GILL IMAGE ANALYSIS: A TOOL FOR ASSESSING PATHOPHYSIOLOGICAL AND MORPHOMETRIC CHANGES IN THE GILL OF ATLANTIC SALMON (*SALMO SALAR* L.)

THESIS SUBMITTED FOR THE DEGREE OF
DOCTOR OF PHILOSOPHY IN
AQUATIC VETERINARY STUDIES

By

Nilantha S. Jayasuriya (BVSc, MSc)

October 2014

INSTITUTE OF AQUACULTURE

UNIVERSITY OF STIRLING

TO MY PARENTS

AND

FAMILY!

DECLARATION

I, hereby declare that the work and the results presented in this thesis have been carried out by myself at the Institute of Aquaculture, University of Stirling, Scotland and have not been submitted for any other degree or qualification. All information from other sources has been acknowledged.

Nilantha S. Jayasuriya

ACKNOWLEDGEMENTS

I would like to pay my sincere gratitude for the knowledge, guidance and the expertise of my supervisors, Dr. Kim D Thompson, Professor James E Bron and Professor Alexandra Adams at University of Stirling and Dr. Charles McGruk and Dr. Julia Mullins from Skretting ARC, Norway. I would also like to acknowledge University of Stirling and Skretting ARC, Norway for providing PhD studentship support for this thesis.

A very special acknowledgment to Professor James E Bron, for your time and effort for writing image analysis script and also for constructive criticisms to keep me right and focused during my PhD, you were one of the key figures for this thesis. Thank you also to Dr. John B Taggart for your assistance in writing Excel Visual Basic aggregation macro for image analysis tool; Dr. Darren Green for your assistance in statistical analysis and Dr. John Taylor for sharing your knowledge about salmon gill physiology. I never forget you, Dr. Andy Shin for your encouragements and coffee while I am working in the Parasitology lab, especially during late evenings. I would also like to convey my sincere gratitude to technical staff of the Institute of Aquaculture, especially, Mrs. Jacqueline Ireland, giving me enormous encouragement and support for molecular techniques and keep me right for the lab matters and also being a truly a friend. Also I would like to thank Mrs. Debbie Faichney for her kind assistance and expertise knowledge on histology. My gratitude is also for Mrs. Hilary McEwan, Mrs. Karen Snedden, Mr. Charlie Harrower, Ms. Jane Lewis, Mr. Niall Auchinachie, Mrs. Fiona Muir, Mrs. Cathryn Dickson, Mrs. Anda Wright, Mrs. Melanie Cruickshank, Mr. Denny Conway and, Mr. Linton Brown. Thank you very much for your skillful practical support! I also like acknowledge Ms. Linda Jensen and others at Skretting

Aquaculture Research Center, Norway, who supplied experimental materials for this study. Also I would like to mention Assistant Professor Christian K. Tipsmark, Department of Biological sciences, University of Arkansas, USA, for providing anti-FXDY antibodies and valuable thoughts on gill osmoregulations.

Big thanks to my friends from the Aquatic Vaccine Unit, University of Stirling, Dr. Sean Monahan, Dr. Gilta Jackel, Mr. José Gustavo Ramírez Paredes and Mr. Christoforos Metochis. Also I would like to thank Dr. Cristian Delannoy for encouragements and friendship. Thanks very much for my office colleagues Mrs. Ngozi Izuchukwu, Miss Zinan Xu (Nancy) and Mr. Philip Lyons for the company, chats and also for your opinion in science and I wish you all good luck for your thesis. Very special thanks Dr. Polyana Da Silva, for being an amazing work mate and also a great friend throughout the PhD. Dr. Rowena Hoare, thanks very much for your kindness and patience on me staying in F3 so often and also for your valuable opinions on science. Apart, thanks all the big family at Institute of Aquaculture your help, support and encouragement kindly remembered.

Finally to my family, my beloved wife Tharangani, I know you are there for me all the time, thanks for giving time and encouragement. Vinethma and Miheli, my two princesses, it was a bless to have you two around, thanks very much for giving me hugs and cuddles, now I can assure that ‘DADDY’S BIG BOOK’ is finished ! Thanks for my parents and my brothers for your support to achieve this goal!

ABSTRACT

In recent decades, farming of Atlantic salmon (*Salmo salar*) has emerged as an important component of the global aquaculture industry. With intensification of aquaculture, a number of constraints arise including those relating to newly emerging and endemic infectious and non-infectious diseases. Development and implementation of appropriate control measures for disease, including prophylaxis, are increasingly becoming a key factor in ensuring the sustainability of the industry and the provision of a high quality protein source. From recent epidemiological investigations conducted to monitor disease occurrence in major salmon producing countries, it has been shown that gill disease has become an increasing problem for the industry and can make commercial stocks more vulnerable to major diseases caused by viral, bacterial and parasitic pathogens. Prompt application of rapid and accurate disease diagnosis tools and large scale gill screening methodologies using modern technologies can contribute to more timely and effective control of disease in salmon aquaculture.

The main goal of this thesis has been to understand and address the challenges associated with developing a gill health monitoring system, which was accomplished by the development of a Gill Image Analysis Tool (GIA tool) based on computer-aided interpretation of high-resolution digital histopathology images of salmonids gills. The research conducted in this thesis has successfully adapted rapidly developing whole-slide digital scanning methodology coupled with image analysis, an approach that has revolutionised human biomedical science, to develop a tool allowing measurement of histomorphometric changes occurring in Atlantic salmon gills. Traditional histopathology, which involves visual light microscopy inspection of histology slides by human readers (histopathologists), has often been criticised due to its

qualitative/subjective approach, which can lead to significant inter- and intra-reader variation. In contrast, the high throughput whole-slide digital scanning system used in this study, coupled with use of image processing and analysis software, can provide consistent, quantitative data that may be used for subsequent analyses. A computerized image analysis (computer assisted diagnosis: CAD) of Atlantic salmon gills allowed extraction of more information, including precise quantitative diagnostic measures of histomorphometric change, which can improve the current evaluation of histopathological data. During the process of developing the GIA tool, an algorithm was developed for key image analysis tasks such as robust adaptive segmentation and intensity based thresholding for feature extraction from different areas of the gills, providing a higher level of accuracy in processing biologically relevant and computationally tractable features, and thus allowing differentiation of the distinct morphometric signatures relating to different pathophysiological conditions of the gills. Furthermore, techniques, used to monitor changes at the tissue level with different special staining methods used to label different tissue components were employed to enhance colour differentiation for feature extraction.

The methodology employed to develop the GIA tool, incorporating prior knowledge of histopathological changes defined for gills, is described in this thesis. Once the GIA tool had been developed, the effectiveness of this approach was assessed using material generated from a number of tank-based trials. This included assessment of gill histomorphometry in salmon fed with functional feeds, evaluation of the effect of therapeutic dose of a chemical treatment (hydrogen peroxide) used by the industry to treat Amoebic gill disease and sea lice infection, on gill histomorphometry, and classification of gill morphometric changes in fish subject to different temperature regimes (low, optimum and high). Application of the GIA tool to scanned histological

images of the experiments created a large quantitative dataset that was expanded with a number of histomorphometric indices derived from the original data. Data were first pre-processed using an Excel Visual Basic aggregation macro and were then subjected to appropriate statistical analysis to interpret differences between treatment and control groups. In parallel to the use of the GIA tool, the immune status of the gill was evaluated using gene expression analysis, focusing on evaluation of pro-inflammatory and immune gene expression as a mechanism for examining the pathophysiological changes that fish undergo when fed functional diets.

The application of the GIA tool, along with various supporting statistical analyses including use of General Linear Models (GLM) and Principal Component Analysis (PCA), allowed evaluation of a range of histomorphometric indices for fish fed different experimental diets and facilitated recognition of dietary impacts highlighting the utility of the newly developed GIA tool. The use of the GIA tool to evaluate histomorphometric changes caused by application of a therapeutic dose of H_2O_2 over a time course of 14 days post exposure, found acute, chronic and recovering gill lesions, suggesting this tool's usefulness in determining sequential histomorphometric changes quantitatively. The GIA tool was also used to investigate the effects of temperature on gill histomorphology to evaluate its usefulness for examining changes associated with gill plasticity. This study found that in fish reared at lower temperatures (4°C) gill morphometric indices changed significantly with respect to fish reared at 10°C, primarily by increasing its cellularity in the primary lamellae. Further, from the experiment performed to evaluate the combined effect of temperature and functional feed on gill plasticity, it was found that changes caused by temperature could be ameliorated through feeding appropriate functional feeds, allowing fish to handle the temperature induced stress more successfully.

In the final chapter, the role of the gill in response to vaccine and pathogen challenge was investigated using the bacterium *Aeromonas salmonicida* as a model using histopathology, immunohistochemistry and immune gene expression to investigate this response. In this study the immune response of the gill to systemic infection with *A. salmonicida* was compared with the response mounted in the spleen and head kidney, the main systemic immune organs. The study found that the gill can elicit an immune response comparable to head kidney and spleen during both vaccination and vaccination challenge.

In conclusion, the new robust image analysis tool developed through the research described in this thesis was employed successfully to measure morphological changes reflecting altered pathophysiological states. Such states were further characterised using immune gene expression analysis. This automated computer-assisted image analysis approach has many advantages compared to conventional routine histology, including the reduced time required to analyse large number of samples, lower user bias and the production of large data sets suitable for quantitation and interpretation of gill and fish health status. This approach can be extended to investigate a broad range of infectious diseases and exogenous environmental factors that are capable of causing responses / pathology in gills. Overall, the new Gill Image Analysis Tool (GIA Tool) promises a new approach that allows the realistic quantitative study of Atlantic salmon gill histopathology with respect to various stimuli. The application of novel image analysis pipelines such as the GIA tool pipeline described in this thesis will serve to improve monitoring and safeguarding of fish health and welfare in the future.

PUBLICATIONS AND PRESENTATIONS FROM THIS THESIS

PUBLICATION IN PREPERATION

1. **N.S. Jayasuriya**, J.E. Bron, C. McGurk, J. Mullins, A. Adams, P. Silva, T.K. Herath and K.D. Thompson. Development of image analysis tool for evaluation of morphometric indices of Atlantic salmon gills. (In preparation to submit to Journal of Aquaculture)

2. **N.S. Jayasuriya**, J.E. Bron, L. B. Jensen, J. Mullins, A. Adams, C McGurk, T.K. Herath and K.D. Thompson. The effects of temperature on gill immunity and morphology in Atlantic salmon fed with different functional diets. (In preparation to submit to Journal of Aquaculture Research)

3. **N.S Jayasuriya**, T.K. Herath, J.E. Bron, A. Adams, J Mullins, C. McGurk, and K.D. Thompson. Immune response of the gill following furunculosis vaccination and experimental challenge with *Aeromonas salmonicida* subspecies *salmmonicida*. (In preparation to submit to Journal of Comparative Immunology)

4. **N.S Jayasuriya**, J Mullins, J.E. Bron, T.K. Herath, C. McGurk, A. Adams, and K.D. Thompson. Evaluation of gill morphometric parameters in Atlantic salmon after treatment with hydrogen peroxide. (In preparation to submit to Journal of Aquaculture)

CONFERENCES PROCEEDINGS AND SEMINARS

1. **N.S. Jayasuriya**, J. Mullins, J.E. Bron, T.K. Herath, C. McGurk, A. Adams and K.D.Thompson (2014). Evaluation of gill morphometric parameters in time course experiments of Atlantic salmon treated with hydrogen peroxide (H_2O_2) therapeutic dose. The 2nd meeting of the 'International gill health initiative', 21-23 May, 2014, Norwegian Veterinary Institute, Oslo Norway. (Oral presentation).

2. **N.S. Jayasuriya,** J.E. Bron, , J. Mullins, C. McGurk, A .Adams, T.K. Herath, and K.D.Thompson (2013). Functional feeds affect gene expression profiles and morphology of the gills of Atlantic salmon reared at different temperatures. 16th International Conference on Diseases of Fish and Shellfish, 2-6th September 2013, Tampere, Finland. (Oral presentation).

3. **N.S. Jayasuriya**, T.K. Herath, J.E. Bron, A. Adams, J. Mullins, C. McGurk and K.D. Thompson (2013). Gene expression profiles in Atlantic salmon gills after vaccination and challenge with *Aeromonas salmonicida* subsp. *salmonicida*. 16th

International Conference on Diseases of Fish and Shellfish, 2-6th September 2013, Tampere, Finland. (Oral presentation).

4. **N.S. Jayasuriya**, J.E Bron, A. Adams, C. McGurk, J. Mullins and K.D. Thompson (2011). Development of an image Analysis tool to evaluate morphometric changes in Salmonid Gills: A preliminary study, 15th International Conference on Diseases of Fish and Shellfish, 2-6th September 2011, Split. Croatia. 12th-16th September, 2011. (Oral presentation).

5. **N. S. Jayasuriya**, J. E. Bron, J. Mullins, A. Adams, C. McGurk, T. K. Herath and K. D. Thompson (2013). Use of image analysis and measurement of immune gene expression to evaluate the health performance of fish from gill samples. Marine Alliance for Science and Technology for Scotland (MASTS) annual science meeting. 27-29th August 2013, Heriot-Watt University, Edinburgh. (E- Poster presentation).

6. **N.S. Jayasuriya**, J.E. Bron, A. Adams, C. McGurk, J. Mullins, K.D. Thompson (2010). Development of a gill model to assess the immune response of Atlantic salmon (*Salmo salar*) to immunostimulant, pathogen challenge, and in disease resistance. Postgraduate Research Conference, University of Stirling (Poster presentation).

7. **N.S Jayasuriya**, J.E. Bron, A. Adams, C. McGurk, J. Mullins and K.D. Thompson (2012). Gill image analysis: A new tool for quantifying gill responses in salmonids. Lunch time seminar, Institute of Aquaculture, University of Stirling

8. **N.S. Jayasuriya**, J.E. Bron, A. Adams, C. McGurk, J. Mullins, K.D. Thompson (2012). Gill image analysis tool: A new tool for quantifying gill response in salmonids. 3rd PhD conference, Institute of Aquaculture, School of Natural Sciences, University of Stirling (Poster presentation).

THE TABLE OF CONTENTS

DECLARATION I
ACKNOWLEDGEMENTS II
ABSTRACT IV
PUBLICATIONS AND PRESENTATIONS FROM THIS THESIS VIII
THE TABLE OF CONTENTS X
LIST OF TABLES XIV
LIST OF FIGURES XVI
ABBREVIATIONS XVII

CHAPTER 1 1
1.1 BACKGROUND 1
1.1.1 Trends in global aquaculture expansion 1
1.1.2 Salmonid diseases and their transmission 2
1.2 THE FISH GILL 4
1.2.1 Anatomy of fish gills 6
1.2.1.1 The gill arch 6
1.2.1.2 Gill Filament 7
1.2.1.3 Respiratory Lamellae 9
1.2.1.4 Epithelial Cells 9
1.2.1.5 Gill Vessels 15
1.3 GILL PATHOLOGIES 16
1.3.1 Assessment of the gill health of fish 18
1.4 TISSUE MORPHOMETRIC ANALYSIS OF GILLS 20
1.4.1 Semi quantitative scoring systems for gill pathologies in salmonids 21
1.5 FISH IMMUNE SYSTEM 22
1.5.1 Components of the fish immune system 22
1.5.2 Immune tissue and cells 23
1.5.2.1 Head kidney 23
1.5.2.2 Thymus 24
1.5.2.3 Spleen 25
1.5.2.4 Liver 26
1.5.2.5 Fish immune cells 27
1.5.3 Immunity in fishes 28
1.5.3.1 Innate immunity of fish 28
1.5.3.2 Adaptive immunity of fish 30
1.5.3.3 Mucosal immunity fish 31
1.5.3.4 Teleost IgT as a marker of mucosal immunity in fish 35
1.6 NUTRITION AND FISH HEALTH 35
1.6.1 Functional feeds as a measure to induce disease resistance in cultured salmonids 37

1.7 IMAGE ANALYSIS 39
1.8 AIMS OF STUDY 42

CHAPTER 2 43

2.1 INTRODUCTION 43
2.2 MATERIALS AND METHODS 48
2.2.1 Dietary trial 49
2.2.2 Sample processing for histology 50
2.2.2.1 Haematoxylin and Eosin (H&E) staining 52
2.2.2.2 Periodic acid shift (PAS) and Alcian blue (AB) staining 52
2.2.3 Light microscopy, imaging and processing 53
2.2.4 Subsampling (cropping) of images through selected randomisation 54
2.2.5 Development of gill image analysis tool (GIA) 54
2.2.5.1 Edge detection 59
2.2.5.2 Noise removal 59
2.2.5.3 Colour thresholding 59
2.2.5.4 Morphological filtering 60
2.2.5.5 Intensity thresholding 60
2.2.5.6 Size scrapping and filling 61
2.2.5.7 Intensity thresholding of inverted images 61
2.2.5.8 Interactive manual object delineation 61
2.2.5.9 Feature extraction and output generation 62
2.2.6 Image analysis using KSRUN software 62
2.2.7 Data analysis 72
2.2.7.1 Pre-processing of data for statistical analysis 72
2.2.7.2 Statistical analysis 74
2.2.8 Gene expression analysis 75
2.2.8.1 RNA extraction 75
2.2.8.2 cDNA synthesis 75
2.2.8.3 Primer optimisation using conventional PCR reaction 76
2.2.8.4 Pre-processing of data, normalisation and relative quantification 80
2.2.8.5 Statistical analysis 80
2.3 RESULTS 81
2.3.1 Conventional histological analysis 81
2.3.2 Morphometric analysis of Atlantic salmon gills after feeding with two functional diets 81
2.3.2.1 Non parametric analysis of morphometric data 85
2.3.2.2 Primary lamellae-associated morphometric parameters 87
2.3.2.3 Secondary lamellae associated morphometric parameters 88
2.3.2.4 Mucous cell associated morphometric parameters 89
2.3.2.5 Total gill area associated morphometric parameters 91
2.3.3 Multivariate analysis of morphometric data (PCA) 92
2.3.4 Gene expression analysis 99
2.4 DISCUSSION 101

CHAPTER 3 107

3.1 INTRODUCTION 107
3.2 MATERIALS AND METHODS 114

3.2.1 Fish....114
3.2.2 Sample processing for histology and Periodic acid shift (PAS) and Alcian blue (AB) staining....115
3.2.3 Light microscopy, imaging and processing....116
3.2.4 Conventional histopathological examination for H_2O_2 treated gills at different time points....117
3.2.5 Image analysis using KSRUN software....119
3.2.6 Data analysis....119
3.3 RESULTS....124
3.3.1 Conventional histological analysis....124
3.3.2 Morphometric analysis of Atlantic salmon gills treated with hydrogen peroxide....132
3.3.2.1 General Linear Model (GLM), univariate analysis of morphometric data 132
3.3.2.2 Multivariate analysis of morphometric data....143
3.3.3 Discussion....149

CHAPTER 4....158

4.1 INTRODUCTION....158
4.1.1 The effects of water temperature on gill physiology....158
4.1.2 The effect of temperature on teleost immunity....164
4.1.3 Gill specific morphometric response to different functional diets....171
4.2 MATERIALS AND METHODS....172
4.2.1 Fish and feeds....
4.2.1.1 ..Experiment 1 – evaluation of morphometric changes of Atlantic salmon gill reared in three different temperatures and fed with a conventional diet....172
4.2.1.2 Experiment 2 – evaluation of morphometric changes, immune gene expression of Atlantic salmon gill reared in two different temperatures and fed with three different diets....173
4.2.2 Sampling of fish....174
4.2.3 Sample processing for histology....174
4.2.4 Light microscopy, imaging and processing....174
4.2.5 Evaluation of gills using GIA tool....175
4.2.6 Gene expression analysis....175
4.2.6.1 Primer optimisation using conventional PCR reaction....175
4.2.6.2 Primer optimisation using RT-qPCR in Realplex Eppendorf platform 179
4.2.6.3 Reverse Transcription Quantitative Polymerase Chain Reaction (RT-qPCR) in Realplex Eppendorf platform....179
4.2.6.4 Gene expression analysis using GenEx software....180
4.2.7 Statistical analysis....181
4.3 RESULTS....183
4.3.1 Experiment 1 - evaluation of morphometric changes of Atlantic salmon gill reared at three different temperatures and fed a conventional salmon diet....183
4.3.1.1 Histology....184
4.3.1.2 Morphometric analysis....186
4.3.1.3 Gene expression analysis....193

4.3.2 ..... Experiment 2 - evaluation of morphometric changes, immune gene expression of Atlantic salmon gill reared in two different temperatures and fed with three different diets 196
4.3.2.1 Histology 197
4.3.2.2 Morphometric analysis 199
4.3.2.3 Gene expression analysis 206
4.3.2.4 PCA Analysis of combined morphometric and gene expression data of Experiment 2 212
4.4 DISCUSSION 215

CHAPTER 5 224

5.1 INTRODUCTION 224
5.2 MATERIALS AND METHODS 228
5.2.1 Fish 228
5.2.2 Vaccination 230
5.2.3 Experimental infection of fish with A. salmonicida after vaccination 232
5.2.4 Sampling of fish post-vaccination and post-infection 235
5.2.5 Histology 236
5.2.5.1 Sample processing for histology 236
5.2.5.2 Haematoxylin and eosin staining 236
5.2.5.3 PAS and Alcian blue staining 237
5.2.6 Immunohistochemistry 237
5.2.7 Laser scanning confocal microscopy (LSCM) 240
5.2.8 Gene expression analysis 240
5.2.8.1 Analysis of gene expression 244
5.3 RESULTS 245
5.3.1 Mortality curve and cause of death 245
5.3.2 Histology and immunohistochemistry 246
5.3.3 Laser scanning confocal microscopy (LSCM) 250
5.3.4 Gene expression analysis results 253
5.3.4.1 Normalised immune gene expression of head kidney, spleen and gill, during A. salmonicida infection post-vaccination 253
5.3.4.2 . Normalised immune gene expression of head kidney, spleen and gill of vaccinated and unvaccinated fish following challenge with A. salmonicida ... 256
5.3.4.3 IL-1β 256
5.3.4.4 INF-γ 257
5.3.4.5 IgM 260
5.3.4.6 IgT 260
5.4 DISCUSSION 264

CHAPTER 6 275

REFERENCES 287

APPENDIX I 310

APPENDIX II 312

LIST OF TABLES

Table 1.1 The infectious agents involved in causing gill diseases or syndromes in salmonids 19

Table 2.1 Different morphometric parameters measured during development of the gill image analysis tool..... 56

Table 2.2 The qPCR primers used to measure changes in the gills of fish following feeding of different functional feeds..... 78

Table 2.3 Thermal cycling conditions used in the Techne Quantica® Thermal cycler for the RT-qPCR assay to quantify target associated genes. 79

Table 2.4 Calculation of mean relative gene expression values using relative the expression software tool (REST) (Schmittgen and Livak, 2008: Pfaffl *et al.*, 2002)..... 80

Table 2.5 Results of measured morphometric variables of Atlantic salmon gill fed with three different diets. 86

Table 2.6 Total variance of extracted first 10 principal components using 25 measured morphometric parameters. 93

Table 2.7 Total variance explained by the first 5 principal components (25 measured morphometric parameters)..... 95

Table 2.8 Component matrices generated from PCA analysis of measured morphometric variable..... 96

Table 2.9 Multiple comparisons test between dietary groups for PC5. Diet as dependent variable, bolded values significant at $p<0.05$ 98

Table 2.10 The slopes, R^2 and efficiencies (% E) values for each of the primers, calculated from the standard curves..... 99

Table 2.11 Summary of the results of gene expression analysis for selected primers across different functional diets. Values are indicated as log2 conversion of relative expression values and significant (*) at $p < 0.05$. N=9..... 100

Table 3.1 A list of possible histopathological lesions recorded in earlier literature. During the present trial few of these lesions could be observed 118

Table 3.2 Results of measured morphometric variables. GLM was performed in Minitab. 134

Table 3.3 Total variance explained by the first 5 principal components (29 measured morphometric parameters).....144

Table 3.4 Total variance of extracted first 10 principal components out of total of 28 measured morphometric parameters.....144

Table 3.5 Component matrices generated from PCA analysis of measured morphometric variable. The parameters indicate greater explanatory power is shaded in grey 146

Table 4.1 Details of the samples prepared for histology for the gill morphometric studies 177

Table 4.2 The PCR primers used to measure immunomodulation induced by diet in the gills of fish reared at different temperature 178

Table 4.3 Univariate statistical analysis of morphometric data generated from gill sections taken from fish held at different experimental water temperatures (4, 10 and 16 °C) in Experiment 1. General Linear Model (GLM) performed using SPSS statistical software.....188

Table 4.4 Total variance of extracted first 10 principal components in Experiment 1.191

Table 4.5 Summary of classification of discriminant analysis for morphometric data generated from experiment 1 193

Table 4.6 Total variance of extracted first 10 principal components in Experiment 1.195

Table 4.7 Univariate analysis of morphometric data generated from gill sections taken from fish held at different water temperatures (4 and 12°C) in Experiment 2. The General Linear Model (GLM) was performed using Minitab statistical software 200

Table 4.8 Analysis of variance for principal component 1 (GLM). The significance is indicated by * when $p< 0.05$.....203

Table 4.9 Analysis of TNF α expression in response to diet and temperature using a general linear model (GLM). Significance has indicated as * when $p< 0.05$.....207

Table 4.10 Analysis of IgT expression in response to diet and temperature using a general linear model (GLM). Significance has indicated as * when $p< 0.05$.....207

Table 5.1 Final experimental groups and nomenclature. The colour code indicates the identity of relevant groups in bar graphs 234

Table 5.2 Immunohistochemistry targets, primary and secondary antibodies, reagents used in the IHC procedures and resulting staining obtained following IHC 242

Table 5.3 The qPCR primers used to measure changes in the gills of fish following vaccination and challenge.....243

ABBREVIATIONS

AB	Alcian blue
AGD	Amoebic gill disease
ANOVA	Analysis of Variance
ARF	Aquaculture Research Facility
ASPV	Atlantic salmon paramyxovirus
BKD	Bacterial kidney disease
BM	Basement membrane
BCP 1	bromo-3-choropropane
BC	blood channels
BHIA	brain heart infusion agar
BBA	Brilliant blue agar
CAD	computer assisted diagnosis
CMS	cardiao-myopathy syndrome
CC or CL	chloride cells
CD8	cluster of differentiation eight
CD4	cluster of differentiation four
CO_2	carbon dioxide
Con A	concanavalin A
CRP	C-reactive protein
CVS	Central venous sinus
Tc	Cytotoxic T-cells
d.p.e.	days post-exposure
h.p.e.	hours post-exposure
DAPI	4',6-diamidino-2-phenylindole
DMC	distal marginal channel
ERM	enteric redmouth disease
ELISA	enzyme linked immunosorbent assay
EGC	eosinophilic granulocytes cells
EDTA	Ethylenediaminetetraacetic acid
FAO	Food and Agriculture Organization
GALT	Gut-associated lymphoid tissues
GIT	gastrointestinal tract
GLM	General Linear Model
GIA	gill image analysis
GIA Tool	Gill Image Analysis Tool
GR	Gill Ratio
SLA/PLA	Gill Ratio g
H&E	Haematoxylin and Eosin
HABs	harmful algal blooms
HSMI	heart and skeletal muscle inflammation
HIF-1α	hypoxia inducible factor 1-alpha
ILT	interbranchial lymphoid tissue
IgT	Immunoglobulin T
IgM	Immunoglobulins M
IHC	immunohistochemistry
IoA	Institute of Aquaculture
ILS	Inter-lamellar space

ILCM	Inter-lamellar cell mass
IL-1β	interleukin interleukin one beta
IL-10	interleukin ten
ILS/SLA	Inter-secondary ratio of gill
ISA	Infectious salmon anaemia
ISR ……	Inter-secondary Ratio
LSCM	laser scanning confocal microscopy
LM	Light microscopy
LPS	lipopolysaccharide
MHC	major histocompatibility complex
MedianFERETMaxSL ……...	Median maximum Feret secondary lamellae
MedianFERETMinSL ……	Median minimum Feret secondary lamellae
MedianSLL ……	Median secondary lamellar length
MMC	melanomacraphage centres
mIgM)	membrane immunoglobulin M
mIgT ……..	membrane immunoglobulin T
MRC.....	mitochondria rich cells
MALT	mucosal associated lymphod tissue
MCA-PLEA ……	Mucous cell area in PLEA
MCA-SLA ……..	Mucous cell area of secondary lamellar area
(MCA-SLA)/SLA ……..	Mucous cell area of secondary lamellar area/ Secondary lamellar area
(MCN-SLA) ……..	Mucus cell number in secondary lamellar area
MC	mucus cells
NKA	$Na^+ K^+$ ATPase
NKs	natural killer cells
NEC	neuroepithelial cells
NBF	neutral buffered formalin
iNOS	nitric oxide synthase
RT minus	no reverse transcriptase enzyme
NTC.....	non template control
NCC	Non-specific cytotoxic cells
O_2	Oxygen
UMC	outer marginal canal
PAMP	pathogen associated molecular pattern
PVC	pavement cells
PD	Pancreas disease
PAS	periodic acid Schiff stain
PBS	phosphate buffered saline
PC.....	pillar cells
pIgR	polymeric immunoglobulin receptor
pIgRL	polymeric immunoglobulin receptor
APC	Antigen presenting cells
PLA……	Primary lamellar area
PLEA……..	Primary lamellar epithelial area
PCA	Principal Component Analysis
PGD	proliferative gill disease
PGI	proliferative gill inflammation
RT-qPCR	quantitative reverse transcription
PCR……	polymerase chain reaction
RAG1 and RAG2	recognition activator genes
ROI	region of interest

RT-PCR	reverse transcription polymerase chain reaction
ISAV	salmon anaemia virus
SAA	salmon serum amyloid A
SGPV	salmonid pox virus
SLA ……	Secondary lamellar area,
SLPL ……	Secondary lamellar perimeter length
SLPL/MeanSLL……..	ratio of secondary lamellar perimeter length / Mean secondary lamellar length
SLPL/SLA……..	ratio of secondary lamellar perimeter length / secondary lamellar area
SALT	skin associated lymphoid tissues
SEM	standard error mean
SLL ……	Secondary Lamellar Length
SOP	standard protocol of operation
Th	T-helper cells
TD	thymus dependent
TI	thymus independent
TLR	Toll-like receptors
TGA ……..	Total gill area
TMCA ……...	Total mucus cell area,
TMCA/TGA ……..	Total mucus cell area / Total gill area
TMCN ……	Total mucus cell number
TMCN/TGA ……..	Total mucus cell number / Total gill area
TEM.....	transmission electron microscopy
TNP.....	tri-nitrophenyl
TSA	tryptone soya agar
TNFα	tumour necrosis factor alpha
T3SS	type III secretory system
VAPL ……..	Vacuolar area of primary lamellae
VASL …….	Vacuolar area of secondary lamellae
WSI ……	whole-slide imaging

LIST OF FIGURES

Figure1.1 Histomicrograph showing H&E stained Atlantic salmon gills (A) low power showing gill filements (primary lamellae) (Long arrow) with cartilaginous rod (C) running in the centre and secoundtry lamellae (short arrow) extending as projections from the primary lamellae. (B) a higher magnification of the primary lamellar area blocked in gray in the plate (A) area showing respiratory epithelia of the gill. Note distal marginal channel (DMC), blood channels (BC), chloride cells (CL) and pillar cells. 8

Figure1.2 (A) Transmission electron micrograph across central marginal canal at mid region of the secondary lamellar. The pillar cells (PC) and cytoplasmic flanges of pillar (PC-F) cells are supported by basement membrane (BM). The two spool shaped PC cells joined together by flanges forming pillar canals. Note red blood cells (RBC), polymophonuclear white blood cells (WBC-PMN) in the pillar canals in the micrograph. **(B)** Transmission electron micrograph across outer marginal canal (UMC) at distal end of secondary lamellar. Spool shaped pillar cells (PC) are supported by two true lamellar epithelial cells (TLE). The cytoplasmic flanges of pillar cells (PC-F) lines the outer lamellar blood space filled with red blood cells in the micrograph. The basement membrane surrounds the pillar cells and endothelium of the UMC. Micrographs Courtesy of Dr Tharangani Herath (unpublished)..... 10

Figure1.3Transverse electron micrograph of mucous cell enriched with membrane bound vesicles (MC), (A) with a nucleus (N) pushed a towards to the base of the cell and an apically located secretory pit (black arrow) and (B) endoplasmic reticulum tightly stacked at the base of the cells. Micrographs are Courtesy of Dr Tharangani Herath (unpublished) 12

Figure1.4 Confocal laser scanner micrograph of a Atlantic salmon gill stained with FITC- anti Na/K ATPase and FITC (A) lower magnification (B) higher magnification showing darkly stained chloride cells. Note size differences in chloride cells in micrograph B. (C) A transmission electron micrograph of a gill at base of the primary lamellae (areas is marked red in micrograph B). The tissue is rich in mitochondria rich chloride cells (CL). The apical membrane of the lamellar epithelium with micro projection (arrow) is surrounded by CL cells. Electron micrographs Courtesy of Dr Tharangani Herath (unpublished) 13

Figure1.5 Electron micrograph of a fresh water reared Atlantic salmon gill epithelim showing a chloride cell enriched with mitochondria (M) and sub epical vesicular system (vc). Cell membrane of the gill epithelium forms as extensions of the apical membrane forming microprojection (ASP). Note nucleus (N). Micrographs Courtesy of Dr Tharangani Herath (unpublished) 14

Figure 2.1 A Schematic diagram of experimental plan. Fish were fed with Diet A- conventional salmon diet (control), Diet B - test diet with 25% of fish meal replaced with soybean meal, Diet C - test diet enriched with additional immune stimulant and sampled at 11 weeks and 20 weeks after introducing test feeds. First sampling (initial

sampling) was carried out 11 weeks and second sampling (final sampling) after 20 weeks after start of test feed. Results of final sampling were analysed and presented in this chapter accordingly. 51

Figure 2.2 A diagrammatic illustration of the different steps involved in histopathological evaluation through whole slide imaging (WSI) technology. (A) different functional feed fed fish, (B) second gill arch, (C) histological slides with different gill sections, (D) Mirax desktop scanner with manual feeding of slides, (E) scanned whole slide images (WSI), (F) defined region of interest (ROI), (G) x40 cropped images through Mirax viewer (or "Pannoramic" viewer), (H) representative image of gill fed with different functional diet using Mirax "x40" magnification setting. Scale bar 100 μm 55

Figure 2.3 A diagrammatic illustration of intermediate analytical steps included in the use of the of GIA tool. Thin (5μm) histological sections of whole gill from fish fed with different functional diets were used to develop the GIA tool. A-E, shows common steps involved in virtual histopathology and GIA tool; F, uploaded cropped image (a subsample) in KS300\KSRUN software; G, region of interest with 5 secondary lamellae on each side (total 10); H-L, intermediate steps which generate different gill histo-morphometric parameters including TGA, SLA, PLA, TMCN and VASL; M, a screenshot of the generated data file, rows comprise individual fish or subsamples, columns comprise relevant morphometric parameters or indices. 58

Figure 2.4 Standardised image orientation and crop using pre sized box 63

Figure 2.5 Selection of the region of interest (ROI) from the cropped gill image 64

Figure 2.6 Initial selected region of interest (ROI) for subsequent processing and analysis.....65

Figure 2.7 Thresholding cropped image to give binary image 65

Figure 2.8 Lines drawn to segment gills into different anatomical areas. 66

Figure 2.9 Different segmented areas of the gill tissue were transformed into binary images for area measurements. A PLA, B PLEA, C CVS and D SLA 67

Figure 2.10 Extractions of mucous cells from secondary lamellar area using intensity thresholding. Mucous cells are marked in blue colour. The small micrographs show x 2 original magnification with more details changes during the process. 69

Figure 2.11 Measurement of secondary lamellar length was performed manually by drawing a line base to the tip of the lamellae 70
Figure 2.12 Extraction of inter-lamellar space (ILS) from interconnected secondary lamellar area by drawing a line connecting the tips of the secondary lamellae.....70

Figure 2.13 Extraction of the vacuolar area of the primary lamellae (VAPL) 71

Figure 2.14 Extraction of the vacuolar area of the secondary lamellae (VASL).....71

Figure 2.15 Extraction of the secondary lamellar perimeter length (SLPL) 72
Figure 2.16 Extraction of mucous cells from primary lamellar area (PLA) using colour thresholding and masking. Mucous cells stain blue. The small micrographs show x 2 original magnification detailing the process of extraction.....73

Figure 2.17 The task-specific Visual Basic Excel aggregation macro developed to tabulate GIA output data.....74

Figure 2.18 Results of RT-qPCR for reference gene β actin (a) standard curve generated from ct values (y-axis) versus 10-fold dilution of pool cDNA of all samples, (b) RT-qPCR amplification curves (c,d) dissociation curve (melting curve) analysis of RT-qPCR of the standard sample to determine specificity of the end product.....79

Figure 2.19 Micrographs of gill derived from dietary group A, stained (A) H & E for conventional histology (B) PAS / Alcian blue with haematoxylin for mucous cell histochemistry. Note normal gill morphology with early stage of clubbing at the distal ends of the secondary lamellae. Scale bar 100 μm. 82

Figure 2.20 Micrographs of gill derived from dietary group B, stained (A) H & E for conventional histology (B) PAS / Alcian blue with haematoxylin for mucous cell histochemistry. Note normal gill morphology with initial stage of clubbing at the distal ends of the secondary lamellae Scale bar 100 μm 83

Figure 2.21 Micrographs of gill derived from dietary group C, stained (A) H & E for conventional histology (B) PAS / Alcian blue with haematoxylin for mucous cell histochemistry. Note normal gill morphology with initial stage of clubbing at the distal ends of the secondary lamellae (A) 125 μm, (B) 100 μm.....84

Figure 2.22 Primary lamella-associated morphometric changes in Atlantic salmon gills fed with different functional diets. (a) vacuolar area of primary lamellae (VAPL); (b) primary lamellar epithelial area (PLEA); (c) primary lamellar area (PLA) Abbreviations: 0H - pre-trial control; H-hours post exposure; D – days post-exposure. Bars represent mean values ± SEM where n=9. Different letters indicate significantly different values ($p < 0.05$) from Kruskal Wallis *post-hoc* tests.....87

Figure 2.23 Secondary lamellae associated morphometric changes in gills of Atlantic salmon fed with different functional diets. (a) vacuolar area of secondary lamellae (VASL); (b) secondary lamellar area (SLA); (c) median minimum Feret value for secondary lamellae (MeanFERETMinSL); (d) median maximum Feret value for secondary lamellae (MedianFERETMaxSL), error bars represent means values ± SEM where n=9. Different letters indicate significantly different values at $p \leq 0.05$ from Kruskal Wallis *post-hoc* tests. 88

Figure 2.24 Secondary lamellae associated morphometric changes in gills of Atlantic salmon fed with different functional diets continued. (e) Secondary lamellar perimeter length (SLPL), (f) SLPL/SLA, (g) (SLPL/MedianSLL). Bars represent means values ± SEM where n=9. Different letters indicate significantly different values at $p \leq 0.05$ from Kruskal Wallis *post-hoc* tests. 89

Figure 2.25 Mucous cell associated morphometric changes in the gills of Atlantic salmon fed with different functional diets. (a) total mucous cell area (TMCA); (b) total mucous cell area / total gill area (TMCA\TGA); (c) mucous cell number in primary lamellar epithelial area (MCN-PLEA); (d) total mucous cell area in primary lamellar epithelial area (MCA-PLEA); (e) mucous cell area in primary lamellar epithelial area / primary lamellae epithelial area (MCA-PLEA)/PLEA; (f) mucous cell number secondary lamellar area (MCN-SLA); Bars represent mean values ± SEM where n=9. Different letters indicate significance of difference at $p \leq 0.05$ from Kruskal Wallis *post-hoc* tests.....90

Figure 2.26 Mucous cell associated morphometric changes in the gills of Atlantic salmon fed with different functional diets continued (g) Mucous cell area of secondary lamellar area (h) mucous cell area of secondary lamellar area / secondary lamellar area (MCA-SLA); (i) total mucous cell number (TMCN), (j) TMCN/TGA. Bars represent mean values ± SEM where n=9. Different letters indicate significance of difference at $p \leq 0.05$ levels from Kruskal Wallis *post-hoc* tests 91

Figure 2.27 Total gill area associated morphometric changes in the gills of Atlantic salmon fed with different functional diets. (a) Interlamellar area (ILS); (b) gill ratio (GR); (c) inter-secondary ratio (ISR); (d) total gill area (TGA). Bars represent means values ± SEM where n=14. Different letters indicate significantly different values ($p \leq 0.05$) from Kruskal Wallis *post-hoc* tests 92

Figure 2.28 Scree plot of Eigenvalues of relevant principal components 94

Figure 2.29 Loading plot for morphometric parameters analysed.....97

Figure 2.30 scatter plot of PC1 vs PC2 from morphometric analysis showing distribution of fish fed different diets 97

Figure 2.31 Boxplot of Principal Component 5 for three diets (A control, B & C functional).....98

Figure 3.1 A composite diagram of common irritant-induced gill lesions. Six respiratory lamellae are shown (a-f), the top one of which is normal (*Oncorynchus mykiss*, modified from Skidmore and Tovell 1972). The lesions are 1, epithelial lifting; 2, necrosis; 3, lamellar fusion (c and d); 4, hypertrophy; 5, hyperplasia; 6, epithelial rupture and bleeding into pharynx; 7, mucous secretion; 8, clavate lamella or lamellar aneurism (e); 9, vascular congestion; 10, mucous cell proliferation; 11, chloride cells damaged early; 12, chloride cell proliferation; 13, leukocyte infiltration of epithelium;14A, lamellar blood sinus dilates; 14B, lamellar blood sinus constricts. For photomicrographs of some of these lesions are illustrated in Eller (1975). Abbreviations: bl, basal lamina; cc, chloride cell; e, typical lamellar epithelial cells; lbs, lamellar blood sinus; ma, marginal blood channel; mu, mucous cell; pi, pillar cell; rbc, erythrocyte. [Adapted from Mallatt (1985)]. 113

Figure 3.2 Experimental layout of H_2O_2 trial, 231 g (N=7) of Atlantic salmon fed with conventional salmon diet and reared at duplicate tanks were exposed to therapeutic dose of H_2O_2 1500 ppm for 20 min prior to sample in time course interval(Fish 1 -82).

Please note only 5 fish were analysed on Day 7 post exposure with a technical problem obtaining high resolution scanned images. 115

Figure 3.3 A diagrammatic illustration of different steps involved in histopathological evaluation through whole slide imaging (WSI) technology. (A) hydrogen peroxide treated fish, (B) preferred second gill arch, (C) histological slides, (D) Mirax desktop scanner, (E) scanned whole slides, (F) defined area of interest, (G) x40 cropped images, (H) representative image of H_2O_2 treated gills using Mirax "x40" magnification setting. Scale bar indicate 100 µm.....120

Figure 3.4 A diagrammatic illustration of intermediate analytical steps including use of the GIA tool, which was used to analyse H_2O_2 treated whole gill archs thin (3µm) histological sections mounted on special adhesive slides. A-E, shows common steps involved in virtual histopathology (Figure 3.1) and GIA tool; F, uploaded cropped image (subsample) in KS300\KSRUN software; G, area of interest with 5 secondary lamellae of each side (total 10); H-L, intermediate steps which generate different gill morphometric parameters including TGA, SLA, PLA, TMCN and VASL; M, a screenshot of generated large data files, rows comprise individual fish or subsamples, columns comprise relevant morphometric parameters or indices. For more details see chapter 2 section 2.4.4. 121

Figure 3.5 The Excel macro developed to tabulate GIA output data. Detailed information is included in Chapter 2 Section 2.2. 123

Figure 3.6 Pre-trial control gill samples (0 H) stained with Alcian blue and counter stained with haematoxylin for mucous cell histochemistry. (A) normal morphology, C-cartilage, SL- secondary lamellae, PL- primary lamellae, ILS- inter-lamellar spase, heavy arrows indicate mucous cells. (B) Low magnitude cell clubbing in the distal end of the secondary lamella was occasionally seen (light arrows). Scale bar 100µm.....125
Figure 3.7 Pre-trial control gill samples (0H) stained with Alcian blue and counter-stained with haematoxylin. (A) Normal morphology with a few lamellae showing clubbing, thick arrows indicate mucous cells. (B) Slight oedema with no epithelial separation at the base of the lamellae and interlamellar area. Square box shows higher magnification of irregular cell 126

Figure 3.8 Gill samples of 4 h.p.e (4H) stained with Alcian blue and counter stained for haematoxylin for mucous cell histochemistry and gill morphology. (A) Histopathological changes in PLEA (small box shows twice the original magnification), ILS filled with some blood cells, occasionally epithelial cells. (B) Increased cellularity in PLEA. Scale bar 100µm 127

Figure 3.9 Gill samples of 24H stained with Alcian blue and counter stained for haematoxylin for mucous cell histochemistry and gill morphology. (A) Histopathological changes in PLEA (small box shows twice the original magnification), increased cellularity in PLEA. (B) Blood cells and scant amount of epithelial cells seen in the ILS could possibly a sampling/processing artefact. Scale bar 100µm 128

Figure3.10 Gill samples of 3 d.p.e (3D) stained with Alcian blue and counter stained for haematoxylin for mucous cell histochemistry and gill morphology. (A) Histopathological changes in PLEA (small box shows twice the original magnification),

decreased magnitude of cellularity in PLEA compared to previous time points. (B) ILS filled with very few blood cells and occasionally fallen epithelial cells. Scale bar 100µm 129

Figure 3.11 Gill samples of 7 d.p.e (7D) stained with Alcian blue and counter stained for haematoxylin for mucous cell histochemistry and gill morphology. (A) Histopathological changes in PLEA (small box shows twice the original magnification), increased cellularity in PLEA is decreased compared to earlier time points. (B) ILS filled with blood cells, occasionally fallen epithelial cells. Scale bar 100µm 130

Figure 3.12 Gill samples of 14 d.p.e (14D) stained with Alcian blue and counter stained for haematoxylin for mucous cell histochemistry and gill morphology. (A) Histopathological changes in PLEA (small box shows twice the original magnification), decreased cellularity in PLEA compared to earlier time points. (B) ILS filled with blood cells, occasionally fallen epithelial cells. Scale bar 100µm..... 131

Figure 3.13 Distribution of data from selected morphometric parameters; (A) GR, gill ratio, (B) TGA, total gill area, (C) SLA, secondary lamellar area and (D) (MCA-SLA)\SLA, mucous cell area of secondary lamellar area over secondary lamellar area. 133

Figure 3.14 Primary lamellae associated morphometric changes in Atlantic salmon post-exposure with 1500 ppm hydrogen peroxide for 20 min at 12°C in salt water: (a) vacuolar area of primary lamellae (VAPL); (b) primary lamellar epithelial area (PLEA); (c) primary lamellar area (PLA) Abbreviations: 0H - pre-trial control; H-hours post exposure; D – days post-exposure. Bars represent mean values ± SEM where n=14. Different letters indicate significantly different values ($p < 0.05$)..... 136

Figure3.15 Secondary lamellae associated morphometric changes in Atlantic salmon post exposure with 1500 ppm hydrogen peroxide for 20 min at 12°C in salt water: (a) vacuolar area of secondary lamellae (VASL); (b) secondary lamellar area (SLA); (c) mean minimum Feret value for secondary lamellae (MeanFERETMinSL); (d) median minimum Feret value for secondary lamellae (MedianFERETMinSL); (e) maximum Feret value for secondary lamellae (MeanFERETMaxSL); (f) median maximum Feret value for secondary lamellae (MedianFERETMaxSL). Abbreviations: 0H - pre-trial control; H-hours post exposure; D – days post-exposure. Bars represent means values ± SEM where n=14. Different letters indicate significantly different values ($p \leq 0.05$). 138

Figure 3.16 Mucous cell associated morphometric changes in Atlantic salmon post exposure with 1500 ppm hydrogen peroxide for 20 min at 12°C in salt water: (a) total mucous cell area (TMCA); (b) total mucous cell area / total gill area (TMCA\TGA); (c) number in primary lamellar epithelial area (MCN-PLEA); (d) total mucous cell area in primary lamellar epithelial area (MCA-PLEA); (e) total mucous cell area in primary lamellar epithelial area / primary lamellae epithelial area (MCA-PLEA)/PLEA; (f) total mucous cell number secondary lamellar area (MCN-SLA); (g) mucous cell area of secondary lamellar area / secondary lamellar area (MCA-SLA); (h) total mucous cell number (TMCN) Abbreviations: 0H - pre-trial control; H-hours post exposure; D – days post-exposure. Bars represent mean values ± SEM where n=14. Different letters indicate significantly different values ($p \leq 0.05$). 141

Figure 3.17 Total gill area associated morphometric changes in Atlantic salmon post exposure with 1500 ppm hydrogen peroxide for 20 min at 12°C in salt water: (a) interlamellar area (ILS); (b) gill ratio (GR); (c) inter-secondary ratio (ISR); (d) total gill area (TGA). Abbreviations: 0H - pre-trial control; H-hours post exposure; D – days post-exposure. Bars represent means values ± SEM where n=14. Different letters indicate significantly different values ($p \leq 0.05$). 143

Figure3.18. A scatter plot generated from PCA analysis, plotting principal component 1 and 2 and showing clear clustering of subsamples of fish belong to different groupings. 147

Figure3.19. Classification of subsamples of fish belonging to different time points using new variables PC1 and PC2. (A) All six sampling points, (B) Control versus 4 h.p.e., (C) control versus 12 h.p.e., (D) control versus 3 d.p.e., (E) control versus 7 d.p.e., (F) control versus 14 d.p.e. 148

Figure 4.1 A Scanning electron micrographs from the 2nd gill arch of crucian carp kept in normoxic or hypoxic water: (a) In normoxia, the gill filaments have no protruding lamellae; (b) The morphology has already changed after 1 day of hypoxia exposure ($0.75\pm0.15 \cdot mg \cdot O_2 \cdot L^{-1}$); (c, d). The change progresses for up to 7·days in hypoxia, but (e) there were no further changes with subsequent exposure; (f) When the fish were moved to normoxic water, the morphological changes were reversed within 7 days. Scale bar, 50 mm (Sollid *et al.*, 2003) 161

Figure 4.2 Light micrographs of gills stained for (a–c) S-phase cells (BrdU) and (d–f) apoptotic cells (TUNEL). Picture series starts with normoxia (a, d), 3·days of hypoxia (b,e) and 7·days of hypoxia (c,f). Arrows point out some of the stained cells seen on the micrographs. ILCM, interlamellar cell mass. Scale bar, 50·mm. (Sollid *et al.*, 2003).162
Figure 4.3 The effects of acclimation temperature on the surface area of ionocytes (as determined by Na+/K+-ATPase immunofluorescence) and their distribution in goldfish (Carassius auratus). (A) The surface area of ionocytes was significantly decreased (indicated by asterisk) in fish acclimated to 25 °C (N=6) when compared with fish kept at 7 °C (N=6); data are presented as means ± 1 s.e.m. (B, C). Representative light micrographs illustrate that the decrease in ionocyte (arrows) surface area in fish acclimated to 25 °C was a result of decreased numbers and sizes of individual cells. Note that the ionocytes were confined to the outer edge of the ILCM in the fish acclimated to 7 °C; scale bars, 20 μm. Sections were labelled with DAPI-containing mounting media to show cell nuclei (blue) (Mitrovic and Perry, 2009).....163

Figure 4.4 Flow chart to show different steps of data processing in GenEx Enterprise software, which included a step of quality assurance, replacement of missing data to fulfil the requirement of balance ANOVA (GLM). Most suitable and recommended normalisation was achieved by using reference gene index. 182

Figure 4.5 Growth performances (fish weight, fish length and condition factor) of fish from experiment 1, reared at three different temperatures. *indicates significant difference compared to the control group (10 ºC) when $p<0.05$. Error bars indicate ±SEM. N= 11. 183

Figure 4.6 Representative gill micrographs of gill sections from fish maintained in Experiment 1, stained with Alcian blue and haematoxylin, (A) fish at 4 °C, (B) fish at 10 °C, (C) fish at 16 °C. All fish were fed with control diet (Diet A). The upper small box shows primary lamellar area displaying different magnitudes of cellularity, while the lower small box shows the distal end of the secondary lamellae at approximately twice the magnification (with arrows indicating the region selected within the gill section). The mucous cells are stained light blue and nuclei are stained dark blue. Scale bars 50 µm. 186
Figure 4.7 Changes in gill area parameters at different rearing temperatures (4, 10 and 16 °C). All fish were fed with control Diet A. (n=6, significance between temperature groups were indicated by * when p< 0.05). 187

Figure 4.8 Score plot of first two principal components (factors) from Experiment 1 showing clear differentiation of individuals from different temperature regimes. n = 6 per state. 192

Figure 4.9 Levels of gene expression in gills sampled from Atlantic salmon in Experiment 1 maintained at three different temperatures (4, 10 and 16 °C) and fed two different diets (control diet A and test diet B). Different colours indicate the groups of fish. Normalised expression values are compared to the control group (Diet A at 10°C). Unlabelled groups are not significantly different between states. Groups labelled with different letters are significantly different ($p < 0.05$) for selected target genes. N=6, bars represent normalised expression values ± SE). 194

Figure 4.10 The scatter plot of PC1 and PC2 generated from the gene expression data in Experiment 1. Individuals are assigned to their relevant sub group representing temperature and diet. Groups colour coded by temperature (4, 10 and 16 °C) and by diet (Control Diet A and Test Diet B).....196

Figure 4.11 Representative gill micrographs from Experiment 2, stained with Alcian blue and haematoxylin. (A) Fish at 4 °C fed with diet B, (B) Fish at 12 °C fed with diet B. The mucous cells were stained light blue with Alcian blue and nuclei were stained purple-blue with haematoxylin. The small insert at twice the magnification of the original shows the prominent cellularity in the primary lamellar area. Scale bar 50 µm 198

Figure 4.12Changes in different gill area parameters at different rearing temperatures (4 and 12 °C). The fish were fed with three different diets (control diet A, B and D). (n=6, significance between temperature groups indicated by * when p< 0.05. The graph indicates individual morphometric parameters at the different combination of temperature and diet. Means that do not share a letter are significantly different as indicated separately for diet, temperature and diet*temperature. 201

Figure 4.13 Interaction plots for mucous cell area of secondary lamellar area secondary lamellar area compared to secondary lamellar area 202

Figure 4.14 Loading plot of measured morphometric variables for gill parameters and indices analysed from Experiment 2 morphometric data. Numbers 1, 2 and 3 indicate three different clustered groups of variables: 1. Secondary lamella-associated direct gill

measurements including indices like GR; 2. Gill indices made from combining two gill parameters *e.g.*, ISR and SLPL compared to SLA; 3. All other gill parameters. 204

Figure 4.15 Plot of first and second principal components for variables relating to gill morphology, showing clear differentiation between fish maintained at different temperatures and those fed a particular diet at specific temperatures. 205

Figure 4.16 Classification of individuals belonging to different dietary groups A, B and D at two different temperatures (4°C and 12° C) by new variables/principal components. Groups are indicated as corresponding letters for dietary groups followed by temperature (A4, A12, B4, B12, D4 and D12). 206

Figure 4.17 Relative expression of immune genes in Experiment 2 in the gills of fish fed Diets A, B and D when maintained at (A) 12oC or (B) 4oC). Means that do not share a letter are significantly different as indicated at $p<0.05$, n=6. 208

Figure 4.18 Loading plot of measured variables *i.e.* measured 10 target genes. Loading plot of measured target genes shows three distinct directional clusters 210

Figure 4.19 Classification of individuals belonging to different dietary groups at different temperatures by plotting PC1 and PC2 (new variables/components). 210

Figure 4.20 Classification of individuals belonging to different dietary groups (A, B and D) by new variables (principal components) at 12^0 C and 4^0 C (Score plots, A and B). 211

Figure 4.21 Loading plot of measured variables *i.e.* measured morphometric and target immune gene data from experiment 2. 213

Figure 4.22 Classification of individuals belonging to different dietary groups based on morphometric and gene expression data at different temperatures by plotting PC1 and PC2.....213

Figure 4.23 PCA classification of individuals belonging to different dietary groups classified by new variables (principal component 1 and 2). Score plots A and B: all diets at two different temperatures (A = 12 °C and B = 4 °C). Score plots D, C & E: Grouping of individuals belonging to the same dietary group at different temperatures. Data were generated from both morphometric and gene expression values from Experiment 2. 214

Figure 5.1 Overview of experimental plan of *Aeromonas salmonicida* vaccination and challenge trial performed on Atlantic salmon. Four sets of duplicate tanks of fish were used and first four tanks (n-35/tank) were vaccinated with a commercial furunculosis vaccine (0.1 ml) eight tanks of fish were injected with 0.1 ml of PBS. Please note that 1080 fish were used for full experiment 229

Figure 5.2 After the vaccination, four fish per tank were sampled for gill, head kidney and spleen from Group 1 at 12, 24, and 59 days post vaccination (d.p.v.). 231

Figure 5.3 Layout of challenge experiment. At 59 d.p.v Group 3 (n= 20/tank)) was challenged with a virulent strain of *A. salmonicida* Hooke strain and group 4 (n=20/tank) was kept as unchallenged (but second PBS injection was given). The samples (8 fish/tank/organ; gill, head kidney and spleen) were collected from group 3 and 4, at 4, 7 and 21 d.p.c analysed for immune gene expression. The group 2 (n=15/tank) was monitored for mortality count. 233

Figure 5.4 Flow chart of different steps of data processing in GenEx Enterprise software which included a step of quality assurance, replacement of missing data to fulfil the requirement of balance ANOVA (GLM). Most suitable and recommended normalisation was achieved by using the reference gene index. 245

Figure 5.5 Cumulative mortality of Atlantic salmon (duplicate tanks) injected with 0.1 ml PBS ml or 0.1 ml commercial furunculosis vaccine following challenge with Aeromonas salmonicida. The relative percentage survival (RPS) of vaccinated fish was 80 %. 246

Figure 5.6 Intraepithelial Lymphoid Tissue (ILT) in the gills. (A) digitally scanned high resolution whole slide image of transversely sectioned Atlantic salmon gill. (B) enlarged image of lymphoid cell aggregation of ILT in the gills. (C) high magnification of highlighted area (left) in B representing closely associated blood vessels, (D) high magnification of highlighted area (right) in B of lymphoid aggregation mostly filled with a homogeneous set of lymphocytes. 247

Figure 5.7 Atlantic salmon posterior kidney from (A) control (unvaccinated unchallenged) fish (7 d.p.c.) (B) unvaccinated challenged fish at 4 d.p.c. (C) lower magnification and (D) high magnification IHC positive tissue from moribund fish scarified at 4 d.p.c. Note bacterial colonisation in interstitial paranchyma (blue arrow), sever diffuse degeneration of kidney tubules and necrosis loss of interstitial tissues (D). Short black thick arrow heads indicate melanomacrophage centres (MMC) aggregated between renal interstitial tissues. Thin brown arrows indicate that different types of crossed sectioned tubules. Scale bar A, B, C 100µm and D 25 µm 248

Figure 5.8 Atlantic salmon gills enriched with Eosinophilic Granular Cells (EGC) in vaccinated challenged fish. (A) EGC stained with anti-caspase 3 polyclonal antibody using immunohistochemistry on *A. salmonicida* infected gills (4 d.p.c.). (B) EGC located around veins (please note the lumen is labelled with * and thin walls around the lumen) and (C) high magnification of presence of EGC around arteries (afferent) (please note the lumen is labelled with * and thick walls around the lumen). Scale bar 200 µm. 249

Figure 5.9 Immunohistochemstry staining of gill of Atlantic salmon vaccinated with *A. salmonicida* stained with CD3 monoclonal antibody. Cytoplasm of CD 3 positive cells (T lymphocytes) stained intensely dark (black arrow) found (A) distal end of the primary lamellae (B) mid region of the primary lamellae however in some instances non-specific staining was also encountered in (C) chondrocytes of the primary lamellae and (D) epithelium of primary and secondary lamellae noted as light brown staining. 100µm. 251

Figure 5.10 Laser scanning confocal micrographs Atlantic salmon gill (A) low magnification (B) high magnification showing eosinophilic granular cells (EGCs) which stained green (blue arrow) with anti-caspase 3 polyclonal antibody and FITC and *A. salmonicida*-infected moribund fish (C) gills and (D) posterior kidney at 7 days post infection confirming the presence of bacteria which stained red with anti-A.salmonicida monoclonal antibody 9F7 and texas red (white arrow). The renal tubules (yellow arrow) are distorted. Scale bar indicates (A) 50 µm, (B) & (D) 20 µm. (D) 10 µm. 252

Figure 5.11 The SYBR green real time PCR results for IgM gene expression in head kidney (A), spleen (B) and gill (C) in Atlantic salmon vaccinated with Aeromonas salmonicida. The mean IgM expression of vaccinated fish (blue) (n=8) and unvaccinated (green) fish (n=8) sampled at Day 12 and 24 post vaccination were normalised to reference gene index (ELF1, cofilin, actin) +/- SE. The significance difference ($P \leq 0.05$) is marked between groups (a) and between time points for vaccinated fish (b) and for unvaccinated fish (c).....254

Figure 5.12 The SYBR green real time PCR results for IgT gene expression in head kidney (A), spleen (B) and gill (C) in Atlantic salmon vaccinated with Aeromonas salmonicida. The mean IgT expression of vaccinated fish (blue) (n=8) and unvaccinated (green) fish (n=8) sampled at Day 12 and 24 post vaccination were normalised to reference gene index (ELF1, cofilin, actin). The significance difference ($P \leq 0.05$) is marked between groups (a) and between time points for vaccinated fish (b) and for unvaccinated fish (c).....255

Figure 5.13 The SYBR green real time PCR results for IL-1β gene expression in head kidney (A), spleen (B) and gill (C) during vaccination and following challenge with *A. salmonicida*. The mean IL-1β expression of un-vaccinated/unchallenged fish (blue) (n=8), vaccinated/unchallenged (green) and vaccinated/challenged (red) fish (n=8) sampled at Day 4, 7 and 21 post challenged were normalised to reference gene index (ELF1, Cofilin, Actin). A different letter within individual time points indicates a significant difference between groups. at that time point. Significance differences between vaccinated unchallenged and vaccinated challenged fish at different time points is indicated with an * or ** respectively.....258

Figure 5.14 The SYBR green real time PCR results for IFN-γ gene expression in head kidney (A), spleen (B) and gill (C) during vaccination and following challenge with *A. salmonicida*. The mean IFN-γ expression of unvaccinated fish (blue) (n=8), vaccinated (green) and vaccinated/challenged (red) fish (n=8) sampled at Day 4, 7 and 21 post challenged were normalised to reference gene index (ELF1, Cofilin, Actin). A different letter within individual time points indicates a significant difference between groups at that time point. Significance differences between vaccinated unchallenged and vaccinated challenged fish at different time points is indicated with an * or ** respectively.....259

Figure 5.15 The SYBR green real time PCR results for IgM gene expression in head kidney (A), spleen (B) and gill (C) during vaccination and following challenge with *A. salmonicida*. The mean IgM expression of un-vaccinated/unchallenged fish (blue) (n=8), vaccinated/unchallenged (green) and vaccinated/challenged (red) fish (n=8) sampled at Day 4, 7 and 21 post challenged were normalised to reference gene index (ELF1, Cofilin, Actin). A different letter within individual time points indicates a

significant difference between groups at that time point. Significance differences between vaccinated unchallenged and vaccinated challenged fish at different time points is indicated with an * or ** respectively. 261

Figure 5.16 The SYBR green real time PCR results for IgT gene expression in head kidney (A), spleen (B) and gill (C) during vaccination and following challenge with *A. salmonicida*. The mean IgT expression of un-vaccinated/unchallenged fish (blue) (n=8), vaccinated/unchallenged (green) and vaccinated/challenged (red) fish (n=8) sampled at Day 4, 7 and 21 post challenged were normalised to reference gene index (ELF1, Cofilin, Actin). A different letter within individual time points indicates a significant difference between groups. at that time point. Significance differences between vaccinated unchallenged and vaccinated challenged fish at different time points is indicated with an * or ** respectively 263

CHAPTER 1

GENERAL INTRODUCTION

1.1 Background

1.1.1 Trends in global aquaculture expansion

Fish remain an important protein source for human consumption, contributing around 6% of protein consumed by man compared to 39 % from animal protein and 55 % other sources. It has been estimated that total human protein consumption will rise by 40 % in 2050 compared to 2008 (Anon, 2010), with significant increases in population predicted in Asia and Africa. The world population is expected to increase to 9 billion by the end of 2050, and one of the major changes faced with respect to this increased growth is the need for proper planning to ensure sufficient food is provided to feed the growing population. Aquaculture has the potential to meet these demands (Bailey, 2014).

The supply of marine-sourced protein is mainly provided through wild fisheries captures and aquaculture production. The wild catch for human consumption is in decline, while aquaculture is growing rapidly *i.e.* in 2012 the aquaculture industry contributed nearly 50 % of the fish consumed by humans (Kontali analyse, 2013). The FAO estimated that by 2030 aquaculture will be increased from 45 million tonnes to 85 million tonnes (FAO, 2014). Salmon farming contributed 4.5 % of the global seafood supplied in 2011 (Kontali analyse, 2013). The supply of aquaculture production has shifted more towards salmon farming with it becoming the dominant aquaculture species, mainly in Europe and globally increasing to 2.1 million tonnes in 2012.

Atlantic salmon farming is a commercially important aquaculture industry to the world economy, delivering a relatively inexpensive, high quality food, especially in terms of protein and highly unsaturated omega-3 fatty acid content, with obvious benefits for human health (FAO, 2013). However, whilst the salmon farming industry is thriving, it does suffer from significant disease issues. The occurrence of disease problems such as infectious salmon anaemia (ISA), pancreas disease (PD), sea lice infections or amoebic gill disease (AGD) severely threatens the salmon farming industry in the world (Evans 2006; Krkošek *et al.,* 2011). The causes of disease outbreaks are complex, resulting in part from the impact of husbandry practices *e.g.* high stocking densities, and environmental conditions such as changing sea temperature. Recent research by the major salmon farming countries of Norway, Scotland, Chile, Canada and Australia has helped to underpin the sustainability of the salmon farming industry by providing new strategies for disease prophylaxis and treatment including vaccines, genetically selected disease resistant fish and new improved functional diets (Kiron, 2012).

1.1.2 **Salmonid diseases and their transmission**

The incidence of disease on farms mainly depends on how the pathogen is transmitted to the fish and the environment associated with intensive fish culture. Understanding the dynamics of an infectious disease involves examination of the portal of entry of the pathogen, discovering how it is disseminated within the body of the fish, observation of clinical signs and signs of recovery, elucidating the mechanisms of transmission of the pathogen from fish to fish, and identifying the existence of potential asymptomatic carriers after recovery. The portal of entry of a pathogen into the fish normally involves mucosal barriers such as the skin, gill and gut (Rombout *et al.,* 2014). The mechanism of entry depends on the extent of intact epithelial membranes (mucosal membranes), which can be disturbed by environmental factors such as low dissolved oxygen content,

high temperatures and compromised mucosal immune responses. The effect of environmental factors (*e.g.* long term hypoxic condition leading to chronic stress) on intestinal health was recently examined in relation to current intensive farming practices by Niklasson *et al.*, (2011), who found the integrity of the gut mucosal barrier to be affected. Although some of the mechanisms governing the barrier function of the Atlantic salmon intestine can be extrapolated to Atlantic salmon gills, the barrier function of the gills is known to vary according to influences from the surrounding environment. Mitchell and Rodger (2011) have reviewed the major infectious diseases of gills in marine salmonid fishes, including amoebic gill disease (AGD) (Rodger & McArdle 1996; Adams & Nowak 2001), proliferative gill inflammation (PGI) (Kvellestad, Dannevig & Falk 2003; Nowak & LaPatra 2006) and tenacibaculosis (Ferguson *et al.*, 2010). There are several other bacterial, viral and parasitic diseases that have or are suspected to have the gill as their portal of entry (*e.g. Renibacterium salmoninarum*, the causative agent of bacterial kidney disease (BKD), Atlantic salmon paramyxovirus (ASPV) (Kvellestad *et al.*, 2005; Nylund *et al.*, 2008), salmon gill poxvirus (SGPV) (Nylund *et al.*, 2008), pancreas disease (PD) and infectious salmon anaemia (ISA).

In 2001, Munday, Zilberg & Findlay were the first to suspect that *Neoparamoeba pemaquidensis* was responsible for causing AGD, but the agent involved was later confirmed to be *Paramoeba (=Neoparamoeba) perurans* (Young *et al.*, 2007). In 2006, Nowak and LaPatra reported epitheliocystis outbreaks in fish, mainly in salmonids. Later in 2007, Rodger published on the emerging gill disorders present in farmed Atlantic salmon in the marine environment.

1.2 **The fish gill**

Fish represent over 50 % of all the vertebrate species present on earth, and they inhabit almost every aquatic environment present, which together occupy around 75 % of the earth's surface. There are more than 35,000 species of fish distributed globally in oceans, lakes and rivers (Evans *et al.*, 2005, Eddy and Handy, 2012). Thus, fish are clearly important to a variety of ecosystems, as well as being a major protein source for humans. However, the aquatic environment can change rapidly due to the presence of infectious agents, shifting climates, and opportunistic predators (Miller *et al.*, 2014). It is therefore important to understand how fish can rapidly respond to environmental changes (Eddy and Handy, 2012).

Aquatic animals have evolved very efficient respiratory mechanisms to meet their metabolic needs. The fish gills are a respiratory organ highly specialised in absorbing oxygen from the water, although some amphibians also exchange gas through their gills (Evans *et al.*, 2005). There are two types of gills: external and internal gills. External gills are present in some larval stages and amphibians as protuberances of the outer skin with increased surface area. Some invertebrates like the starfish, aquatic worms, mussels, crustacean, and snails have simple forms of gills. Internal gills are characterized by an enlarged respiratory membrane within the body of the animal. They are mainly present in some molluscs, arthropods, and fish (Helfman *et al*., 2009).

The fish gill is a multifunctional organ, acting as the primary site for respiration, osmoregulation, acid/base balance, nitrogen excretion and metabolism of circulating hormones (Evans *et al*., 2005). Gills serve to facilitate oxygen and carbon dioxide diffusion to and from the capillaries, which form a superficial network of blood vessels containing red blood cells making the gills appear red in colour (Evans *et al.*, 2005).

Blood flow within the capillaries is in counter-current direction, meaning that the blood flows in an opposite direction to the movement of water past the gill lamellae. This provides a concentration gradient for gas exchange between the water and the blood. Another significant role of the gill is the elimination of CO_2 produced during respiration, which is expelled at the same time as oxygen absorption (Roberts and Rodger, 2012). In air-breathing animals, this occurs in two different stages with inspiration of O_2 and expiration of CO_2.

Due to the high level of vascularization present in the gills, they are highly vulnerable to mechanical injury (Maina, 2002). One advantage of the aquatic environment is that the respiratory membrane is kept moist and fully functional. Gills are capable of taking up oxygen from the air if the respiratory epithelium is covered with a thin layer of water, however, if the respiratory membrane is exposed to air, the moisture will evaporate very quickly and the gills dry out, resulting in the lamellae sticking together and decreasing the efficiency of the gas exchange, and in turn leading to CO_2 toxicity (Perry and Tufts, 1998). Compared to the lungs of air breathing animals breathing air containing 21% O_2, the fish gill is surrounded by water containing only 5–10 % oxygen (Bone and Moore, 2008). The oxygen concentration of water is, however, dependent on temperature and salinity. Therefore, respiration is most problematic in warmer regions, especially with an increased salt concentration (Maina 2002). The counter current flow system described above facilitates a constant exchange of water at the respiratory surface to maximise exchange of gas, a process referred to as ventilation.

1.2.1 **Anatomy of fish gills**

1.2.1.1 The gill arch

The gill is derived from a series of paired pouches in the lateral wall of the mouth cavity of the embryonic fish, which forms a pathway for the water to flow from the mouth to the exterior, where the tissue later becomes the gill arch and supports the gill filaments (Olson 2011). The anatomical structure of fish gills comprises a row of several arches, with each arch projecting two filaments with a series of lamellae. In bony fish the gill arch is a relatively simple bow-shaped structure, the ends of which are attached to the dorsal and ventral surfaces of the buccal cavity, with the curved portion projecting posterior-laterally. Teleost' gills consist of eight gill arches arranged as four pairs on either side of the buccal cavity, which is associated with an extra vestigial gill hemiarch called the pseudo branch, covered by a thick epithelium known to be functionally insignificant, but suspected to be involved in oxygen transportation in to the eye (Ferguson 2006, Helfman *et al*., 2009, Roberts 2012).

The gill arch holding the gill filaments is supported by three flexible bones *i.e.* starting from a ventral aspect, hypobranchial, ceratobranchial, and epibranchial, which are functionally involved in jaw movement during feeding and respiration (Olson, 2011). The projections from the arch known as gill rakers are located on the opposite side of the filaments where they serve as filters. These arches provide a matrix for gill blood vessels including afferent and efferent branchial arteries and branchial veins (Evans *et al.*, 2005).

Each of the arches supports paired rows of long blade-like filaments where gaseous exchange occur (Ferguson, 2006). There are two types of muscles, the adductor and the abductor muscles, connected to these arches as mechanical supports to connect the

cartilaginous rod in the filament to the arch (Evans *et al.*, 2005). The contraction of the muscles generates a motion allowing the buccal cavity movements during respiration. Recent findings have confirmed that the IS structurally support the newly discovered intrabrachial lymphoid tissue (ILT) in the gills (Haugarvoll *et al.*, 2008). In some fish species such as tuna, elasmobranchs, and a few others, the intrabrachial septum extends all the way into the body wall.

1.2.1.2 Gill Filament

The functional anatomical unit of the gill, the gill filament (Figure 1.1), is consisted of different types of cells and tissues. The long, slender and flat gill filament supports numerous respiratory secondary lamellae. The gill filaments offers minimal resistance to the flow of water over it and counter current mechanism of blood and water flow across the gill filament ensures gaseous exchange (Olson, 2011).

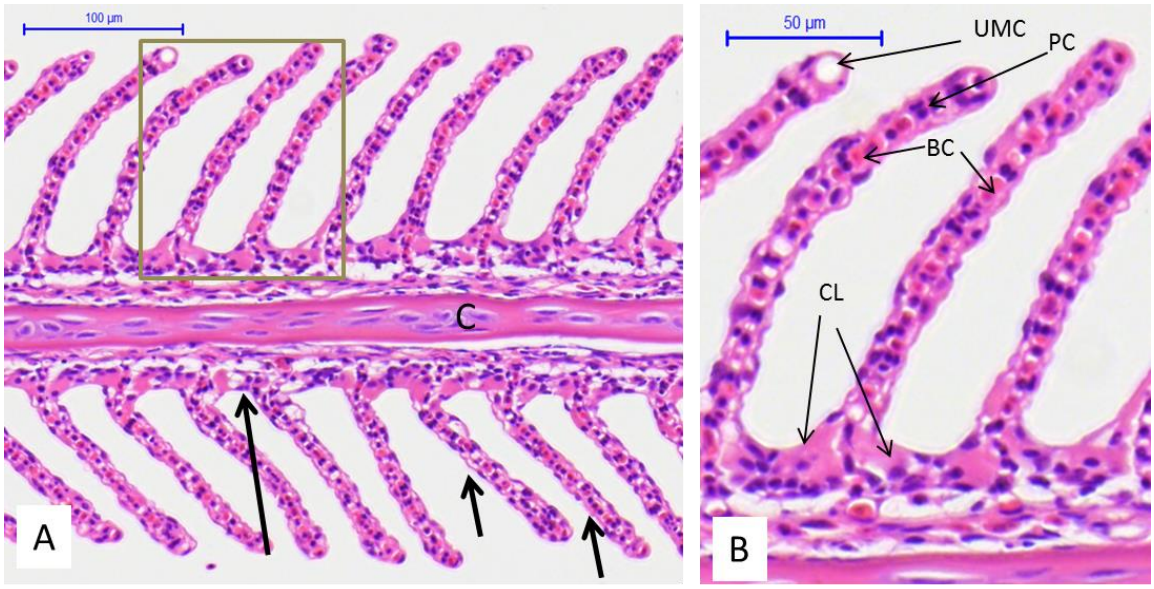

Figure1.1 Histomicrograph showing Haemotoxylin and Eosin (H&E) stained Atlantic salmon gills (A) low power showing gill filaments (primary lamellae) (Long arrow) with cartilaginous rod (C) running in the centre and secondary lamellae (short arrow) extending as projections from the primary lamellae. (B) a higher magnification of the primary lamellar area blocked in gray in the plate (A) area showing respiratory epithelia of the gill. Note outer marginal channel (UMC), blood channels (BC), chloride cells (CL) and pillar cells (PC).

1.2.1.3 Respiratory Lamellae

The respiratory lamellae or secondary lamella of the gill filaments are plate-like structures projected at right angles from both sides of the filaments. They spread the blood out into the periphery of the tissue creating a minimal diffusion distance between the blood and the water (Ferguson, 2006). Each lamella consists of two rows of epithelial cells held apart by a series of centrally located cells called pillar cells (Figure 1.2). Pillar cells provide structural support to hold two squamous epithelial cell layers together. Pillar cells are unique in shape (spool-shaped cells) with a large central nucleus and broad cytoplasmic flanges that radiate out from the top and bottom of the cell. The adjacent pillar cells are joined together through pillar cell flange forming vascular lacunae called pillar channels that are enriched with RBCs (Figure 1.2). The lamellae dramatically increase the surface area of the respiratory epithelium, resulting in a small diffusion distance between the blood water barrier (Evans *et al.,* 2005; Ferguson, 2006).

1.2.1.4 Epithelial Cells

A number of different cell populations are characterised on the respiratory lamellae, including pavement cells (PVC), chloride cells (CL), mucous cells (MC), neuroepithelial cells (NEC), and undifferentiated cells located on germinal epithelium (Evans *et al.,* 2005). Pavement cells, the most abundant epithelial cells found on the epithelium form a relatively impermeable barrier between the water and the tissue. These relatively thin, often hexagonal cells have a surface enriched with micro-ridges or microvilli believed to help trap a protective coat of mucus, as well as increasing the surface area for gaseous exchange (Mallatt, 1985) (Figure 1.2B).

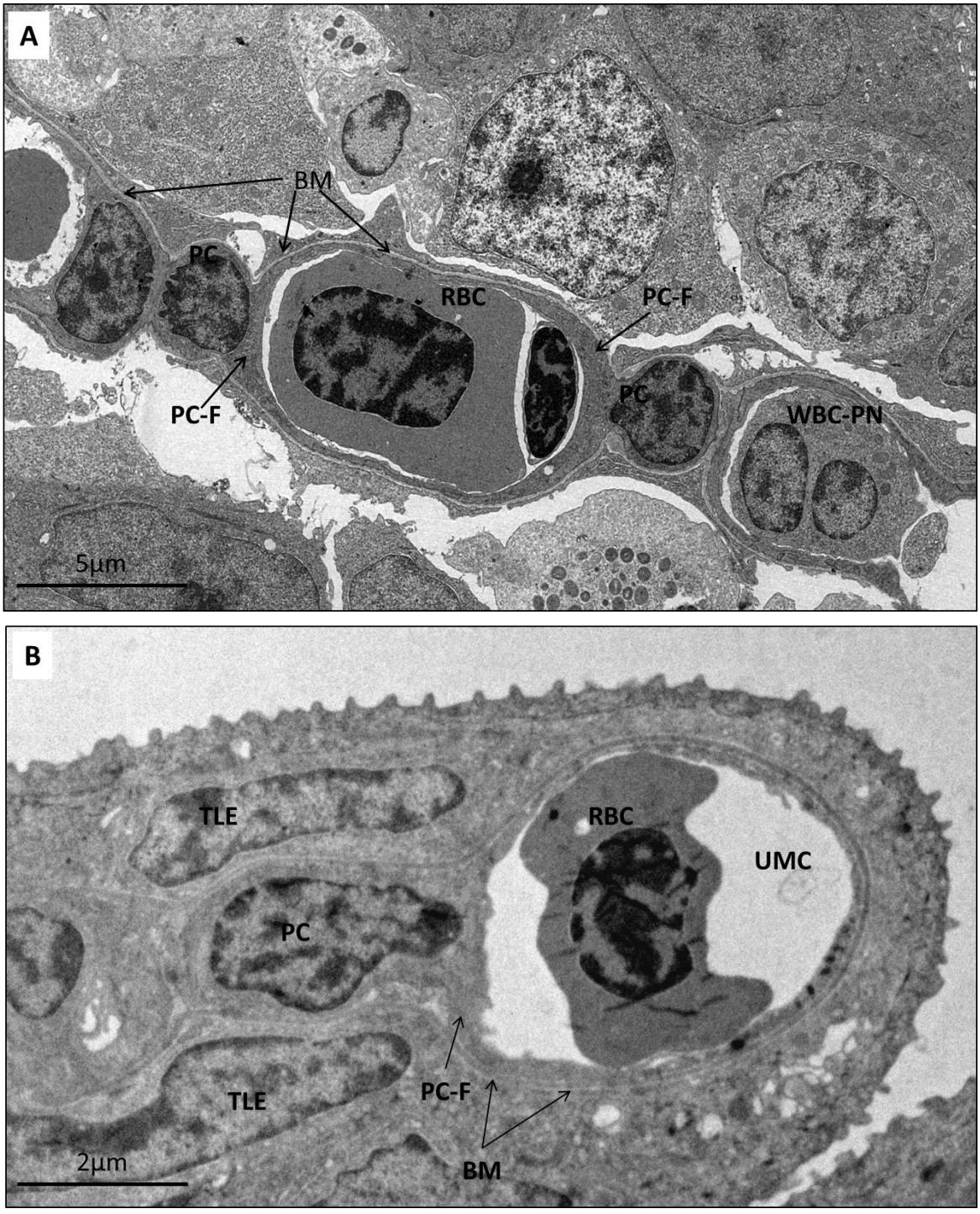

Figure1.2 (A) Transmission electron micrograph across central marginal canal at mid region of the secondary lamellar. The pillar cells (PC) and cytoplasmic flanges of pillar (PC-F) cells are supported by basement membrane (BM). The two spool shaped PC cells joined together by flanges forming pillar canals. Note red blood cells (RBC), polymorphonuclear white blood cells (WBC-PMN) in the pillar canals in the micrograph. **(B)** Transmission electron micrograph across outer marginal channel (UMC) at distal end of secondary lamellar. Spool shaped pillar cells (PC) are supported by two true lamellar epithelial cells (TLE). The cytoplasmic flanges of pillar cells (PC-F) line the outer lamellar blood space filled with red blood cells in the micrograph. The basement membrane surrounds the pillar cells and endothelium of the UMC. Micrographs courtesy of Dr Tharangani Herath (unpublished).

Mucous cells (also called goblet cells) are often scattered throughout the gill including gill arch, the filament and more predominantly on the edge of the filament facing the water current and basal regions of the lamella (Evans *et al.,* 2005). These polarised cells are filled with large membrane bound mucus droplets (Figure 1.3 A&B), basal nucleus (Figure 1.3 A), and tightly packed rough endoplasmic reticulum and Golgi apparatus (Figure 1.3 B). These cells contained acidic glycoproteins, neutral glycoproteins, or a combination of those two (Fletcher *et al.,* 1976). It is also known that the mucus has antibacterial properties against pathogens (Rakers *et al.,* 2013).

Changes in mucous cell number, their size and secretion of mucus from these cells has been described during parasitic infections such as AGD (Roberts and Powell, 2003: Peyghan and Powell, 2006). Furthermore, mucous cell numbers change, as observed using histochemistry, during exposure to high salinity seawater (*i.e.* increase) (Olson, 1996), ion-poor water, mechanical abrasion, high environmental water temperature (*i.e.* increase) and a variety of waterborne contaminants including metal ions, therapeutic drugs, organophosphates and aquatic pathogens. In addition to the commonly observed mucous cells, another cell type that has been reported in the gills is granular cells, which are embedded slightly deeper in the epithelium, secreting mucus intermittently (Hidalgo *et al.,* 1987). Their secretory products contained glycoproteins with abundant sialic acid residues and they appear similar to mucous cells.

Ion-transporting cells known as ionocytes, chloride cells (CCs) or mitochondria rich cells; (MRC) are most commonly located on the body or the lamellar portion of the filament, especially along the afferent margin of the filament and interlamellar filament epithelium located between adjacent lamellae (Figure 1.4 A-C) (Evans *et al.,* 2005).

Ionocytes, present on the lamellar epithelium, are most commonly located near the filament and are rarely observed on the more lateral areas of the lamella (Figure 1.4 B).

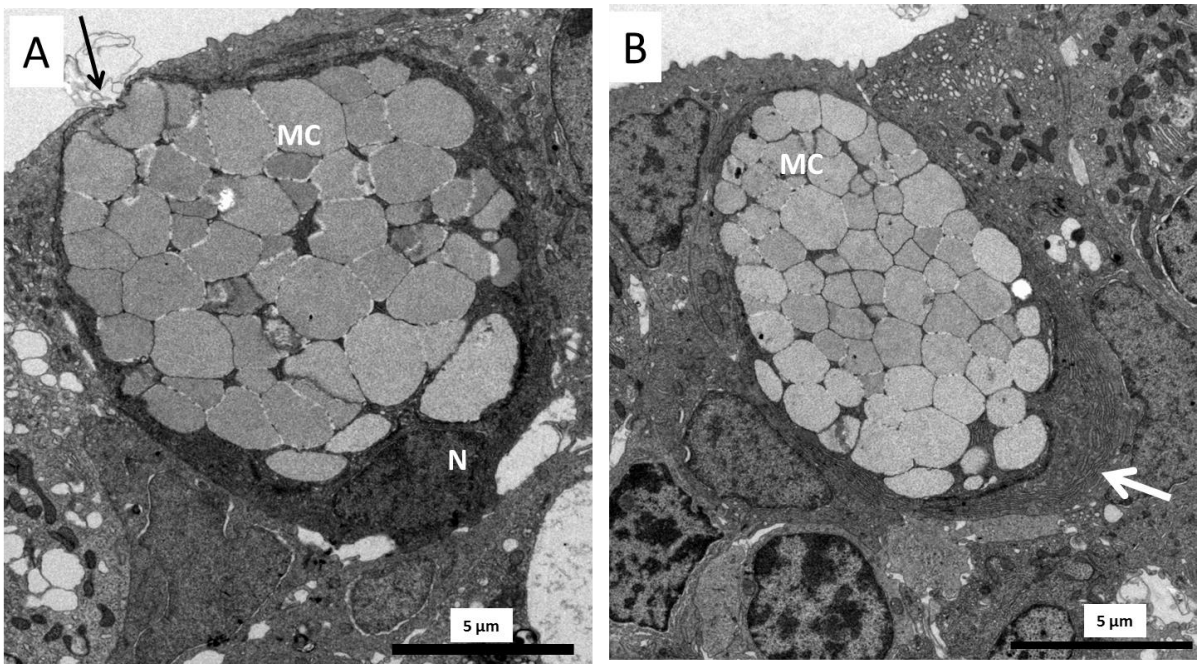

Figure1.3Transverse electron micrograph of mucous cell enriched with membrane bound vesicles (MC), (A) with a nucleus (N) pushed a towards to the base of the cell and an apically located secretory pit (black arrow) and (B) endoplasmic reticulum tightly stacked at the base of the cells. Micrographs are courtesy of Dr Tharangani Herath (unpublished)

The chloride cells are broadly classified into two different categories, depending on the water fish in (i) surface cells with an apical membrane exposed to the environment, (ii) recessed cells, with an apical membrane, opening into a pit that is partially covered by overlaying pavement cells. Freshwater fish have more surface cells (Figure 1.5) than saltwater fish, which have recessed chloride cells. A number of chloride cell subtypes have been described *i.e.* light and dark cells, microvillous and smooth surface cells, A cells and B cells, α and β cells, accessory cells etc. (Pisam *et al.,* 1987, 1988). Both classes of ionocytes have two striking features important for ion regulation: (i) abundant mitochondria to generate large amount of energy, which are needed for ion regulation

and (ii) an extensively invaginated basolateral membrane. The apical region of the cell is filled with a tubular reticulum (Evans *et al.*, 2005, Olson 1996).

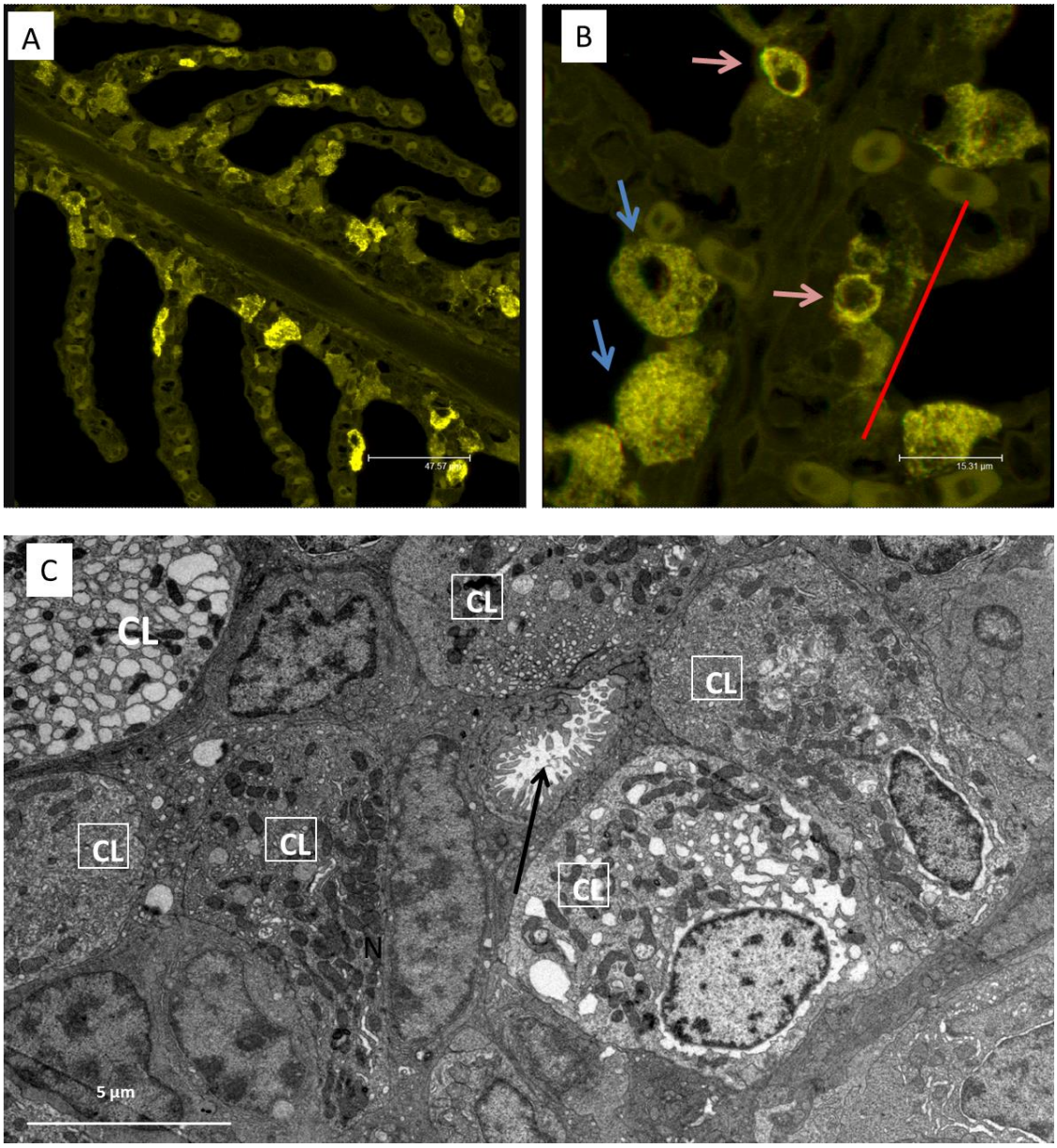

Figure1.4 Confocal laser scanner micrograph of an Atlantic salmon gill stained with fluorescence isothiocyanate (FITC) conjugated anti mouse secondary antibodies bind to anti-Na/K ATPase primary antibodies (A) lower magnification (B) higher magnification showing darkly stained chloride cells. Note size differences in chloride cells in micrograph B (pink arrows; smaller cells and blue arrows; larger cells. (C) A transmission electron micrograph of a gill at base of the primary lamellae (areas is marked red in micrograph B). The tissue is rich in mitochondria rich chloride cells (CL). The apical membrane of the lamellar epithelium with micro projection (arrow) is surrounded by CL cells. The size of the scale bar of micrograph A and B, are approximately 48 and 16 µm. TEM micrographs courtesy of Dr Tharangani Herath (unpublished)

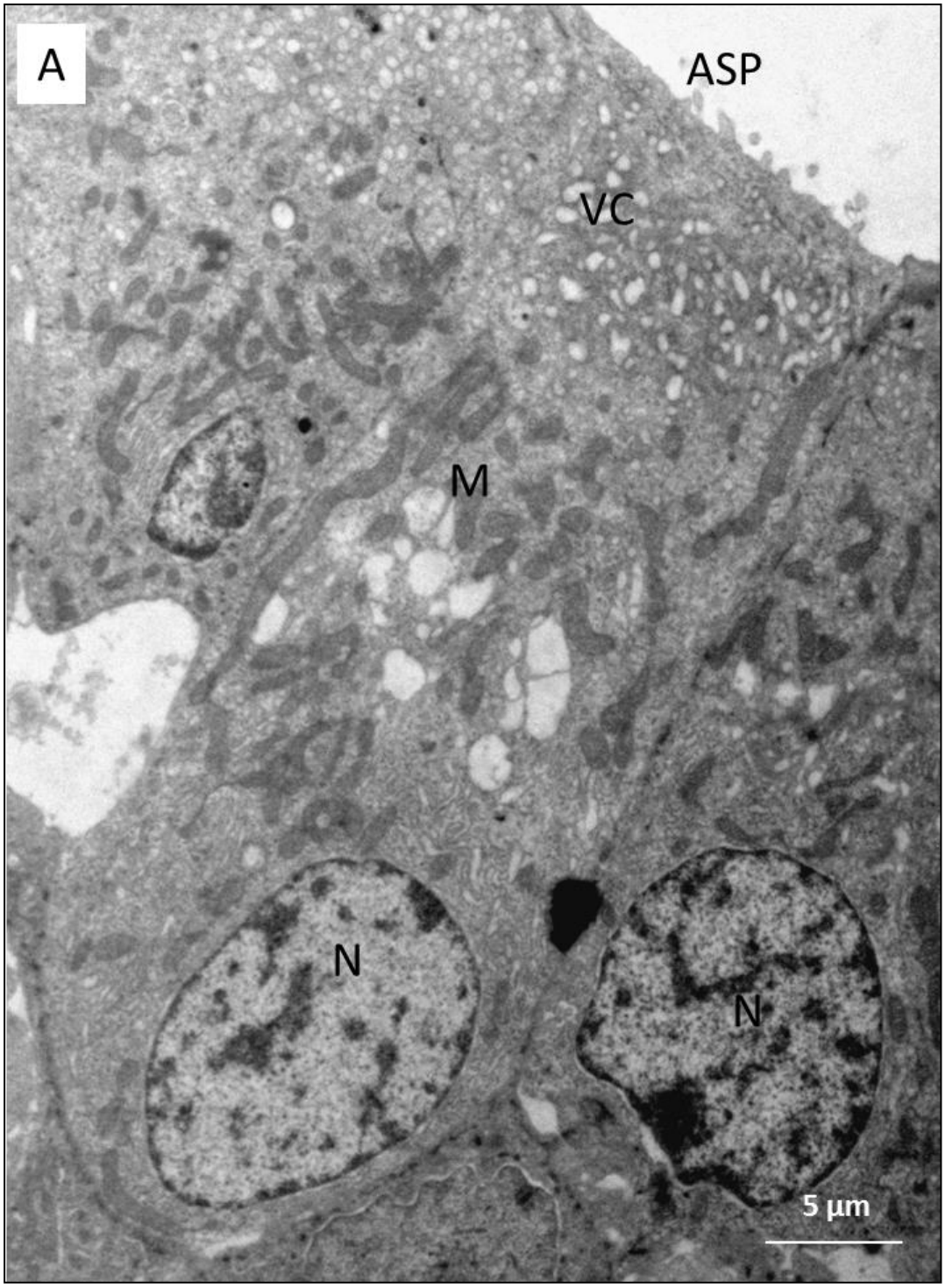

Figure1.5 Electron micrograph of a fresh water reared Atlantic salmon gill epithelium showing a chloride cell enriched with mitochondria (M) and sub-apical vesicular system (VC). Cell membrane of the gill epithelium forms as extensions of the apical membrane forming microprojection (ASP). Note nucleus (N). Micrographs courtesy of Dr Tharangani Herath (unpublished)

Neuroepithelial cells, which serve as chemoreceptor cells and monitor the oxygen tension in both water and blood (Dunel-Erb-Erb *et al.*, 1982, 1994; Bailly *et al.*, 1992), are thinly scattered along the efferent margin beneath the epithelium. In addition, interstitial and undifferentiated cells are found throughout the body of the filament. Undifferentiated cells embedded in the area of the margin of the lamella differentiate into lamellar pillar cells, and the lamellae essentially grow outward from the filament as the fish grows (Ostrander, 2000). Rodlet cells, also called X cells, are pale staining cells, and are thinly dispersed on the gills arch, the body of the filament, on the interlamellar filamental epithelium, and the basal areas of the lamellae. Rodlet cells appear to be secretory, however reveal an enigma. However, recently rodlet cells were defined as a type of eosinophilic granulocytes at its immature stage and in response to stimuli, rodlet cell may act in a similar way to mast cells acting against parasites (Reite and Evensen 2006).

1.2.1.5 Gill Vessels

The gill is richly supplied with blood. The afferent brachial artery (ABA) delivers blood to, and distributes it along, the gill arch. The branches of AB, filamental arteries (AFAs) distribute blood to the respiratory lamellae (L) via afferent lamellar arterioles. The oxygenated blood drain out from the gill lamellae via efferent lamellar arterioles (ELAs), and then into efferent filamental arteries (EFAs) and lastly into efferent branchial artery (EBA) before leaving the gill (Olson *et al.*, 1991). Nutrient supply to the arch tissues, including gill rakers, comes from numerous small arterioles that arise from either the EBA or the EFAs near their junction with the EBA. These arterioles

anastomose repeatedly with each other to form the nutrient arteries. Nutrient vessels ultimately drain into the branchial veins (Evans *et al.,* 2005).

1.3 **Gill pathologies**

1.4.1 The causes of gill pathologies

The causative agents for gill pathologies appear to be multifactorial and the gill damage that results can cause severe respiratory distress leading to osmoregulatory imbalance and eventually even death (Baxter *et al.,* 2011, Rodger *et al.,* 2011). The possible causes for commonly known gill pathologies in salmon can broadly be classified into 5 main groups, including 1) zooplankton, 2) phytoplankton, 3) parasitic 4) bacterial and 5) viral (Rodger 2007). Environmental factors capable of causing mechanical damage should also be added to this list *e.g.* the presence of high levels of suspended solids in the water column. Zooplankton damage is recognised particularly for contact with some species of gelatinous zooplankton such as jellyfish, while some species of phytoplankton can cause damage when present in high numbers during harmful algal blooms (HABs), which are reported to be encouraged by eutrophication, intensified aquaculture activities and environmental pollution. These have received a great attention in marine farmed salmonids in particular, and have been considered as non-infectious aetiologies for gill diseases (Rodger *et al.,* 2011). The main mechanisms that cause mortalities of fish during harmful algal blooms are considered to be due to 1) physical damage 2) asphyxiation due to oxygen depletion 3) gas bubble trauma due to oxygen super-saturation caused by algal photosynthesis and 4) toxins (Rodger *et al.,* 2011; Black *et al* 1991). In addition some zooplankton can also act as vectors of bacterial diseases (Ferguson *et al.,* 2010; Delannoy *et al.,* 2011) in which physical

damage caused by zooplankton (*e.g. Pelagia noctiluca*) could initiate introduction of bacterial pathogens (*e.g. Tenacibaculum maritimum*), which appeared to be also acting as a carrier for them (Delannoy *et al.,* 2011). Apart from recently described plankton-induced pathologies, environmental factors, nutritional deficiencies genetic and congenital disorders could also cause gill pathologies of a non-infectious nature (Rodger 2007; Rodger *et al.,* 2011).

The main infectious agents that are associated with gill pathologies include parasites, bacteria and viruses (Mitchell and Rodger, 2011) (Table 1.1). Protozoan parasites including Trichodina and costia (*Ichthyobodo* sp.) can cause significant pathologies in the gill (Bermingham and Mulcahy, 2006). Amoebic gill disease (AGD) caused by *Paramoeba perurans* (=*Neoparamoeba perurans*) has become one of the greatest challenges that salmon farmers have faced recently, particularly in Tasmania and Western Europe (Young *et al.,* 2007). *Desmozoon lepeophtherii* (family Desmozoa) was also recently found to be associated with proliferative gill inflammation (PGI) in Atlantic salmon (Steinum *et al.,* 2010). Bacteria directly associated with gill pathology include *Flavobacterium branchiophilum*, *Tenacibaculum maritimum* and epitheliocystis, which have been associated with *Piscichlamydia salmonis*, and *Clavochlamydia salmonicola*. *Aeromonas salmonicida*, the causative agent of furunculosis, which induces severe septicaemia, can also be found in the gill lamellae during acute infection, although no pathological changes are manifested in the gills (Ferguson, 2006, Bruno *et al.,* 2013). Viruses that cause gill pathologies are rarer, although two viruses, Atlantic salmon paramyxovirus (ASPV) and salmonid pox virus (SGPV) have been reported to be associated with a low number of cases of PGI in salmon farmed in Norway recently, their role in the pathogenesis of the disease has yet to be confirmed (Kvellestad *et al.,* 2005; Falk *et al.,* 2008; Nylund *et al.,* 2008).

Furthermore, although it exerts no apparent pathological damage, infectious salmon anaemia virus (ISAV) was also observed in the gill epithelium (Workenhe *et al.*, 2007).

1.3.1 **Assessment of the gill health of fish**

Regular assessment of fish health, including examination of the gills, is fundamental for the prevention of disease outbreaks. Due to the multifunctional nature of the gill, changes in gill function and morphology have been widely studied using various techniques including histopathology, molecular biology and serological methods. Modern infectious disease investigations are based on the rapid detection of the causative agent in diseased tissues in parallel with the analysis of the potential risk factors for the disease outbreak. The same principles are employed in the investigation of gill-related diseases. Some of the multi-pathogen and environmental interactions recently identified provide new insights into the multifactorial nature of gill diseases (Anon, 2013). The fish gill is a rapidly changing organ, due to the plasticity it exhibits, and histomorphometric changes are vital to assess predict the health status of the gill at a given time. A state-of-the-art histopathological-based tool enabling the monitoring of health and performance of fish in farm conditions is a priority for salmon farming industry (*e.g.* GIA; gill image analysis).

Table 1.1 The infectious agents involved in causing gill diseases or syndromes in salmonids.

Disease category	**Pathogen Aetiology**	**Disease or disease syndrome**	**Salmonids species affected**
Parasite	*Desmozoon lepeophtherii*	Proliferative gill inflammation (PGI)	AS, RT
Parasite	Salmincola salmonea	Mild gill inflammatioin	AS
Bacterial	'*Candidatus Piscichlamydia salmonis'*	Epitheliocystis	AS, AC
Bacterial	'*Candidatus Clavochlamydia salmonicola'*	Epitheliocystis	AS, BT
Bacterial	*Tenacibaculum maritimum*	Tenacibaculosis	AS, RT, CS
Parasite	*Neoparamoeba perurans*	Amoebic gill disease	AS, RT, CO, CS
Parasite	*Ichthyobodo* spp.	Marine costiasis	AS, RT
Parasite	*Loma salmonae*	Microsporidean gill disease	CS, CO, RT[a]
Parasite	*Gyrodactyloides bychowskii*	Obstructive gill damage	AS
Parasite	*Trichodina* sp	Trichodinosis	All salmonids
Viral	Salmon gill poxvirus (SGPV)	Proliferative gill inflammation (PGI)	AS
Viral	Atlantic salmon paramyxovirus (ASPV)	Proliferative gill inflammation (PGI)	AS

AS, Atlantic salmon; RT, rainbow trout; CS, chinook salmon; BT, brown trout; CO, coho salmon; AC, Arctic char; PGI, proliferative gill inflammation.
[a]Fresh water only (Mitchell and Rodger, 2011).

1.4 **Tissue morphometric analysis of gills**

Tissue morphometric analysis, which generally involves the measurement or quantification of particular tissues, cell populations or subcellular components *e.g.* cell number, nuclear size and shape, mitochondria or secretory vesicles, has been widely used in studying gill associated changes in the past (Hughes *et al*., 1979 Measurements of interest have been achieved by 'point counting', for example counting chloride cell number (Maina, 1991) or estimating surface area changes (*e.g.* volume and surface areas of secondary lamellae). Detailed information about morphological changes in the dimensions of the water / blood barrier, which is relevant to the gill's function in gas exchange, has been widely measured to assist assessment of the gill health of fish (Hughes & Wright, 1970; Morgan & Toveil, 1973, Maina and West 2005).

Pinkney *et al.*, (1989) published a morphometric study on the effects of tributyltin (TBT), an active ingredient used in antifouling paints on vessels and for coating nets for marine fish farming, on the gill of morphology of the mummichog, *Fundulus heteroclitus*. After 6 weeks of sub-lethal exposure to the compound, the morphometric analysis of gill tissue measured by point counting revealed hypertrophy of the lamellar epithelium with significant decrease in relative diffusion capacity and this compound was later banned in the U.K. on small boats and fish farming equipment (Abel, 1987).

In general, morphometric assessments are performed using light microscopy based on histopathological examination and subsequent counting of points of interest, which is a rather laborious and time consuming exercise. However, advances in virtual microscopy and digital image analysis have ushered in a new era, allowing rapid and accurate quantification of morphometric data (Bandyopadhyay, 2011; Bhattacharjee *et al.*, 2014).

1.4.1 Semi quantitative scoring systems for gill pathologies in salmonids

Histopathology is one of the most frequently used tools to diagnose infectious or degenerative diseases in fish (Ferguson, 2006; Roberts and Rodger, 2012). In general, histopathology assessments are qualitative, with diagnosis based on morphological alterations of the tissue examined, however, in some instances diagnoses by observers can also involve subjective measurements of the degree of the severity of the lesion by ranking the lesion of interest using an arbitrary scale, for instance with low, medium or high grade considering the clinical relevance of the lesion (Mitchell *et al.*, 2012).

New and rapid assessment tools for monitoring gill pathology are in demand, however, there are no defined systems established for monitoring gill health status. More recently, however, reports of novel semi-quantitative gill scoring systems, involving pathogen quantification and environmental impact have been published by Mitchell *et al.*, (2012) and a further gill scoring system has been recently reported (Gjessing 2014, unpublished data). Previously, a grading system for pathological changes was established in order to assess the negative effect of hydrogen peroxide as a delousing agent for Atlantic salmon by Thomassen (1993) and also to monitor aquatic ecosystem pollution, however these scoring strategies have not considered gill pathologies to any great degree. The 2nd meeting for the gill health initiative held in Oslo in 2014 highlighted that lack of standardisation of a gill scoring or monitoring system, that could universally be used for monitoring gill health in farmed salmon (Gjessing, 2014). With the rapid increase in gill related issues in farmed salmon, a standardised user friendly evaluation system is urgently required in this thesis a novel image analysis system using digital pathology and quantitative statistics has been successfully attempted.

1.5 Fish immune system

1.5.1 Components of the fish immune system

Fish comprise a heterogeneous group of species, which include the agnathans (hagfishes and lampreys), chondrichthyans (sharks and rays) and teleosteans (bony fish) (Zapata *et al.,* 1996). From an evolutionary perspective fish are the first vertebrate group to have both cellular and humoral immune responses (Jimeno, 2008). Compared to mammals they show some similarities and some differences regarding immune function (Nelson, 1994; Zapata *et al.,* 1996; Press & Evensen, 1999; Tort *et al.,* 2003; Cabezas, 2006; Randeli *et al.,* 2008). The basic cellular components of the fish defence system are similar to those described in mammals, with fish having phagocytic cells similar to macrophages, neutrophils, and natural killer (NK) cells, as well as specific T and B lymphocytes involved in adaptive immunity (Fischer *et al.,* 2013). The main feature of the teleost immune system is a well-developed innate immune system consisting of both cellular and humoral factors such as complement (classical and alternative pathways), lysozyme, natural haemolysin, transferrin and C-reactive protein (CRP). The cytokines are proteins or protein derivatives known to play a major role in eliciting inflammatory reactions (pro-inflammatory cytokines like IL1β, TNFα, IFNγ) and subsequently linking with the adaptive immune response (IL-12, IL-4), via another set of cytokines known as anti-inflammatory in nature and which help to regulate the immune system (*e.g.* IL-10). To date, almost all major cytokine families have been identified in different fish teleost species. In addition to pro-inflammatory and anti-inflammatory cytokines, several other cytokines have been identified in different fish species (Aoki *et al.,* 2008). In addition to these cytokines, a family of chemoattractant cytokines regulating immune cell migration are also recognised and are known as chemokines (Alejo and Tafalla, 2011).

The key tissues of the fish immune system are different from those of mammals, in spite of the previously mentioned functional similarities. Instead of bone marrow and lymph nodes as primary lymphoid organs, as possessed by mammals, the head kidney of fish serves as a major lymphoid organ in addition to the thymus and spleen (Zapata *et al.,* 1996; Press & Evensen, 1999; Alvarez-Pellitero, 2008; Jimeno, 2008). According to recent findings, fish mucosal immune tissues consist of less organised lymphoid aggregations known as mucosal associated lymphoid tissue (MALT) (Rombout *et al.,* 2011), which are specialised in mounting a localised mucosal immune response (Zhang *et al.,* 2010). Gut-associated lymphoid tissues (GALT) predominantly serve as major mucosal lymphoid organs, and have been shown to function in eliciting immune responses in fish (Rombout *et al.,* 1993; Joosten *et al.,* 1996; Picchietti *et al.,* 1997; Salinas *et al.,* 2011). In addition, gill-associated intrabranchial lymphoid tissue (ILT) (Haugarvoll *et al.,* 2008, Koppang *et al.,* 2010) and skin associated lymphoid tissues (SALT) have recently been discovered as further important lymphoid tissues involved in mucosal immunity (Xu *et al.,* 2013). In comparison to mammals, fish are not equipped with a lymphatic system connecting the blood with lymph and tissue fluids. Some teleosts, such as plaice, *Pleuronectes platessa,* do possess a lymphatic system that is differentiated from the blood vascular system, although demonstrating the existence of such a system in other species has been challenging (Hølvold, 2007).

1.5.2 **Immune tissue and cells**

1.5.2.1 Head kidney

The head kidney, or anterior kidney (pronephros), has a well-innervated structure, displaying a neuroendocrine function homologous to that of mammalian adrenal glands, releasing corticosteroids and other hormones. The head kidney, therefore, serves as a

valuable organ with key regulatory functions and the central organ for immune-endocrine interactions (Press & Evensen, 1999; Tort *et al.,* 2003). The anatomical and structural organisation of head kidney is also closely related to its function as a primary lymphoid organ, which involves haematopoiesis and lymphogenesis (Press & Evensen, 1999). During early development, the kidney is involved in the production of immune cells and the early immune response.

The anterior part of kidney is mainly haematopoietic (Doñate Jimeno, 2008; Meseguer *et al.,* 1995; Tort *et al.,* 2003), and unlike higher vertebrates represents the principal immune organ responsible for pathogen clearance (Dannevig *et al.,* 1994; Galindo-Villegas & Hosokowa, 2004), antigen processing through antigen-presenting cells, production of immunoglobulins and is important for the induction of immune memory. Melanomacrophage centres (MMC) have an active involvement in this response (Tort *et al.,* 2003; Agius and Roberts, 2003). Furthermore MMCs have been evaluated in terms of marker tissues for fish health monitoring (Wolke *et al.,* 1985)

1.5.2.2 Thymus

The thymus is an important organ in juvenile fish, located beneath the pharyngeal epithelium in the dorsolateral region of the gill and initially appears as a paired bilateral organ, but as the fish grows it starts to reduce in size. The size of the thymus also varies with seasonal changes and hormonal cycles (Meseguer *et al.,* 1995; Zapata *et al.,* 1996; Press & Evensen, 1999; Galindo-Villegas & Hosokowa, 2004). The thymus appears to have no executive function; however, it is responsible for producing pools of virgin lymphocytes in the circulation and other lymphoid organs. Research has shown that the thymus is responsible for the development of T-lymphocytes, as in other jawed vertebrates (Alvarez-Pellitero, 2008; Galindo-Villegas & Hosokowa, 2004). However,

much of the evidence supporting this is indirect, obtained either by immunizing with T-dependent antigens (Ellsaesser *et al.,* 1988), using monoclonal antibodies as cell surface markers (Passer *et al.,* 1996) or functional assays *in vitro*. It has been shown in trout that lymphocytes migrate through the thymus before reaching the spleen and kidney (Tatner & Findlay, 1991), suggesting that the teleost thymus has the same function as in higher vertebrates, and is the main source of immuno-competent T cells (Zapata *et al.,* 1996).

1.5.2.3 Spleen

The spleen is a major secondary lymphoid organ in fish, which contains fewer haematopoietic and lymphoid cells than the kidney, being composed mainly of blood held in sinuses, and it is believed to be involved in immune reactivity and blood cell formation (Galindo-Villegas & Hosokowa, 2004; Manning, 1994; Zapata *et al.,* 1996). The fish spleen is not distinctly organized into red and white pulp as in mammalian spleen. It contains different sized lymphocytes, numerous developing and mature plasma cells and macrophages in a supporting network of fibroblastic reticular cells. Lymphocytes and macrophages are present in the spleen of fish, contained in specialized capillary walls, termed ellipsoids. In addition, ellipsoids appear to have a specialised function for plasma filtration, particularly for immune complexes. In spleen, most macrophages are arranged in MMCs, which can retain antigens as immune complexes for long periods of time. Although the lymphoid tissue is poorly developed in teleosts, in the spleen an increased amount of lymphoid tissue appears after antigenic stimulation, which indirectly suggests the presence of T-like and B-like cells (Espenes *et al.,* 1995; Galindo-Villegas & Hosokowa, 2004; Zapata *et al.,* 1996). The spleen of teleosts has also been implicated in the clearance of blood-borne antigens and immune complexes in splenic ellipsoids and also has a role in antigen presentation and in the

initiation of the adaptive immune response (Alvarez-Pellitero, 2008; Chaves-Pozo *et al.,* 2005; Whyte, 2007).

1.5.2.4 Liver

In mammals, the liver is responsible for production of components of the complement cascade and acute phase proteins (such as C reactive proteins CRP), which are important in the natural resistance to infectious agents in animals, and the liver has been previously suggested to play a similar role in fish (Fletcher, 1981). However, some consider that research to support this claim is lacking (Galindo-Villegas & Hosokowa, 2004; Shoemaker *et al.,* 2001). Recent research has explored the liver transcriptome of the innate immune response in Atlantic salmon subjected to starvation and then acute bacterial challenge to examine their altered immune gene signature. In those fish that were starved, decreased immune gene transcription were highlighted and genes responsible for plasma protein showed reduced expression, and upon infection there was a further decrease in expression of genes encoding plasma proteins but a large increase in acute phase response proteins. The latter was greater in magnitude than in the fish that had been fed prior to infection (Martin *et al.*, 2010). A cDNA microarray study was performed to examine the acute phase response pathway, an important systemic reaction that occurs within hours of an inflammatory signal caused by physical bodily injury or microbial infection, such as in olive flounder, *Paralichthys olivaceus,* liver after infection with *Edwardsiella tarda* (Moon *et al.,* 2014). The results showed that a set of genes involved in the acute phase response (APR) was strongly up-regulated in the liver especially toll-like receptor 5, a soluble form, which has not been detected in mammals, was up-regulated as much as 250-fold indicating that liver pays key role in innate immunity.

1.5.2.5 Fish immune cells

All multicellular organisms possess a selection of cells and molecules that interact in order to ensure protection from pathogens (Abbas *et al*., 2006). This wider collection of highly specialised cells makes up most of the physiologically important immune system, governing a defence against invading microbes (Doñate Jimeno, 2008). Fish immune cells are derived from both the lymphoid and the myeloid systems and share functional and morphological similarities with mammalian lymphocytes, granulocytes and monocytes (Zelikoff, 1998). The key cell types involved in non-specific cellular defence responses of teleost fish include the phagocytic cells monocytes/macrophages, non-specific cytotoxic cells (or NK cells), thrombocytes, and granulocytes (mainly neutrophils) (Buonocore & Scapigliati, 2010; Hamerman *et al.,* 2005; Hølvold, 2007; Magnadóttir, 2006; Doñate Jimeno, 2008; Shoemaker *et al.,* 2001).

The immune response is initiated upon injury or pathogen invasion through phagocytic and inflammatory processes (Corbel, 1975), assisted by non-specific immune cells such as monocytes/macrophages, neutrophils and NCCs. Monocytes and macrophages are probably the single most important cell type involved in the immune response of fish. Macrophages also have a role in antigen-presentation, thus acting as a link between the innate and acquired immune responses (Balfry & Higgs, 2001; Galindo-Villegas & Hosokowa, 2004; Doñate Jimeno, 2008; Shoemaker *et al.,* 2001; Vallejo *et al.,* 1992). Recently, phagocytic activity has been reported for trout B lymphocytes (Li *et al.,* 2006; Sunyer 2012). Fish also have eosinophilic granular cells (EGCs) associated with the mucosal regions of the gut and gills, where these cells become functionally active and capable of responding to pathogens (Secombes, 1996). The different functions of EGCs (also known as mast cells), recently reviewed by Sfacteria *et al.,* (2014), indicate that they play a central role in the immune system of teleost fish. It has recently been

observed that basophilic granular cells (acidophilic/eosinophilic granule cells or mast cells) of fish from the Perciformes order, the largest and most evolutionarily advanced order of teleosts, produce histamine (Garcia-Ayala & Chaves-Pozo, 2009; Doñate Jimeno, 2008; Magnadóttir, 2006; Mulero *et al.*, 2007; Whyte, 2007). Non-specific cytotoxic cells (NCC) are present in both blood and lymphoid tissues including mucosal sites responding to virus-infected host cells and protozoan parasites (Secombes, 1996). Thrombocytes appeared to be the nucleated version of the mammalian platelet involved in blood clotting and also have some phagocytic properties (Balfry & Higgs, 2001; Secombes, 1996). There is a growing interest in knowing whether red blood cells function as a component of the fish immune system. Though their primary function remains respiratory gas exchange, other functions including interactions with the immune system have been attributed to these cells (Morera and Mackenzie, 2011). In fish the principal finding for RBC immune-related function includes the fact that they appear to regulate specific pattern recognition receptor (PRR) mRNAs capable of specific pathogen associated molecular pattern (PAMP) detection that is central to the innate immune response (Morera *et al.*, 2011).

1.5.3 **Immunity in fishes**

1.5.3.1 Innate immunity of fish

Similar to most other multi-cellular organisms, in fish the innate immune system plays an integral part in the defence against pathogens acting as ‘the first line of defence’ and as a ‘signal of danger’ to the presence of foreign material, including pathogens (Magnadóttir, 2006). In teleosts, innate immunity is considered to be highly developed with an underdeveloped, slowly responding adaptive immune system, compared to mammals. It also helps to activate the adaptive immune system during an infection to

elicit specific and long-lasting immune memory (Whyte, 2007). Similarly to mammals, the fish innate immune system comprises physical, humoral and cellular factors (Magnadóttir, 2006). The mucous layers of skin, gill and gut act as the main physical barriers that protect fish from pathogen entry and are rich in a variety of biologically active substances including lysozyme, lectins, proteolytic enzymes, flavoenzymes, immunoglobulins M and T (IgM, IgT), C-reactive protein, apolipoprotein A–I and antimicrobial peptides (Alexander and Ingram, 1992; Kaattari and Piganell, 1996; Ellis, 2001; Villarroel *et al.,* 2007 and Kitani *et al.,* 2008). The recently discovered mucosal specific immunoglobulin IgT also plays a pivotal role in the innate immunity of fish (Sunyer *et al.,* 2009). The main humoral factors involved in the innate immunity of fish incude various lytic factors (lysozymes, cathepsin, chitinase), complements (classical, alternative or lectin dependent), agglutinins, precipitins, natural antibodies, cytokines including interleukin (IL)-1, IL-6, tumour necrosis factor- α (TNF-α), growth inhibitors, serum protease inhibitors (α2 macroglobulin, α1 anti-trypsin), chemokines, acute phase proteins and antibacterial peptides.

The fish innate immune system recognises foreign stimuli (*i.e.* pathogens) as non-self by binding to Toll-like receptors (TLR) (Kawai and Akira, 2005). TLRs can differentiate and respond accordingly to the molecules that are associated with different types of microbes (*e.g.* polysaccharides, lipopolysaccharides, peptidoglycans, bacterial DNA and double stranded viral RNA) (Eaton, 1990; Lockhart *et al.,* 2004). In addition the derivatives of tissue damage can also trigger the innate immune reaction (*e.g.* host DNA, RNA, heat shock proteins, chaperones). In addition to physical and biological factors, human interventions such as handling, diet and food additives such as immunostimulants and probiotics, drugs, vaccines, and importantly pathogens can

easily modulate the innate immune system in fish (Bowden, 2008; Tort, 2011; Kiron, 2012).

1.5.3.2 Adaptive immunity of fish

Modern bony fishes, including salmonids, represent one of the first groups to possess the molecules of the classical adaptive immune system (Cooper & Alder, 2006; Boehm & Bleul, 2007). The adaptive immune system in fish appeared to be less sophisticated than mammals presumably indicating its lesser importance to fish with respect to their biological functions, rather than inferiority compared to mammals (Kaattari, 1994; Watts *et al.*, 2001). The adaptive immune system in fish is comparable to that of higher vertebrates, with the presence of all fundamental features including immunoglobulins (Ig), T-cells and T-cell receptors, the major histocompatibility complex (MHC) and recognition activator genes 1 and 2 (RAG1 and RAG2) (Watts *et al.*, 2001). In comparison to mammals, the adaptive immune system of fish lacks immune memory and has a low antibody repertoire (Magnadóttir, 2006), although it is still able to elicit a long lasting immune response during infection, especially with respect to vaccines.

Information on specific cell-mediated immunity is not widely established for teleosts. Both T and B-lymphocytes are present in fish including salmonids, although the types and function of different cell repertoires are still to be confirmed (Fischer *et al.*, 2006). The signatures for the presence of T-cells were reported in fish a few decades ago and the cloning of T-cell receptors, MHC-I, MHC-II molecules and T-cell surface markers CD3, CD4 and CD8 represented a breakthrough in studies on T-cells, allowing examination of the question of how adaptive immune mechanisms operate in fish (Secombes & Zou, 2005; Alvarez-Pellitero, 2008; Randelli *et al.*, 2008). Two types of T-cell are present: T-helper cells (Th), which are enriched with CD4 on their surface

and cytotoxic T-cells (Tc), which express CD8 receptors. The antigen bound to the MHC class I and II are recognised by CD8 and CD4 present on the T cells respectively. The MHC molecules also act as a bridge connecting the innate and adaptive immune response. However, recent finding suggested that Atlantic cod lack MHC II, which has been substituted with an alternative mechanism of adaptive immune response (Wigmore 2011; Star and Jentoft, 2012; Malmstrøm *et al.,* 2013). Until the recent discovery of IgD, IgT and IgZ, IgM was regarded as the only antibody thought to be present in fish (Randelli *et al.,* 2008; Sunyer *et al.,* 2009). The molecular arrangement of teleost IgM is different from mammals as the light and heavy chains are held together by a non-covalent bond instead of di-sulphide bonds seen in mammalian IgM. The monomers of fish IgM are present as single monomers or in tetrameric form, while IgM in mammals is a pentamer (Watts *et al.,* 2001). The non-covalent binding of IgM tetramers found in fish is believed to enhance the ability of the molecule to bind to different types of epitopes, adjusting their orientation (Solem & Stenvik, 2006). The antibody molecules of fish possess relatively low intrinsic affinity and the antigen binding sites are limited in heterogenicity compared to mammals (Kaattari, 1994; Solem & Stenvik, 2006). The teleost IgM molecule is capable of opsonising pathogens to enhance phagocytosis by macrophages (Secombes & Fletcher, 1992; Solem & Stenvik, 2006). They are also able to activate the classical complement pathway, and act as effective agglutinators for foreign molecules. Due to the temperature dependent nature of the specific immune system, the antibody response of fish can take weeks to be established (Watts *et al.,* 2001).

1.5.3.3 Mucosal immunity fish

Organised lymphoid tissues like lymph nodes and Peyer's patches do not exist in fish. Nevertheless, in 2008, Haugarvoll reported the first identification of lymphoid

aggregates in the gills of the Atlantic salmon. Two years later, Koppang *et al.,* (2010) showed that the lymphoid aggregates are intraepithelial having a distinct organisation mainly consisting of T-cells embedded in epithelial cells similar to the organisation pattern of the thymus. However, there are distinct differences between the gill lymphoid tissue and the thymus both in gene expression patterns and in the anatomical construction. Further research by Koppang *et al.,* (2010) showed that fish undergoing a viral infection had a shrunken ILT compared to control fish.

The skin, gills and gut are identified as the mucosal associated lymphoid tissue (MALT) of immune system of fish (Doñate Jimeno, 2008; Press & Evensen, 1999; Tort *et al.*, 2003). Skin is the primary barrier providing both physical and chemical protection, mainly through an association with mucus that comprises glycoproteins, proteoglycans and proteins. The mucus constitutes an interface between the fish and the environment (Dalmo *et al.*, 1997) and it is well established that antimicrobial factors found in the mucus inhibit the colonization of potentially harmful microorganisms (Alexander and Ingram, 1992; Ruangsri *et al.*, 2010).

The teleost gill has been identified as an important organ involved in fish immune function, through the MALT, mainly consisting of T-lymphocytes (Haugarvoll *et al.*, 2008; Koppang *et al.*, 2010). The gills also contain other major immune cell types including macrophages, neutrophils, lymphocytes and mast cells/eosinophilic granulocytes (EGCs), normally scattered around different stimulated and non-stimulated tissues (Pratap and Wendelaar Bonga, 1993; Reite and Evensen, 2006; Powell and Kristensen, 2014). Haugarvoll *et al.,* (2008) was first to describe the intrerbranchial lymphoid aggregation of T lymphocytes, similar to those described in mammalian mucosa, which is found at the interbranchial septum at the base of gill

filaments extending up to 2/3 of the filament, suggesting their involvement in immune surveillance. More recently, Austbo *et al.,* (2014) performed a transcriptional study to evaluate the immune gene in the gills and separated ILT by laser micro dissection of Atlantic salmon challenged with infectious salmon anaemia virus (ISAV). The results suggested a strong innate immune response in both conventionally processed gills and laser micro dissected ILT as well as mid kidney, despite the fact that no virus could be detected in any of those tissues. Furthermore immune gene expression of IgT (a marker for mucosal immunity) showed a small delayed increase in ILT indicating the ILT's role as a secondary lymphoid organ, with clonal expansion of IgT expressing B-cells. Further studies carried out by Aas *et al.,* (2014) concluded that ILT can be regarded as a strategically located T-cell reservoir and possibly an evolutionary forerunner of mammalian MALTs. Due to its location at the interface with the external environment and the diversity of the lymphocyte population, measured transcriptional changes may reflect the shift in the T-cell population to optimize local gill defence mechanisms. This was initially proven to occur in the gut (Zhang *et al.,* 2010) and skin (Xu *et al.,* 2013) of rainbow trout. Furthermore, compared to other tissues (*e.g.* the mid kidney of the same fish), gills displayed the earliest replication of the virus, further supporting this tissue as the main entry route for the ISAV. Due to this, most of the earliest immune signatures were seen in teleost gill rather than head kidney or spleen.

Similar to the gill, the gastrointestinal tract (GIT) of teleosts serves as an organ with multiple functions including nutrient absorption, digestion and acting as a mucosal immune barrier preventing entry of pathogens (Gomez *et al.,* 2013). The organisation of the GALT of teleosts is less complex and more diffused than that of the mammalian counterparts known as Peyer's patches, which are organized as an aggregated lymphoid tissue (Rombout *et al.,* 2011). The teleost gut has various types of immune cells

including lymphocytes, plasma cells, eosinophilic (mast cell-like) granulocytes (EGCs), and macrophages, which can elicit various types of local responses against various stimuli (Press and Evensen, 1999). In healthy fish, intestinal microbiota and the mucosal immune response need to be balanced, with the microbes being in direct contact with the gut mucosa and the GALT distinguishing between them to initiate either tolerance or an immune response (Montalto *et al.*, 2009).

Although teleosts lack organised MALT, there is evidence that skin, gills and intestine contain populations of leucocytes (Doñate Jimeno, 2008; Press & Evensen, 1999) and intraepithelial plasma cells (Dorin *et al.*, 1994; Moore *et al.*, 1998; Tort *et al.*, 2003). Several additional defences have been discovered in fish mucous membranes (Bols *et al.*, 2001), such as the production of nitric oxide by the gill as well as antibacterial peptides and proteins by skin (Campos-Perez *et al.*, 2000; Galindo-Villegas & Hosokowa, 2004; Ebran *et al.*, 1999; Tort *et al.*, 2003). Not only is the mucous membrane of these tissues an important physical barrier in fish, but they also contain several components with a role in the host-pathogen interaction, and release antimicrobial agents or proteins. Among the epidermal secretions, complement, lysozyme, lectins (or pentraxins), alkaline phosphatase and esterase, trypsin (or trypsin-like), natural antibodies or immunoglobulins are prominent. Their levels and activities depend on the fish species, and haemolysins are among the substances present with biostatic or biocidal activities (Alexander & Ingram, 1992; Arason, 1996; Ellis, 2011; Aranishi & Mano, 2000; Shoemaker *et al.*, 2001; Balfry & Higgs, 2001; Jones, 2001; Fast *et al.*, 2002; Tort *et al.*, 2003; Galindo-Villegas & Hosokowa, 2004; Magnadóttir, 2006; Palaksha *et al.*, 2008; Alvarez-Pellitero, 2008).

Mucous or goblet cells secrete mucus, which has at least three different types of defensive roles: (1) mucus interrupts the establishment of microbes by being continually sloughed off; (2) if establishment is accomplished, mucus acts as a physical barrier; (3) The mucus on skin, and presumably the other surfaces, contains a variety of humoral factors with antimicrobial properties (Galindo-Villegas & Hosokowa, 2004; Tort *et al.,* 2003).

1.5.3.4 Teleost IgT as a marker of mucosal immunity in fish

Teleost immunoglobulin T (IgT) is a specialized component of mucosal immunity (Zhang *et al.,* 2010). Although IgT is present in serum as monomers, in the gut mucus it forms mainly multimers, similar in mass to those of IgM. However, IgT multimers are associated in a noncovalent manner. An additional lineage of teleost B cells that uniquely express surface IgT has been identified in rainbow trout and has been found to represent the main B cell subset in the gut (Zhang *et al.,* 2010). Mucosal IgT and IgM in trout associate with a polymeric immunoglobulin receptor (pIgR) for their transport into the gut lumen (Zhang *et al.,* 2010; Yoshimizu *et al*., 2009). Consistent with the prevalent roles of IgT in gut immunity it has been revealed that most bacteria in the gut lumen of rainbow trout are coated with IgT. The IgT responses to gut parasites are measurable only in the gut, whereas IgM responses were confirmed to serum (Zhang *et al.,* 2010).

1.6 Nutrition and fish health

Fish health is partially dependent on what the fish are fed and therefore provision of appropriate feed and feeding regimes is pivotal to fish health and immune status. In the initial stages of aquaculture feed studies the nutritional requirements of the fish were

assessed independently from their immune responses, but with the advancement of knowledge on fish nutrition and fish immunology, more recent research efforts are attempting to integrate biochemistry, physiology, microbiology and pathology in nutritional studies (Pohlenz and Delbert, 2014).

The major commercial players in the international aquaculture feed industry (Skretting, Biomar Ltd, Marine Harvest, Ewos) have emphasised the importance of manufacturing sustainable diets for the aquaculture industry. There is a wider acceptance that the quality of feeds should not only ensure superior fish growth, but also promote optimal fish health (Sealey *et al*., Gatlin, 2001). The role of different dietary nutrients or feed additives on the immune function of fish has been investigated since the 1980s. The main nutrients that were investigated from the outset were vitamins C, E and saturated fatty acids. In addition, immunostimulants, and pre and probiotics have more recently attracted scientific attention in terms of their ability to protect fish from stress or disease. It is surprising that energy-macronutrient intake, an aspect of great importance in animal nutrition, has not been addressed in fish. It may partly be due to the fact that commercial aquaculture feeds generally contain a surplus of essential nutrients. For a number of years, the fish nutrition field focused mainly on establishing the minimum nutrient requirements for normal growth of different fish species (NRC, 2011). Although macronutrient deficiencies are not prominent, the high energy of the current aqua feeds and ingredients may inadvertently cause micronutrient imbalances that could compromise the functionality of the immune system. Nowadays nutritional deficiencies are seldom reported from farms. However, undetected subclinical deficiencies may possibly have a link to incidence of diseases that often occur during production cycles. Functional feeds, which are defined as specially formulated feeds with special nutrients, essential or non-essential, fed either singly or in combination, which can influence

immune function and fish health (Kiron, 2012). Similarly, micronutrients are also considered as additives when they are supplemented in feeds at levels higher than the animal's normal requirements (Kiron, 2012).

Bricknell and Dalmo (2005) defined an immunostimulant as "a naturally occurring compound that modulates the immune system by increasing the host's resistance", however, the basic functional mechanisms that alter immune response of these functional feeds have been not widely explored. Initially it was thought that immunostimulants were involved in stimulating mononuclear phagocyte systems alone, however it was later identified that there was an effect on the pattern recognition receptors (PRR) of different leucocytes, mainly in macrophages (Kiron, 2012). Functional feeds have been developed to address specific issues such those involving infectious diseases *e.g.* salmon pancreas disease (PD), heart and skeletal muscle inflammation (HSMI), cardiac myopathy syndrome (CMS) and also to boost specific components of immune systems including mucosal immunity, although understanding of mechanisms of action for functional feeds are frequently lacking (Martinez-Rubio *et al.,* 2012, Martinez-Rubio *et al.,* 2014).

1.6.1 Functional feeds as a measure to induce disease resistance in cultured salmonids

The term disease resistance relates to the susceptibility of fish to disease. There are two main factors that need to be considered (1) genetically or inherent resistance, (2) acquired resistance through vaccination, antibiotics, functional feeds etc (Houston *et al.,* 2012; Kiron *et al.,* 2012). Currently, vaccination is used as one of the most favoured disease control measures used in animal husbandry, helping to replace the need for chemical treatments (Sommerset *et al.,* 2005; Brudeseth *et al.,* 2013; Tafalla *et al.,* 2013). It also serves to slow down the development of drug resistance towards

antibiotics currently being used against fish, terrestrial farm animal species and human pathogens (Alderman & Hasting, 1998; Aoki, 1992; Horsberg, 2003). The major vaccines available for bacterial diseases in salmonids include those targeting vibriosis, enteric red mouth disease (ERM) and furunculosis Hastein and Gudding, 2005). In addition, with the recent advances in vaccinology, several commercial vaccines against viral diseases in salmonids, including those against salmon pancreas disease and infectious pancreatic necrosis virus have also been deployed (Biering *et al.,* 2005).

In salmonids, several recent studies have highlighted the acquisition of resistances to infectious diseases *e.g.* viral diseases, through provision of special diets (functional feeds) (Oliva-Teles, 2012) that modify host responses by reducing inflammation (Martinez-Rubio *et al.*, 2012; 2014) and immune enhancement by supplementing immunostimulants (Dalmo and Bøgwald, 2008). Various internal and external factors *e.g.* temperature fluctuations; stress due to high rearing densities, have suppressive effects on innate immune parameters that can be overcome by adding several food supplements and immunostimulants (Magnadottir, 2006, 2010).

Most immune-nutritional studies in fish have been based on alteration of single nutrients, employing only selected humoral and cellular immune markers and disease challenge models rather than focusing on the underlying different mechanisms of response at the tissue or cellular level. A range of feed additives, including vitamins, carotenoids, probiotics, prebiotics, symbiotic and herbal remedies, have been tested (Kiron, 2012), with a reduction in stress, increased innate immune activity and improved disease resistance noted (Austin & Brunt, 2009; Hoffmann, 2009; Magnadóttir, 2010; Nayak, 2010).

Application of clinical nutrition strategies to improve stock health would benefit farmed organisms in many ways including more rapid growth, resistance to infections, enhance ability to cope with stress more efficiently. Functional feed have been considered as an alternative measure for controlling viral diseases (Martinez Rubio *et al.,* 2013 a, b; 2014) and therefore health management through nutrient supplementation is a strategy which would improve the sustainability of the aquaculture industry.

1.7 **Image analysis**

1.5.1 Image analysis for health assessment

Light microscopy (LM) is a vital tool for the interpretation of tissue changes by trained histopathologists. This approach currently involves two definitive methods (a) confirmation of the presence or absence of disease and (b) assessing the extent of the disease, or quantifying the progression of the disease. Both methods are subject to sampling bias and also operator variation (Ramsey *et al*., 2011). The recently development of computer-assisted diagnosis (CAD), using high-throughput digital scanners and virtual microscopy have revolutionised histopathology (Ghaznavi *et al.*, 2013; Bhattacharjee *et al.,* 2014). Conventional histopathological diagnostic methods, already established using thin tissue sections on glass slides, can now be applied using the scanning and high resolution digitisation of whole-slide imaging (WSI). The WSI coupled with CAD analysis, has led to the development of tools for detection, diagnosis, and prediction of prognosis and provides a key complement to the opinion of the pathologist (Gurcan *et al.,* 2009). The digitised images can be shared between experts in the field based at different locations. The images can be easily archived and subjected to computerised quantitative image analysis (Gurcan *et al.,* 2009). The computer aided digital image analysis allows the extraction of more objective and

precise quantitative diagnostic targets, helping to improve histopathological data obtained from histological sections. The computer assisted whole slide digital imaging has become a common application especially in human disease diagnosis such as early diagnosis of cancer by marker assisted cytological investigations (Camparo *et al.,* 2012). Rojo *et al.,* (2006) has identified 31 commercially available digital slide systems are now available in histopathology investigations through CAD system.

Quantitative morphology at the microscopic level has become a valuable tool in studying morphological differences between fish parasites and subtle tissue changes occurring during early stages of disease progression (Hanzelova *et al.,* 2005). Computer aided image analysis is based on a framework that establishes image hierarchy, image segmentation, feature extraction, construction and representation. The morphometric data can be obtained by various means including stereological analysis of tissue sections on digitally scanned WSI (Daunoravicius *et al.,* 2014). Briefly stereology is a technique based on geometric principles that allows the derivation of three-dimensional structures from two-dimensional sections of these structures. By stereological methods, three different aspects; the volume (V), surface (S) and number (N) of structural features in tissues and cells can be determined quantitatively (Reid, 1980).

As with many of the advanced techniques emerging from biomedical science, computer-assisted quantitative digital image analysis has been successfully modified and applied to various other cross-disciplinary areas including commercial aquaculture. For example, computerised image analysis has been successfully employed to morphometric discrimination of parasites in fish including *Gyrodactylus salaris* Malmberg (Monogenea) (Shinn *et al.,* 2001) and *Benedenia* and *Zeuxapta* in Australian aquaculture (Whittington *et al.,* 2011). Furthermore, digital image analysis was also successfully employed to evaluate spinal and skull deformities quantitatively in

vaccinated and unvaccinated farmed Atlantic salmon (Berg *et al.,* 2012), the estimation of lipid quantities present in processed salmon fillet (Borderias *et al.,* 1999) and also the effects of dietary phosphorus on bone growth and mineralisation of vertebrae in haddock (*Melanogrammus aeglefinus* L) (Roy *et al.,* 2002). Most recently digital image analysis has been successfully used for histomorphological assessment of gut morphology in Atlantic salmon, proving to be very powerful tool in classifying soya bean enteritis from normal tissue and allowing quantification of subtle changes in diseased or affected tissues (Silva, 2014). This advanced technique remains to be utilised to its full potential in aquaculture, especially in disease diagnosis and health related research such as emerging gill diseases in salmonid aquaculture.

In the recent past, with the increase in the incidence of gill pathologies in commercial salmonid aquaculture, gills have received greater attention in terms of characterising aetiology and mitigating possible control measures (Rodger *et al.,* 2010). In addition to the gills ability to act as a first line barrier, recent research has also demonstrated gill associated immune functions (Haugarvoll *et al.,* 2008; Austbo *et al.,* 2010). However, our understanding of immune-modulation in the gill is limited and our knowledge of how to detect and monitor enhanced disease resistance in response to vaccines, functional feeds and pathogens is similarly incomplete. The work presented in this thesis sought to advance the understanding of the salmonid gill, its response to various stimuli and the evaluation of those responses through the development of a robust monitoring tool, employing capture processing and analysis of digital images of gill histology through Gill Image Analysis Tool (GIA tool). The described work also sought to explore the use of such a tool for quantifying morphological and pathophysiological changes and also immune modulation and disease resistance in the gill.

1.8 **Aims of study**

The main aim of this study was to develop a robust method for quantifying morphological changes in Atlantic salmon gills in response to a variety of nutritional, chemical and pathogen-derived stimuli. This was addressed through the individual objectives presented in following chapters:

1. A development of an advanced gill image analysis tool (GIA tool) to measure histomorphometric changes in the gills of Atlantic salmon. This was used to explore pathophysiological changes in gills of fish fed with two different functional diets and compared to a conventional salmon diet **(Chapter 2).**
2. Application of the GIA tool, developed in Chapter 2, to evaluate and validate morphometric changes in the gills of Atlantic salmon treated with hydrogen peroxide **(Chapter 3).**
3. Use of the GIA tool to study the effect of different temperature regimes on the morphology and protein expression of gills of Atlantic salmon fed with different functional feeds, and assessment of the role of this tool as part of a potential strategy for monitoring the health status of the fish **(Chapter 4).**
4. Evaluation of the immune response of the gills of Atlantic salmon vaccinated with a commercial furunculosis vaccine and challenge with *Aeromonas salmonicida* subsp. *salmonicida* as a model for studying gill-associated changes (immune response) reflected in systemic immune response **(Chapter 5).**

CHAPTER 2

DEVELOPMENT OF AN IMAGE ANALYSIS TOOL FOR EVALUATION OF MORPHOMETRIC INDICES OF ATLANTIC SALMON GILLS

2.1 Introduction

In recent years gill diseases and disorders have emerged as a key challenge to health and welfare in Atlantic salmon farming across the globe (Rodger *et al.,* 2011). Currently, the salmon farming industry in Northern Europe faces severe challenges from a complex of gill diseases including proliferative gill inflammation (PGI) (Kvellestad *et al.*, 2005), epitheliocystis (Nowak and Lapatra, 2006) and AGD (Rodger and McArdle, 1996; Brown and Zarza, 2012), the latter of which has become endemic in Ireland and has recently been reported in Scotland and Norway. These complex disorders in farmed Atlantic salmon appear to involve both infectious and non-infectious aetiologies (Rodger *et al.,* 2011; Mitchell and Rodger, 2011; Rodger, 2014) and therefore early, accurate, differential diagnosis of such diseases and disorders are regarded as being highly important for ensuring the health of farmed salmon. At present, routine gill health monitoring is recommended for salmon farms in at-risk areas as a precautionary measure to protect the welfare status of fish (Segner *et al.,* 2012).

Conventionally, histology, which provides the gold-standard method for assessing structural alterations in the organ, is used as the preferred method for health assessments of gills (Adams and Nowak, 2003; Ferguson, 2006; Roberts and Rodger, 2012). In general this is performed by a trained histopathologist, observing stained histology sections under light microscope and who is able to provide a qualitative description about ongoing histological alterations to provide a histopathological

diagnosis. This methodology remains largely qualitative with respect to changes and presence of pathogens or other aetiologies, however, quantitative assessment of changes in the gill or pathogen load are not generally attempted in routine disease diagnosis. In general this type of histological assessment only measures morphological changes and those reflected in changed staining properties within tissue lesions. It is also important to examine the tissues close to lesions, where apparently healthy looking cells may in fact be in the initial stages of cellular changes, which cannot be detected by human observers under conventional microscopy. Furthermore, use of conventional methods based on subjective assessments could potentially be inconsistent depending on the person who examined the tissues, and this is regarded as a drawback in the use of histopathology in research (Belsare and Mushrif, 2012).

The quantification of the extent of histopathology using semi-quantitative assessment or scoring has been previously used in fish research, targeting different organs to understand disease pathologies (Christie *et al.,* 2007; Herath *et al.,* 2013; Martinez-Rubio *et al.,,* 2012; Martinez-Rubio *et al.,,* 2014) and also to determine migratory measures. These methods are still laborious and also limited to relatively small-scale specialist research studies (Fonyad *et al.,* 2012). However, such systems can easily be complemented by user-friendly automated digital image analysis systems which would allow analysis of larger numbers of samples in a shorter period of time with lower errors than that obtained using routine histopathology. Automated digital image analysis platforms are widely used in human medicine, however, in aquaculture the use of such tools is still in its infancy and they are hardly ever used in pathophysiological studies of fish (Madabhushi *et al.,* 2009).

In 2012, Mitchell and others developed a semi-quantitative scoring system to investigate gill pathologies during a longitudinal study carried out in west coast of Ireland, using a quantitative scale, which assessed the severity and the extent of pathology present in samples derived from a field-based longitudinal study. This system assessed both, pathological changes that occur in response to any insult (index criteria) and minor or less freeqent indicators of gill pathology (ancillary criteria) using a scale ranges from 0 to a maximum of 24. In assessing gill diseases using this scoring system usually denotes; lesion score of 0–3 reflects no substantial pathology, a score of 4–6 mild gill pathology of minor clinical significance, a score of 7–9 moderate gill pathology of clinical significance, and finally a score greater than 10 was associated with severe gill pathology of high clinical significance. Further, this scoring system also allowed assessment of some other parameters such as pathogen load and a range of environmental factors (*e.g.* water temperature, pH and oxygen saturation). Screening large numbers of gill samples at a commercial scale is not, however, possible without the improvement of a semi-quantitative scoring system for gills. Quantitative assessment of the gill, both grossly and using histology, remains an important aspect of monitoring fish health (Au, 2004), mainly due to the huge surface area of gills, high water throughput and their direct exposure to the ambient environment, which makes them excellent markers for the effects on fish of a range of exogenous factors, including chemical bath treatments and exposure to different pathogens in ambient water (e.g. *Neoparamoeba* sp.).

Image processing and analysis, using digital images as a starting point, provide a set of tools ideally suited to quantification of pathology / plasticity in the gill. Image analysis may be defined in terms of a number of processes undertaken to obtain data, be it objects recognition or quantitative data, from images, now largely conducted using

digital media. Image analysis depends critically upon successful completion of three consecutive processes: (1) image capture, (2) image processing, (3) image analysis. Although the successful performance of all three stages is vital for the final outcome, also depends very much on accurate sampling of fish and how the sample is handled and processed. During the image capture phase, the intensity / colour distribution of the selected subject or scene is acquired with a suitable camera or through scanning of the targeted object. During this step, digitisation of the image may also take place. The subsequent image processing step involves a series of transformations that allow the entire image or key regions of the image to be subsequently recognised / analysed. Such transformations include a range of image processing functions such as contrast enhancement or normalisation, smoothing (median), edge improvement (Laplace), grey morphology (grey erosion / dilation) and image arithmetic (addition / subtraction). The process termed image segmentation is used to detect and separate key regions or phases from their environment on the basis of their grey values. This process creates a binary image from a grey value or true colour image. Processing of the segmented binary image can further improve segmentation results *e.g.* arithmetic operations, filling of holes or filtering on the basis of size.

Following image processing, image analysis is then performed to produce the required quantitative data, which is then stored in database files. The measurement values are obtained from the image and its components during the measurement process. In general there are two possible cases (1) field specific measurements where a record of measurements is extracted from a given image, for example percentage area covered, (*e.g.* total gill area; TGA), the number of particular regions in an image (*e.g.* total mucous cell number; TMCN), its overall size (*e.g.* total mucous cell area; TMCA), *etc*., (2) region specific measurements where every region generates a record containing

measurement values. Examples are the size and shape of regions, their mean grey value, optical density or the number of holes in a region (*e.g.* secondary lamellar area; SLA, circularity of mucous cells).

It may be suggested that the development of a robust computerised image analysis tool might allow evaluation of a range of factors that impact gill and fish health. This can include assessment of the effects of functional diets upon gill structure, the subtle changes that may occur due to different temperature regimes and the effects of different chemical treatments (therapeutic and non-therapeutic doses). To employ image analysis techniques most successfully, image capture methodologies must also be optimised. One of the most important contributions to recent quantitative histology has been the development and use of high resolution digitised WSI histology slides, scanned using high-throughput digital slide scanners (Wetzel *et al*., 2000; Ghaznavi *et al.,* 2013). Such technologies are capable of making a significant contribution to the assessment of morphometric changes in gill structure.

Digital image capture and analysis systems are increasingly used to diagnose human diseases including human breast cancer (Loukas *et al.,* 2013) and human prostate cancer (Parimi *et al.,* 2014), where data are digitised and enable specialised pathologists to examine samples from patients anywhere in the world through virtual digital microscopy (Mencarelli *et al.,* 2008; Nakayama *et al.,* 2012). Similarly for fish, researchers at Skretting's ARC in Stavanger, Norway have recently implemented new methodologies for image-based assessment of fish health and nutrition, using image analysis methodologies to generate large datasets with relatively little user input (Silva, 2014).

Development of an image analysis pipeline described in this chapter seeks to develop a pipeline for the detection and quantitative description of histomorphological changes occurring in the gills of Atlantic salmon in response to a range of exogenous factors / pathogens. To achieve this, new approaches to image capture, processing and analysis have been developed, including the use of digital whole slide image capture and the development of a novel gill image analysis (GIA) tool. The aim of the work conducted has been to develop a system for rapid detection of histomorphometric changes in Atlantic salmon gills through provision of robust semi-automated histomorphometric assessment tools capable of quantitating pathophysiological changes occurring in response to different functional feeds, chemical treatments, environmental changes and pathogen challenges. In this chapter the procedures involved in developing the initial GIA tool and its application to the classification of differential responses to functional feeds are described, allowing initial validation of the approach. The use of the aforementioned technologies, coupled with multivariate statistical analyses, provides a new approach to histopathology-based gill health monitoring.

2.2 **Materials and methods**

In order to provide histological samples for developing the proposed image analysis pipeline and material for validation of the approach, a feed trial was conducted comparing standard and functional diets. In addition to gill tissue samples, a range of relevant immune/physiological parameters were also obtained from the trial in order to provide supporting data. Following the trial and completion of sampling, histological processing and staining methods were optimised and image capture conducted. Using the gill histopathology images obtained, a new gill image analysis (GIA) tool was developed and validated. The component elements of this analytical pipeline are described below:

2.2.1 **Dietary trial**

A feed trial for post-smolt Atlantic salmon weighing 65 to 75 g was conducted at Lerang Research Station Norway (Figure 2.1). The three experimental diets used for the experiment were comprised of a fishmeal-based control diet (Diet A), a diet containing 25 % soya bean meal concentrate (Diet B) and a fishmeal-based diet with an added immunostimulant (Diet C). Diets were trialled in triplicate tanks, with the nine flow-through 100 L tanks being maintained under 24 hour light photoperiod at 11±2 °C. Two test feeds (Diet B & C) were introduced to 2 groups of fish after feeding control diet for 2 weeks. The control group was maintained on the control diet (Diet A.) Each tank contained 30 fish.

For sampling, fish were euthanised by overdosing with benzocaine (100 mgL^{-1}) (Sigma, Norway) in compliance with recommended guidelines established to maintain animal welfare standards (Norwegian National Legislation for Laboratory Animals). Three fish from each tank from all three groups were sampled at 11 weeks (initial sampling) and 20 weeks (final sampling) after introducing test diets. Samplings were carried out in order to monitor growth rates, establish basic immunological parameters and assess histomorphometric changes (Table 2.1).

Blood was collected by caudal venipuncture, using heparinised syringes, prior to sampling the second arch from the right side of the gill into 10 % neutral buffered formalin (NBF) (=4 % formaldehyde) for histological analysis and the second arch of the left side of the gill was sampled into 1 mL of RNAlater (Sigma, Missouri, USA) for gene expression analysis. Samples taken into 10 % NBF were kept at room temperature in Norway and transferred to Scotland by rapid courier service. After 48 h fixation at 4 °C, RNAlater (Sigma) was removed and samples were transported to the Institute of

Aquaculture (IoA) and kept at -20 °C until being processed according to manufacturer's guidelines.

2.2.2 **Sample processing for histology**

The processing of the gill for histology involved an optimised standard protocol of operation (SOP, Histology lab, IoA) and key details are highlighted in the discussion accordingly. The SOP was conducted as follows. Processing of gills was performed using an automated tissue processor (Leica, Shandon Excelsior, Thermo Scientific, UK) where tissue samples were dehydrated through 100 % alcohol and cleared with several baths of xylene. Finally, the tissue samples were infiltrated with paraffin wax at 60°C (Histowax, Sweden or Q-Path, France). The gills were carefully placed on the histo-cassettes with the second gill arch being laterally orientated and placed level on the bottom of the cassette by gentle pressing from blunt end of forceps. Histo-cassettes were placed into diluted commercial fabric conditioner (final sampling point only) which is routinely used as a soft decalcifier solution, for 30-45 minutes allowing decalcification to take place without causing any architectural damage. Initially tissue blocks were carefully trimmed (20 μm) to expose tissue and then 5 μm thick paraffin sections were made using a Shandon Finesse® microtome (Thermo Scientific, Waltham, MA, U.S.A.) with disposable metal knives (Sigma, UK). The sections were dried on either conventional microscope slides (conventional and special staining) or poly-L-lysine coated microscope slides for immunohistochemistry (IHC) (Solmedia, UK.) at 60°C in a drying cabinet for a minimum of one hour prior to staining.

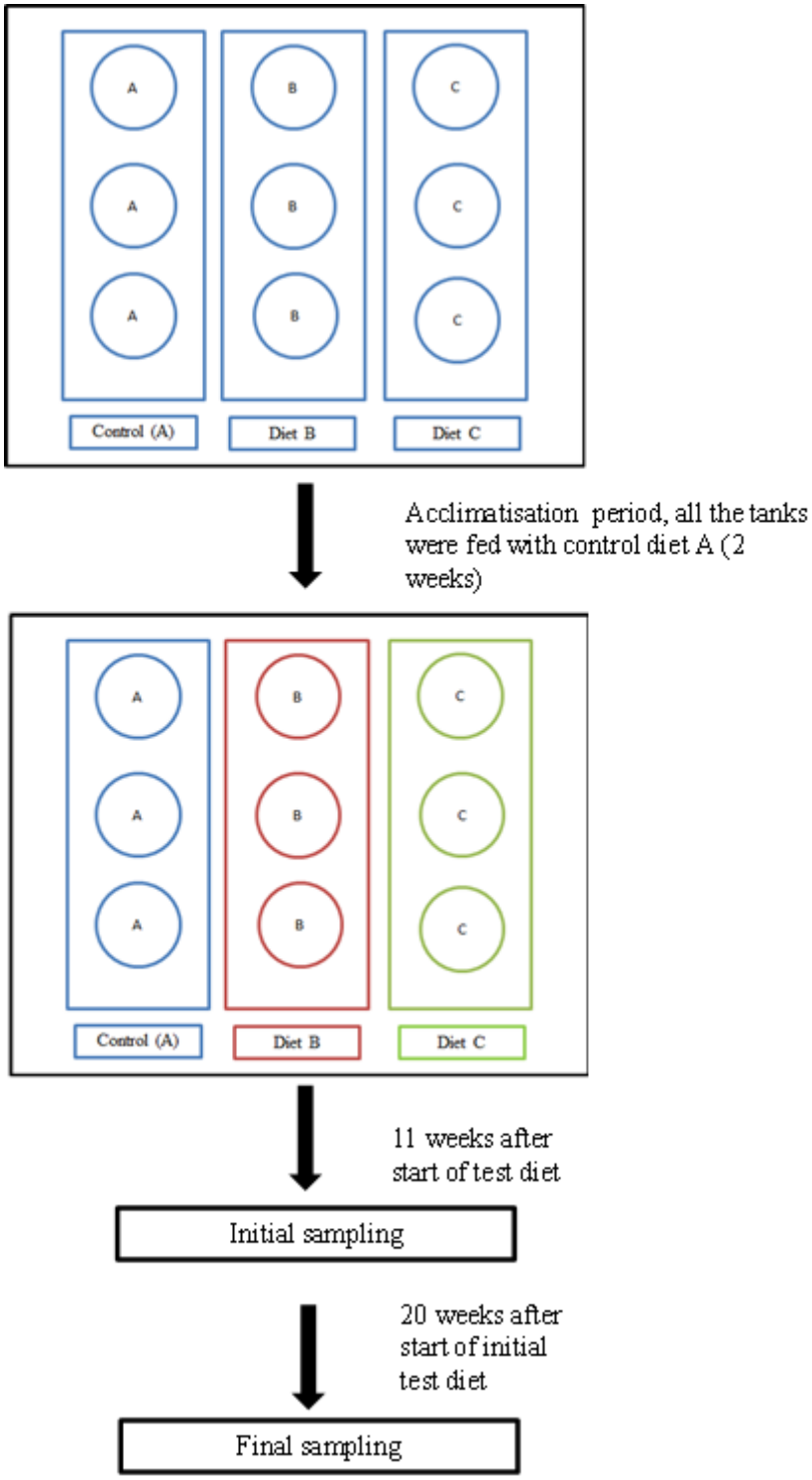

Figure 2.1 A Schematic diagram of experimental plan. Fish were fed with Diet A- conventional salmon diet (control), Diet B - test diet with 25% of fish meal replaced with soybean meal, Diet C - test diet enriched with additional immune stimulant and sampled at 11 weeks and 20 weeks after introducing test feeds. First sampling (initial sampling) was carried out 11 weeks and second sampling (final sampling) after 20 weeks after start of test feed. Results of final sampling were analysed and presented in this chapter accordingly.

2.2.2.1 Haematoxylin and eosin (H&E) staining

Haematoxylin and eosin (H&E) is the most widely used histology stain in routine pathology providing a broadly differentiated nuclear and tissue visualisation. The 5 μm thick paraffin wax sections were stained with H&E. Slides were pre heated in an oven at 60 °C for 1 h before being deparaffinised through two xylene baths for 5 min each, then transferred into absolute alcohol for 2 min before being placed into methanol for 1.5 min. Slides were then washed in running tap water before placing in them in haematoxylin Z for 5 min and again washing them in tap water until clear (30 sec to 1 min) before 3 quick dips in 1 % acid alcohol to differentiate. Slides were then washed in tap water and Scott's tap water substitute for 1 min then brought back into water before placing them in eosin for 5 min. Slides were then given a quick wash in tap water before placing them in methanol for 30 sec. Stained slides were then dehydrated through an ethanol series before clearing through two xylene baths (5 min each) and mounting under coverslips using Pertex (Cellpath, UK).

2.2.2.2 Periodic acid Schiff (PAS) and Alcian blue (AB) staining

The combined alcian blue (pH 2.5) periodic acid Schiff stain (PAS) (=AB-PAS), allows staining of acid and neutral mucopolysaccharides, this being particularly useful for staining of mucous cell populations in gills. The Alcian blue component, when applied at correct pH, (pH 2.5) effectively blocks staining of acid mucopolysaccharides by PAS leaving neutral polysaccharides free for binding. 5μm paraffin wax sections were pre-incubated at 60 °C in an oven before being deparaffinised in two consecutive xylene baths for 5 min each. Slides were then transferred to alcohol for 2 min before passing to methanol for one and half minutes and being washed in tap water for 30 seconds to 1 min. Slides were then immersed in Alcian blue (Sigma, UK) solution (Alcian blue 1 g

dissolved in 3 % acetic acid, 100 ml at pH 2.5) for 10 min. Where Alcian blue was to be employed without a combined periodic acid Schiff's stain it was immersed for an additional 30 min. Once slides were stained with Alcian blue, they were washed in tap water and then in distilled water for 30 min and transferred into 1 % aqueous periodic acid for 5 min before rinsing well in distilled water. Then they were transferred to Schiff's reagent (Sigma, UK) for 15 min and washed in running tap water for 5 min before counter-staining with Mayer's haematoxylin for 2 min. After washing in tap water for 2 min, 2 quick dips were performed in 1 % acid alcohol to differentiate, then rinse in alcohol for dehydration and clearing through xylene (5 min each) before mounting under coverslips with Pertex (Cellpath, UK).

2.2.3 **Light microscopy, imaging and processing**

The H&E stained gill sections and Alcian blue-PAS stained gill sections were assessed blind for the different functional diets using light microscopy observation (LM) for any histomorphometric changes. Light microscope images were taken with a Zeiss AxioCam MRC colour digital camera attached to an Olympus BX51TF light microscope. MRGrab version 1.0 software (Zeiss) was used to capture and save images (tiff images approximately 8 MB in size, 2290x 1200 pixels) and a slide graticule scale was used to calibrate test images. Initially, during tool development, camera-acquired images (AxioCam) were used to develop the prototype GIA tool but this capture methodology was later replaced by WSI technology and the GIA tool customised to accommodate the change. To develop the final gill image analysis tool, histology slides were scanned (WSI) using a Mirax desktop scanner with single slide feed (3DHISTECH Ltd) at Skretting ARC Norway.

2.2.4 Subsampling (cropping) of images through selected randomisation

Digital high resolution images of whole gill arches were acquired using WSI technology. From these cropped subsamples (4 subsamples per fish) were used to give equal size images for downstream processing and analysis using the GIA tool. Initially large WSI whole gill images (normal file size was 1.5 GB) were uploaded into the Mirax viewer (Freeware-Version Rel 1.6.2.4, Carl Zeiss) or Panoramic Viewer software (3DHISTECH Ltd). At low magnification (x 1.5), a suitable intact rectangular tissue area, of the gill filaments, were selected for further cropping of subsamples (Figure 2.2.F). Then equal size digital tiled tiff images (approximately 8 MB in size, 2290x 1200 pixels) were cropped inside the large pre-selected area (Figure 2.2). The size of the cropping image was kept constant using equal sizes similar to the slide viewing panel of the Mirax viewer software. The images were exported using a consistent protocol (decided by conducting experiments on image size and quality in order to ensure acceptable quality in KS300) as illustrated in Figure 2.2. Later those images were transformed into a more standard tiff file format using IrfanView software (www.irfanview.com) before analysing in KS300 for histomorphometric gill changes (Figure 2.2).

2.2.5 Development of gill image analysis tool (GIA)

Development of the Gill Image Analysis (GIA) tool was carried out using the KS300 image analysis platform (Carl Zeiss, GmbH, Germany, 1997). The developed tool was used to examine differences in a total of 25 morphometric variables and indices, which were developed and evaluated with respect to three different diets (Table 2.1).

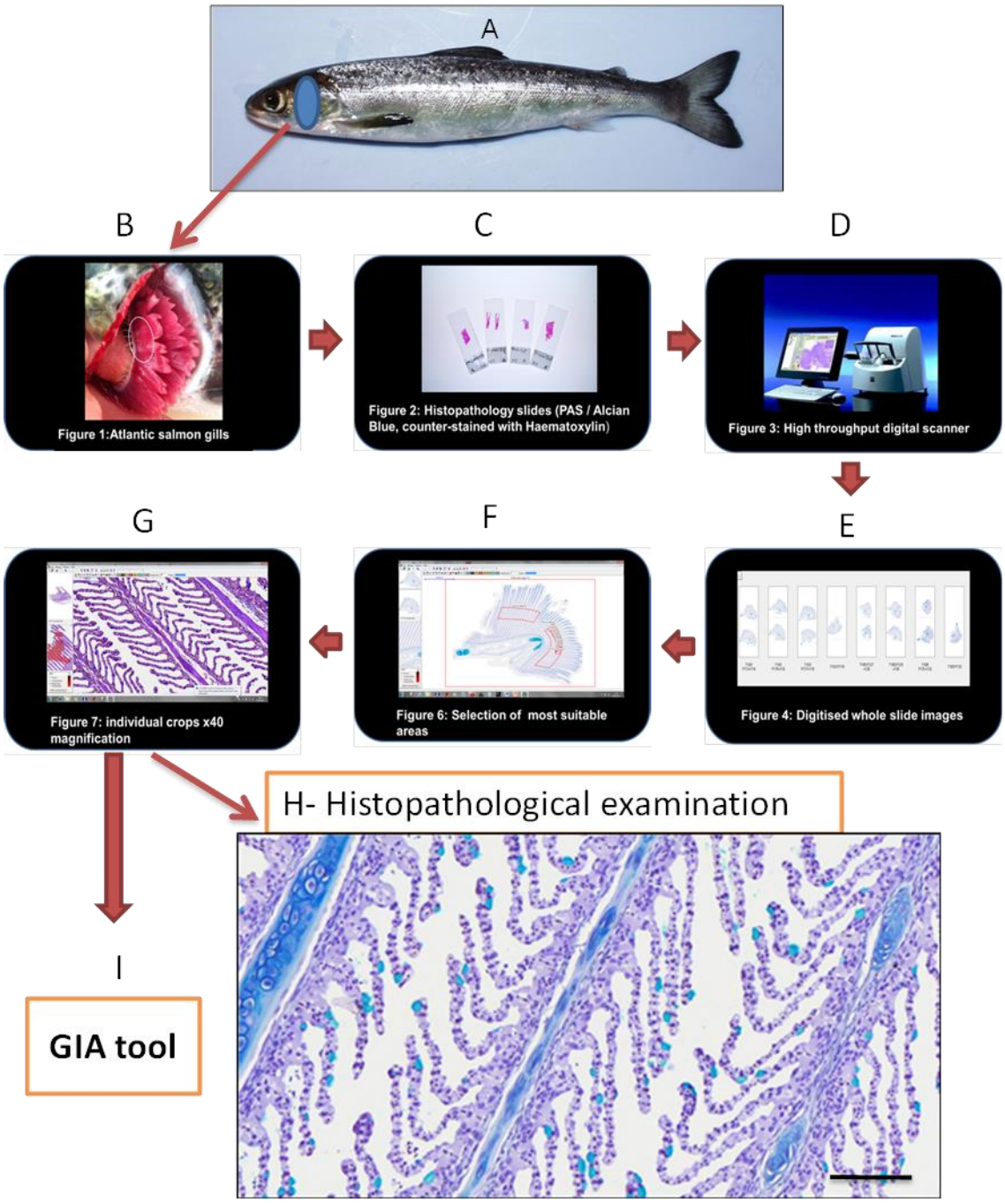

Figure 2.2 A diagrammatic illustration of the different steps involved in histopathological evaluation through whole slide imaging (WSI) technology. (A) different functional feed fed fish, (B) second gill arch, (C) histological slides with different gill sections, (D) Mirax desktop scanner with manual feeding of slides, (E) scanned whole slide images (WSI), (F) defined region of interest (ROI), (G) x40 cropped images through Mirax viewer (or "Pannoramic" viewer), (H) representative image of gill fed with different functional diet using Mirax "x40" magnification setting. Scale bar 100 µm

Table 2.1 Different morphometric parameters measured during development of the gill image analysis tool

	Gill parameter or indices	Acronyms
Primary lamellae associated morphometric parameters		
1	Vacuolar area of primary lamellae	VAPL
2	Primary lamellar area	PLA
3	Primary lamellar epithelial area	PLEA
Secondary lamellar associated morphometric parameters		
4	Vacuolar area of secondary lamellae	VASL
5	Secondary lamellar area	SLA
6	Secondary lamellar perimeter length	SLPL
7	Median minimum Feret secondary lamellae	MedianFERETMinSL
8	Median maximum Feret secondary lamellae	MedianFERETMaxSL
9	Median secondary lamellar length	MedianSLL
10	Secondary lamellar perimeter length / Secondary lamellar area	(SLPL/SLA)
11	Secondary lamellar perimeter length / Mean secondary lamellar length	(SLPL/MeanSLL)
Mucous cell associated morphometric parameters		
12	Total mucous cell area	TMCA
13	Total mucous cell area / Total gill area	TMCA/TGA
14	Mucous cell number in PLEA	MCN-PLEA
15	Mucous cell area in PLEA	MCA-PLEA
16	(MCA-PLEA)/PLEA	(MCA-PLEA)/PLEA
17	Mucous cell number in secondary lamellar area	(MCN-SLA)
18	Mucous cell area of secondary lamellar area	(MCA-SLA)
19	Mucous cell area of secondary lamellar area/ Secondary lamellar area	(MCA-SLA)/SLA
20	Total mucous cell number	TMCN
21	Total mucous cell number / Total gill area	TMCN/TGA
Total gill area associated morphometric parameters		
22	Total gill area	TGA
23	Inter-lamellar space	ILS
24	Gill Ratio (SLA/PLA)	GR
25	Inter-secondary ratio of gill (ILS/SLA	ISR

Development of the GIA involved planning of the key processing and analysis requirements followed by writing of a custom macro script in association with Prof James Bron, Institute of Aquaculture (IoA), University of Stirling. This script allowing interactive quantification of a number of morphometric and densitometric features of target features of the fields (in the selected area of the image) or individual objects (*e.g.* mucous cells). These features included the area measured (including geometric measurements), mean colour intensity and counts. The GIA script produced output measurement data for each image in the form of an Excel data file (tab-delimited format) (Microsoft) for use in subsequent statistical analysis. In addition, for each processed image the GIA archived a number of additional images for quality control and visual interpretation. The GIA script encoded a fixed series of operations with minimal user-interaction, in order to ensure consistency between measurements of histomorphometric changes and removal of user bias. It has been widely reported that the use of digital image analysis in this context is much faster than taking manual measurements and analysis of gill morphometric data. It is more accurate and allows improved inter-user repeatability allowing handling of a large number of samples over a very short period of time.

A series of steps were performed during the development of GIA tool to measure common histomorphometric changes *i.e.* image segmentation, edge detection, noise removal, colour thresholding, morphological filtering, intensity thresholding, Size scrapping and filling, intensity thresholding of inverted images, manual object delineation and feature extraction and output generation (Figure 2.3). Key processes are described below.

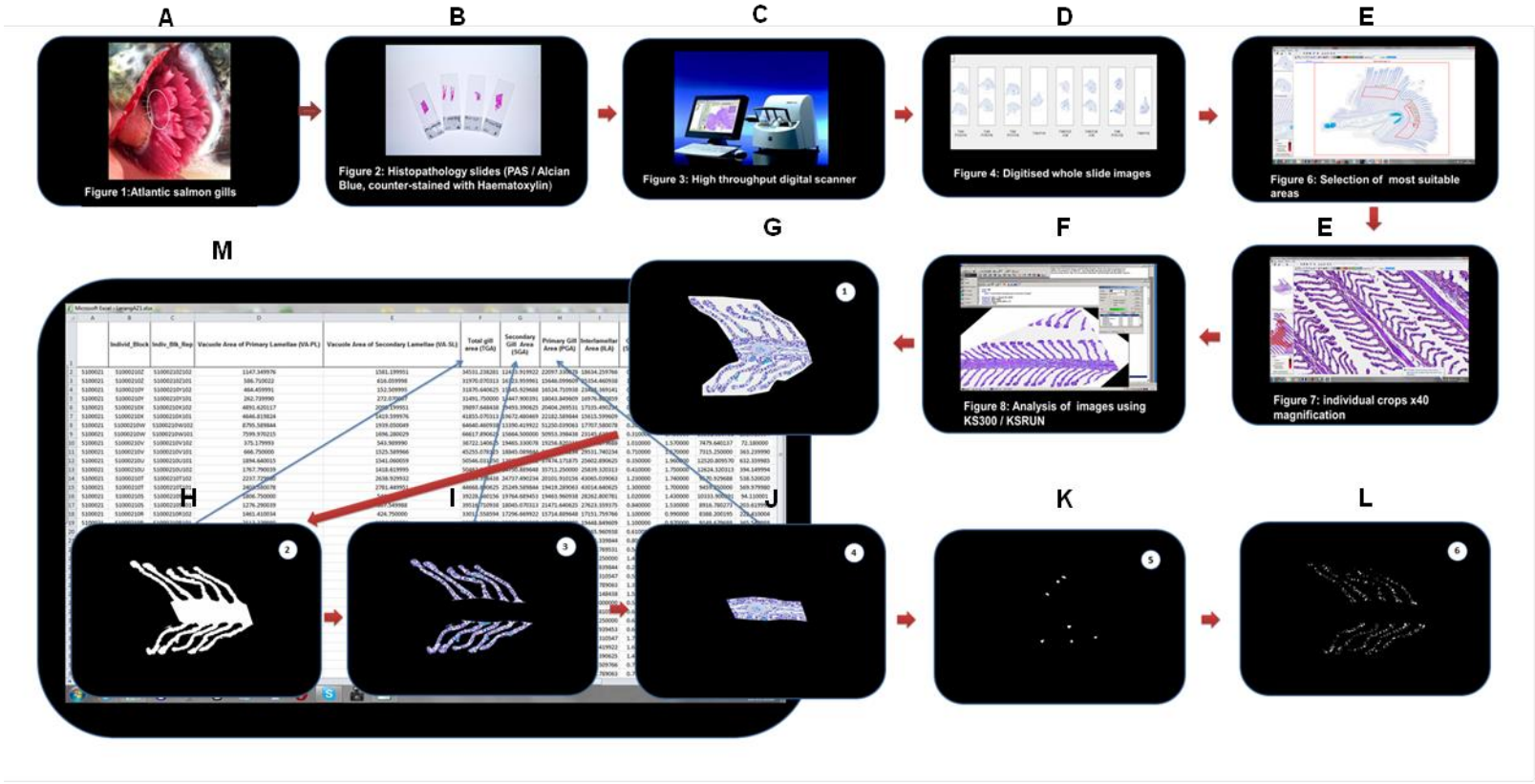

Figure 2.3 A diagrammatic illustration of intermediate analytical steps included in the use of the of GIA tool. Thin (5µm) histological sections of whole gill from fish fed with different functional diets were used to develop the GIA tool. A-E, shows common steps involved in virtual histopathology and GIA tool; F, uploaded cropped image (a subsample) in KS300\KSRUN software; G, region of interest with 5 secondary lamellae on each side (total 10); H-L, intermediate steps which generate different gill histo-morphometric parameters including TGA, SLA, PLA, TMCN and VASL; M, a screenshot of the generated data file, rows comprise individual fish or subsamples, columns comprise relevant morphometric parameters or indices.

2.2.5.1 Edge detection

Edges are defined as boundaries between objects useful for defining discrete elements (*e.g.* surface of gills, mucous cells) in 2D images. In a colour image it is difficult to find salient edges, strong edges or the object boundaries. Quantitatively, edges can be detected at the boundaries between regions of different colour, intensity, or texture. The segmentation of an image into coherent regions is a difficult task and it is preferable to detect edges using only purely local information. In the GIA tool, edge detection was used to identify different objects from other adjacent tissue areas and their boundaries from normal tissue.

2.2.5.2 Noise removal

Noise removal and sharpening are commonly used image enhancement methods in image processing. Digital images are prone to a variety of types of noise which could cause errors in the image analysis process and which result in pixel values which do not reflect the true intensities of the real objects *e.g.* tissue in the image. Noise can be introduced into an image in many ways but this relates to the method of image creation. Digital images captured from the light microscope, for instance, were noisier than images from scanned WSI technology.

2.2.5.3 Colour thresholding

The number of colours that may be represented (displayed) and stored in a digital image is governed by the number of bits per pixel of the image. The more bits per pixel an image has, the higher the number of colours that may be represented / stored and hence, during initial image capture / creation, the number of colours depends on the technology or device employed *e.g.* camera, software. The number of bits per pixel, known as a display screen's bit depth, similarly determines the number of colours it can display.

Most computer displays use 8, 16, or 24 bits per screen pixel. Depending on the system, the screen bit depth may be specifically selected. In general, 24-bit colour provides the best colour resolution, with 16-bit being preferable to 8-bit. For the described work, colour thresholding was used to distinguish different tissue areas stained with different colours. Different colour intensities generated from different tissue areas were used to identify tissue areas or individual cells by colour thresholding *e.g.* mucous cells stained turquoise (Alcian blue) are markedly different from adjacent tissue areas counter-stained with haematoxylin.

2.2.5.4 Morphological filtering

Morphological filters comprise a collection of non-linear operations which relate to the shape or morphology of features in the image. To use such filters, colour images need to be transformed into binary images. Binary morphological operations change the shape of the underlying binary objects (Ritter and Wilson 2000).

During the development of the GIA tool, histological images were initially transformed into binary images and then a series of morphological operations were conducted including dilation and erosion, during which objects were dilated by adding one or more layers of pixels to the outside of the object or eroded through removal of pixels. In both operations, boundary pixels may be subject to change causing separation of merged objects (*e.g.* closely associated mucous cells) or merging of accidentally separated regions.

2.2.5.5 Intensity thresholding

Intensity values (brightness/darkness) vary across different regions of an image, with different regions representing corresponding objects in a scene, and with similar objects sharing similar intensity values. Intensity thresholding is one of the operations

performed during image segmentation. Thresholding is used to extract an object from its background by assessing an intensity value for each pixel and, from that value, classifying the pixel as either an object point or a background point. During development of the GIA tool, intensity thresholding was used to discriminate gill tissue from non-tissue (background).

2.2.5.6 Size scrapping and filling

In binary images, in order to remove regions that are larger or smaller than the target object (*e.g.* mucous cells) size scrapping allowed regions above or below a selected pixel number threshold to be removed from the image. This allows removal of debris, noise and some scanning artefacts. In addition, heterogeneity in staining / intensity / tissue structure may lead to regions having holes in them, which are known to be artifactual *e.g.* mucous cells shaped like an "O". In these instances, filling operations may be used to fill holes surrounded by a continuous recognised region.

2.2.5.7 Intensity thresholding of inverted images

Positive binary images (white objects on a black background) may be inverted to negative images (black objects on a white background). Size scrapping of inverted binary images was used to remove specific features (holes in tissue/vacuoles) and to clean up the image.

2.2.5.8 Interactive manual object delineation

Interactive manual object delineation was included as an option to allow the user to remove capture artefacts and unwanted material such as mucous aggregates/tissue debris. This ensures accurate tissue capture and quantification. As a final operation, during quantification, objects to be measured are highlighted in green and can be deselected before the final measurements are taken.

2.2.5.9 Feature extraction and output generation

Once the final processed images have been derived, remaining features (objects *e.g.* mucous cells, tissue) are automatically extracted and enumerated / measured according to the parameters selected by the user

2.2.6 Image analysis using KSRUN software

After pre-processing, each captured image (microscope or scanner derived) was uploaded into the KSRUN image analysis environment (Once developed, the GIA macro script was run for every pre-processed image, and subsequent data files and post analysis images were screened for accuracy against observer observations *e.g.* checking that mucous cells had been successfully recognised).

To standardise images, the original images (8 MB captures) were cropped give to a defined size and orientation (secondary lamellae running from "top" to "bottom" in order to give consistent images before analysis) (Figure 2.4). While gills might be examined using a "whole" gill arch or "whole" primary lamella analysis, it was decided from initial pre-trials that analysis of a defined and replicable region would provide both higher consistency and, through the ability to use a higher image magnification, better resolution of key features. Initially, therefore, the region of interest (ROI) was defined by drawing a box that encompassed five pairs of secondary lamellae and the associated primary lamella and passed above the tips of the secondary lamellae and through the interlamellar space surrounding the region (Figure 2.5).

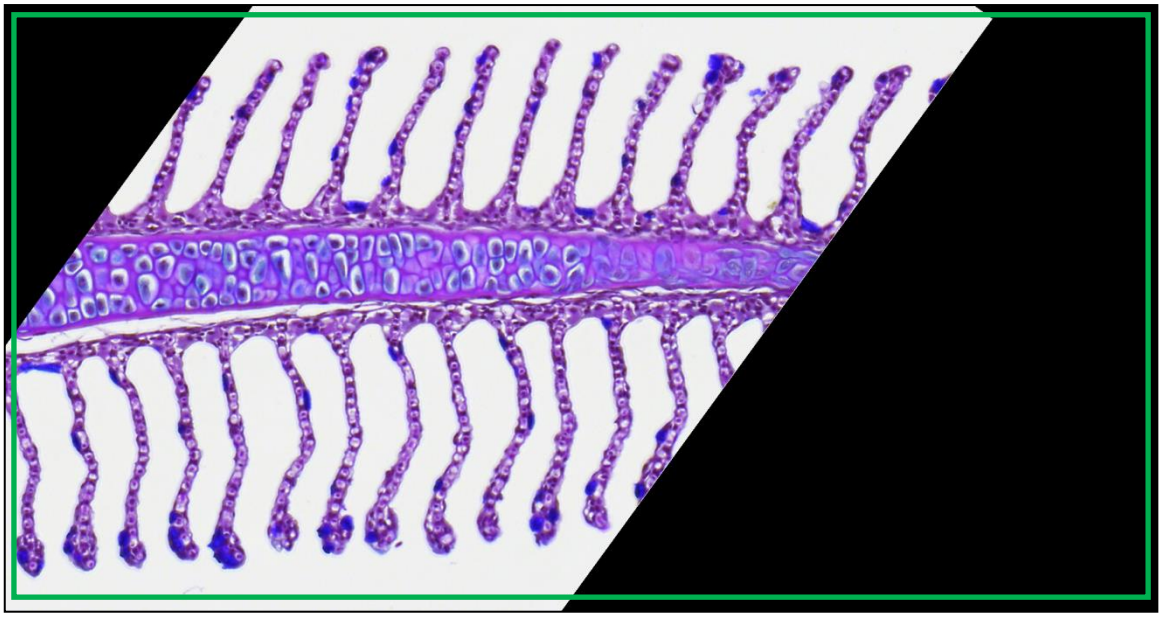

Figure 2.4 Standardised image orientation and crop using pre sized box

The selected crop was then subjected to thresholding in order to segment out the tissue area from the background to produce a binary tissue image for subsequent image processing (Figure 2.6). Using the binary image, a vertical line was then drawn if necessary to separate fused or touching secondary lamellae. Subsequently a series of lines were interactively drawn on the image to divide the gill area into to sub-areas enabling measurement (histomorphometric measurements) of key features of the gill primary and secondary lamellae (Figure 2.7).

To achieve this a line was drawn for both the dorsal and ventral side connecting the lowest point of each interlamellar space including one extra point at each end of the crop lying outside the original boundaries (marked by white line) (Figure 2.8). As suggested by many authors, the most active and proliferative area of the primary lamella (filament) of the gill is defined as the primary lamellar epithelial area (PLEA), which is anatomically distinguished in terms of the epithelium overlying the basal cell layer *i.e.* germinal layer, resting on the basement membrane. In order to separate the

primary lamellar area (PLA) into primary lamellar epithelial area (PLEA) and central venous sinus (CVS) or cartilage (C), a continuous line was drawn along each epithelial boundary (lying along the basement membrane) located on both dorsal and ventral side of the filament (Figure 2.9). Automated measurements of the resulting image segments were carried out (PLA, PLEA and CVS) in order to calculate the area of each segmented tissue.

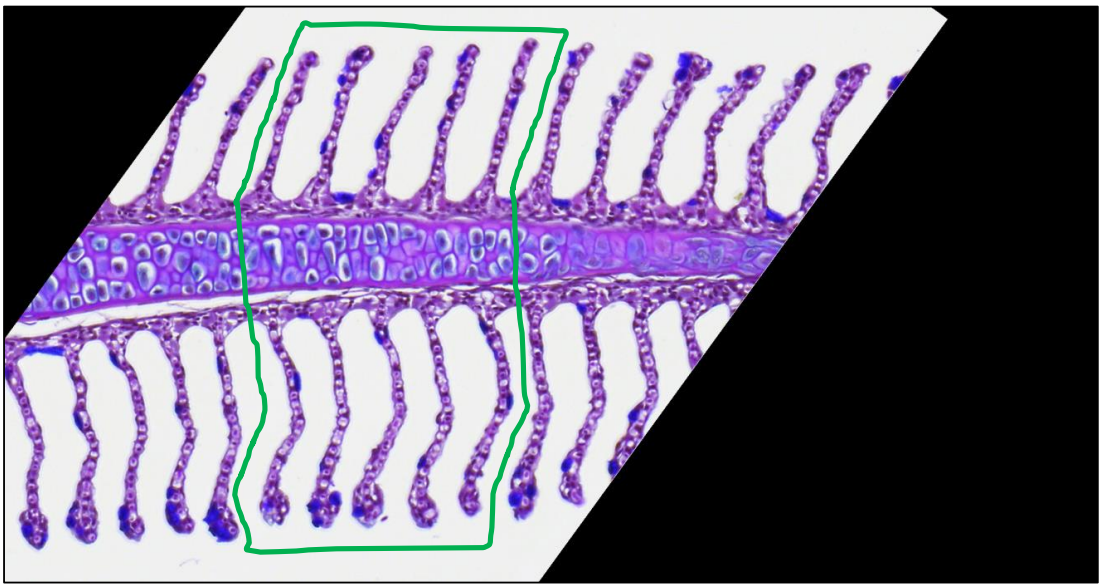

Figure 2.5 Selection of the region of interest (ROI) from the cropped gill image

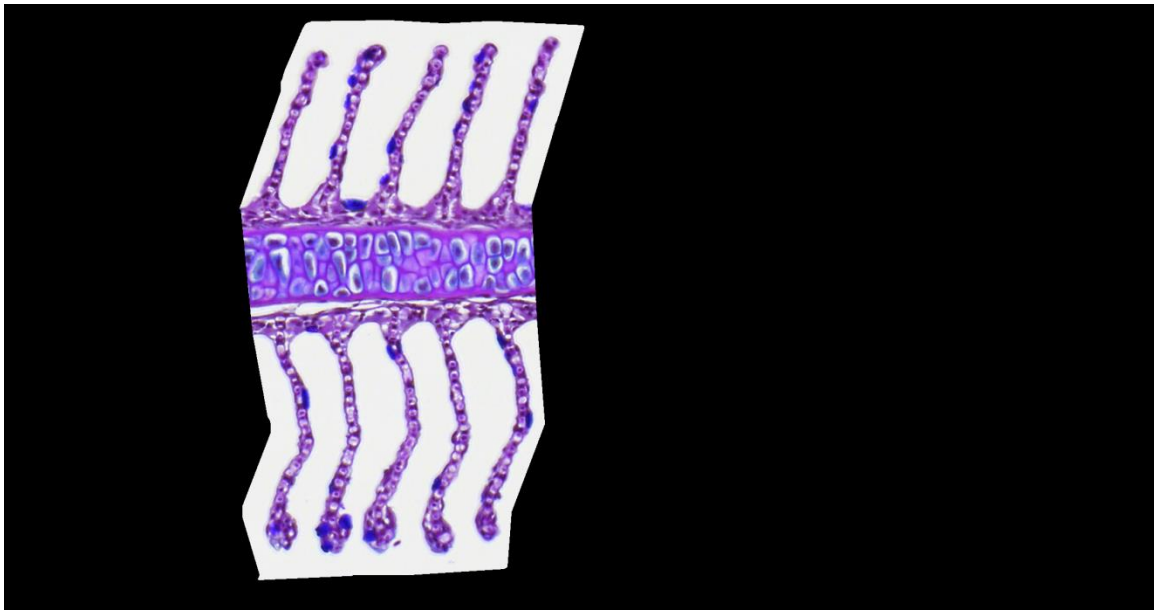

Figure 2.6 Initial selected region of interest (ROI) for subsequent processing and analysis

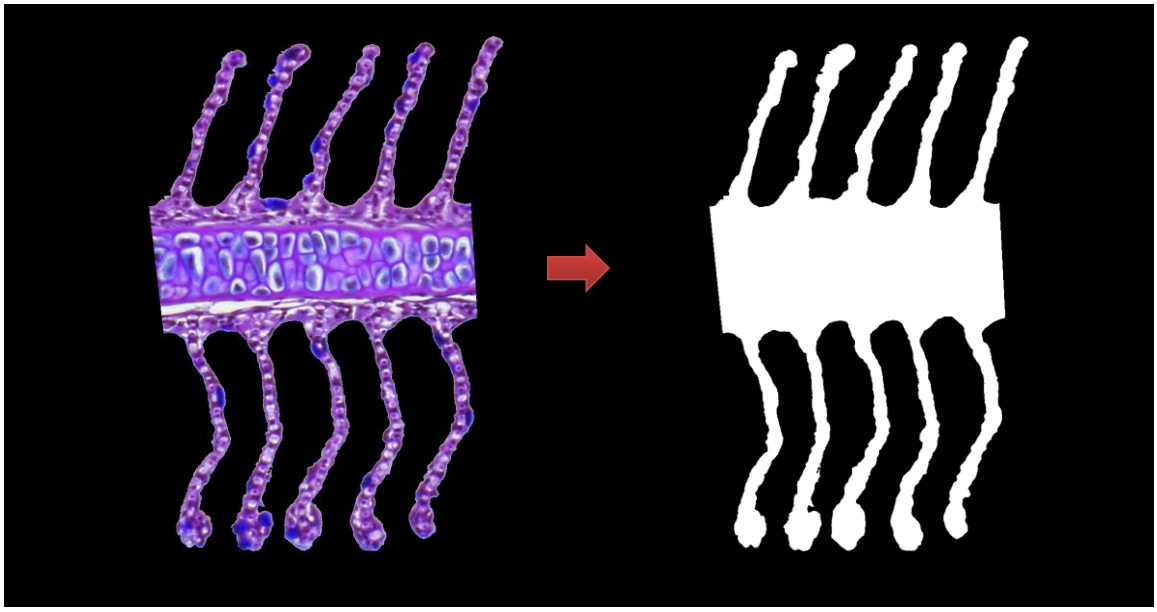

Figure 2.7 Thresholding cropped image to give binary image

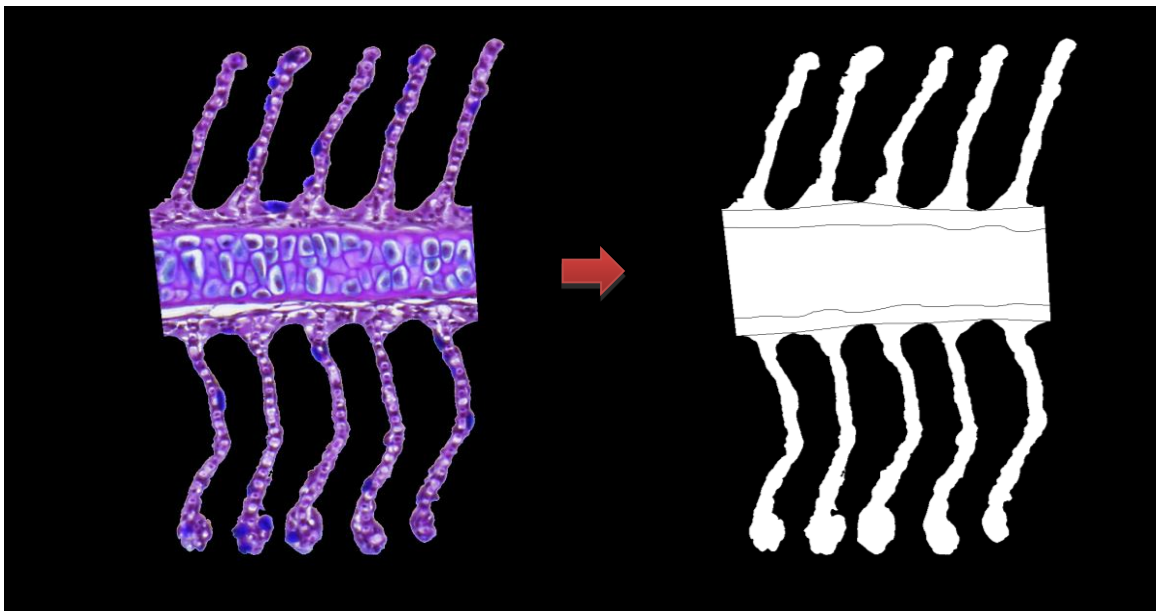

Figure 2.8 Lines drawn to segment gills into different anatomical areas.

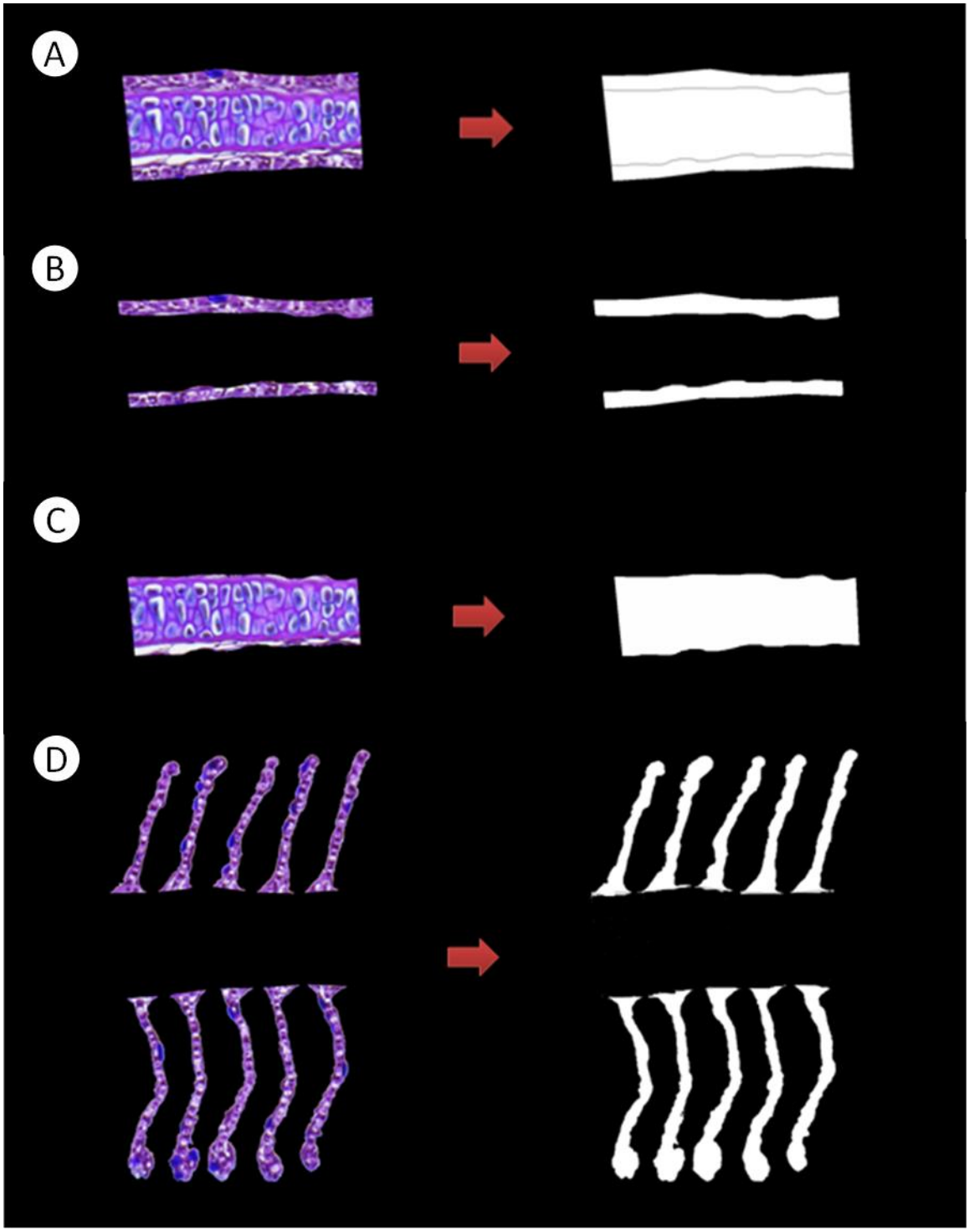

Figure 2.9 Different segmented areas of the gill tissue were transformed into binary images for area measurements. (A) primary lamellar area; PLA, (B) primary lamellar epithelial area ; PLEA, (C) central venous cinus; CVS and (D) secondary lamellar area; SLA

The measurement of mucous cell area (MCA) and mucous cell number (MCN) was carried out by implementing a colour thresholding operation (HLS colour model; Hue,

Brightness and Saturation). For the initial starting point, colour samples of mucous cells were taken (blue mucous cells stained with Alcian blue) to allow colour thresholding, with thresholds extended as necessary on a per-image basis to ensure accurate capture. This task was assisted by viewing a high magnification of the image for better accuracy (Figure 2.10).

An interactive point to point measurement of the length of the secondary lamellar length was performed (median secondary lamellar length; MSLL) on the ten secondary lamellae by drawing a line from middle of base to tip of filament (Figure 2.11). Between the secondary lamellae lies the inter-lamellar space (ILS), which can be used as an indicator of gill remodelling. The cells located on the primary lamella between the secondary lamellae are termed the inter-lamellar cell mass (ILCM), and are particularly important to the shrinking or enlarging of the size of the ILS. To define the ILS, a line was drawn connecting the tips of the secondary lamella along the dorsal / ventral aspects of the gill (Figure 2.12). The subsequent step automated measurement of the ILS. Total gill area (TGA) was generated from corresponding binary images after screening and removing any artefacts or unwanted inclusions *e.g.* tissue debris, which were accidently included. An intermediate quality control step was included to separate the secondary lamellae from the base when it interconnected accidently even after segmenting into secondary lamellae. Each tissue area measured has unstained areas appearing to represent vacuoles The vacuolar area of the primary lamellae (VAPL) comprised unstained areas of the tissue stained with Alcian blue and counterstained with haematoxylin and the vacuolar area of the secondary lamellae (VASL), representative of blood channels, were captured by thresholding (highlighting) of the vacuolar area while keeping the epithelial area unselected (Figure 2.13).

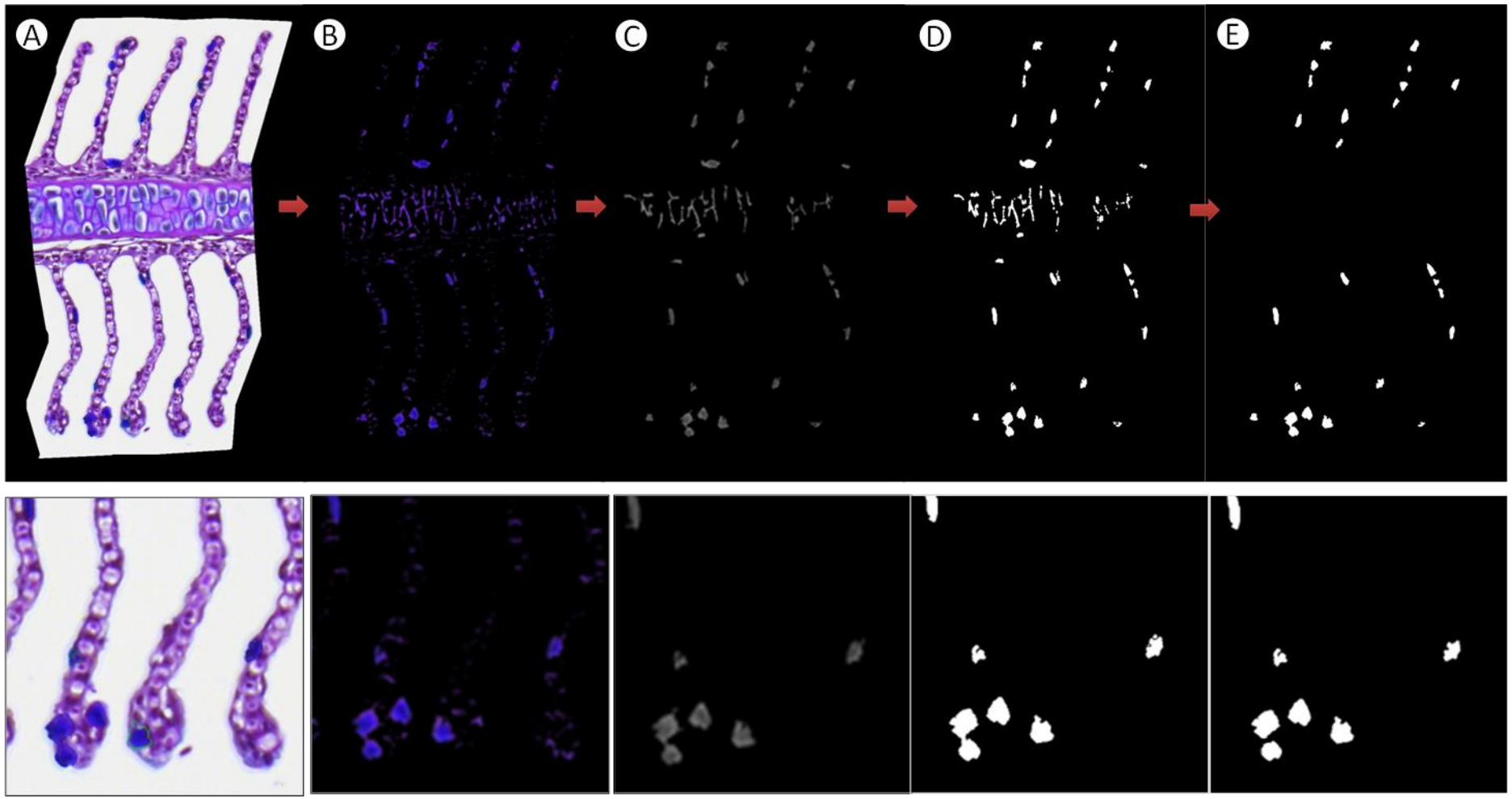

Figure 2.10 Extractions of mucous cells from secondary lamellar area using intensity thresholding. Mucous cells are marked in blue colour. The small micrographs show x 2 original magnification with more details changes during the process.

The area selected in the central venous sinus (CVS) /C (cartilage) was excluded for these automated measurements. Using a region reject operation, mucous cells of the PLA and SLA were screened for any accidental inclusion, these being manually removed. Automated measurement of the SLA was achieved following clicking on selected filaments. Automated measurements of CVS/C, VAPL and VASL were performed after deselecting unwanted accidental inclusions.

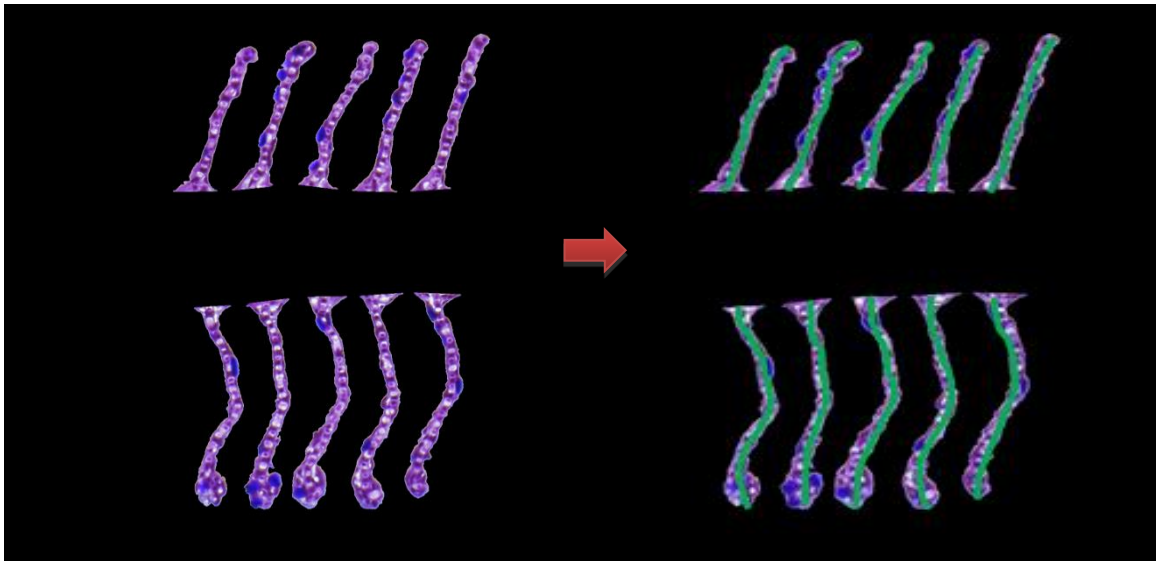

Figure 2.11 Measurement of secondary lamellar length was performed manually by drawing a line base to the tip of the lamellae

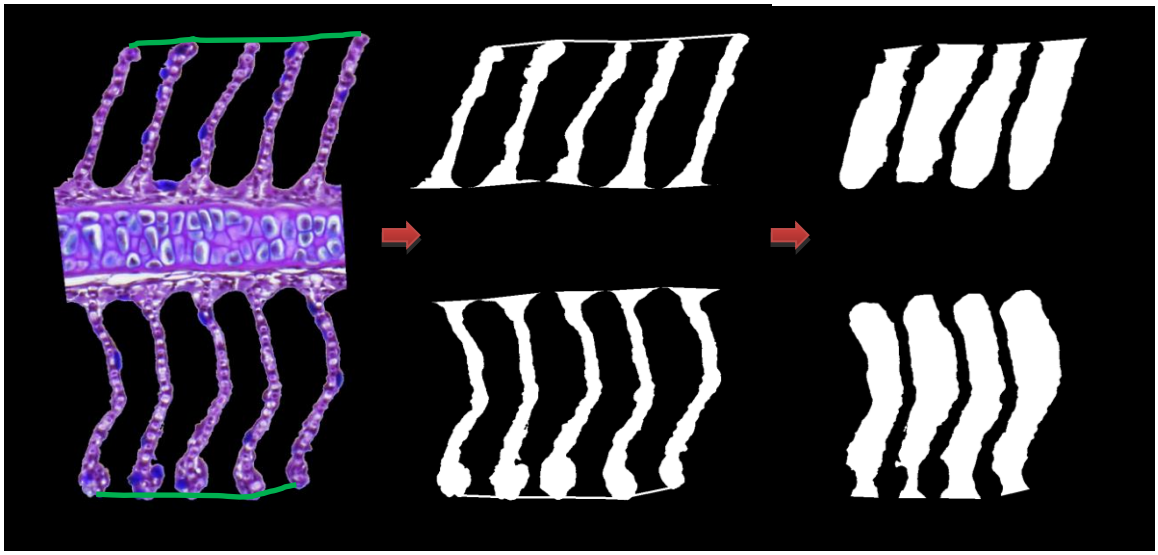

Figure 2.12 Extraction of inter-lamellar space (ILS) from interconnected secondary lamellar area by drawing a line connecting the tips of the secondary lamellae

The perimeter of the secondary lamellae (secondary lamellar perimeter length; SLPL) was measured using an edge detection function which allowed detection/distinction of the boundary of the object from the background. (Figure 2.12). SLPL is an important morphometric measurement of the gills reflecting the cross sectional area of the respiratory surface area of the gills.

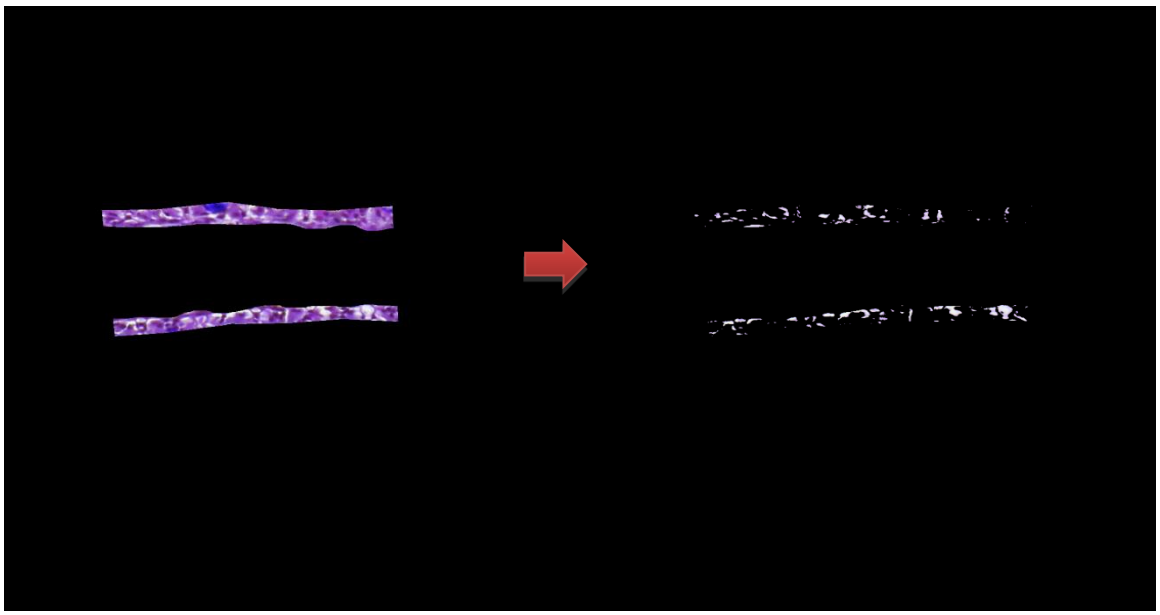

Figure 2.13 Extraction of the vacuolar area of the primary lamellae (VAPL)

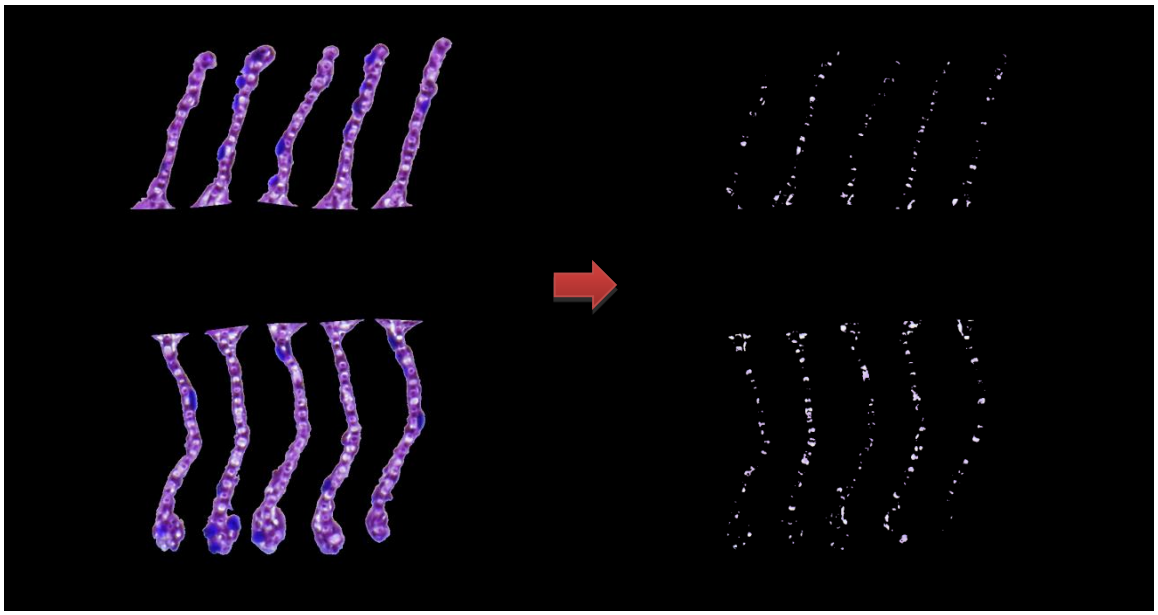

Figure 2.14 Extraction of the vacuolar area of the secondary lamellae (VASL)

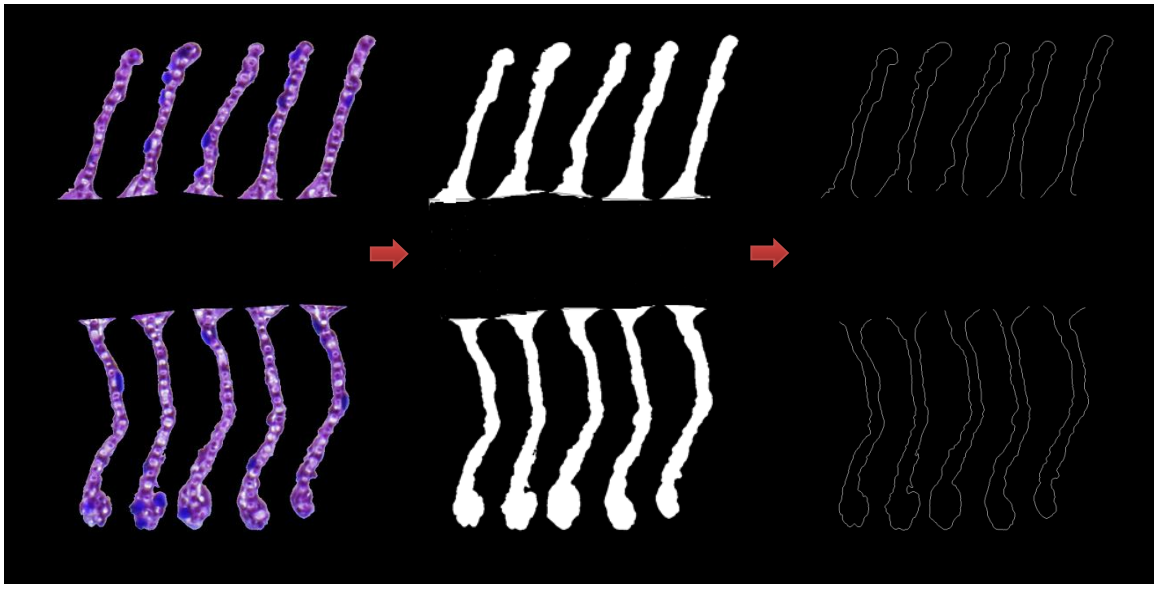

Figure 2.15 Extraction of the secondary lamellar perimeter length (SLPL)

2.2.7 **Data analysis**

2.2.7.1 Pre-processing of data for statistical analysis

After performing GIA tool analysis, data files were uploaded into a software "file-rename utility" to reorganise the files so that they could then be recognised by a task-specific Visual Basic Excel aggregation macro (written by Dr John Taggart, IoA). The complete path and file names were copied using ExplorerXP software (Nikolay Avrionov, 2003-2005.) and subsequently pasted into the Excel segregation macro. The execution of this segregation macro, enabled basic statistical calculations to be undertaken (calculation of mean and median of parameters, *e.g.* meanSLL, medianSSL) and other basic calculations (subtraction of areas to produce new parameters *e.g.* PLEA was generated by subtracting CVS/cartilage from PLA) for a number of measured variables including calculations of some derived variables (ISR, GR) automatically. After performing data aggregation, a large Excel file was generated tabulating all the cases and numerical values for the morphometric variables measured. Before proceeding further, randomly selected files belonging to a few individual cases (sub-samples) were manually calculated to verify the accuracy of the final tabulated results

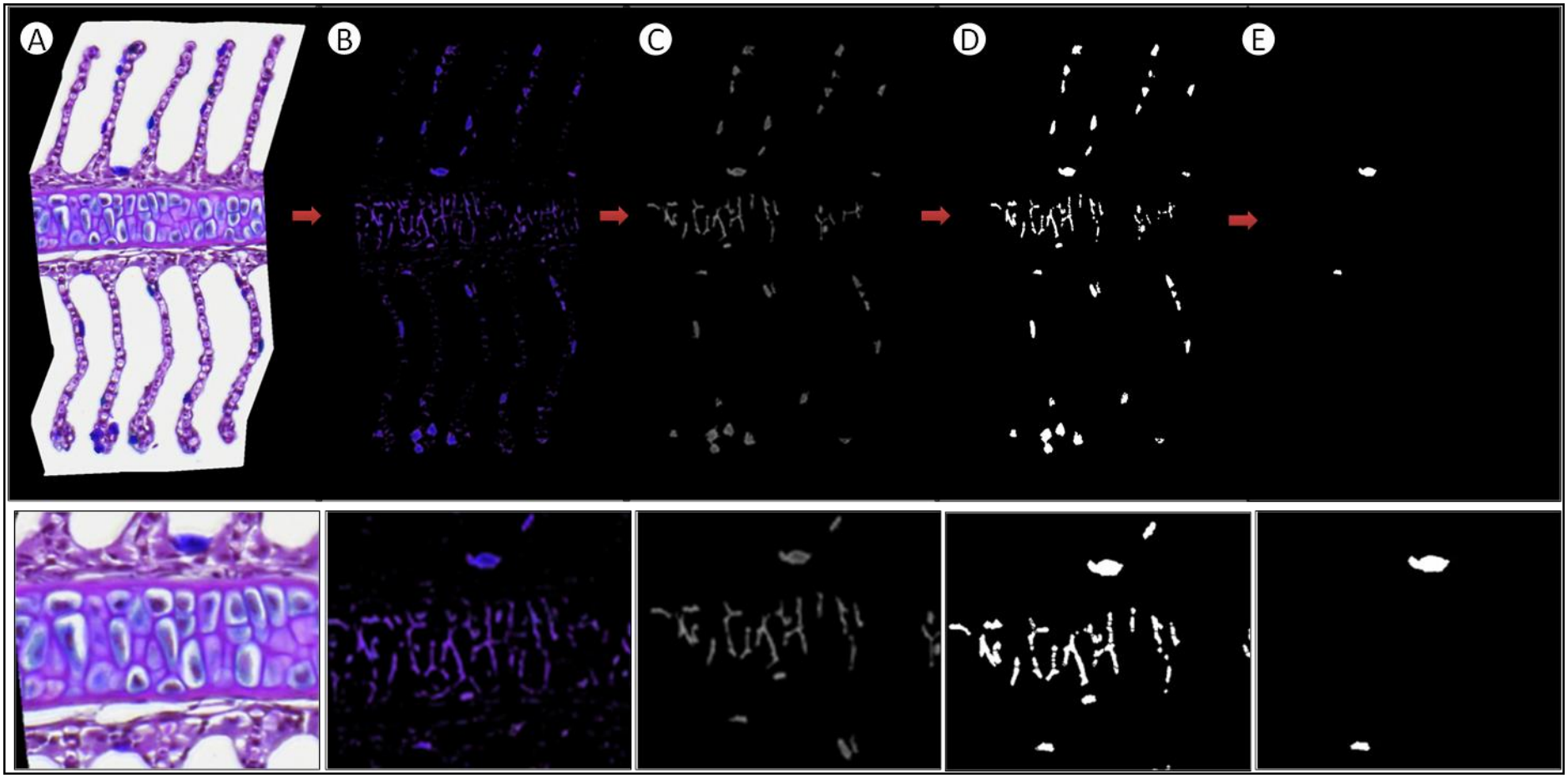

Figure 2.16 Extraction of mucous cells from primary lamellar area (PLA) using colour thresholding and masking. Mucous cells stain blue. The small micrographs show x 2 original magnification detailing the process of extraction.

2.2.7.2 Statistical analysis

Once the data had been verified for accuracy, statistical analyses were performed using Minitab version 16 (Minitab Ltd, Brandon Court, Unit E1-E2, Progress Way, Coventry, CV3 2TE, UK) and SPSS version 19 (IBM, SPSS UK Ltd, First Floor St Andrew's House, West Street, Woking, Surrey, GU21 1EB, UK) software. First, parameters were evaluated for normality by observing individual plots for residuals and normalised plots of residuals. At the same time, behaviour of the data was evaluated by using residuals versus fit and residual versus order plots. Due to the fact that majority of morphometric parameters were not normal, non-parametric analysis of variance (ANOVAs) (Kruskal-Wallis test) were performed in SPSS.

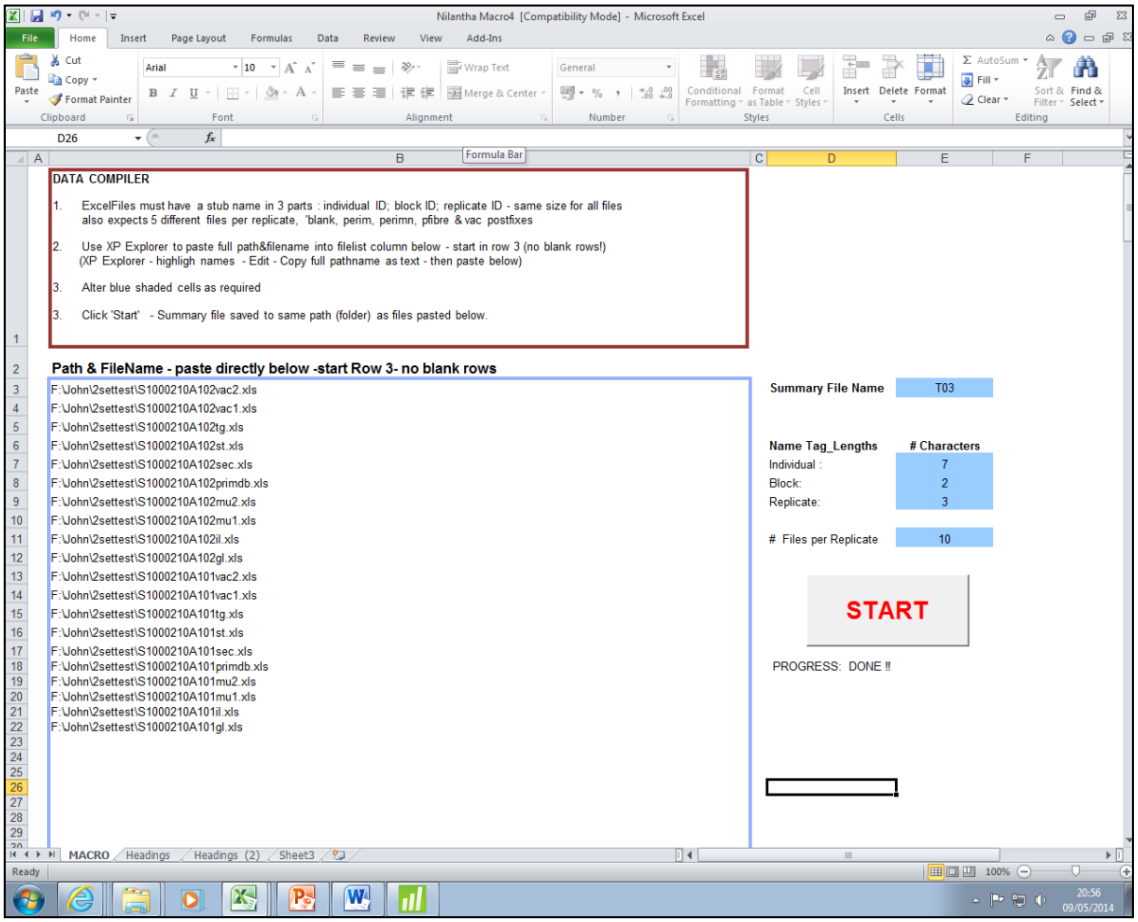

Figure 2.17 The task-specific Visual Basic Excel aggregation macro developed to tabulate GIA output data

2.2.8 **Gene expression analysis**

2.2.8.1 RNA extraction

Total RNA from gills was extracted using an organic solvent extraction method, employing TriReagent (Sigma, Dorset, UK) according to manufacturer's instructions. Briefly, tissue samples (1 ml of TRI reagent for 100 mg of tissue) were incubated at room temperature for 15 min and homogenised using a Polytron mechanical homogenizer (Kinematica; PT1300D) for 2-3 min. Then 100 µl of BCP (1-bromo-3-choropropane, Sigma) was added and shaken vigorously for 15 sec at room temperature before centrifuging at 12,000 g for 15 min at 4 ^{o}C. The aqueous upper phase was transferred to a new nuclease free tube without disturbing the remaining two layers, before adding 250 µl of isopropanol and RNA precipitation solution. Samples were gently inverted 4-6 times and incubated at room temperature for 10 min before centrifuging at 12,000 g for 10 min at 4 ^{o}C. After removing the supernatant, the pellet was washed with 75 % ethanol (Fisher scientific, Loughborough, UK) before samples were centrifuged at 7500 g for 5 min at 4^{o} C. After removing ethanol, the RNA pellet was air dried for 3-5 min at room temperature. Finally, the pellet was dissolved in RNA/DNAse free water for at least 1 h at 4 °C prior to quantification using a Nanodrop 1000. RNA was also subjected to quality assessment by running the sample in 1 % agarose gel made using 0.5 % TAE buffer and stained with ethidium bromide (40 min).

2.2.8.2 cDNA synthesis

The extracted total RNA was reverse transcribed using a high capacity cDNA reverse transcription kit (Applied Biosystems, Paisley, U.K.) following manufacturer's instructions. During the reverse transcription, a mixture of random primers and Oligo dT was used. Prior to the RT reaction, the total RNA was heated at 70 °C for 5 min in a

dry heating block and then placed immediately on ice in order to remove any secondary structures. In brief, 1µg total RNA from gills was dissolved in 10 µL RNase free water and then each sample was combined with 2µL of x10 RT buffer, 0.8µL dNTP mix (100mM mM each), 2µL 500ng/µL anchored oligo-dT 0.5 µL (400 ng/µL) (Eurofins MWG Operon, Ebersberg, Germany) plus random hexamer solution (1:3 ratio), 1µL MultiScribe TM reverse transcriptase, 1 µL of RNase inhibitor and 3.2 µL of nuclease free water to make final reaction volume of 20 µL in total. Negative controls (RT-) were set up without enzyme to confirm that no genomic DNA contamination existed in the samples. Then samples were placed on a Biometra R thermocycler to perform the reverse transcription reaction by incubating at 25 ^{o}C for 10 min followed by 37 ^{o}C for 2 h prior to 85 ^{o}C for 5 min to inactivate the DNA polymerase. The cDNA samples were placed directly on ice for immediate PCR or frozen at -20 °C for later analysis.

2.2.8.3 Primer optimisation using conventional PCR reaction

Conventional PCR was used to optimise the target primers for subsequent reverse transcription polymerase chain reaction RT-PCR (Table 2.2). Primer annealing temperature was established by amplifying them at a 5 degree lower temperature than the calculated mean value of the melting temperatures of the forward and reverse primers. The PCR was performed using Reddy Mix PCR Master mix (Thermo Scientific, Epsom, Surrey, UK), which includes Taq DNA polymerase and $MgCl_2$ with appropriate amount of random hexamers. For the RT-PCR reaction, 10 µL of Reddy Mix PCR master mix were added with a 1 µL volume of each forward and reverse primer (Eurofins, MWG, Germany) of 10 µM concentration and 3 µL volume of undiluted cDNA, with 5 µL of PCR grade water to make a 20 µL total reaction volume. The PCR was performed on a Biometra R thermo cycler with an initial denaturation of 95 °C for 5 min, followed by 36 cycles of 95 °C for 25 sec, annealing temperature 48-

63^{o}C (see the Table 2.2 for annealing temperatures for each individual primers) for 35 sec and 72 °C for 65 sec, followed by a single final extension cycle step of 72 °C for 5 min.

PCR products were examined on a 1% agarose gel stained with 83 ng/ml ethidium bromide (Sigma, UK). Four microlitres of the PCR product were mixed with 1µL 6 x loading dye (Roche, West Sussex, UK) and loaded onto the agarose gel and electrophoresis run at 80 V for 45 min in 0.5 % TAE buffer. The size of the PCR product was determined relative to a GeneRularTM 100 bp DNA ladder (Roche). Gel imaging was performed under UV illumination. If products were not reliable, a further evaluation by temperature gradient PCR was performed in a Biometra R thermocycler to select the best temperature to obtain a reliable product. Only primers that produced a specific band corresponding to the expected PCR product size were used for primer efficiency testing for real time PCR.

The quantitative reverse transcription polymerase chain reaction (RT-qPCR) analysis of each sample was carried out in triplicate, using a Techne Quantica Real Time PCR Thermal Cycler (Techne, UK). Individual qPCR reactions of 20 µl were prepared in the wells of 96 well clear plates (Starlab, UK), consisting of 5 µl of 10^{-1} dilution of the total RNA derived cDNA, 1 µl of 10 µM forward and reverse primer, 10 µl of PCR master mix and 3 µl of nuclease free water. The cycling conditions used for the assays are given in Table 2.3 together with the optimised annealing temperatures. Primer efficiency (E) and relative co-efficiency of the standard curve were optimised before use in the actual test.).

Table 2.2 The qPCR primers used to measure changes in the gills of fish following feeding of different functional feeds

Transcript (Target genes)	Primer name	Primer sequence	Fragment	Tm	Accession No	Source
Mx protein	As_Mx_F As_Mx_R	ACGTCCCAGACCTCACACTC GTCCACCTCTTGTGCCATCT	200	58°C	NM_001123582.1	Herath *et al.*, (2010)
CHE chemokine like protein	As_CHE_F As_CHE_R	TGGACCGCCTCATCAAGAAGTGC ATGGGGGTGGAGGTGGTGGTGTT	131	59° C	BT125321.1	New primer
SAA5	As_SAA_F As_SAA_R	ACTTCCACGCTCGGGGCAACT CCCTGAACCATCTCCCGGCCA	97	58°C	NM_001146565.1	New primer
Reference genes						
Beta actin	As_ βactin_F As_ βactin_R	ACTGGGACGACATGGAGAAG GGGGTGTTGAAGGTCTCAAA	157	58°C	NM_001123525.1	Herath *et al.*, (2010)

The mean of Ct values of triplicates used in the assay were exported into Excel (Microsoft, USA) and expression levels of the CHE chemokine like protein, SAA and Mx protein were calculated using Relative Expression Software Tool (REST® software) (REST 2009 and REST 284) relative to β actin (Figure 2.18) (Pfaffl, *et al.*, 2002)

Table 2.3 Thermal cycling conditions used in the Techne Quantica® Thermal cycler for the RT-qPCR assay to quantify target associated genes.

Enzyme activation	15 min	at	95°C	
Denaturation	20s	at	95°C	45 cycles
Annealing	20 s	at optimal temperature		
Extension	30s	at 72°C		
Dissociation peak 70-90°C measured every 0.5°C				

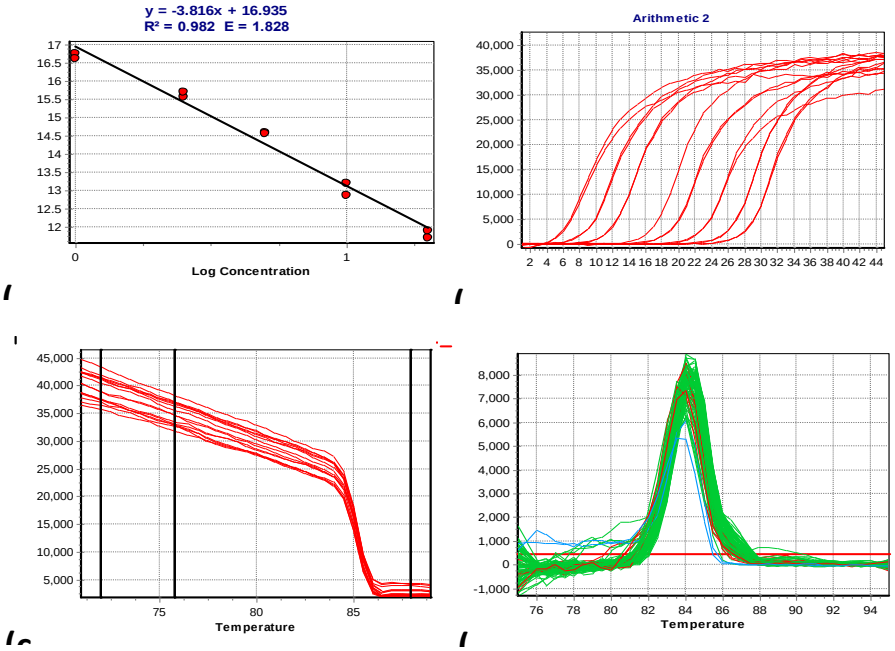

Figure 2.18 Results of RT-qPCR for reference gene β actin (a) standard curve generated from ct values (y-axis) versus 10-fold dilution of pool cDNA of all samples, (b) RT-qPCR amplification curves (c,d) dissociation curve (melting curve) analysis of RT-qPCR of the standard sample to determine specificity of the end product

2.2.8.4 Pre-processing of data, normalisation and relative quantification

In parallel to the histomorphometric analysis of Atlantic salmon gills, a set of key genes was evaluated to see whether any pathophysiological alteration related to inflammation, acute phase response or antiviral response were elicited. The genes selected for gene expression analysis comprised β actin (reference gene), CHE chemokine like proteins (CHE CC), Atlantic salmon serum amyloid A (SAA) and Mx protein. For analysis, the mean Ct values were calculated per technical replicate sample prior to calculating a mean for each dietary group. The reaction efficiency of each test gene and reference gene was between 1.8 to 2.0 (maximum 2).

2.2.8.5 Statistical analysis

Statistical differences between groups were calculated using REST® 2009 software. The normalised mean gene expression values (normalised to reference gene β actin) were transformed to log 2 ratios and expressed as fold change.

Table 2.4 Ccalculation of mean relative gene expression values using relative expression software tool (REST) (Schmittgen and Livak, 2008: Pfaffl *et al.*, 2002).

$$R = \frac{(E_{target})^{\Delta CP target\ (MEAN\ control - MEAN\ sample)}}{(E_{ref})^{\Delta CP ref\ (MEAN\ control - MEAN\ sample)}}$$

2.3 Results

2.3.1 Conventional histological analysis

No significant histopathology changes were observable between dietary groups for H&E stained gills or Alcian blue/PAS (mucous cell) stained sections under light microscope observation. The bulbous enlargements observed at the tip of the lamellae (Figure 2.19, 2.20 and 2.21) was regarded as nonspecific.

2.3.2 Morphometric analysis of Atlantic salmon gills after feeding with two functional diets

Quantification of possible histomorphometric changes resulting from long-term feeding of functional diets (final sampling) was conducted using the developed GIA tool. The results were categorised and presented according to different areas of the gills: (1) primary lamellar area associated gill parameters, (2) secondary lamellar associated gill parameters, (3) mucous cell associated morphometric parameters, (4) total gill area associated morphometric parameters. The morphometric parameters that significantly changed over time are evaluated and graphically presented below.

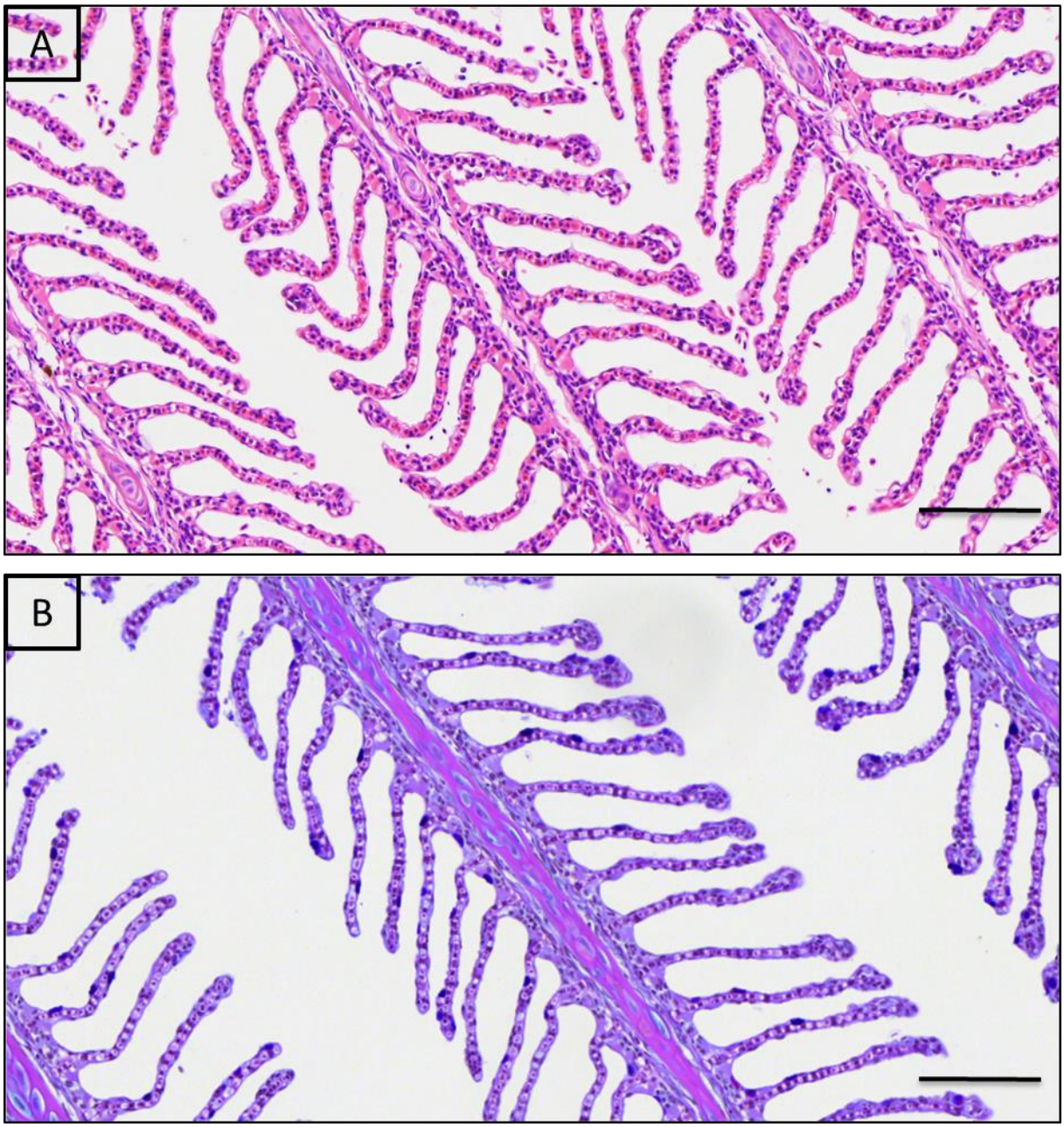

Figure 2.19 Micrographs of gill derived from dietary group A, stained (A) H & E for conventional histology (B) PAS / Alcian blue with haematoxylin for mucous cell histochemistry. Note normal gill morphology with early stage of clubbing at the distal ends of the secondary lamellae. Scale bar 100 μm.

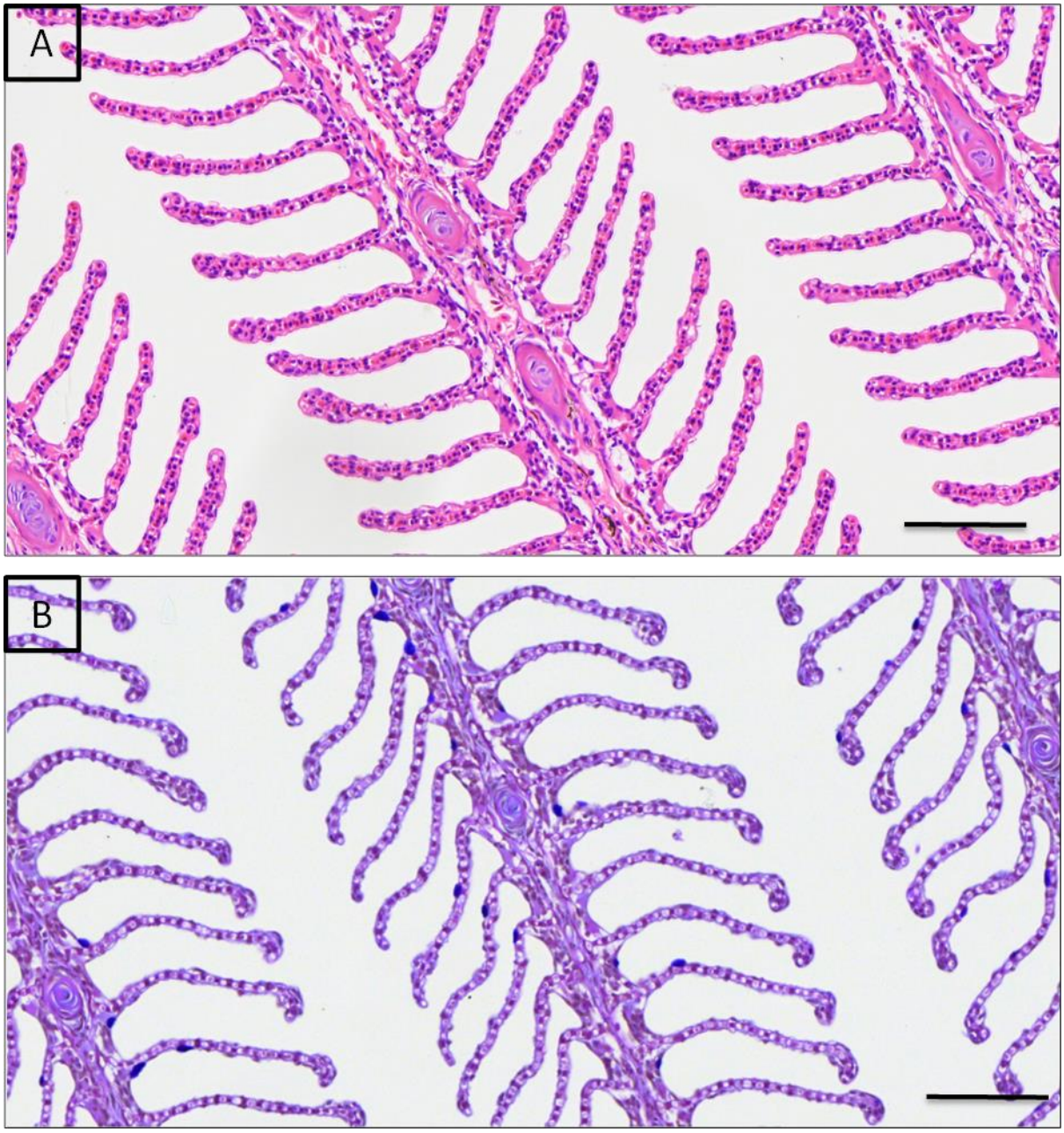

Figure 2.20 Micrographs of gill derived from dietary group B, stained (A) H & E for conventional histology (B) PAS / Alcian blue with haematoxylin for mucous cell histochemistry. Note normal gill morphology with initial stage of clubbing at the distal ends of the secondary lamellae Scale bar 100 μm

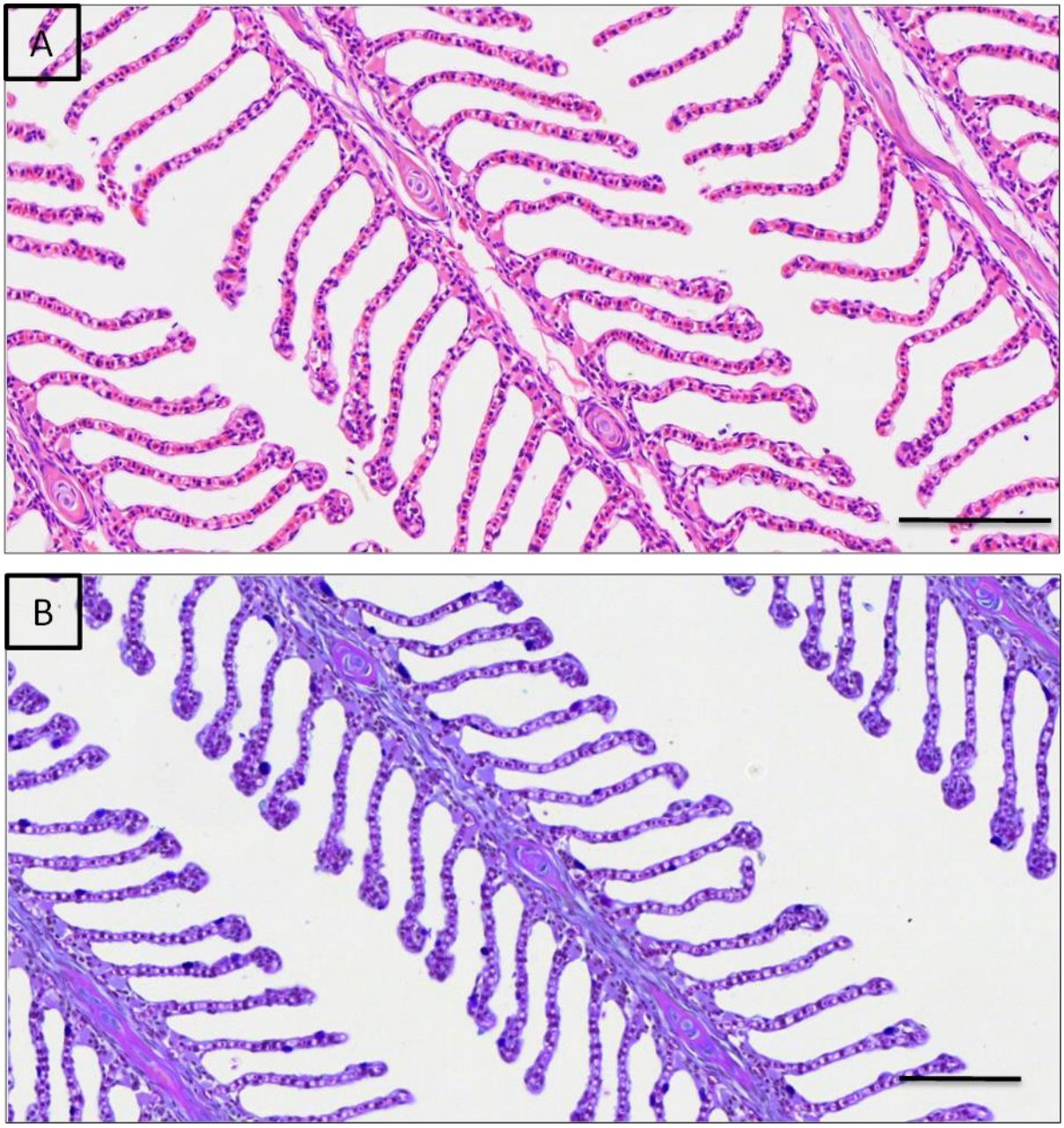

Figure 2.21 Micrographs of gill derived from dietary group C, stained (A) H & E for conventional histology (B) PAS / Alcian blue with haematoxylin for mucous cell histochemistry. Note normal gill morphology with initial stage of clubbing at the distal ends of the secondary lamellae (A) 125 µm, (B) 100 µm.

2.3.2.1 Non parametric analysis of morphometric data

The newly developed GIA tool was used to quantify morphometric changes in the gills fed with two different functional diets compared to control diet. The raw data generated from the KSRUN GIA platform were tabulated to obtain mean morphometric values for various gill parameters obtained from four replicate sections per individual fish. Statistical analysis was performed in SPSS version 19. Data were first subjected to quality assurance and then tested using relevant statistical tests to identify their significance. First, the data were tested for normality, and where not normal, they were subjected to a number of transformations. Despite testing a number of transformations *e.g.* Log 10, square root, the normality and homogeneity of variance assumptions were not met and thus appropriate non-parametric tests were employed. Each parameter was evaluated using a Kruskal Wallis test and the results of multiple comparisons between diets were performed using *post hoc* tests following the Kruskal Wallis. The cut off value for significance was $p \leq 0.05$. The *post hoc* test for multiple comparison between functional feeds were conducted using Mann-Whitney U tests where significance of the parameter was indicated when $p < 0.05$. Summary data comprised mean value, standard error mean (SEM) and data on statistical significance are provided in Table 2.5. Of the measured parameters, the vacuolar area of secondary lamellae (VASL) and the total gill area (TGA), were found to be significantly different across the test diets relative to the control salmon feed (Table 2.5).

Table 2.5 Results of measured morphometric variables of Atlantic salmon gill fed with three different diets.

Acronyms	Kruskal Wallis test	Multiple comparison between diets (Mann-Whitney U test)								
	Diet	Diet A			Diet B			Diet C		
	p value	Mean	SEM	Significance	Mean	SEM	Significance	Mean	SEM	Significance
VAPL	0.576	1154.58	124.05	A	1369.12	182.56	A	2231.30	441.07	A
VASL	0.036*	687.02	74.33	B	1054.82	152.38	A	1042.82	95.51	AB
TGA	0.012*	33679.64	1116.57	B	40246.72	1485.69	A	36091.73	1779.15	AB
SLA	0.183	16002.04	522.52	A	16920.04	693.23	A	17166.36	408.36	A
PLA	0.066	17677.60	928.54	A	23326.69	1647.44	A	18925.38	1767.95	A
ILS	0.523	25040.75	1032.18	A	27665.71	1458.67	A	26451.48	1184.33	A
GR	0.122	1.00	0.06	A	0.86	0.08	A	1.09	0.07	A
ISR	0.858	1.63	0.09	A	1.63	0.05	A	1.55	0.07	A
PLEA	0.208	8062.61	326.40	A	9278.55	392.24	A	9750.42	799.24	A
TMCA	0.528	352.14	52.91	A	281.31	32.10	A	243.18	24.21	A
TMCA/TGA	0.243	0.0104	0.0015	A	0.0072	0.0009	A	0.0070	0.0007	A
SLPL	0.152	3585.00	98.29	A	3966.61	160.28	A	3734.32	79.14	A
MedianFERETMinSL	0.114	37.56	1.26	A	39.68	1.55	A	35.37	0.81	A
MedianFERETMaxSL	0.072	142.77	3.29	A	155.03	4.64	A	152.36	2.91	A
MCN-PLEA	0.462	1.28	0.19	A	1.38	0.27	A	1.52	0.20	A
MCA-PLEA	0.549	45.74	7.48	A	52.43	11.12	A	55.88	8.12	A
(MCA-PLEA)/PLEA	0.735	0.0059	0.0010	A	0.0058	0.0012	A	0.0065	0.0010	A
(MCN-SLA)	0.734	8.36	1.08	A	7.38	0.65	A	6.45	0.69	A
(MCA-SLA)	0.410	306.76	49.67	A	229.37	26.30	A	187.57	21.85	A
(MCA-SLA)/SLA	0.247	0.02	0.00	A	0.0138	0.0015	A	0.0108	0.0012	A
TMCN	0.880	9.64	1.17	A	8.75	0.79	A	7.97	0.73	A
TMCN/TGA	0.477	0.00029	0.00004	A	0.00023	0.00002	A	0.00023	0.00002	A
MedianSLL	0.193	143.26	3.59	A	154.95	5.42	A	149.20	3.24	A
(SLPL/SLA)	0.057	0.2278	0.0053	A	0.2372	0.0056	A	0.2203	0.0057	A
(SLPL/MeanSLL)	0.751	25.10	0.23	A	25.47	0.30	A	25.18	0.39	A

* indicates significance level at $p \leq 0.05$, Different letters across the three diet significance columns for a given parameter (row) indicate significant differences between diets. The highest mean of time points of each measured parameter was denoted as A and subsequent time points were indicated in alphabetical order considering the mean value highest to lower. Letters correspond to graphs shown below

2.3.2.2 Primary lamellae-associated morphometric parameters

During the feed trial, primary lamellae associated measured morphometric parameters were not significantly changed ($p>0.05$) after feeding with the different functional diets *i.e.* vacuolar area of primary lamellae (VAPL), the primary lamellar epithelial area (PLEA) and the primary lamellar area (PLA) (Figure 2.22).

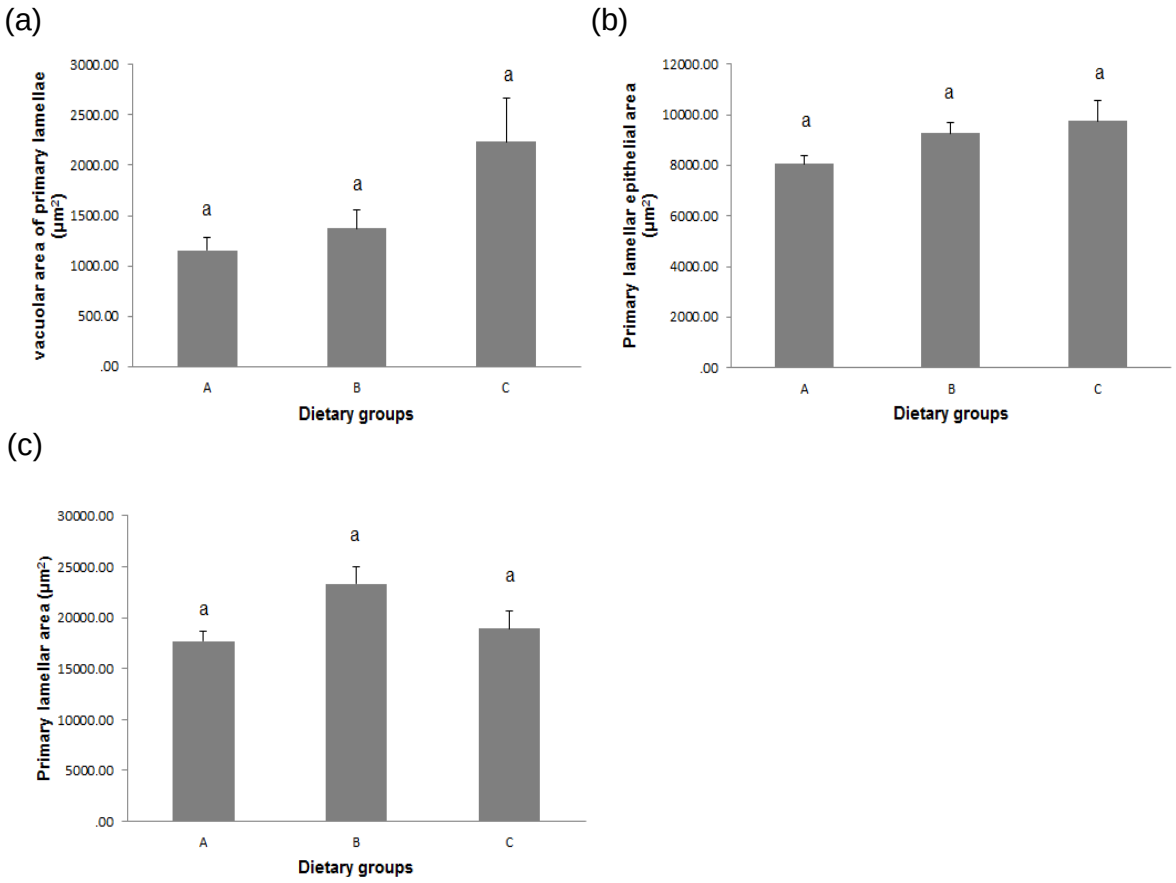

Figure 2.22 Primary lamella-associated morphometric changes in Atlantic salmon gills fed with different functional diets. (a) vacuolar area of primary lamellae (VAPL); (b) primary lamellar epithelial area (PLEA); (c) primary lamellar area (PLA) Abbreviations: 0H - pre-trial control; H-hours post exposure; D – days post-exposure. Bars represent mean values ± SEM where n=9. Different letters indicate significantly different values ($p< 0.05$) from Kruskal Wallis *post-hoc* tests

2.3.2.3 Secondary lamellae associated morphometric parameters

The majority of secondary lamellae associated morphometric parameters were not found to be significantly different in functional feeds compared to control group (Figures 2.23, 2.24), however VASL were significantly different in diet B compared to control diet A but not diet C.

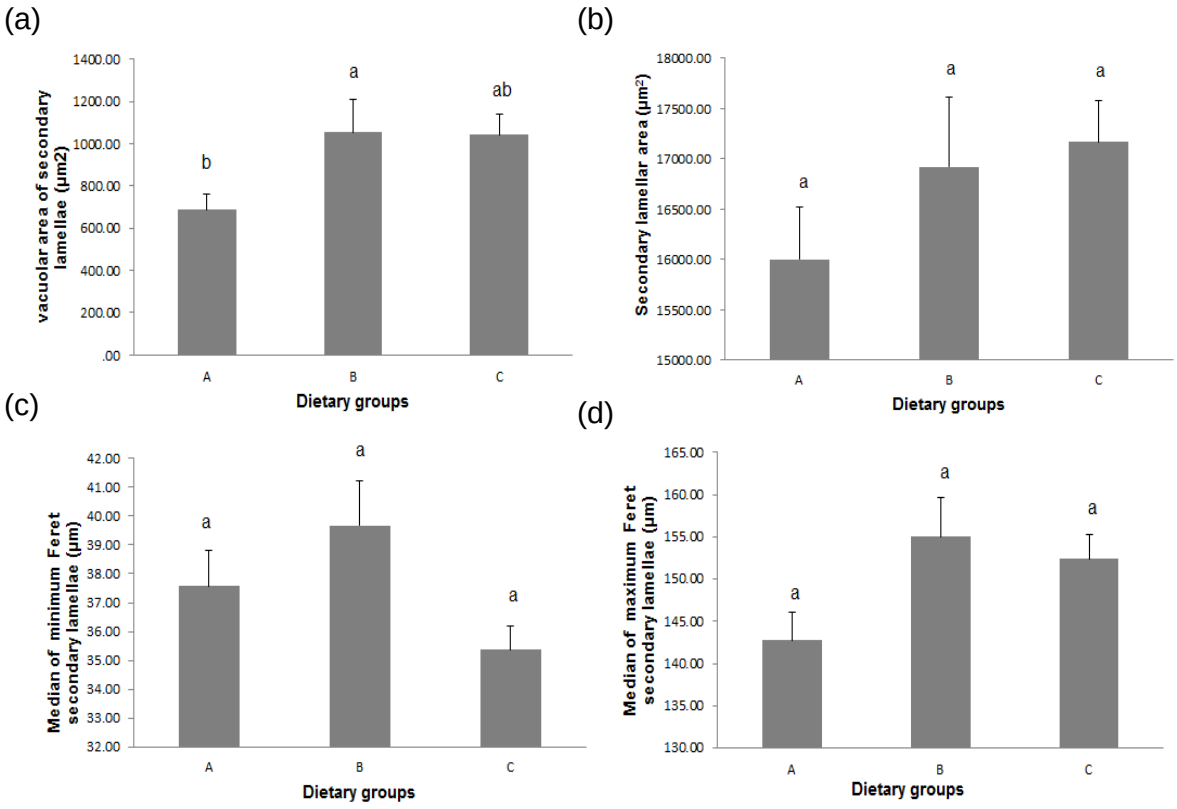

Figure 2.23 Secondary lamellae associated morphometric changes in gills of Atlantic salmon fed with different functional diets. (a) vacuolar area of secondary lamellae (VASL); (b) secondary lamellar area (SLA); (c) median minimum Feret value for secondary lamellae (MeanFERETMinSL); (d) median maximum Feret value for secondary lamellae (MedianFERETMaxSL), error bars represent means values ± SEM where n=9. Different letters indicate significantly different values at $p \leq 0.05$ from Kruskal Wallis *post-hoc* tests.

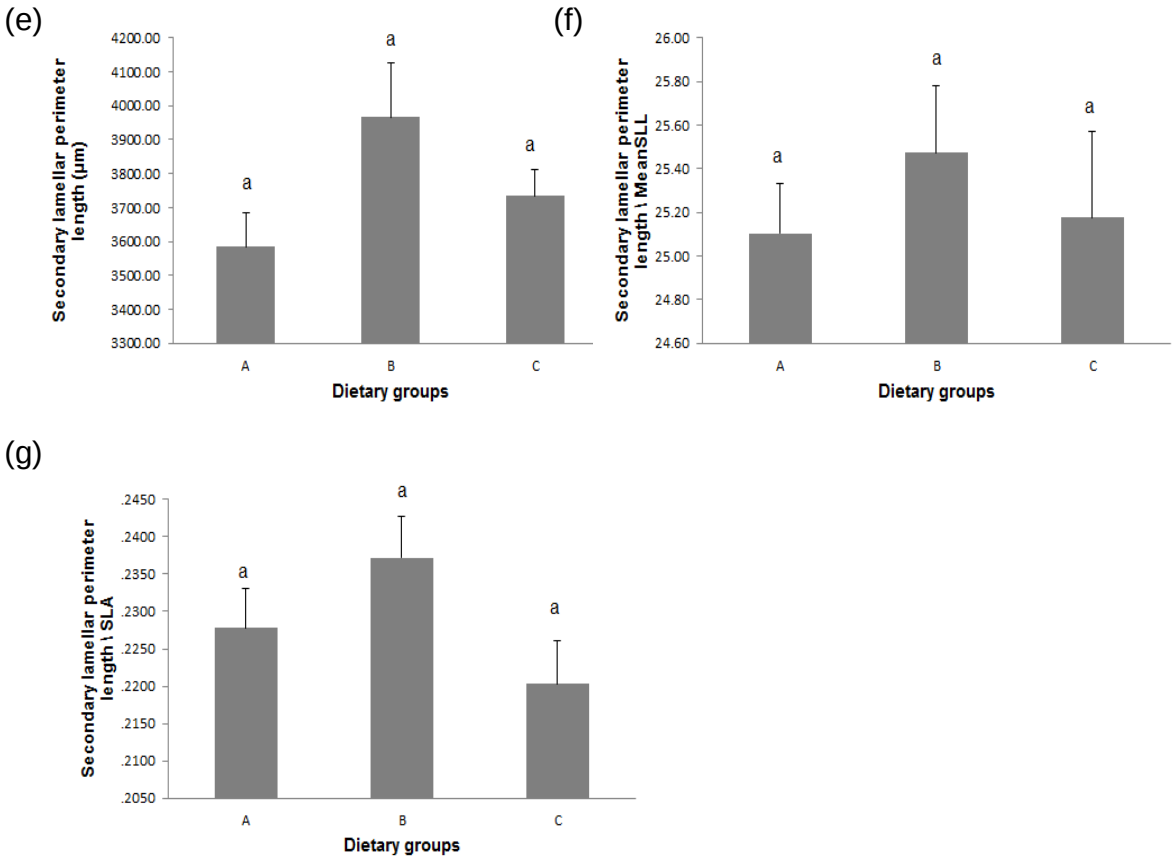

Figure 2.24 Secondary lamellae associated morphometric changes in gills of Atlantic salmon fed with different functional diets continued. (e) Secondary lamellar perimeter length (SLPL), (f) SLPL/SLA, (g) (SLPL/MedianSLL). Bars represent means values ± SEM where n=9. Different letters indicate significantly different values at $p \leq 0.05$ from Kruskal Wallis *post-hoc* tests.

2.3.2.4 Mucous cell associated morphometric parameters

The mucous cell associated morphometric parameters were not found to be significantly different in functional feeds compared to control group (Figures 2.25, 2.26).

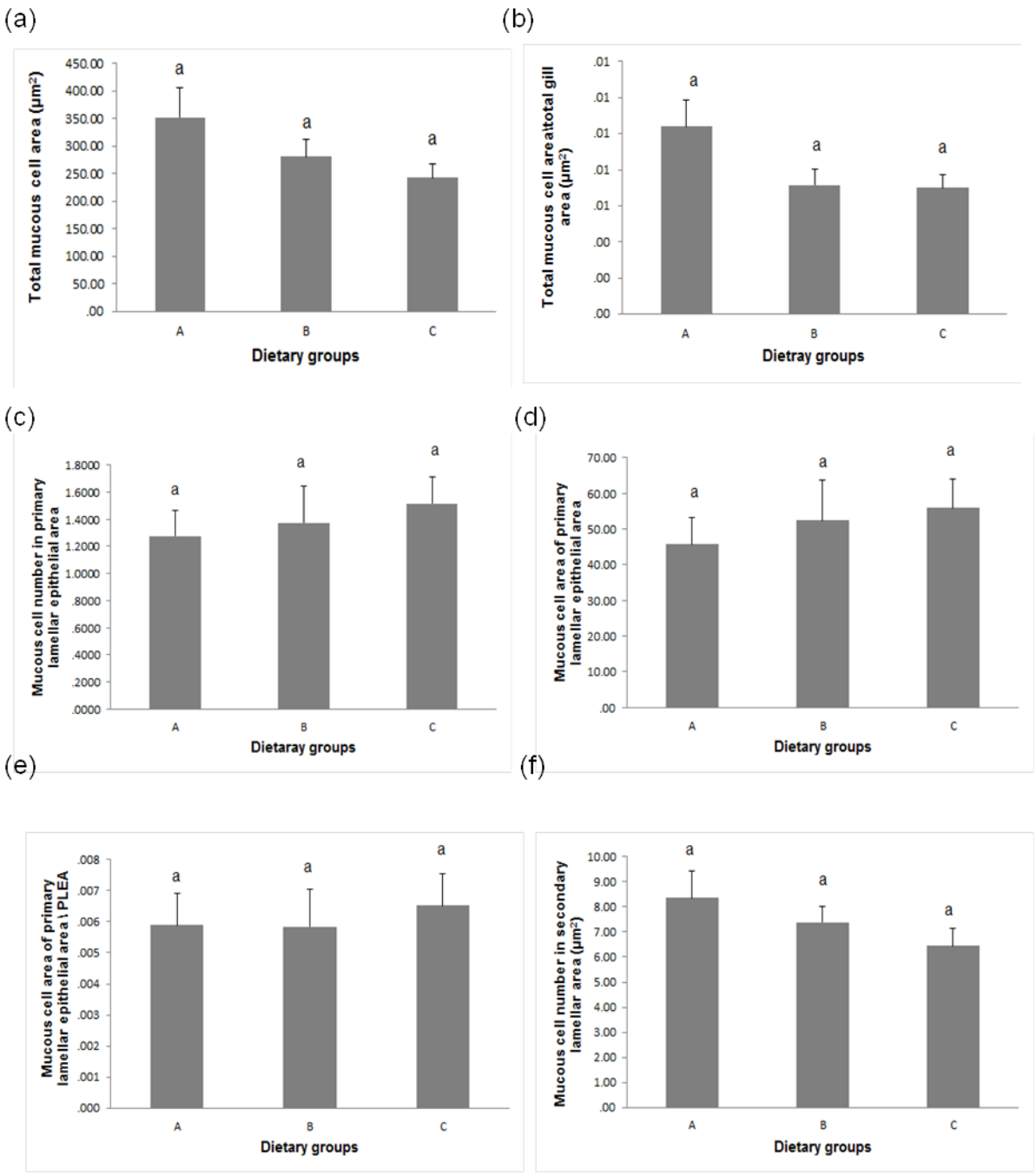

Figure 2.25 Mucous cell associated morphometric changes in the gills of Atlantic salmon fed with different functional diets. (a) total mucous cell area (TMCA); (b) total mucous cell area / total gill area (TMCA\TGA); (c) mucous cell number in primary lamellar epithelial area (MCN-PLEA); (d) total mucous cell area in primary lamellar epithelial area (MCA-PLEA); (e) mucous cell area in primary lamellar epithelial area / primary lamellae epithelial area (MCA-PLEA)/PLEA; (f) mucous cell number secondary lamellar area (MCN-SLA); Bars represent mean values ± SEM where n=9. Different letters indicate significance of difference at $p \leq 0.05$ from Kruskal Wallis *post-hoc* tests.

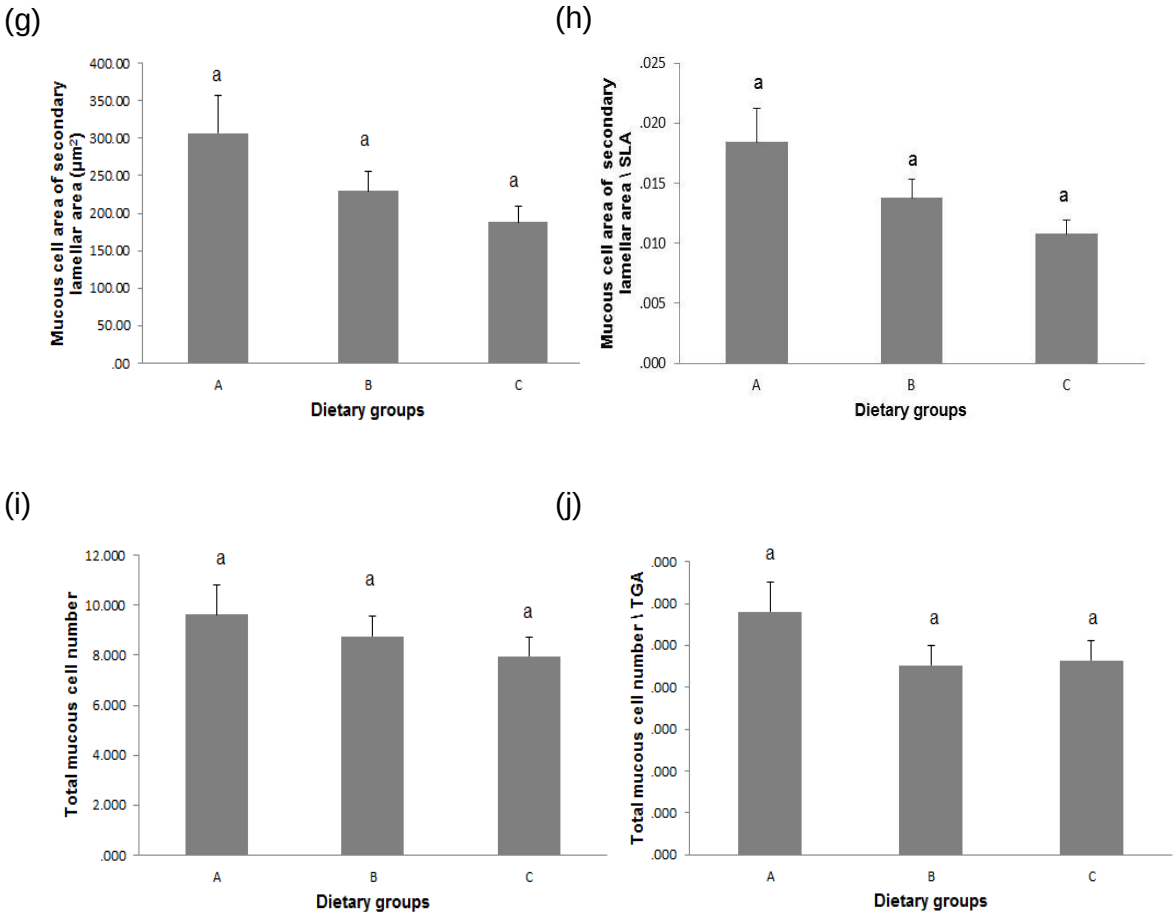

Figure 2.26 Mucous cell associated morphometric changes in the gills of Atlantic salmon fed with different functional diets continued (g) Mucous cell area of secondary lamellar area (h) mucous cell area of secondary lamellar area / secondary lamellar area (MCA-SLA); (i) total mucous cell number (TMCN), (j) TMCN/TGA. Bars represent mean values ± SEM where n=9. Different letters indicate significance of difference at $p \leq 0.05$ levels from Kruskal Wallis *post-hoc* tests

2.3.2.5 Total gill area associated morphometric parameters

Generally, total gill area associated morphometric changes in functional with respect to standard diets were not found to be altered significantly ($p>0.05$) (Figure 2.27). However TGA in diet B was significantly higher (($p<0.05$) compared to control diet A, not to diet C (Figure 2.28).

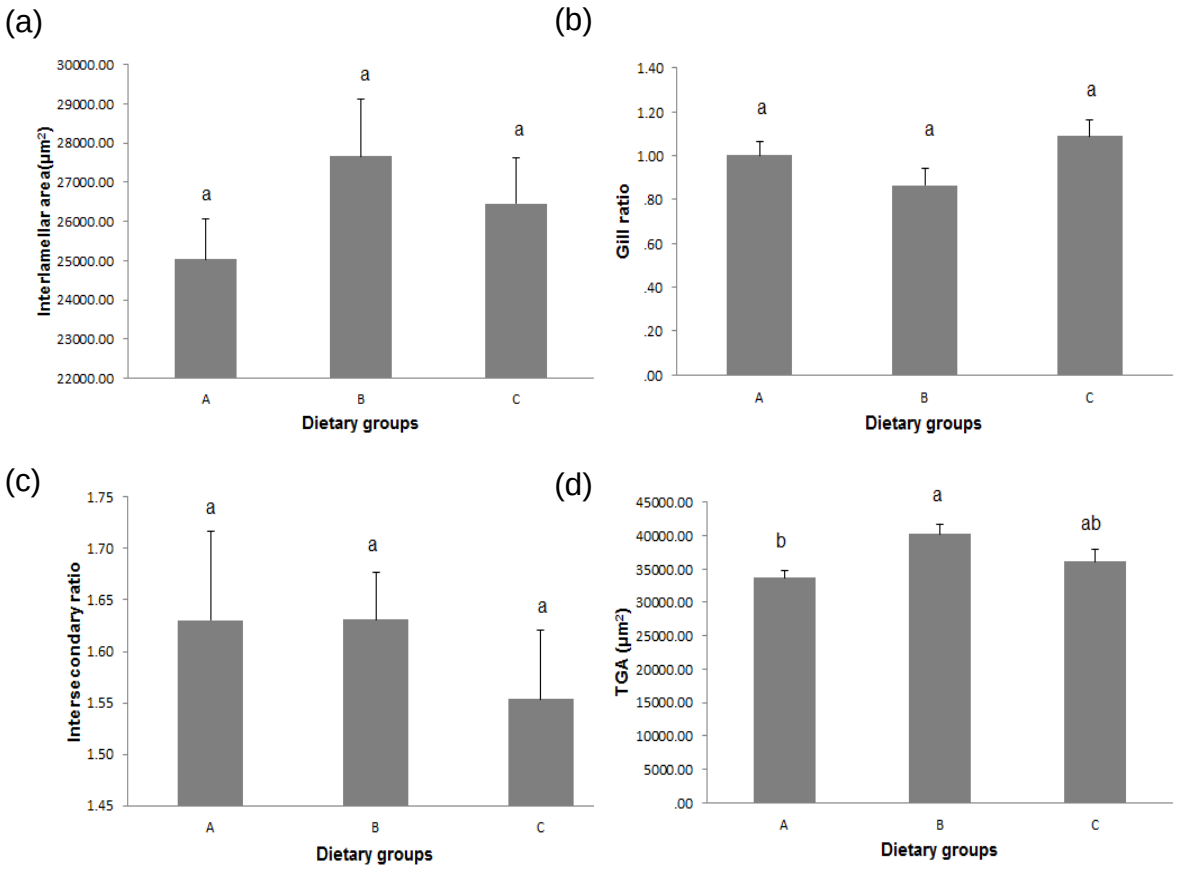

Figure 2.27 Total gill area associated morphometric changes in the gills of Atlantic salmon fed with different functional diets. (a) Interlamellar area (ILS); (b) gill ratio (GR); (c) inter-secondary ratio (ISR); (d) total gill area (TGA). Bars represent means values ± SEM where n=14. Different letters indicate significantly different values ($p \leq 0.05$) from Kruskal Wallis *post-hoc* tests

From the above results, it was clear that the histomorphometric changes in the gill induced by the functional and standard diets were not significantly different to be discriminated by univariate analysis.

2.3.3 **Multivariate analysis of morphometric data (PCA)**

Multivariate analysis of the morphometric data derived from the Lerang feed trial (final sampling) was performed using PCA in Minitab (Minitab Ltd, UK) statistical software, to explore the relationships between variables (morphometric parameters) (Kvalheim and Karstang, 1987). All measured variables were used to perform PCA, the results of which are shown in Table 2.6 – 2.8. The column "Total" gives the eigenvalue or the

amount of variance in the original variables accounted for by each component. The '% variance column' gives the ratio, expressed as a percentage of the variance, accounted for by each component of the total variance. The'Cumulative % column' gives the percentage of variance accounted for by the first 10 components (only the first 10 components are displayed in the Table 2.6).

Table 2.6 Total variance of extracted first 10 principal components using 25 measured morphometric parameters.

Communalities		
Morphometric variables	**Initial**	**Extraction**
Vacuolar area of primary lamellae (VAPL)	1.000	0.719
Vacuolar area of secondary lamellae (VASL)	1.000	0.810
Total gill area (TGA)	1.000	0.931
Secondary lamellar SPASE (SLS)	1.000	0.971
Primary lamellar area (PLA)	1.000	0.938
Interlamellar area (ILS)	1.000	0.904
Gill Ratio (GR) (GR=SLA/PLA)	1.000	0.843
Intersecondary ratio of gill (ISR)	1.000	0.805
Primary lamellar epithelial area (PLEA)	1.000	0.913
Total mucous cell area (TMCA)	1.000	0.979
Total mucous cell area over total gill area (TMCA / TGA)	1.000	0.953
Secondary lamellar perimeter length (SLPL)	1.000	0.976
Median minimum Feret secondary lamellae (MedianFERETMinSL)	1.000	0.565
Median maximum Feret secondary lamellae (MedianFERETMaxSL)	1.000	0.917
Mucous cell number in PLEA	1.000	0.949
Mucous cell area in PLEA	1.000	0.964
(MCA-PLEA)/PLEA	1.000	0.883
Mucous cell number in secondary lamellar area	1.000	0.955
Mucous cell area of secondary lamellar area	1.000	0.973
Mucous cell area of secondary lamellar area over with secondary lamellar area	1.000	0.938
Total mucous cell number (TMCN)	1.000	0.965
Total mucous cell number corrected for total gill area (TMCN / TGA)	1.000	0.947
Median secondary lamellar length (MedianSLL)	1.000	0.977
Secondary lamellar perimeter length over secondary lamellar area (SLP/SLA)	1.000	0.954
Secondary lamellar perimeter length over mean secondary lamellar length (SLP/MeanSLL)	1.000	0.810

The first ‘Component’ has the largest eigenvalue and explains the most variance. The first component explains nearly 31% of the variation between individuals. The first two ‘components’ combined explain 53% (‘Cumulative %’) of the variation between individuals between them. A scree plot (Figure 2.28) shows the key principal components, levelling off after the fifth principal component (Table 2.7).

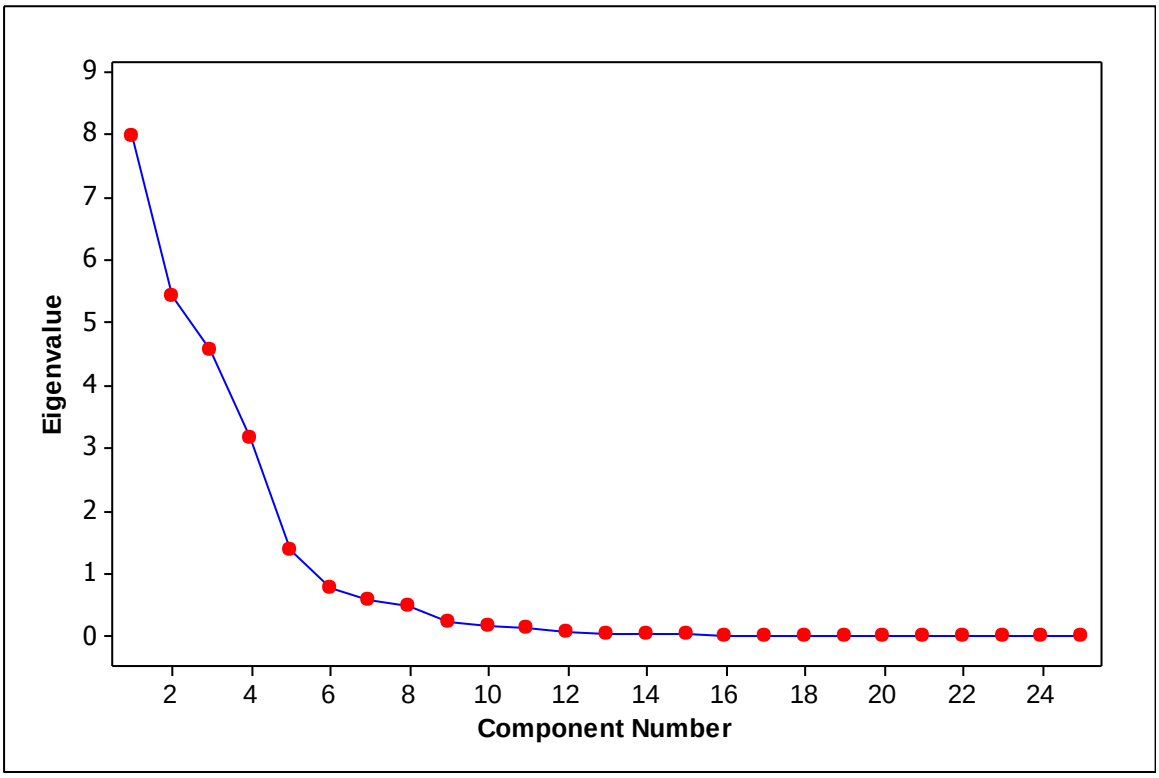

Figure 2.28 Scree plot of Eigenvalues of relevant principal components

Table 2.7 Total variance explained by the first 5 principal components (25 measured morphometric parameters)

Total Variance Explained						
	Initial Eigenvalues			**Extraction Sums of Squared Loadings**		
Component	Total	% of Variance	Cumulative %	Total	% of Variance	Cumulative %
1	7.983	31.931	31.931	7.983	31.931	31.931
2	5.432	21.728	53.658	5.432	21.728	53.658
3	4.567	18.269	71.927	4.567	18.269	71.927
4	3.169	12.676	84.604	3.169	12.676	84.604
5	1.381	5.525	90.129	1.381	5.525	90.129

The rotated component matrices (Table 2.8) were used to compare the relationships of the variables contributing to the key Principal Components. 2D scatterplots of pairs of components (for PC1-PC5) showed minimal structuring save for the plotting of PC3 vs PC5. A plot of component loadings for PC3 vs PC5 is given in Figure 2.29. PC3 can be seen to be largely dependent upon TGA, PLA, ILS, ISR, PLEA and MedianSLL of which, TGA, PLA ILS and PLEA provide the greatest explanatory power. PC5 is seen to be largely dependent upon SLPL / SLA and SLPL / MeanSLL of which, SLPL / MeanSLL provides the greatest explanatory power.

Plotting of Components 3 vs 5 from the PCA analysis discriminates fish belonging to different dietary groups with respect to the multivariate parameters measured using the GIA. From the plot it can be seen that fish from the control diet, Diet A (black dots), are largely clustered in the upper part of the scatter plot while functional Diet C fish (green diamonds) are largely clustered in the lower half of the graph, suggesting that there may be a difference in the response of fish belonging to those two groups reflected in differences in their gill response to functional feeds as analysed by the GIA tool (Figure 2.30).

Table 2.8 Component matrices generated from PCA analysis of measured morphometric variable

Morphometric parameters	Component				
	1	2	3	4	5
VAPL	-.387	.464	.570	-.051	-.162
VASL	-.376	.751	.081	-.193	.246
TGA	-.161	.691	.632	.145	-.079
SLA	.273	.616	-.088	-.600	-.387
PLA	-.266	.501	.692	.367	.057
ILS	.160	.674	-.642	.069	-.086
GR	.445	-.177	-.557	-.520	-.181
ISR	-.075	.168	-.638	.571	.195
PLEA	-.310	.574	.655	.138	-.201
TMCA	.933	.175	.267	.059	.052
TMCATGA	.959	-.059	.113	-.030	.128
SLPL	.133	.874	-.364	-.210	.137
MedianFERETMinSL	-.224	.428	-.503	.245	-.137
MedianFERETMaxSL	.342	.739	-.405	-.300	.004
MCNPLEA	.577	.267	-.026	.642	-.363
MCAPLEA	.483	.269	-.043	.752	-.301
MCAPLEA_PLEA	.595	.000	-.298	.631	-.206
MCNSLA	.906	.016	.296	-.162	.141
MCASLA	.917	.134	.302	-.090	.121
MCASLASLA	.866	-.010	.376	.072	.203
TMCN	.936	.063	.266	-.037	.064
TMCNTGA	.933	-.192	.053	-.125	.147
MedianSLL	.273	.692	-.601	-.247	.034
SLPL_SLA	-.151	.131	-.430	.543	.659
SLPL_MeanSLL	-.205	.690	.358	-.075	.398

The principal components (PC1-PC5) generated by the PCA were further analysed using a Kruskal Wallis non-parametric ANOVA (with diet as the independent grouping variable and each PC as the dependent variable). Differences between diets were non-significant ($p<0.05$) for all principal components save for PC5, which showed a significant difference ($p<0.03$) between dietary groups. A follow-up *post-hoc* test for multiple comparisons showed that the significant difference was between Diet A and Diet C ($p<0.03$) Table 2.9.

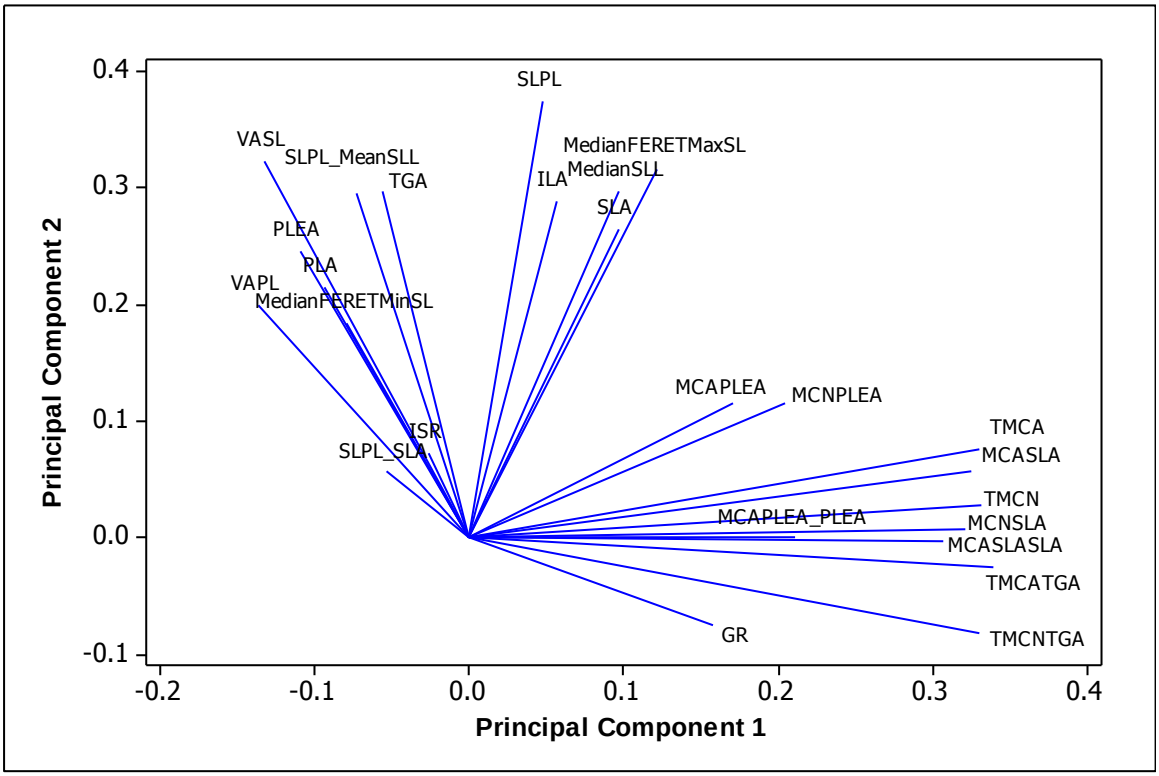

Figure 2.29 Loading plot for morphometric parameters analysed

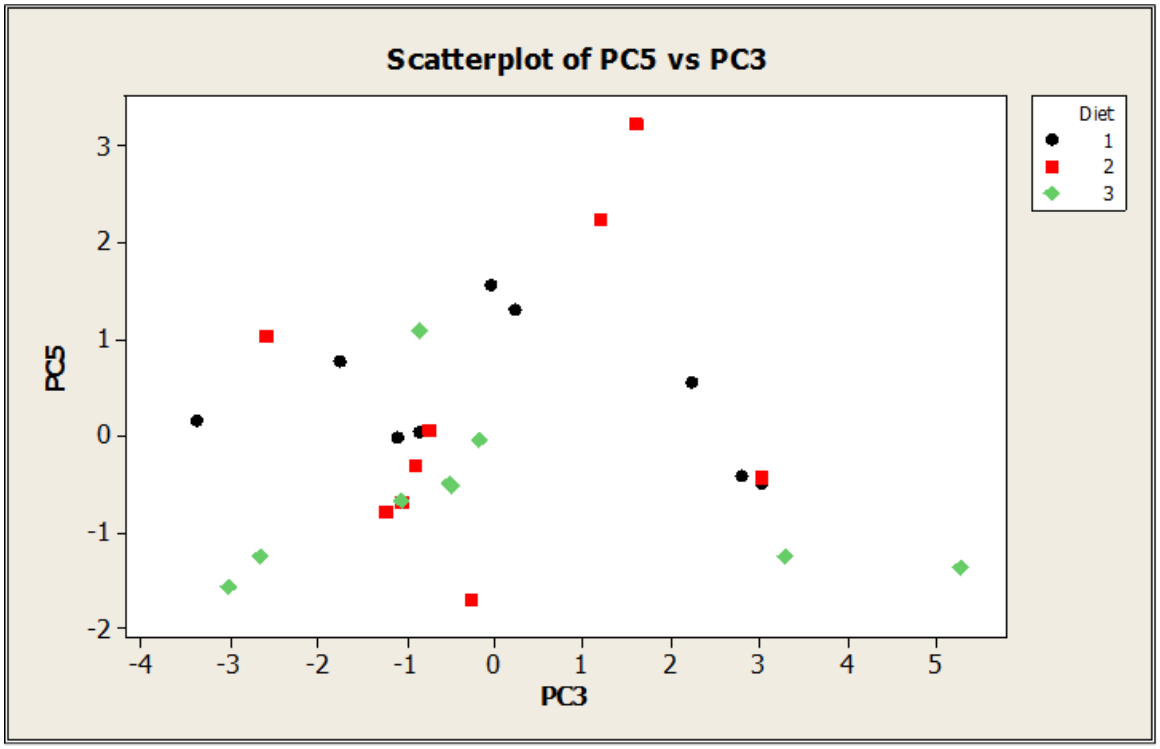

Figure 2.30 scatter plot of PC1 vs PC2 from morphometric analysis showing distribution of fish fed different diets

Following boxplot illustrate

further details of all three dietary groups and their distribution for PC5 (Figure 2. 31)

Table 2.9 multiple comparisons test between dietary groups for PC5. Diet as dependent variable, bolded values significant at p<0.05

	Multiple Comparisons Test p-values (2-tailed); PC5 Independent (grouping) variable: Diet		
Depend.: PC5	Kruskal-Wallis test: H (2, N= 27)		
	1 R:18.444	2 R:14.778	3 R:8.7778
1	x	0.981	**0.029**
2	0.981	x	0.326
3	**0.029**	0.326	x

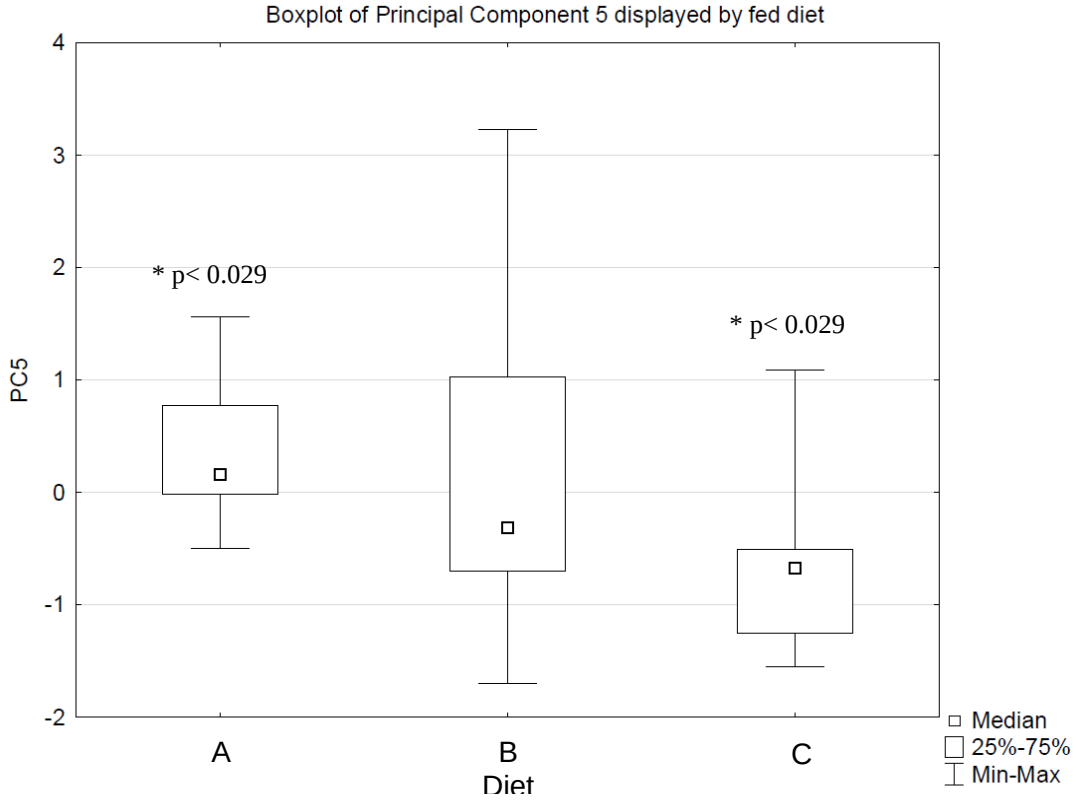

Figure 2.31 Boxplot of Principal Component 5 for three diets (A control, B & C functional)

2.3.4 **Gene expression analysis**

The relative ratio of gene expression of each target gene was calculated using the REST® softwear (Pfaffl, 2001). The calculation of relative expression in the REST is based on deviation of the Ct value of the sample and control of target gene normalised to the mean crossing point deviation of the reference gene. In the present study, for normalisation of the expression of target genes, β actin was used as the reference gene. Before normalisation, the efficiency (E) of each target gene and the reference gene were calculated based on the formula [E=(10-1/slope)-1] in the Quantsoft software of the Quantica thermal cycler (Techne, UK) (Table 2.10). The relative expression of normalised target gene expression of test samples compared to control sample and statistical analysis was performed using pairwise fixed reallocation randomization test (http://www.geen-quantification.info). in the REST software (Table 2.11). Significant differences were observed for Diet A vs Diet B for expression of Mx ($p< 0.001$) and between Diet A and Diet C for chemokine-like protein ($p<0.020$). No significant differences in expression between diets were observed for serum amyloid A (Table 2.11).

Table 2.10 The slopes, R^2 and efficiencies (% E) values for each of the primers, calculated from the standard curves

Target gene	**Slope**	**R^2**	**% E**
β actin	-3.816	0.982	1.828
Mx protein	-3.871	0.987	1.813
Serum amyloid A (SAA)	-4.504	0.992	1.667
CHE chemokine like protein	-3.982	0.998	1.783

Table 2.11 Summary of the results of gene expression analysis for selected primers across different functional diets. Values are indicated as log2 conversion of relative expression values and significant (*) at $p < 0.05$. N=9.

	Mx			SAA			CHE		
	Fold change	**±SD**	**p value**	**Fold change**	**±SD**	**p value**	**Fold change**	**±SD**	**p value**
A compared to B	-1.97	±0.149	0.001*	1.02	±0.237	0.840	-1.57	±0.173	0.080
A compared to C	-1.21	±0.361	0.610	-1.26	±0.277	0.200	-1.9	±0.207	0.020*
B compared to C	1.63	±0.608	0.110	-1.29	±0.244	0.120	-1.21	±0.288	0.380

2.4 **Discussion**

Examination of histopathology remains the gold standard for disease diagnosis in fish and is thus an essential tool for the diagnosis of gill disease in salmonids (Ferguson, 2006; Roberts and Rodger, 2012). The development of automated or semi-automated gill health monitoring tools, employing advanced image analysis techniques, could provide major benefits, such as rapid and accurate interpretation of histological changes associated with gill diseases benifiting global Atlantic salmon aquaculture industry. The combination of advanced image processing and analysis for histomorphometric analysis, together with various recently developed modern technologies and approaches such as WSI (Ghaznavi *et al*., 2013) and CAD (Gurcan *et al.*, 2009) has been employed to develop a gill analysis pipeline to assist future analysis and understanding of gill plasticity and pathology.

This chapter described the successful development of a gill analysis pipeline and, in particular, the development of a prototype semi-automated gill image analysis tool (GIA), which has allowed quantification of a broad range of gill histomorphometric parameters. This robust, interactive tool allows rapid, accurate, quantitative measurement of a range of traditional and novel markers of gill state, providing complementary data to that provided by light microscopic observation as well as sensitive detection of gill changes below normal observational thresholds.

Development of a successful pipeline begins with the initial sampling. One key factor for sampling clean gills is bleeding the fish to remove blood from the gill before fixation (Speare and Ferguson 1989), which minimises processing artefacts caused by reaction of blood constituents (*e.g.* haemoglobin) with fixative chemicals like 10 %

NBF. The preservation of gills in a medium providing adequate fixation allows minimum alteration in the observed gill histopathology, which is essential both to human observation and to optimal image processing and analysis. Automated processing of all tissue samples at the same time is also important, although with very large numbers of samples, in order to risk loss of all samples in a catastrophic processing failure, a structured randomisation of samples to batches might be undertaken. In this instance processing was successfully carried out according to conventional protocols optimised in the IoA using the existing tissue processor. This was followed by embedding with particular consideration to specimen orientation , which needs to be homogeneous across the samples in order to obtain consistent longitudinal (routine sections) across the gill arch (Wolf *et al.*, 2014) and transverse sections through the mid-arch to explore the ILT (interbranchial lymphoid tissue). Protocols were successfully optimised to standardise slides for capture of images using the WSI system, which were representative of the whole gill arch, displaying similar sectioning depths and profiles *e.g.* showing a similar pattern of gill structure including central venous sinus or cartilage.

The GIA gill parameters (Table 2.1) were developed in order to measure histomorphometric changes that occured in the gills. Initially, a list of recognised morphometric changes that had been described in the gills by previous authors (*e.g.* Mallatt, 1985) was summarised (Appendix, Table.3). At the same time image analysis software (KS300 and KSRUN) was examined for possible geometric measurements that might be incorporated into the GIA morphometric tool. After trialling a range of possible measurements a defined set was arrived at that appeared capable of describing a number of elements of gill plasticity /pathology and these were built into the prototype GIA tool and tested on a number of samples deriving from a dedicated feed

trial. The results of this chapter provide some evidence for the expected hypothetical correlation of selected GIA morphometric parameters to conventional histological descriptions.

Examination of the effect of functional feeds on gill histomorphometry was investigated using conventional histological methods and, for the first time, with the GIA tool. The identity and the composition of the feeds used for experiment was kept blind until the final results had been generated from GIA tool and similarly a range of gut parameters (Appendix, Table 2.1) were measured using the semi-automated gut image analysis tool developed for classification of functional feeds (Silva, 2014). The univariate analysis of morphometric data revealed that from all the parameters measured, only VASL and TGA were significantly affected by the functional feeds analysed. The mean value of VASL in gills of fish fed with Diet B was significantly higher than control Diet A fed fish as showen after performing *post hoc* Mann-Whitney U test. By definition VASL indicate the vacuoles present in the centre of the secondary lamella (empty spaces), presumably the cross sectional area of lamellar blood channels present in secondary lamellae that was captured by GIA tool quantitatively. According to the literature, increased blood lamellar space, also known as blood channels, is representative of an increased blood supply through the gill arch, secondary to alteration in blood circulation around the body (Mallatt¸1985). This can also occur as a sign of a local inflammatory response. However, there were no clear signs of inflammation observed in gills stained with H&E, as well as by PAS / Alcian Blue stains in Diet B. However, considering the ingredients of the functional diet, the enlargement of the blood channels in the gill could be a secondary manifestation of the effects in the gut of soya bean enteritis (Diet B), which may also have caused alteration in blood circulation, increasing the diameter of blood channels in the secondary lamellae. For fish with enteritis (Diet B) where high

cell turnover and tissue regeneration occur there is a demand for high metabolism. Thus, if fish are still suffering from chronic enteritis, restoration of body homeostasis requires increased circulation, which could potentially explain not only increased VASL but also increased TGA. The fish suffering from enteritis have high demand for ATP, generated through aerobic tissue respiration. Eventually this could lead to a high demand for oxygen uptake across the secondary lamellae of the gills. This may also have been evidenced in the increased trend (not statistically significant) for secondary lamellae associated morphometric changes; SLPL (representative of respiratory surface area), SLPL / MedianSLL and SLPL / SLA as shown in graphs (Figure 2.24).

One of the highlights of this study was the implementation of various statistical analyses to compare treatments and interpret different findings in a meaningful manner in relation to gill health and fish biology. In this second chapter the results of the GIA histomorphometric analysis were statistically analysed using GLM, however, univariate analysis found only very few parameters that were significantly different between functional diets (*i.e.* VASL and TGA). Hence, while histopathological investigation using H&E and PAS / Alcian Blue stained gill sections were unable to resolve any changes in the gill in response to the different diets, application of statistics to the GIA results was able to pick up statistical differences.

The univariate analyses, which only examined a single parameter at a given time across the group, were further extended to multivariate analysis, performing a PCA analysis, which examines various responses of individuals at a given time to give a detail description to the biological response. The PCA analysis of morphometric data allowed generation of scatterplots, revealing differences between fish belonging to groups fed different functional diets. In particular differences were seen between diet A (control)

and the functional diet C. PC5 is seen to be largely dependent upon SLPL / SLA and SLPL / MeanSLL of which, SLPL / MeanSLL provides the greatest explanatory power The mechanisms underlying these differences remain to be resolved.

During this feed trial, conventional histological analysis did not reveal any histological changes in the gills except lamellar clubbing which is observed as bulbous enlargments of the lamellar tips. Lamellar clubbing which often results from misoriented positioning of gill during histological processing, is commonly misdiagnosed as pathological change (Wolf *et al*., 2014). However, application of the GIA tool revealed histomorphological features that were significantly different between test diets. At the same time, parallel to the gill work, the distal gut of the same fish was also analysed using a semi-automated gut image analysis tool (quantitative histology), which demonstrated significant histological changes associated with soya bean induced enteritis (Silva, 2014) as previously described for unrefined soya bean inclusion in Atlantic salmon diets (Baeverfjord and Krogdahl 1996; Knudsen *et al.*, 2007). In the gill there were limited changes thought to reflect the on-going enteritis, except for the increase in size of the VASL.

At the start of this work, feed details were blinded by the manufacturer and therefore, before developing the GIA tool, little information was known about the diets. To improve our understanding of the pathophysiology associated with the given functional diets, a few immune-related gene transcripts were selected for analysis using RT-qPCR . These included those concerned with persistence of any acute phase response (Atlantic salmon serum amyloid A5; SAA5) (Lund and Olafsen, 1999: Jorgensen *et al.*, 2000), any inflammation in the gills (CHE chemokine like protein) and also any antiviral response initiated by the diets (Atlantic salmon Mx protein). According to the results,

CHE chemokine like protein transcript was significantly increased in Diet C compared to control Diet A. This could be due to immuno-stimulant enrichment in Diet C (Appendix Table 2.2). The Mx transcripts were increased in Diet B compared to Diet A. The function of the Mx transcript in the gills is unclear with regards to soyabean enrichment in Diet B and enteritis, unless antiviral gene pathways have been stimulated non-specifically in the gill as part of a general alert associated with barrier leakiness from the ongoing gut enteritis (and hence potential viral entry). Collectively, this study found that gene expression provided a useful tool to study immune responses; however, examining a limited number of immune gene transcripts as performed here is sufficient to define the effects of dietary inclusions. Instead, a selected larger snap-shot of genes or whole transcriptomic analysis (Sahlmann *et al.,* 2013) would have been better employed in this study to define dilatory responses.

In conclusion, during this study a robust highly sensitive semi-automated image analysis tool was successfully developed and subsequently applied to classify two different functional feeds with comparison to a conventional salmon feed, using histomorphological change in the gills of Atlantic salmon. These analyses were strongly assisted by the use of multivariate statistical analysis techniques such as PCA. In addition to conventional histological examination and use of the GIA tool, the expression of three selected genes was also evaluated by RT-qPCR to examine underlying pathophysiological mechanisms. Examination of the behaviour of the gills in term of morphometric change allowed us to distinguish the functional feeds provided. This novel approach may allow feed manufacturers to evaluate impacts of their feed through use of advanced image analysis in association with the more conventional tools currently applied.

CHAPTER 3

EVALUATION OF GILL MORPHOMETRIC PARAMETERS IN ATLANTIC SALMON AFTER TREATMENT WITH HYDROGEN PEROXIDE

3.1 Introduction

As the most versatile and physiologically diversified organ found in vertebrates (Olson, 2002; Ferguson, 2006), the fish gill endures a range of extreme challenges from its aquatic environment including osmotic effects, harmful solutes and various pathogens. It has an extraordinary ability to cope with these through rapid structural and functional re-modelling with very little impact on the organ's physiological function.

Bath-treatments with various chemical compounds, such as copper sulphate, chloramine-T (for the treatment of bacterial gill disease), sodium chloride (for the treatment of external parasitic protozoans), formalin and hydrogen peroxide (H_2O_2), are routinely used to treat against pathogens in aquaculture (Jokumsen and Svendsen, 2010). H_2O_2 has been used since 1800 as an oxidative disinfectant to treat bacterial and parasitic conditions in aquaculture. In Denmark, H_2O_2 is used as a humane and environmentally friendly alternative to formalin for treating skin parasites and bacterial gill infections in fish and also to treat mould on eggs (Pedersen *et al*., 2010; Sortkjær, 2000). Several studies have investigated potential adverse effects of using H_2O_2 on salmonids to establish recommendations for safe therapeutic doses (Pedersen *et al.,* 2010; Sortkjær *et al.,* 2000; Tort *et al.,* 2002; Gaikowski *et al.,* 1999; Rach *et al.,* 1997; Arndt and Wagner, 1997). The damage caused by H_2O_2 depends on several factors, including the dose, exposure time, frequency of treatment, life stage of the fish and also upon the water temperature during treatment in particular. The larger fish appear to be

more susceptible to H_2O_2 treatment than smaller fish and tissue damage mainly occurs in the gills (Adams *et al*., 2012). In an experiment carried out by Bruno & Raynard (1994), 1.2 % H_2O_2 was applied for 20 min at 10 °C with no mortalities, however, treating at 13.5 °C resulted in 35 % mortality during a 2 h treatment. Clearly the water temperature is a critical factor to consider during bath treatments with H_2O_2. Further trials by Johnson *et al.,* (1993) and Kiemer & Black (1997) found that the timing of treatments was also critical, with a significant correlation seen between the length of exposure and the degree of gill damage and mortality observed (*i.e.* 10 % mortality following a 1.5 g L^{-1} (1500 ppm) treatment at 11 °C for 20 min rising to 26 % mortality when the treatment period was extended to 40 min).

In Australia, where AGD has been endemic for a long time, freshwater bath treatment for 2–3 h is the most preferred means of treatment (Adams *et al.,* 2012). During the last few years, especially in Scotland, Ireland and Norway, H_2O_2 has been used extensively to control sea lice infections as well as to treat newly emerged AGD. As recorded by Rodger (2014), in Scotland fish are generally treated for AGD at a temperature 10-12 °C (up to 16 °C), using 1000-1200 ppm of H_2O_2 for 20-30 min (or less according to temperature) . In Ireland, H_2O_2 treatment has been carried out in confined environments in well-boats and full tarpaulin enclosures using 600 to 1200 ppm for 18 to 22 min. In general, before H_2O_2 treatment, the status of the gill is assessed together with environmental conditions (*e.g.* water temperature fluctuations, oxygen concentrations, occurrence of algal blooms and size of the fish (biomass) as a practice. Hydrogen peroxide has become popular treatment for AGD with minimal harmful impact, excellent clearance and lack of harmful residues in the environment. However, possible development of pathogen resistance with frequent treatments and also high costs and logistical difficulties (use of high volumes) appear to be clear disadvantages.

The first record of H_2O_2 being used as a therapeutic for sea lice came from Norway (Thomassen, 1993) and it was later adopted in Scotland in the early 1990s (Rae, 2002) after resistance development to Aquagard (dichlorvos). As H_2O_2 releases oxygen that helps to maintain dissolved oxygen levels during the treatment, it became an environmentally-friendly therapeutic product.

The mechanism by which H_2O_2 kills sea lice is uncertain, however, visible effects of treatment include apparent mechanical paralysis of the sea lice caused by the formation of bubbles in the haemolymph, which detaches the lice from its host and they float to the water surface (Thomassen, 1993; Bruno and Raynard, 1994; Treasurer *et al.*, 2000). Manufacturers have recommended a concentration of 1.5 g L^{-1} for 20 min based on the work performed by Thomassen (1993). The effectiveness of H_2O_2 was found to be reduced by an increased organic load in the water or heavily fouled nets (Johnson *et al.*, 1993).

In Chile, the first use of H_2O_2 to treat sea lice was in 1994, however, it soon became less popular due to its poor effectiveness against some life stages of *Caligus rogercresseyi* (i.e. it gave good control against the adult Caligus but was less effective against the chalimus stage) (Bravo *et al.*, 2010). In this respect it should be noted that H_2O_2 treatment is being reinstated in Scotland after an absence of 10 years. This renewed interest and the likelihood that this treatment may be re-established in Chile in the near future has led to work establishing optimal treatment regimes. There is also a need to examine the physiological effect of H_2O_2 on gills, including their morphology, immune competence and disease resistance after treatment.

The list of gill responses described by Mallatt (1985) has been widely used by other researchers to evaluate gill pathology or morphological changes in response to chemical

treatments, especially H_2O_2 treatment (Bruno and Raynard, 1994; Kiemer and Black, 1997; Speare *et al.*, 1999; Bowers *et al*., 2002). Histological lesions observed, include changes in the gill epithelium (e.g. cell lifting, necrosis, hyperplasia, hypertrophy, and ruptured cells, bulging or fusion of gill lamellae, hypersecretion and proliferation of mucocytes, and changes in chloride cells and gill vasculature. Some of these lesions were more abundant in studies using organic toxicants and other irritants, and include necrosis and hypertrophy of gill epithelial cells together with mucous hypersecretion (due to mucous cell hyperplasia and hypertrophy), and several studies have reported damage to pillar cells and marginal cells (Schmid and Mann 1961; Brown and Jones, 1968; Skidmore and Tovell 1972; Abel and Skidmore 1975; Abel 1976; O'Conner *et al.,* 1976; Rombough and Garside 1977; Dalela *et al.,* 1979; Segers *et al.*, 1984). This type of vascular damage was only really found in animals exposed to very high doses of irritants or fish that were terminally affected as a result of the exposure. Thus, cells composing the branchial blood vessels seem relatively resistant to irritant substances. For example, during his analysis, Mallatt (1985) found few types of gill lesions associated with the branchial blood vessels, and these were only reported a few times in the literature, e.g. glycoprotein precipitate in branchial blood vessels (Cope *et al.,* 1970; Kennedy *et al*., 1970) and proliferation of cartilage cells within the gill rays (Mahajan and Singh 1973; Dalela *et al*., 1979).

The distribution of gill lesions, tended to vary widely in their intensity for a given set of exposure conditions, and many authors found that different gills and lamellae within a single fish tended to show differing degrees of severity in the morphological changes that occurred (Mackie *et al*., 1975; Ternmink *et al*., 1983), and also between fish (Van Valin *et al*., 1968). Mallatt (1985) further concluded that non specificity of the branchial changes seen in response to irritants suggests that these changes might

represent a generic physiological reaction by the gills to stress, and many of these are considered as a first line defence responses by the gills. Some branchial morphological changes have been considered to be inflammatory in nature, but Mallatt concluded that the literature he reviewed did not fully support this hypothesis. Some authors have suggested that the branchial defence responses represent an inflammatory reaction to injury caused by irritants (Skidmore and Tovell 1972; Abel 1974; Abel and Skidmore 1975; Abel 1976; Rombough and Garside 1977; Walters and Plumb 1980). Some of the irritant-induced lesions reported in fish gills are indicative of inflammation, i.e. dilation of blood vessels, congestion of blood cells in these vessels, and leukocyte migration from the blood into the lamellar epithelium.

Nowak *et al.*, (2014) commented on a general lack of inflammatory infiltrate in AGD lesions of the gills in histopathological sections despite suggested inflammatory changes from gene expression studies. However, recent finding have shown that irritant-induced morphometric changes in the branchial epithelium have some inflammatory characteristics associated with them, which have been corroborated through gene expression studies in which differentially regulated immune and pro-inflammatory cytokine genes were seen after treating fish with H_2O_2. Henriksen *et al.*, (2013) found that the immune gene expression of head kidney was affected by treatment of gills with H_2O_2, and this treatment made the fish more susceptible to infection by *F. psychrophilum*. Some previous studies, which agreed with these findings, are supported by ultra-structural morphological changes showing signs of tissue damage including cytoplasmic vacuolisation, autophagosome formation and inclusions, loss of microvilli and abnormal mitochondria and nuclei.

It is important to note that most of the branchial lesions resulting from various chemical treatments are reversible and once the stimulus is removed, the morphology of the gill returns to normal (i.e. pre-treatment) and a normal physiological status, assuming that lethal doses of the substances in question were not used. The time scale for this repair and full recovery of the gill from damage can take days to weeks, and also depends largely on the water temperature (Ferguson, 2006), and therefore the recovery time should also be taken into consideration when designing a treatment regime.

As described for the mammalian inflammatory model, there are three distinct steps involved in the inflammation process (Robbins and Cotran 1979). First, blood vessels near the injury site become dilated. Second, permeability of the capillary walls increases and produces an exudation of fluid that leads to a congestion of blood cells in these vessels, termed vascular stasis (Figure 3.1). This involves increased permeability and the migration of leukocytes out of the capillaries and into nearby epithelium (Roberts 2012; Robbins and Cotran 1979). However, subsequent stages of inflammation become chronic if there is a continuous infiltration of extravascular material containing leukocytes (especially monocytes/ macrophages). Where inflammation has been studied in fish (skeletal muscles, peritoneum, peri-orbital connective tissue) it resembles the process seen in mammals (Finn and Nielson 1971). The final stage in this protective process is the proliferation of fibroblasts associated with scar tissue formation. Gills have a remarkably fast healing time compared to other tissues (Ferguson, 2006).

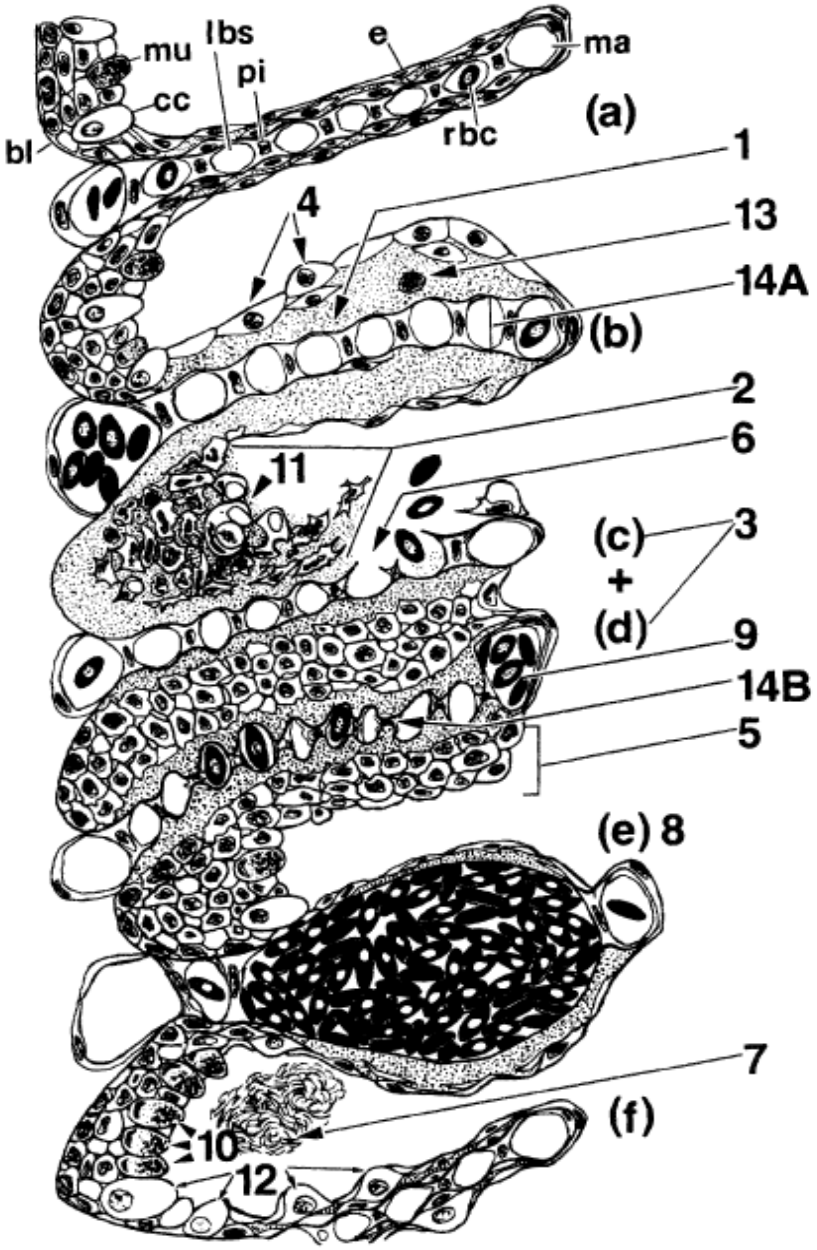

Figure 3.1 A composite diagram of common irritant-induced gill lesions. Six respiratory lamellae are shown (a-f), the top one of which is normal (*Oncorhynchus mykiss*, modified from Skidmore and Tovell 1972). The lesions are 1, epithelial lifting; 2, necrosis; 3, lamellar fusion (c and d); 4, hypertrophy; 5, hyperplasia; 6, epithelial rupture and bleeding into pharynx; 7, mucous secretion; 8, clavate lamella or lamellar aneurism (e); 9, vascular congestion; 10, mucous cell proliferation; 11, chloride cells damaged early; 12, chloride cell proliferation; 13, leukocyte infiltration of epithelium;14A, lamellar blood sinus dilates; 14B, lamellar blood sinus constricts. For photomicrographs of some of these lesions are illustrated in Eller (1975). Abbreviations: bl, basal lamina; cc, chloride cell; e, typical lamellar epithelial cells; lbs, lamellar blood sinus; ma, marginal blood channel; mu, mucous cell; pi, pillar cell; rbc, erythrocyte. [Adapted from Mallatt (1985)].

Toxicant-induced ultrastructural changes include cytoplasmic vacuolization, mitochondrial and nuclear alterations, loss of microvilli, increased numbers of lysosomes and inclusions, and alterations in cytoplasmic density, these being mainly reported in the typical squamous epithelial cells on the gill lamellae and osmoregulatory ionocytes (chloride cells or mitochondria rich cells). Most of those changes were associated with cell damage or death (Sandritter, 1976), however some of them also reflect increased cellular activity, swelling of intracellular tubules, and the appearance of an apical pit (Pisam 1981). None of those changes are indicative of toxicant-specific alterations. This has raised the question of using transmission electron microscopy (TEM) to help characterise toxicant-induced lesions since this might show early signs of nonspecific branchial changes (*i.e.* subtle cytological changes), which might not be detectable by light microscopy (LM) examination. Obviously more research has been published and numerous techniques *e.g.* laser scanning confocal microscopy (LSCM), IHC, microarrays (Olsvik *et al.*, 2005) have been used to identify toxicant-induced gill histopathological changes.

The aim of the study reported in this chapter was to examine the effect of H_2O_2 exposure on key aspects of gill morphology, pathology and plasticity, using a single therapeutic dose widely used in the aquaculture industry. The morphometric changes that occurred in the gill after treatment were elucidated using image processing and subsequent analysis to quantify these changes.

3.2 **Materials and methods**

3.2.1 **Fish**

Disease-free (n=200) Atlantic salmon, with a mean weight of 334.35±41.9 g, were placed in duplicate tanks and acclimated for two weeks in salt water, where they were

fed continuously with a conventional feed for salmon (Skretting, Norway). The fish were then treated with $H_2O_2$1500 ppm (mg L^{-1}) for 20 min at 12 °C in salt water. Seven fish from each tank were sampled before conducting the H_2O_2 treatment as pre-trial controls. Subsequent to treatment, seven fish from each tank were sampled at 4h, 12h, 3 days, 7 days and 14 days post exposure (h.p.e / d.p.e.), (Figure 3.2). For sampling, fish were killed using an overdose of benzocaine (100mg L^{-1}) (Sigma, Norway) anaesthesia, in compliance with recommended guidelines established to maintain animal welfare standards by Norwegian National Legislation for Laboratory Animals. Prior to excising gill tissue into 4% NBF, fish were bled from caudal vein and tissues were fixed for 24-48 h at 4° C and processed for histology.

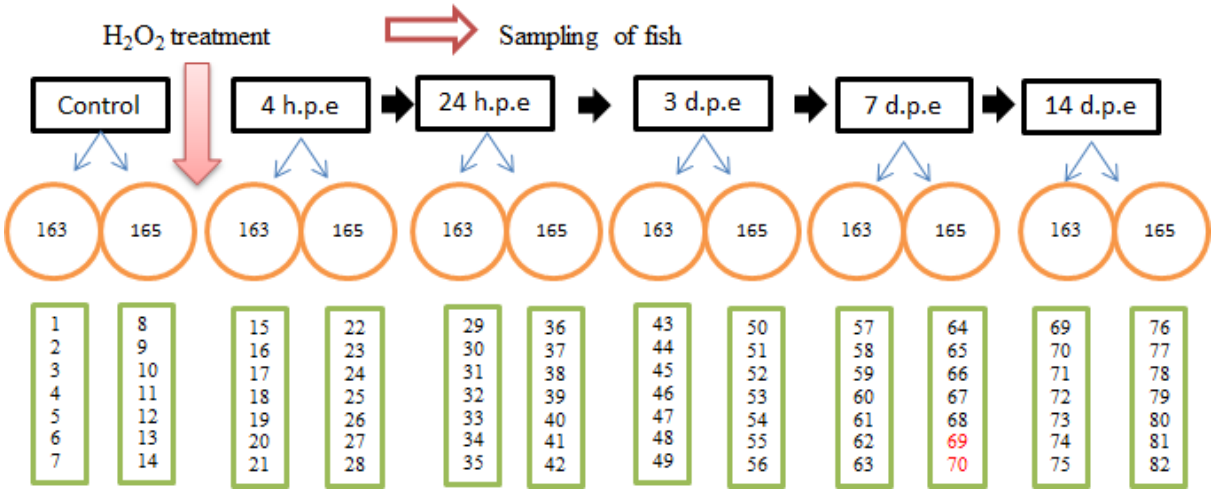

Figure 3.2 Experimental layout of H_2O_2 trial, 231 g (N=7) of Atlantic salmon fed with conventional salmon diet and reared at duplicate tanks were exposed to therapeutic dose of H_2O_2 1500 ppm for 20 min prior to sample in time course interval(Fish 1 -82). Please note only 5 fish were analysed on Day 7 post exposure with a technical problem obtaining high resolution scanned images.

3.2.2 Sample processing for histology and Periodic acid shift (PAS) and Alcian blue (AB) staining

Gill samples fixed in 4 % buffered formalin were processed for histology at the Diagnostic laboratory, General Hospital, Stavanger, Norway. The gills were dissected,

laterally orientated and placed flat on the bottom in histo-cassettes (ChemiTeknikk, Norway). Then histo-cassettes were placed into ethylenediaminetetraacetic acid (EDTA) (ChemiTeknikk, Norway) solution, which was prepared in un-buffered 4 % formalin, pH adjusted to 7 with sodium hydroxide for 2 days to allow decalcification to take place without causing any structural damage. Tissue processing was performed using an automated tissue processor (Leica, Shandon Excelsior) where tissue samples were dehydrated through an alcohol series to 100% and cleared with several baths of xylene. Finally, the tissue samples were infiltrated with paraffin (Histowax, Sweden or Q-Path, France) at 60 ^{o}C. The paraffin embedded tissue samples were sectioned with a semi-automated Microtome (Leica) preparing 3 µm sections, which were mounted on Super frost plus slides (Menzel, Braunschweig, Germany) and dried overnight at 37 ^{o}C in an oven. The sections were deparaffinised, rehydrated and tissue sections stained using a BenchMark automated special stainer (Roche, France). Sections were stained with Alcian blue (AB) pH 2.5 and PAS using ready-to-use staining kits (Roche, UK) followed by counter stain haematoxylin. Finally, sections were dehydrated and automatically cover-slipped by the automated stainer.

3.2.3 **Light microscopy, imaging and processing**

Conventional histological slides were scanned (WSI) using a Mirax desktop scanner located at Skretting ARC Norway. The large image files (mrxs format) were processed and analysed using the customised image analysis software developed for image analysis of gill tissue (gill image analysis; GIA tool) as describe in Chapter 2. Briefly the original large tiled tiff files were uploaded into Mirax viewer (or “panoramic” (*sic*.) viewer) software (3DHISTECH Ltd.), cropped approximately to produce predetermined equal sized images (tiff images approximately 8 MB in size, 2290x 1200 pixels), which were then either used to assess the gill using the developed GIA tool or were manually

examined for histopathological changes (Figure 3.3) with findings finally compared with previous findings from similar studies published in the literature.

3.2.4 Conventional histopathological examination for H_2O_2 treated gills at different time points

The histopathological evaluation of Alcian blue/PAS stained gill tissues were carried out using the same set of images (tiff images approximately 8 MB in size, 2290x 1200 pixels) that were used for GIA tool. (Figure 3.3). All individual images were uploaded into IrfanView software (or any compatible programme in Windows) to evaluate histopathological alterations following the list published by Mallatt (1985) with some modification in terminology (Table 3.1).

Table 3.1 A list of possible histopathological lesions recorded in earlier literature. During the present trial few of these lesions could be observed

Lesion number	Histological gill lesion
1	Epithelial cells lifting with intraepithelial oedema
2	Epithelial cells lifting without intraepithelial oedema (there is no fluid inside tissue space)
3	Necrosis of gill epithelium, characterised by round dark nuclei, destruction of tissue margins and tissue debris present
4	Lamellar fusion with lacunae where tissue debris, bacteria or parasite present
5	Epithelial cells swelling (epithelial cell hypertrophy), characterised by irregular cell walls
6	Hyperplasia of gill epithelium (acute <12h, chronic <96h), increased number of squamous cell layers. The hyperplasia in the distal end of the secondry lamellae is referred as clubbing.
7	Rupture of lamellar epithelium (bleeding into pharynx), associated with other lesions or without other prominent lesions (mechanical injury)
8	Mucous cell proliferation, mucus hypersecretion (mucous cell hyperplasia and hypertrophy), increased number of mucous cells and increased size of mucous cells
9	Clavate-globate lamellae (haemorrhaging, aneurisms, telangiectasia), sudden circulatory disturbance
10	Congested blood cells in lamellae (stasis), sudden circulatory disturbance, lamellar blood channel has more than one RBC, distal marginal channel has considerable amount of RBC
11	Chloride cells, preferential early damage, difficult to see from light microscope in H&E staining, TEM is the best to explore ultrastructure level
12	Chloride cell proliferation, or features of increased activity, could be as a result of gill remodelling
13	Leukocyte infiltration of gill epithelium, macrophages, natural killer cells (NKC), lymphocytes, eosinophilic granular cells (EGC), antigen secreting cells (ASC)
14	Lamellar blood sinus either dilates or constricts.

3.2.5 **Image analysis using KSRUN software**

Development of the Gill Image Analysis (GIA) algorithm was carried out on the KS300 platform 1997 (Carl Zeiss, GmbH, Germany) as described in Chapter 2, Section 2.3.6. This platform was used here to examine differences in total of 25 morphometric variables and indices with respect to the different pre- and post-treatment timepoints (Figure 3.4). A list of parameters examined and the analyses used are detailed in Chapter 2, Table 2.1.

3.2.6 **Data analysis**

The data files obtained from GIA tool analysis, were uploaded into a software "file-rename utility" to reorganise the files so that they could then be recognised by a task-specific Excel segregation macro (written by Dr John Taggart, IoA). The segregation macro was written in Visual Basic and all the instructions were included in the first page (Figure 3.5).

After performing the segregation, a large Excel file was generated tabulating all the cases and numerical values for morphometric variables measured (Figure 3.5). Before proceeding further, randomly selected files belonging to a few individual cases (sub-samples) were manually calculated to verify the accuracy of the final tabulated results. Once the data were verified for accuracy, statistical analysis was performed on Minitab and/or SPSS software. A Two-way ANOVA was performed with timepoint as a fixed factor and tank as a random factor (independent variables).

Parameters were evaluated for normality by observing individual plots of residuals and normalised plots of residuals. At the same time behaviour of the data were evaluated by

using residuals versus fit and residual versus order plots. Difference between time points were considered as significant when $p < 0.05$. Multiple comparison of time points were performed using a Tukey's *post hoc* test.

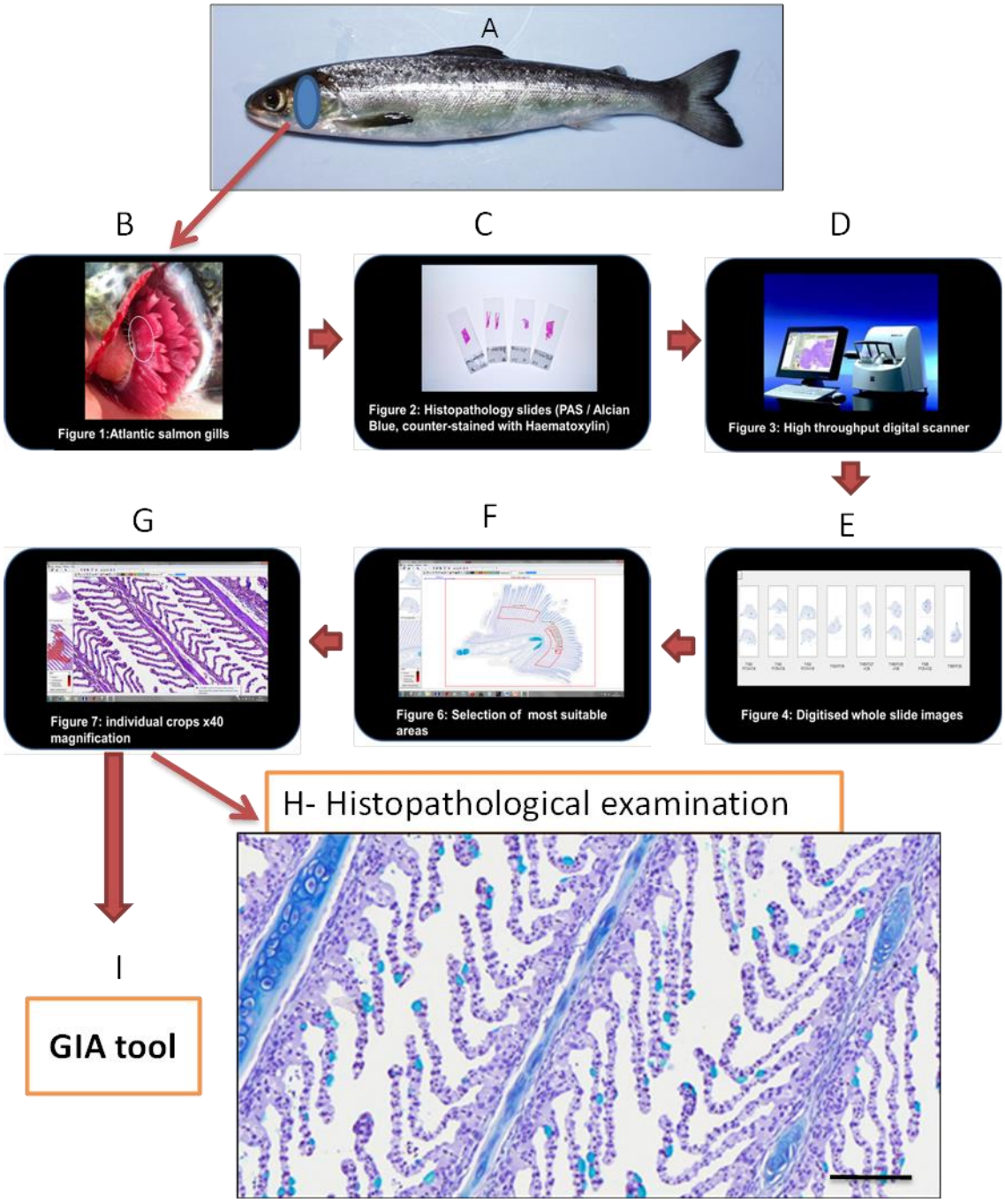

Figure 3.3 A diagrammatic illustration of different steps involved in histopathological evaluation through whole slide imaging (WSI) technology. (A) hydrogen peroxide treated fish, (B) preferred second gill arch, (C) histological slides, (D) Mirax desktop scanner, (E) scanned whole slides, (F) defined area of interest, (G) x40 cropped images, (H) representative image of H_2O_2 treated gills using Mirax "x40" magnification setting. Scale bar indicate 100 µm.

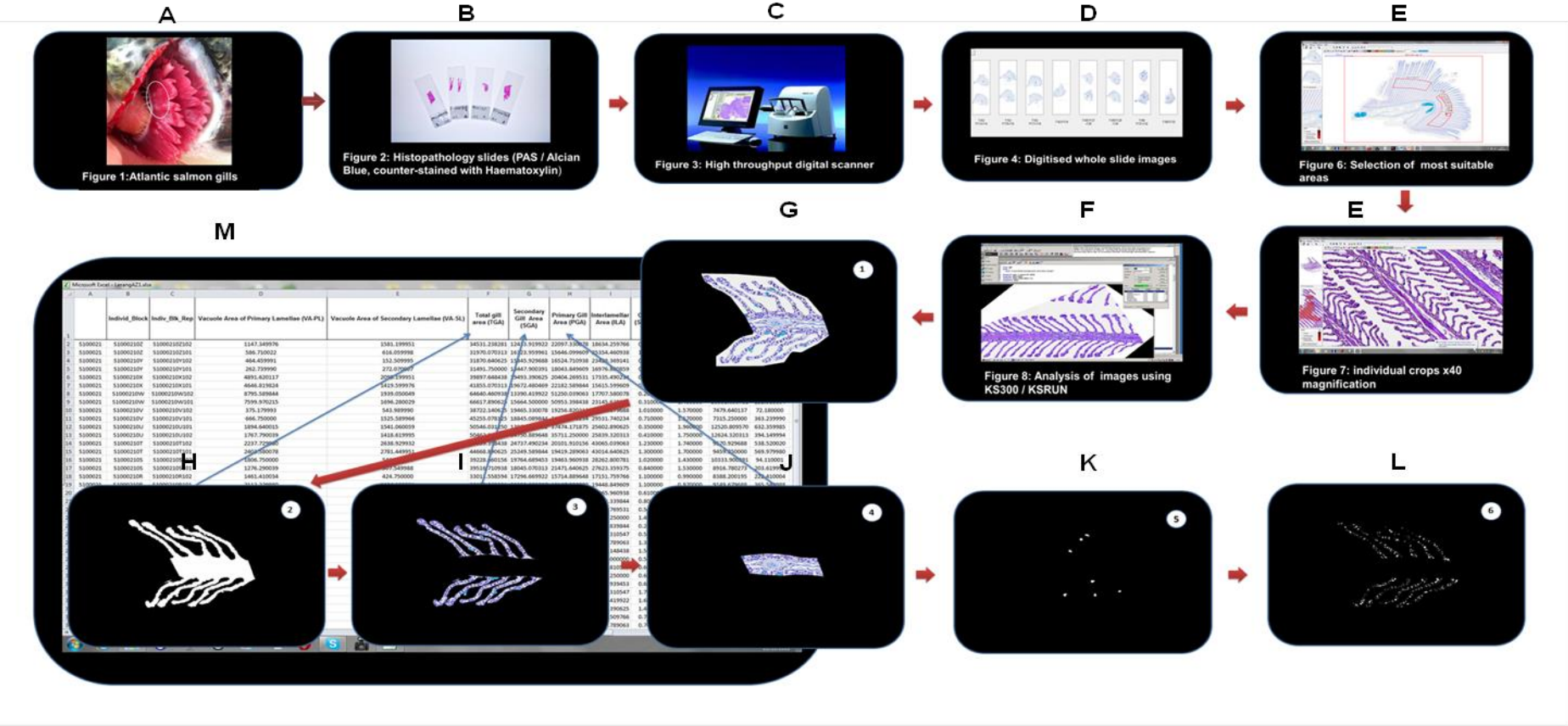

Figure 3.4 A diagrammatic illustration of intermediate analytical steps including use of the GIA tool, which was used to analyse H_2O_2 treated whole gill archs thin (3µm) histological sections mounted on special adhesive slides. A-E, shows common steps involved in virtual histopathology (Figure 3.1) and GIA tool; F, uploaded cropped image (subsample) in KS300\KSRUN software; G, area of interest with 5 secondary lamellae of each side (total 10); H-L, intermediate steps which generate different gill morphometric parameters including TGA, SLA, PLA, TMCN and VASL; M, a screenshot of generated large data files, rows comprise individual fish or subsamples, columns comprise relevant morphometric parameters or indices. For more details see chapter 2 section 2.4.4.

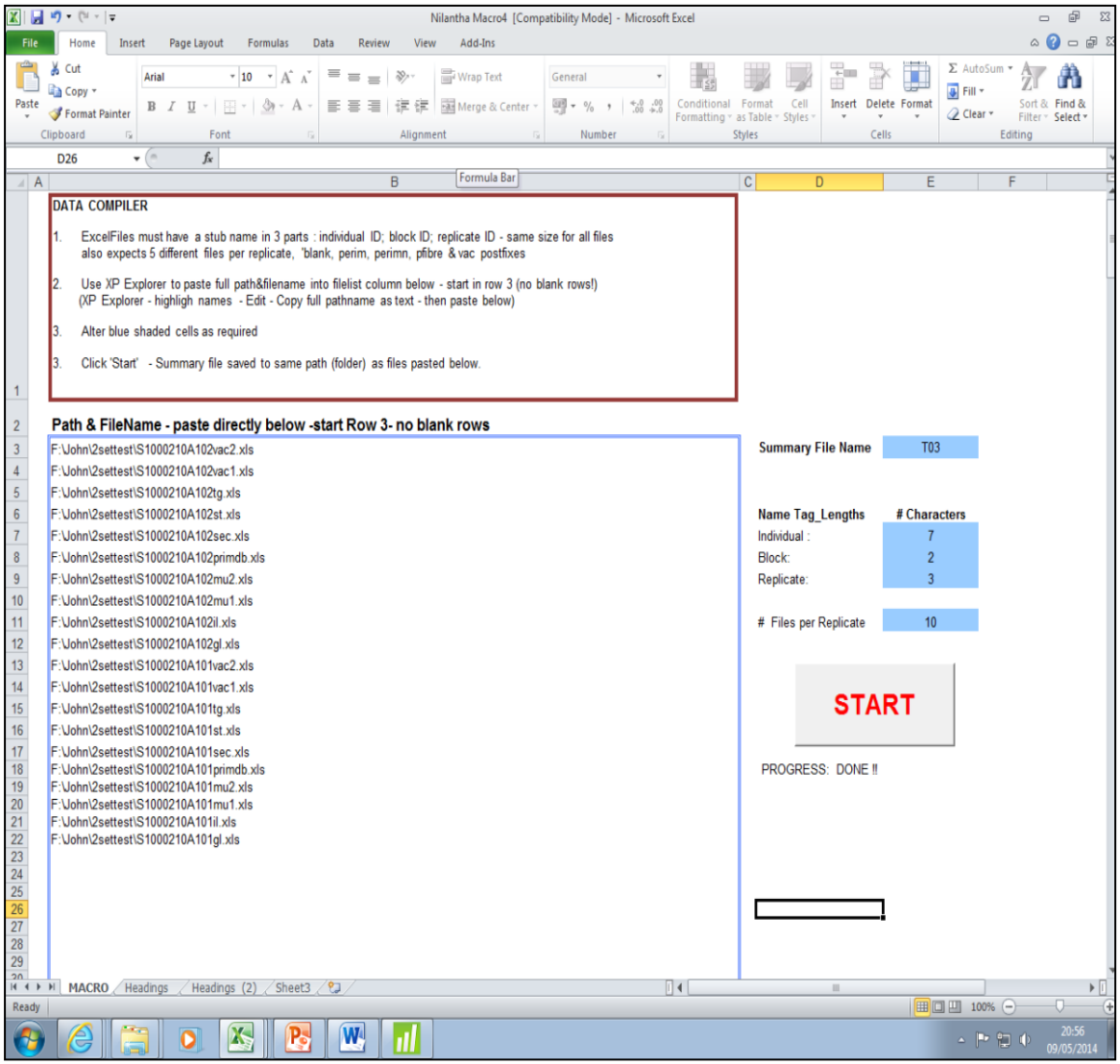
Nilantha Macro4 [Compatibility Mode] - Microsoft Excel
DATA COMPILER
1. ExcelFiles must have a stub name in 3 parts : individual ID; block ID; replicate ID - same size for all files also expects 5 different files per replicate, 'blank, perim, perimn, pfibre & vac postfixes
2. Use XP Explorer to paste full path&filename into filelist column below - start in row 3 (no blank rows!) (XP Explorer - highligh names - Edit - Copy full pathname as text - then paste below)
3. Alter blue shaded cells as required
3. Click 'Start' - Summary file saved to same path (folder) as files pasted below.
Path & FileName - paste directly below -start Row 3- no blank rows
F:\John\2settest\S1000210A102vac2.xls
F:\John\2settest\S1000210A102vac1.xls
F:\John\2settest\S1000210A102tg.xls
F:\John\2settest\S1000210A102st.xls
F:\John\2settest\S1000210A102sec.xls
F:\John\2settest\S1000210A102primdb.xls
F:\John\2settest\S1000210A102mu2.xls
F:\John\2settest\S1000210A102mu1.xls
F:\John\2settest\S1000210A102il.xls
F:\John\2settest\S1000210A102gl.xls
F:\John\2settest\S1000210A101vac2.xls
F:\John\2settest\S1000210A101vac1.xls
F:\John\2settest\S1000210A101tg.xls
F:\John\2settest\S1000210A101st.xls
F:\John\2settest\S1000210A101sec.xls
F:\John\2settest\S1000210A101primdb.xls
F:\John\2settest\S1000210A101mu2.xls
F:\John\2settest\S1000210A101mu1.xls
F:\John\2settest\S1000210A101il.xls
F:\John\2settest\S1000210A101gl.xls
Summary File Name
T03
Name Tag_Lengths
Characters
Individual :
7
Block:
2
Replicate:
3
Files per Replicate
10
START
PROGRESS: DONE !!
MACRO
Headings
Headings (2)
Sheet3
Ready

Figure 3.5 The Excel macro developed to tabulate GIA output data. Detailed information is included in Chapter 2 Section 2.2.

3.3 **Results**

3.3.1 **Conventional histological analysis**

The histological examination of all gill samples was performed on digitalised images. Except for the presence of low magnitude changes that were occasionally observed, the pre-treatment control gills (0 h.p.e.) were absent of histological alterations (Figure 3.6). The low magnitude changes observed included slight oedema of the secondary lamellae (Figure 3.7) and initial stages of clubbing (Figure 3.7), however these changes were negligible compared to magnitude of the changes seen at the other time points.

At time points 4 and 12 h.p.e, the histological changes were particularly confined to the primary lamellar epithelial area (PLEA) of the primary lamellae area (PLA). Increased proliferation of cells (dark round nuclei) in the PLEA (Figure 3.8) was clearly observed in the gill micrographs at 4 h.p.e (4 H). Furthermore, increased cellularity in the PLEA with slight epithelial separation and lifting towards the distal end of the secondary lamellae were also noted (Figure 3.8 B). At 24 h.p.e, a continuous increase in the cellularity at basal layer of the PLEA was clearly evident (3.9 B). In some sections, RBC and exfoliated epithelial cells results from processing artefacts rather than true pathological changes were also observed in the ILS regardless to the time point of sampling.

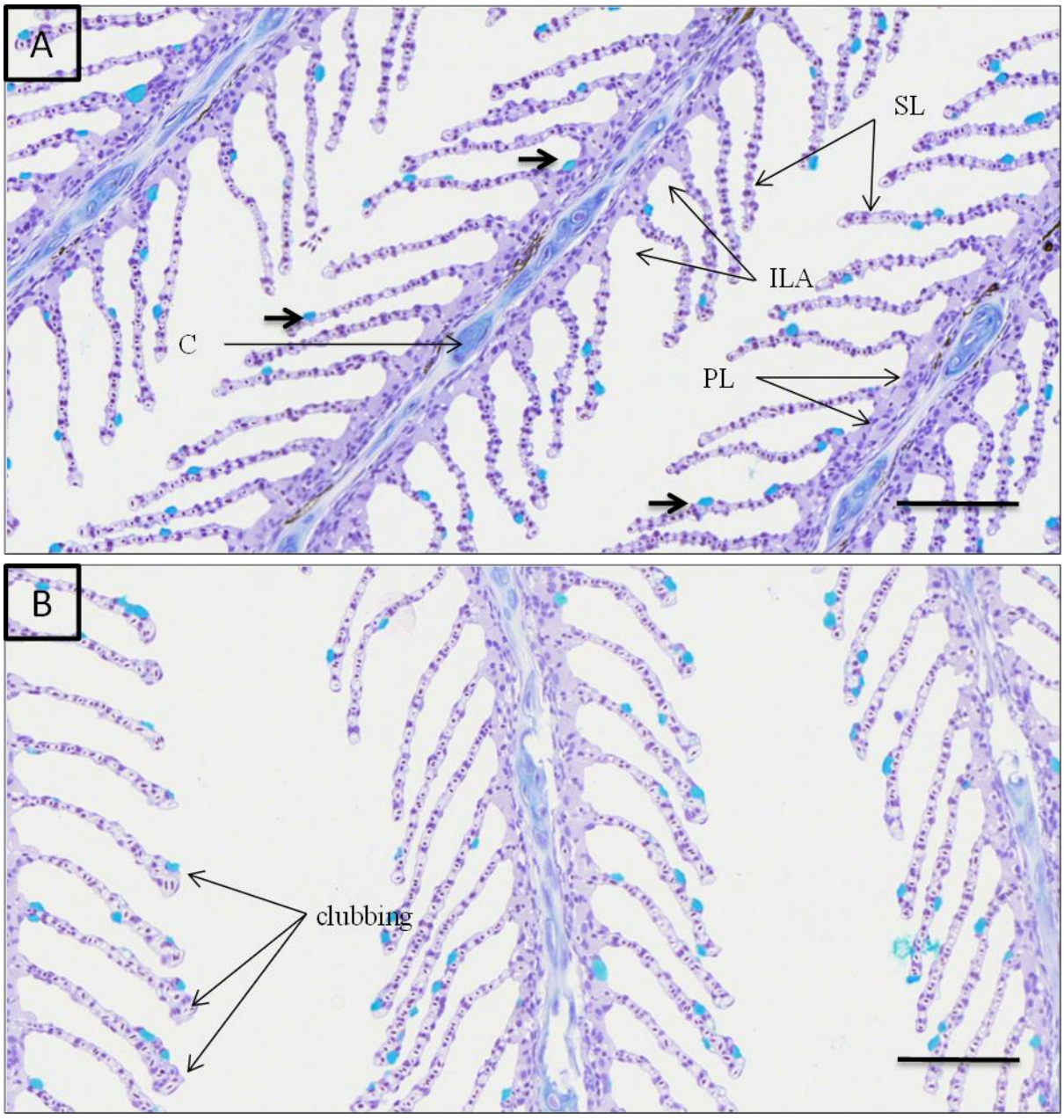

Figure 3.6 Pre-trial control gill samples (0 H) stained with Alcian blue and counter stained with haematoxylin for mucous cell histochemistry. (A) normal morphology, C-cartilage, SL-secondary lamellae, PL- primary lamellae, ILS- inter-lamellar spase, heavy arrows indicate mucous cells. (B) Low magnitude cell clubbing in the distal end of the secondary lamella was occasionally seen (light arrows). Scale bar 100µm.

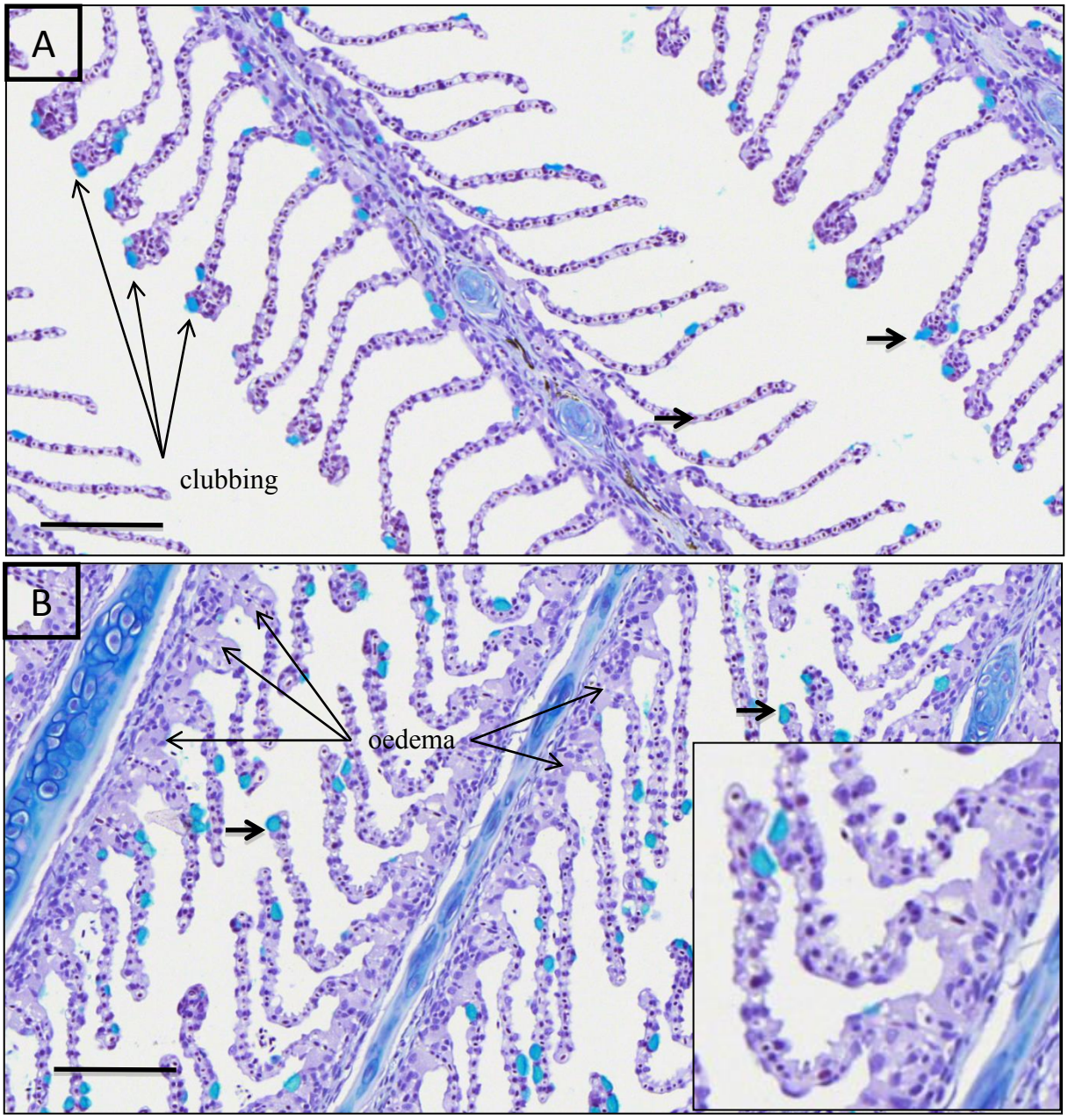

Figure 3.7 Pre-trial control gill samples (0H) stained with Alcian blue and counter-stained with haematoxylin. (A) Normal morphology with a few lamellae showing clubbing, thick arrows indicate mucous cells. (B) Slight oedema with no epithelial separation at the base of the lamellae and interlamellar area. Square box shows higher magnification of irregular cell membranes (Wrinkled cell membranes), scale bar 100µm.

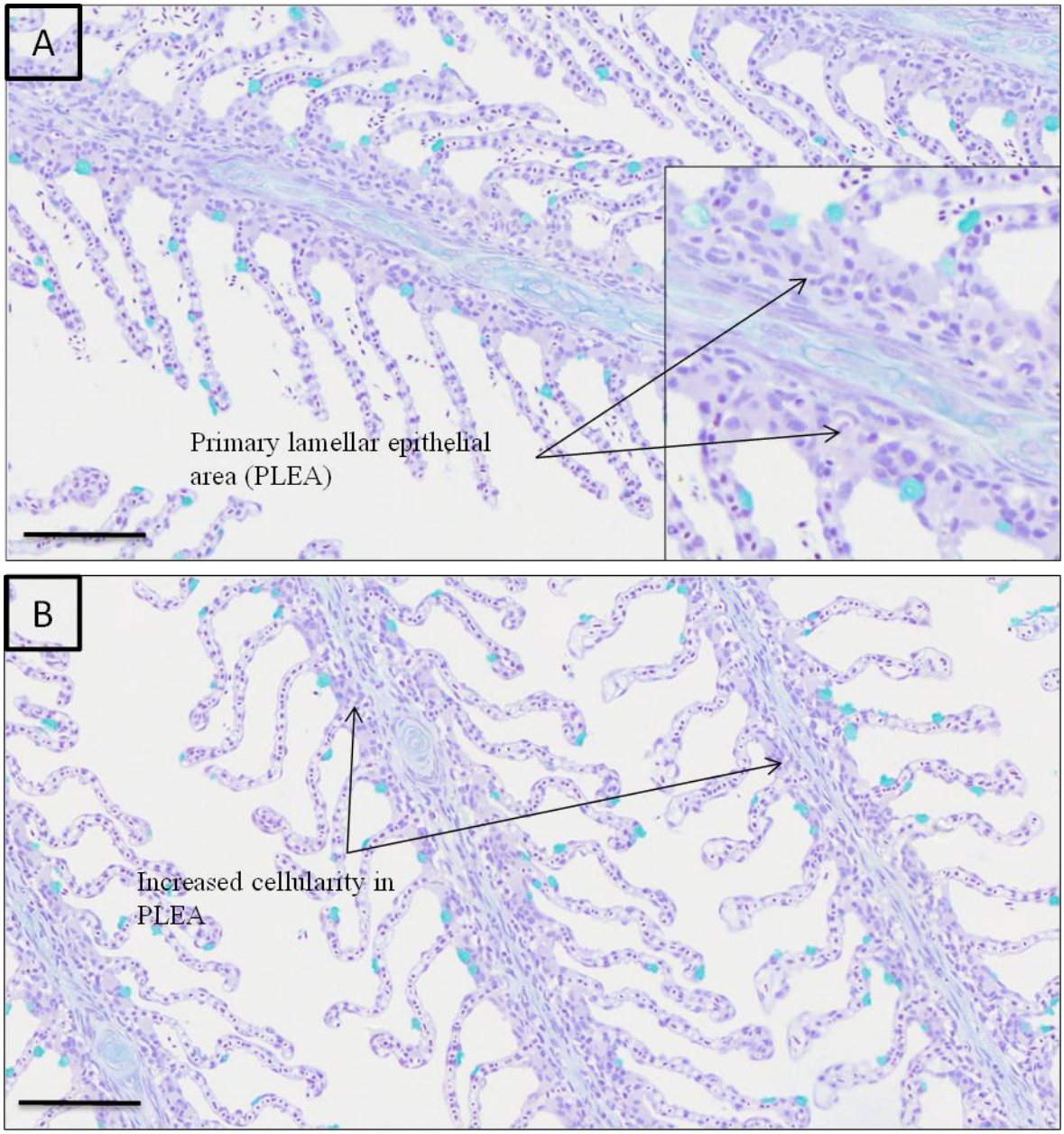

Figure 3.8 Gill samples of 4 h.p.e (4H) stained with Alcian blue and counter stained for haematoxylin for mucous cell histochemistry and gill morphology. (A) Histopathological changes in PLEA (small box shows twice the original magnification), ILS filled with some blood cells, occasionally epithelial cells. (B) Increased cellularity in PLEA. Scale bar 100µm

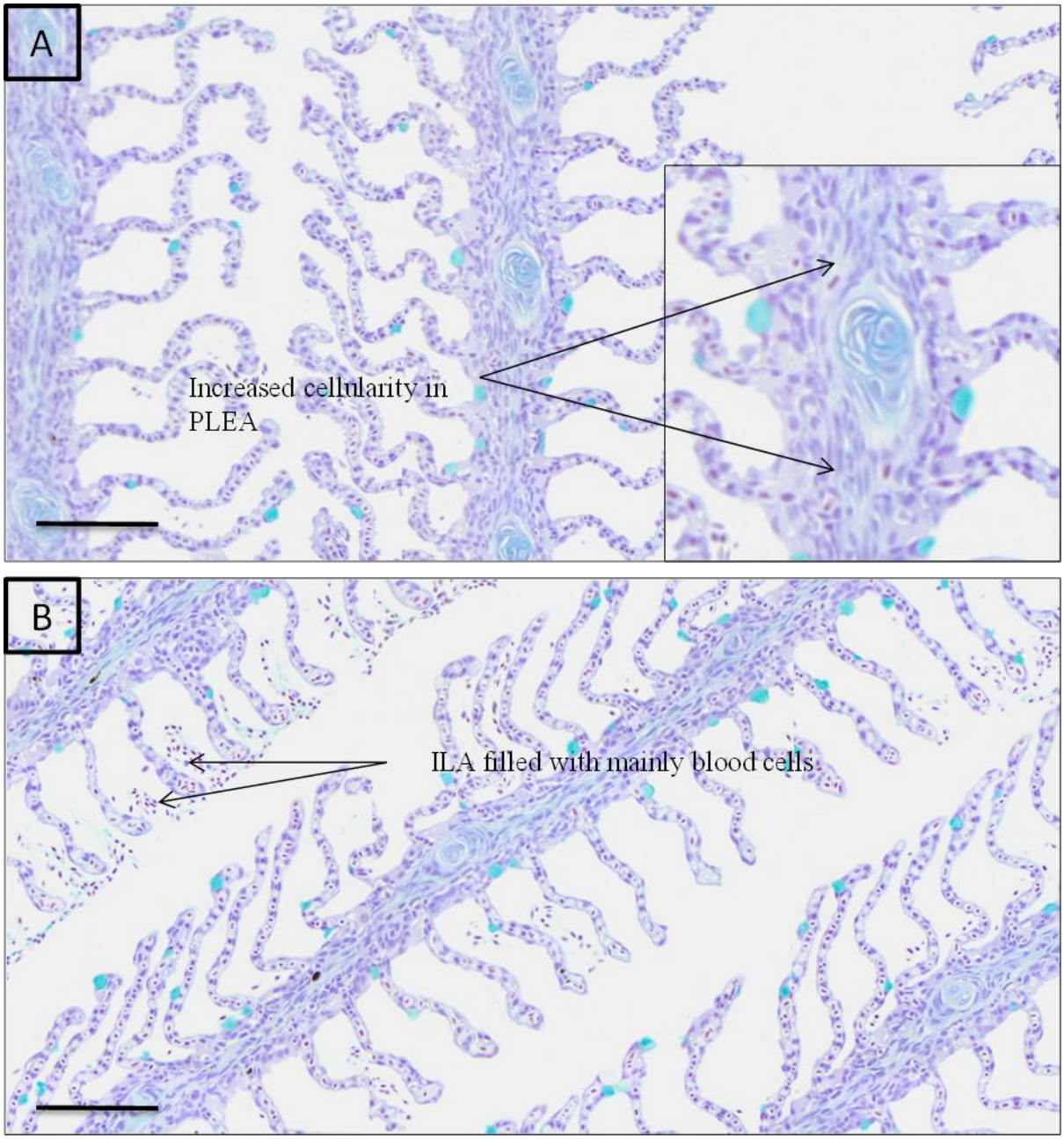

Figure 3.9 Gill samples of 24H stained with Alcian blue and counter stained for haematoxylin for mucous cell histochemistry and gill morphology. (A) Histopathological changes in PLEA (small box shows twice the original magnification), increased cellularity in PLEA. (B) Blood cells and scant amount of epithelial cells seen in the ILS could possibly a sampling/processing artefact. Scale bar 100µm

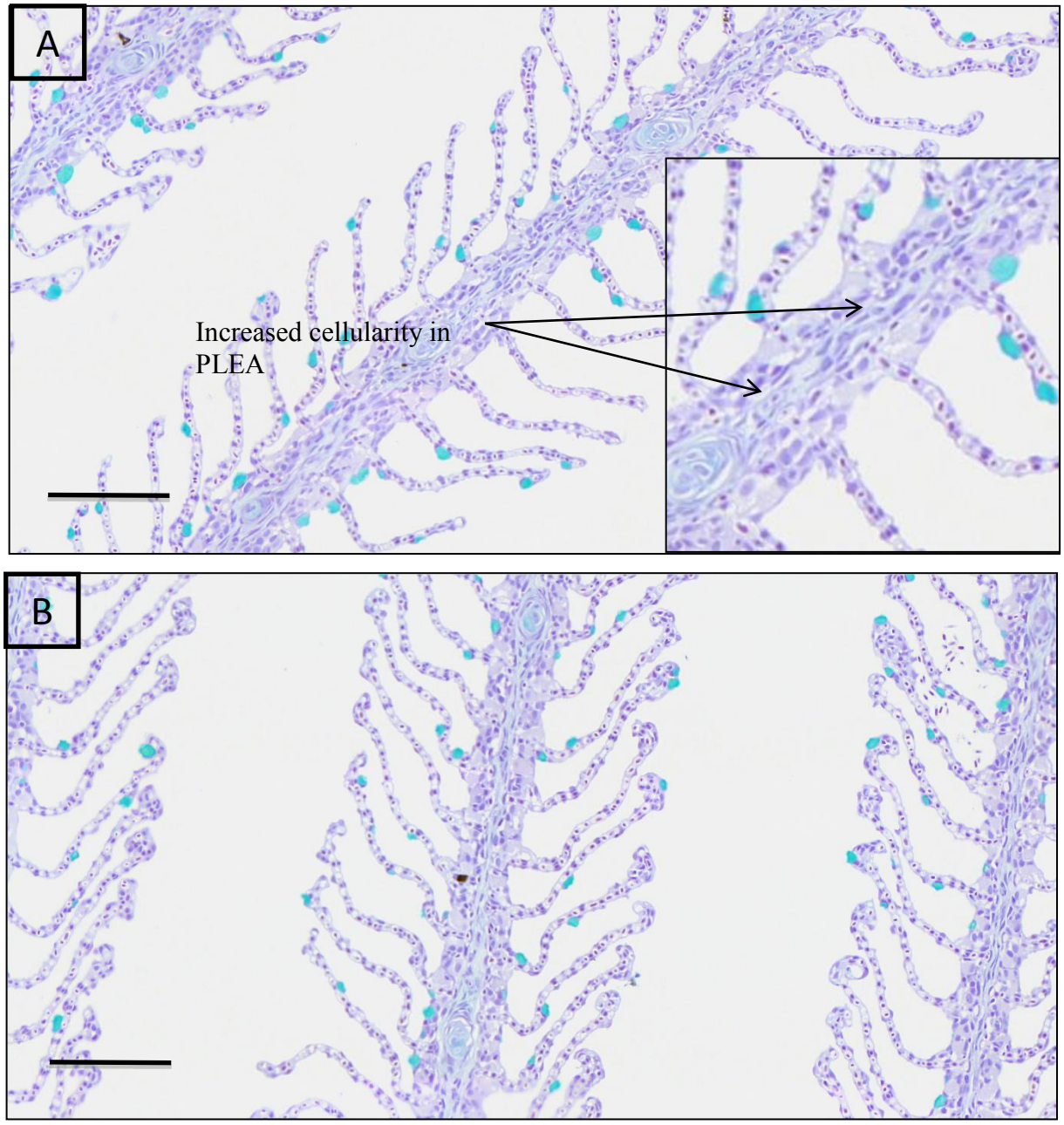

Figure3.10 Gill samples of 3 d.p.e (3D) stained with Alcian blue and counter stained for haematoxylin for mucous cell histochemistry and gill morphology. (A) Histopathological changes in PLEA (small box shows twice the original magnification), decreased magnitude of cellularity in PLEA compared to previous time points. (B) prominant clubbing of secondary lamellae. Scale bar 100µm

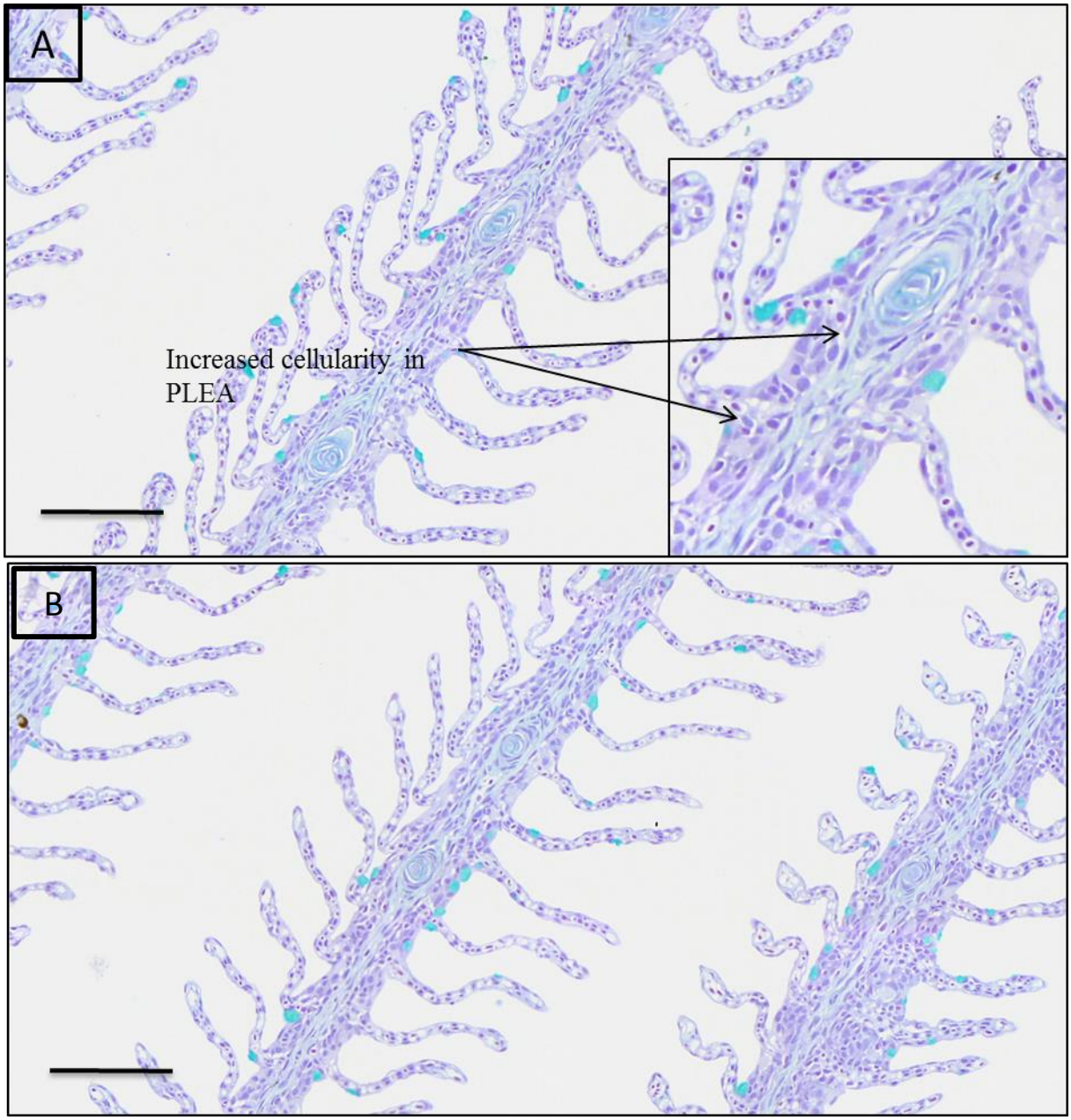

Figure 3.11 Gill samples of 7 d.p.e (7D) stained with Alcian blue and counter stained for haematoxylin for mucous cell histochemistry and gill morphology. (A) Histopathological changes in PLEA (small box shows twice the original magnification), increased cellularity in PLEA is decreased compared to earlier time points. (B) Prominent ncreased cellurarity in PLEA. Scale bar 100µm

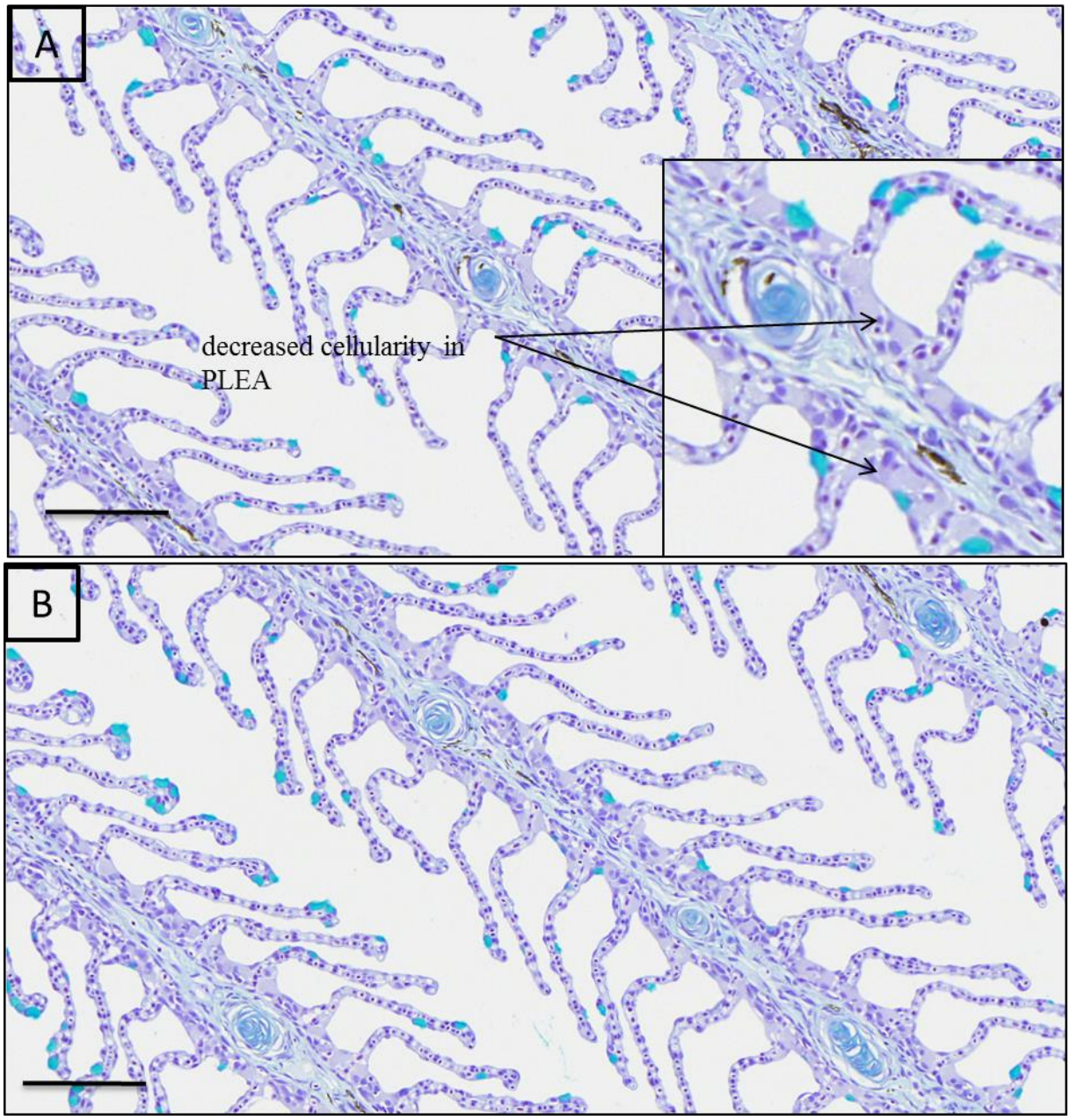

Figure 3.12 Gill samples of 14 d.p.e (14D) stained with Alcian blue and counter stained for haematoxylin for mucous cell histochemistry and gill morphology. (A) Histopathological changes in PLEA (small box shows twice the original magnification), decreased cellularity in PLEA compared to earlier time points. (B) Except few clubbing decreased cellularity across the histology micrographs. Scale bar 100µm

3.3.2 Morphometric analysis of Atlantic salmon gills treated with hydrogen peroxide

The morphometric analysis of Atlantic salmon gills treated with H_2O_2 was carried out using the gill image analysis tool (GIA) developed in Chapter 2. The raw data generated from the KSRUN GIA platform were tabulated and comprised the mean morphometric values for the various gill parameters obtained from five replicate sections per individual fish. The data were first subjected to quality assurance. During the evaluation of data for normalisation, the resulting normal probability plots and histograms corresponded with patterns of typical normal data (Figure 3.13). Hence no unusual behaviour in the data was observed, and it was further analysed using parametric tests including both 1) General linear model; univariate analysis (GLM), 2) Multivariate analysis; principal component analysis.

3.3.2.1 General Linear Model (GLM), univariate analysis of morphometric data

The statistical analysis was performed in Minitab version 16 (Minitab, UK) using general linear modelling (GLM). The cut off significance was $p < 0.05$. The majority of parameters measured during the hydrogen peroxide trial appeared significantly different between different time points compared to pre-trial control groups (Table 3.2). The highest mean of the group has been designated as A in each parameter tested and according to the results of multiple comparisons were tested using *post hoc* test Tukey HSD test following GLM and significant groups were indicated as different letters (this was compatible with graphs). Summary data and the results of statistical testing are given in Table 3.2 Results were categorised and presented according to different areas of the gills: (1) primary lamellar area associated gill parameters, (2) secondary lamellar associated gill parameters, (3) mucous cell associated morphometric changes and (4)

total gill area associated morphometric changes. Most of the morphometric parameters evaluated were significantly changed over time and are graphically illustrated in Figure 3.14-3.17.

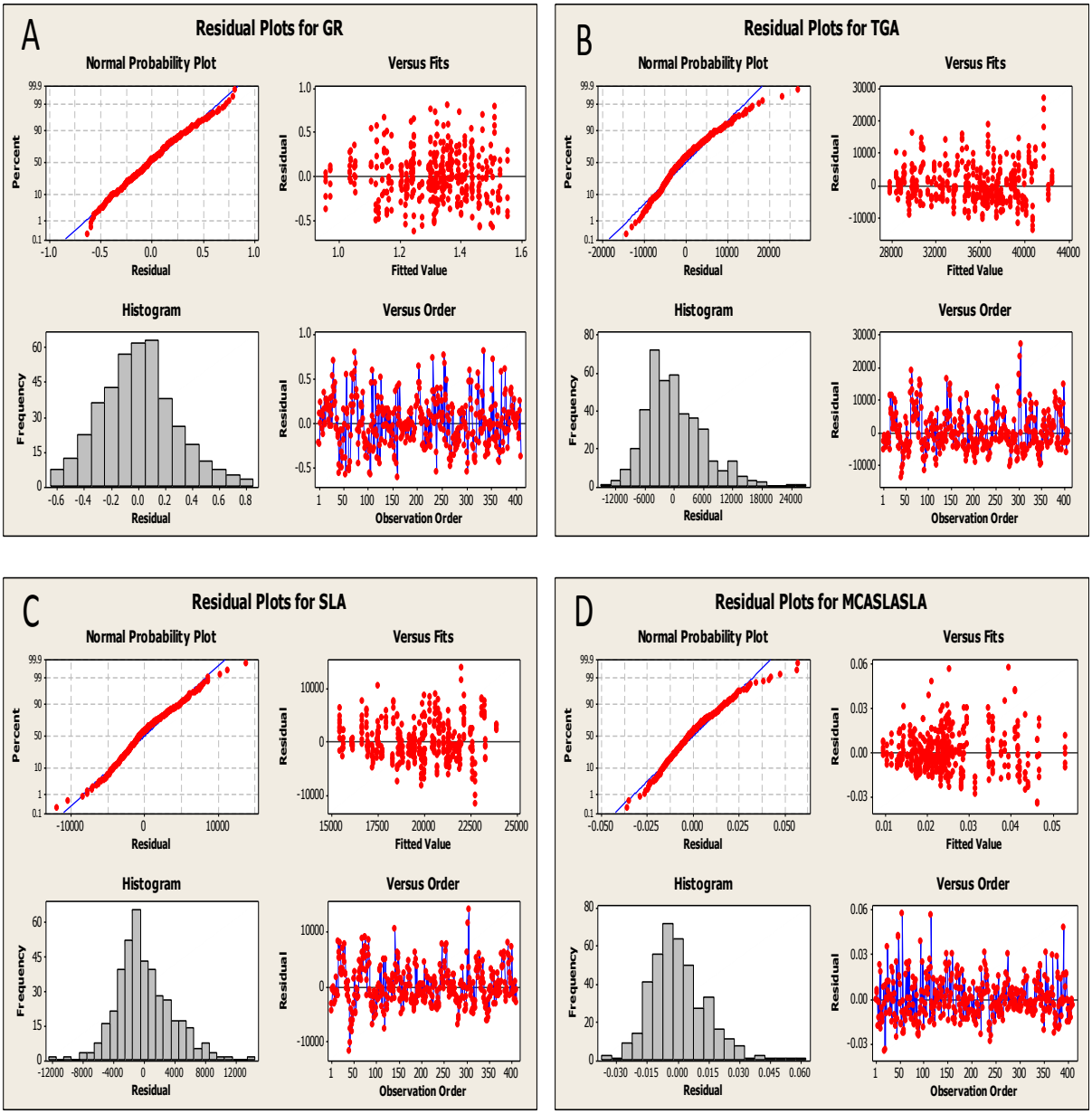

Figure 3.13 Distribution of data from selected morphometric parameters; (A) GR, gill ratio, (B) TGA, total gill area, (C) SLA, secondary lamellar area and (D) (MCA-SLA)\SLA, mucous cell area of secondary lamellar area over secondary lamellar area.

Table 3.2 Results of measured morphometric variables. GLM was performed in in Minitab.

GLM univariate analysis				Multiple comparisons between time points											
Total cases = 410	**Time points**	**Tanks**	**Fish (Tanks)**	**0 h.p.e**		**4 h.p.e**		**1 d.p.e.**		**3 d.p.e.**		**7 d.p.e..**		**14 d.p.e..**	
Acronyms	**p value**	**p value**	**p value**	**Mean**	******	**Mean**	******	**Mean**	******	**Mean**	******	**Mean**	******	**Mean**	******
VAPL	0.001*	0.765	0.001*	38590.8	D	35487.90	B	31428.50	C	30671.80	B C	37792.70	A	38239.50	B C
VASL	0.001*	0.762	0.001*	762.5	E	1935.20	B	1358.60	C D	1646.40	B C	2326.90	A	1294.80	D
TGA	0.001*	0.645	0.001*	38590.8	A	35487.90	B	31428.50	C	30671.80	C	37792.70	A B	38239.50	A B
SLA	0.001*	0.091	0.001*	21802.6	A	20464.00	A B	17367.40	C	17411.90	C	19879.50	B	21184.80	A B
PLA	0.001*	0.513	0.001*	16736.6	A B	15023.90	B C	14061.10	C D	13259.90	D	17902.90	A	17054.70	A
ILS	0.001*	0.116	0.001*	24475.2	C D	25341.40	B C D	26759.20	A B C	27838.70	A	23594.10	D	27511.30	A B
GR	0.001*	0.159	0.001*	1.3	A	1.40	A B	1.30	A B C	1.40	A	1.20	B	1.30	A B
ISR	0.001*	0.921	0.001*	1.2	B	1.30	B	1.60	A	1.60	A	1.20	B	1.30	B
PLEA	0.001*	0.953	0.001*	8778.7	A	8219.10	A B	7384.70	B C	6871.60	C	8823.60	A	8774.20	A
TMCA	0.001*	0.042*	0.001*	1113.3	A	739.70	B	634.80	B C	530.40	C D	356.00	D	707.40	B C
TMCA/TGA	0.001*	0.031*	0.001*	0.02857	A	0.020516	B	0.01947	B	0.01706	B	0.01074	C	0.01820	B
SLPL	0.018*	0.009	0.001*	4582.3	A	4564.20	A B	4436.40	A B	4473.10	A B	4263.60	B	4344.80	A B
MedianFERETMinSL	0.001*	0.898	0.002*	39.5	C	40.80	B C	43.10	B C	43.50	B	42.50	B C	47.70	A
MedianFERETMaxSL	0.001*	0.012*	0.034*	166.1	A	157.50	A B	145.20	C	154.20	B C	151.00	B C	157.90	A B
MCN-PLEA	0.001*	0.025*	0.178	2.5	B	3.50	A	3.20	A B	2.80	A B	1.40	C	2.70	A B
MCA-PLEA	0.001*	0.027*	0.249	204.3	A	244.40	A	196.10	A	169.30	A	84.50	B	195.40	A
(MCA-PLEA)/PLEA	0.001*	0.019	0.457	0.022607	A	0.02814	A	0.0258	A	0.02357	A	0.01208	B	0.02149	A
(MCN-SLA)	0.001*	0.153	0.001*	13	A	7.90	B C	8.10	B C	6.40	B C	6.20	C	8.50	B
(MCA-SLA)	0.001*	0.087	0.001*	909.3	A	495.40	B C	438.70	B C	361.10	C D	271.50	D	512.10	B
(MCA-SLA)/SLA	0.001*	0.158	0.001*	0.041975	A	0.02378	B	0.02461	B	0.02051	B C	0.01494	C	0.02348	B
TMCN	0.001*	0.072	0.001*	15.6	A	11.50	B	11.30	B	9.20	B C	7.60	C	11.20	B
TMCN/TGA	0.001*	0.042*	0.001*	0.000397	A	0.000319	B	0.000349	A B	0.000299	B	0.00022	C	0.00029	B
MedianSLL	0.002*	0.009*	0.001*	166.2	A	166.70	A	159.70	A B	163.30	A B	153.80	B	169.20	A
(SLP/SLA)	0.001*	0.556	0.001*	0.213396	C	0.22651	B	0.25695	A	0.25921	A	0.21703	B C	0.20897	C
(SLP/MedianSLL)	0.001*	0.900	0.001*	27.6	A	27.60	A	27.80	A	27.50	A	27.90	A	25.70	B

* indicates significance level at p <0.05, ** different letters indicate significant differences between time points. The highest mean of time point of each measured parameter was denoted as A and subsequent time points were indicated in alphabetical order considering the mean value. ; h.p.e.- hours.post-exposure; d.p.e. – days post-exposure.

Primary lamellae associated morphometric parameters

Primary lamellae, the structural unit of the teleost gill, were significantly affected by the H_2O_2 treatment, with almost all measured gill parameters (variables) examined changing significantly in response to H_2O_2 treatment. Statistically significant differences ($p< 0.05$) were observed at one or several time points in the vacuolar area of primary lamellae (VAPL), the primary lamellar epithelial area (PLEA) and the primary lamellar area (PLA). The VAPL increased significantly at almost all the time points compared to the pre-treatment control group, with the highest mean at 7 d.p.e. (Figure 3.14a). A significant reduction of PLEA was observed within 24 hours soon after treatment (4 h.p.e. and 24 h.p.e.), which was still observed at 3 d.p.e., but gradually this returned to pre-treatment control levels by 7 d.p.e., (Figure 3.14b). The PLA, which includes the central venous sinus (CVS) / cartilage (C), showed a similar trend to the PLEA with a gradual decrease in size until 3 d.p.e. and then recovered to pre-treatment levels by 7 d.p.e. (Figure 3.14c)

Secondary lamellae associated morphometric parameters

The VASL had significantly increased at all the time points after H_2O_2 exposure with the highest levels observed at 7 d.p.e., which was similar to the VAPL (Figure 3.15a). The SLA gradually decreased in size, with a significant decline by 24 h.p.e, with further decreases seen between 3 d.p.e. and 7.d.p.e. Levels gradually increased after this time, reaching close to the level seen in the pre-trial control. Only 24 h.p.e, 3 d.p.e. and 7 d.p.e. were significantly altered compared to the pre-trial control group levels (0 h.e.p) (Figure 3.15b).

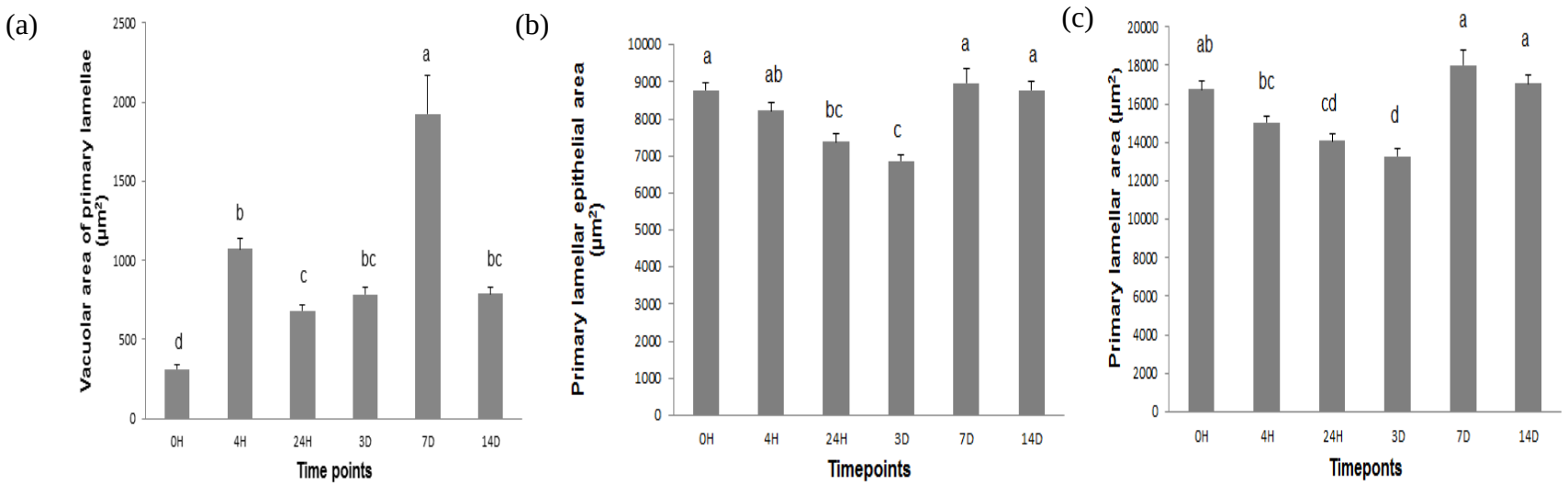

Figure 3.14 Primary lamellae associated morphometric changes in Atlantic salmon post-exposure with 1500 ppm hydrogen peroxide for 20 min at 12°C in salt water: (a) vacuolar area of primary lamellae (VAPL); (b) primary lamellar epithelial area (PLEA); (c) primary lamellar area (PLA) Abbreviations: 0H - pre-trial control; H-hours post exposure; D – days post-exposure. Bars represent mean values ± SEM where n=14. Different letters indicate significantly different values ($p < 0.05$)

The mean minimum Feret value for the secondary lamellae (MeanFERETMinSL) had increased significantly at 14 d.p.e., but not in fish sampled from other time points compared to the control group (Figure 3.15c). The median minimum Feret value for the secondary lamellae (MedianFERETMinSL) had increased significantly compared to the control group by 3 and 4 d.p.e., when it reached its highest value (Figure 3.15d).

In contrast to previous patterns of changes, the median maximum Feret value for the secondary lamellae (MeanFERETMaxSL) had decreased at all-time points, being significantly lower at 24 h.p.e., 3 d.p.e and 4 d.p.e. Its rapid decrease was observable within a day (24 h.p.e.) (Figure 3.15e). It was not a surprise that median maximum Feret value for secondary lamellae (MedianFERETMaxSL) showed the same pattern of change (Figure 3.15f).

However, SLPL gradually decreased and was significantly lower at 7 d.p.e. compared to the pre-trial control, and then started to increase after day 14 d.p.e. (Figure 3.15g). The median secondary lamellar length (MedianSLL) of Atlantic salmon gills treated with hydrogen peroxide had decreased significantly by 7 d.p.e. and then increased to pre-trial control levels (Figure 3.15i). The median SLL was significantly reduced by 7 d.p.e. following the same pattern as above. The SLPL/SLA (known as lamellar index) was significantly increased at 4 h.p.e. and 24 h.p.e., and this started to decrease at 7 d.p.e and 14 d.p.e. (Figure 3.15j). The SLPL/MeanSLL was found to change slightly, but was not significantly different from pre-trial controls until 7 d.p.e. A significant decrease of SLPL\ManSLL was observed at 14 d.p.e (Figure 3.15k).

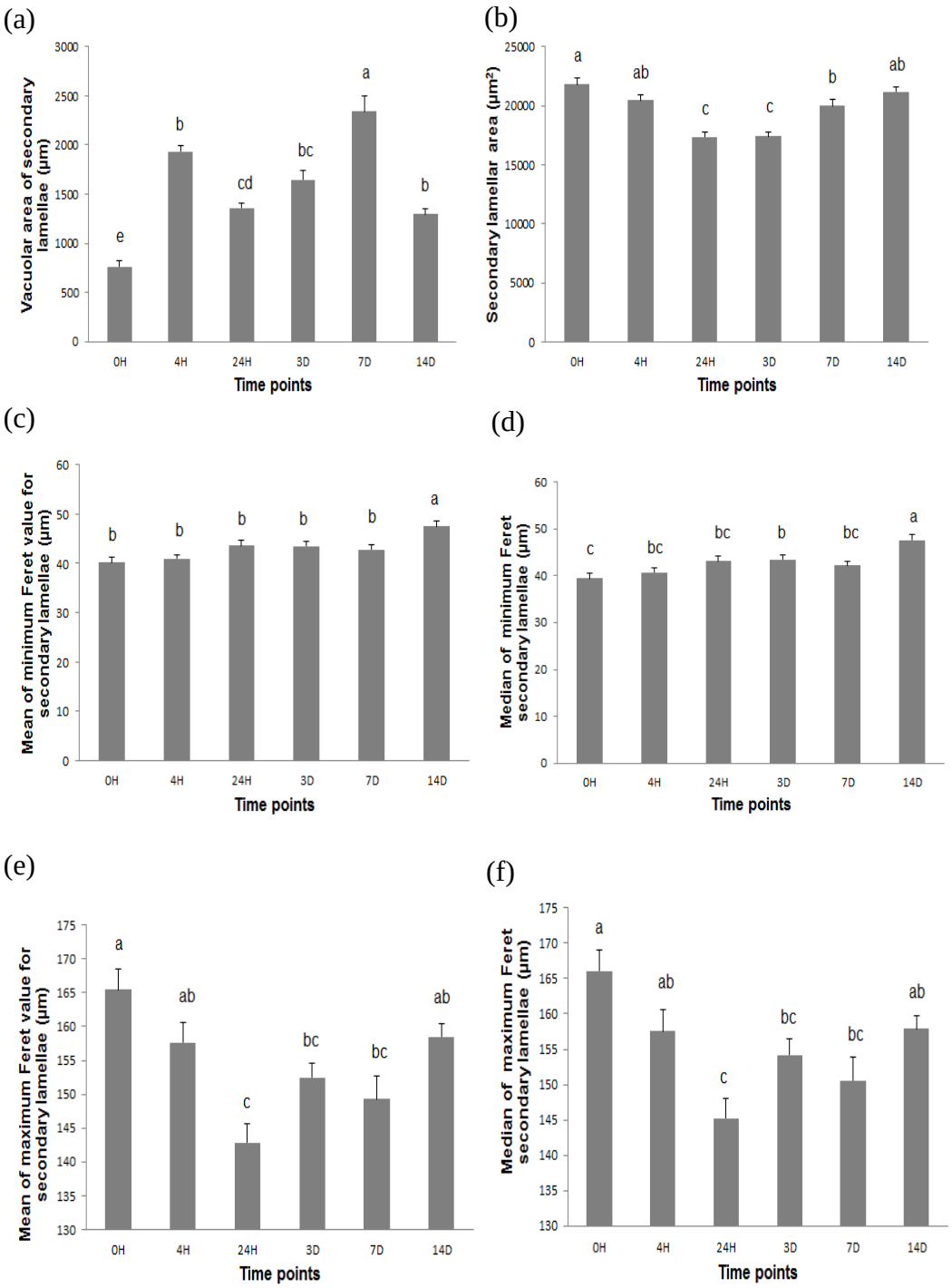

Figure3.15 Secondary lamellae associated morphometric changes in Atlantic salmon post exposure with 1500 ppm hydrogen peroxide for 20 min at 12°C in salt water: (a) vacuolar area of secondary lamellae (VASL); (b) secondary lamellar area (SLA); (c) mean minimum Feret value for secondary lamellae (MeanFERETMinSL); (d) median minimum Feret value for secondary lamellae (MedianFERETMinSL); (e) maximum Feret value for secondary lamellae (MeanFERETMaxSL); (f) median maximum Feret value for secondary lamellae (MedianFERETMaxSL). Abbreviations: 0H - pre-trial control; H-hours post exposure; D – days post-exposure. Bars represent means values ± SEM where n=14. Different letters indicate significantly different values ($p \leq 0.05$).

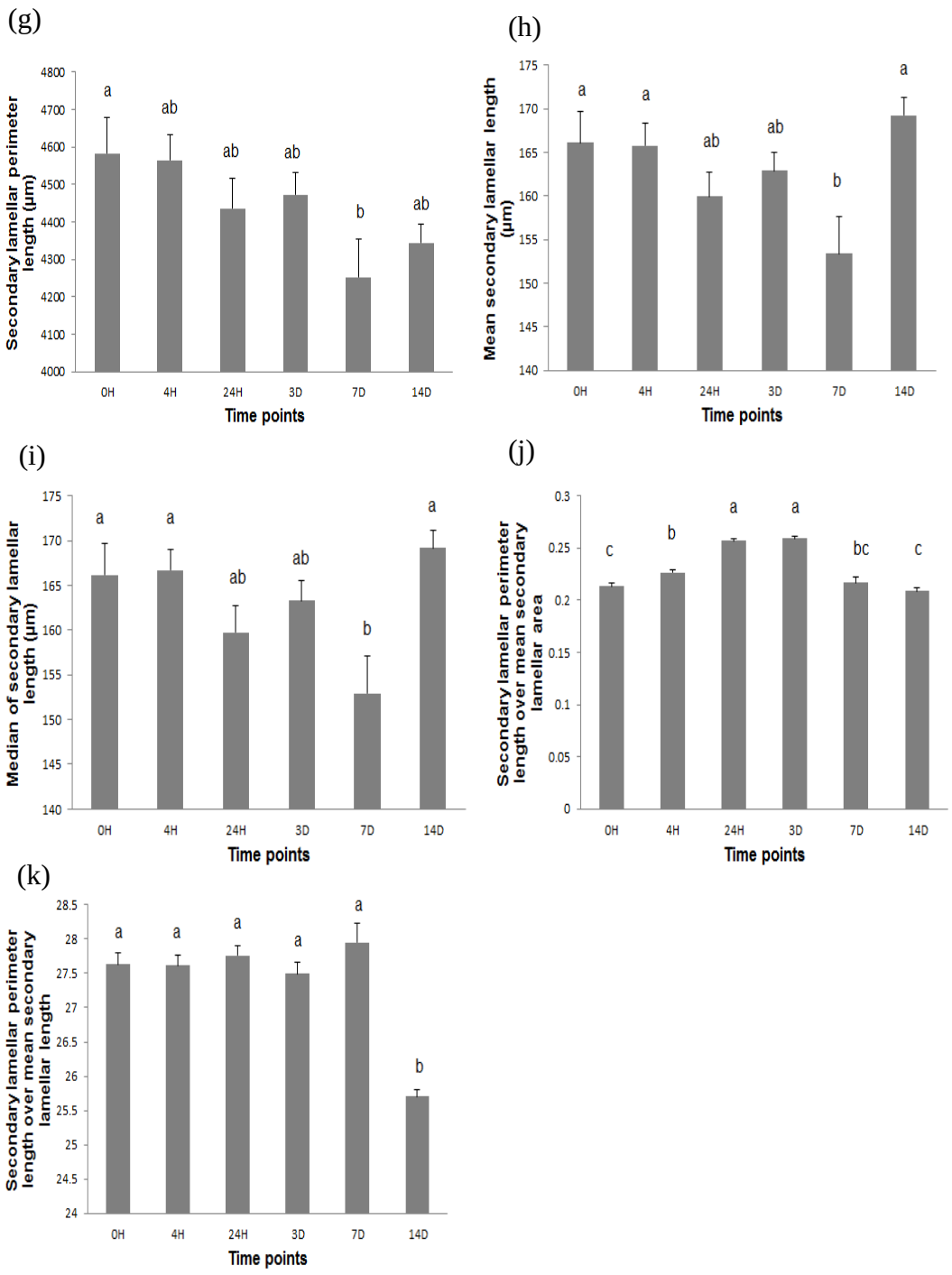

Figure 15 (cont.) Secondary lamellae associated morphometric changes in Atlantic salmon post exposure with 1500 ppm hydrogen peroxide for 20 min at 12°C in salt water: (g) secondary lamellar perimeter length (SLPL); (h) secondary lamellar length (MeanSLL); (i) median secondary lamellar length (Median SLL); (j) (SLPL/SLA); (k) (SLPL/MeanSLL). Abbreviations: 0H - pre-trial control; H-hours post exposure; D – days post-exposure. Bars represent means values ± SEM where n=14. Different letters indicate significantly different values ($p \leq 0.05$).

Mucous cell associated morphometric parameters

According to the results obtained from GIA analysis, mucous cell associated morphometric parameters were significantly changed in Atlantic salmon gills exposed to H_2O_2. The total mucous cell area (TMCA) *i.e.* number of cells in the selected gill area of interest were significantly different over time, reaching the lowest level at 7 d.p.e. and then increasing again by to 14 d.p.e (Figure 3.16a). When TMCA was standardised against total gill area (TMCA\TGA), the same pattern of changes was observed as seen for TMCA (Figure 3.16b). The number of mucous cells in the primary lamellar epithelial area (MCN-PLEA) had significantly increased at 4 h.p.e compared to pre-treatment controls, and then gradually decreased until 7 d.p.e., at which point values were significantly lower than those seen in pre-trial controls. This number was seen to increase to pre-trial levels by 14 d.p.e. (Figure 3.16c). In contrast to the TMCA, total mucous cell area in the primary lamellar epithelial area (MCA-PLEA) increased, showing a similar pattern to MCN-PLEA (Figure 3.16d). Total mucous cell area in primary lamellar epithelial area / primary lamellae epithelial area (MCA-PLEA)/PLEA was seen to be increased in treated fish at 4 h.p.e., then gradually decreased until 3 d.p.e. to significantly lower levels than seen in the pre-trial controls (Figure 3.16e). Initially, PLA values were significantly changed compared to control fish. The total mucous cell number of the secondary lamellar area (MCN-SLA) decreased with a similar pattern to the TMCA and was significantly decreased from 4 h.p.e. until 3 d.p.e., then gradually increased after 7 d.p.e and 14 d.p.e., with mean values of all the time points being lower than the pre-trial control (Figure 3.8f). In contrast to the (MCA-PLA)\PLA, the mucous cell area of the secondary lamellar area \ secondary lamellar area (MCA-SLA) was significantly lower than pre-trial controls. The mean values of

MCA-SLA\SLA observed at all timepoints were lower than pre-trial controls (Figure 3.16g). The total mucous cell number (TMCN) followed

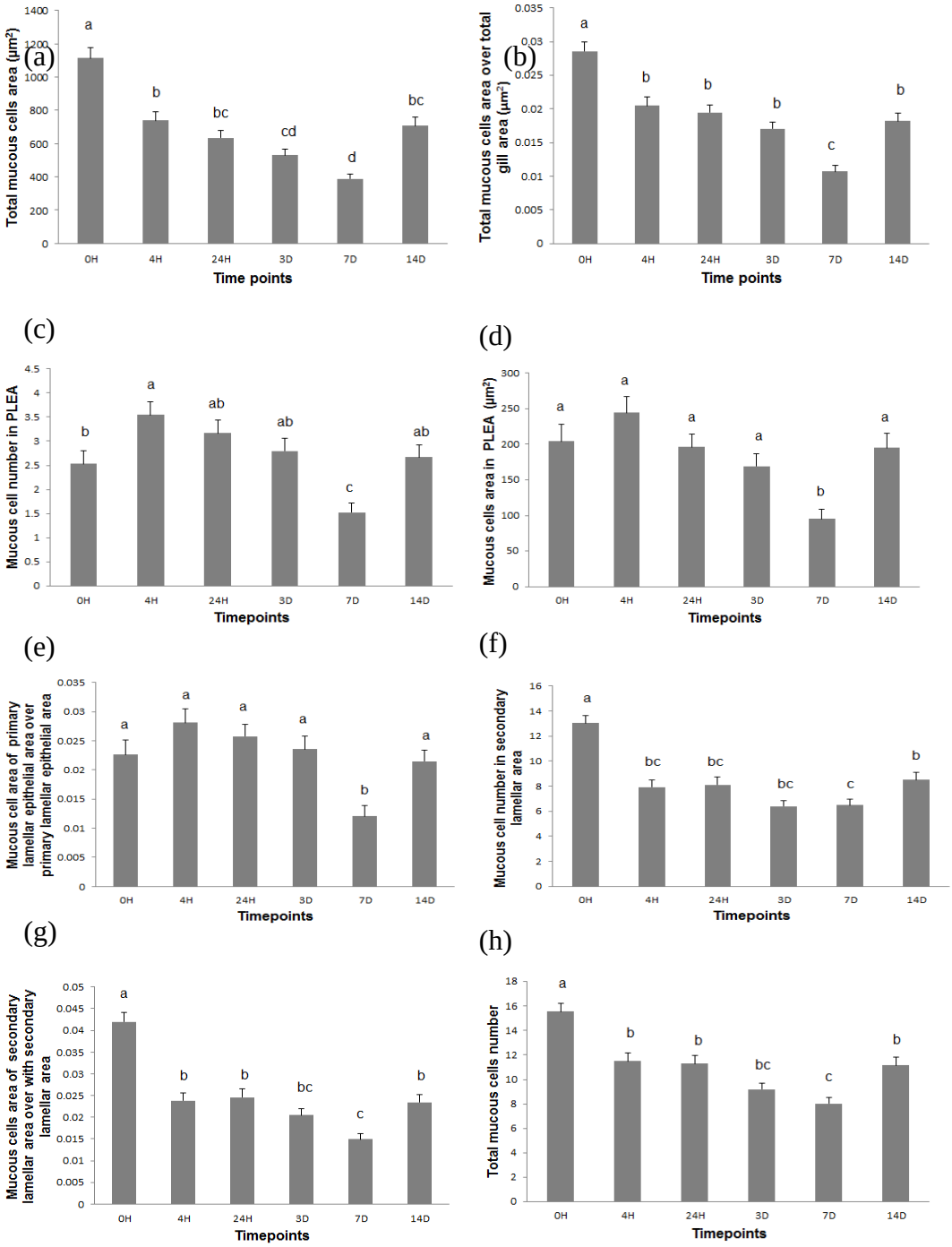

Figure 3.16 Mucous cell associated morphometric changes in Atlantic salmon post exposure with 1500 ppm hydrogen peroxide for 20 min at 12°C in salt water: (a) total mucous cell area (TMCA); (b) total mucous cell area / total gill area (TMCA\TGA); (c) number in primary lamellar epithelial area (MCN-PLEA); (d) total mucous cell area in primary lamellar epithelial area (MCA-PLEA); (e) total mucous cell area in primary lamellar epithelial area / primary lamellae epithelial area (MCA-PLEA)/PLEA; (f) total mucous cell number secondary lamellar area (MCN-SLA); (g) mucous cell area of secondary lamellar area / secondary lamellar area

(MCA-SLA); (h) total mucous cell number (TMCN) Abbreviations: 0H - pre-trial control; H-hours post exposure; D – days post-exposure. Bars represent mean values ± SEM where n=14. Different letters indicate significantly different values ($p \leq 0.05$).

a similar pattern, where TMCA was initially decreased until 7 d.p.e. then started increasing at 14 d.p.e. (Figure 3.16h).

Total gill area associated morphometric parameters

The total gill area associated morphometric parameters changed significantly in one or more time points compared to their pre-trial controls including interlamellar space (ILS), gill ratio (GR), inter-secondary ratio (ISR) and total gill area (TGA). ILS is known to be a representative area for available oxygen for respiration. According to the results the interlamellar area was significantly increased ($p \leq 0.05$) until 3 d.p.e. then decreased at 7 d.p.e. but regained a significant increase at 14 d.p.e. (Figure 3.9a). However, GR showed no significant changes except at 7 d.p.e. where it was reduced significantly to its lowest level (Figure 3.17b). The ISR index was shown to be gradually increased until 3 d.p.e. and was significantly different from their pre-trial control at 24 h.p.e and 3 d.p.e ($p \leq 0.05$) then gradually decreased at 7 d.p.e. and increased again by 14 d.p.e, to levels higher than the pre-trial controls (Figure 3.17c). Finally TGA (selected area of interest from cropped subsamples) showed a significant gradual reduction at 24 h.p.e, and started to increase again at 7 d.p.e. and 14 d.p.e. to similar levels seen in pre-trial controls (Figure 3.17d).

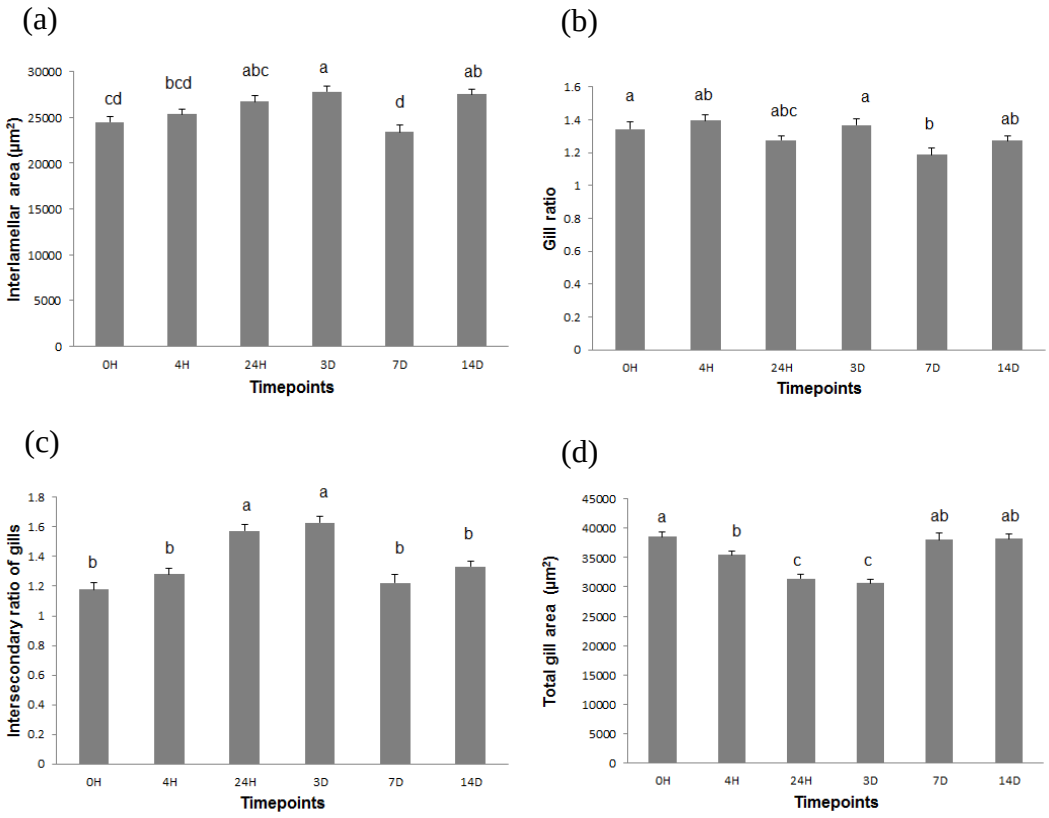

Figure 3.17 Total gill area associated morphometric changes in Atlantic salmon post exposure with 1500 ppm hydrogen peroxide for 20 min at 12°C in salt water: (a) interlamellar area (ILS); (b) gill ratio (GR); (c) inter-secondary ratio (ISR); (d) total gill area (TGA). Abbreviations: 0H - pre-trial control; H-hours post exposure; D – days post-exposure. Bars represent means values ± SEM where n=14. Different letters indicate significantly different values ($p \leq 0.05$).

3.3.2.2 Multivariate analysis of morphometric data

Multivariate analysis of the morphometric data derived from the hydrogen peroxide trial was performed using Principal Component Analysis (PCA) in Minitab (Minitab Ltd) statistical software, to explore the relationships between variables (morphometric parameters). Initially, 28 measured morphometric variables were tested and verified as normally distributed. Almost all measured variables were used to perform PCA and the results were shown in Table 3.3. The column "Total" gives the eigenvalue or the amount of variance in the original variables accounted for by each component. The '% variance column' gives the ratio, expressed as a percentage of the variance accounted for by each component to the total variance. The 'Cumulative % column' gives the

percentage of variance accounted for by the first 10 components (only the first 10 components are displayed in the Table 3.4.

Table 3.3 Total variance explained by the first 5 principal components (29 measured morphometric parameters)

Total Variance Explained						
	Initial Eigenvalues			Extraction Sums of Squared Loadings		
Component	Total	% of Variance	Cumulative %	Total	% of Variance	Cumulative %
1	8.335	24.513	24.513	8.335	24.513	24.513
2	5.451	16.033	40.546	5.451	16.033	40.546
3	4.849	14.260	54.807	4.849	14.260	54.807
4	2.782	8.182	62.989	2.782	8.182	62.989
5	2.245	6.602	69.591	2.245	6.602	69.591

Table 3.4 Total variance of extracted first 10 principal components out of a total of 28 measured morphometric parameters

Communalities		
Morphometric variables	**Initial**	**Extraction**
Weight (W)	1.000	.980
Length (L)	1.000	.893
Condition factor (K)	1.000	.776
Vacuolar area of primary lamellae (VAPL)	1.000	.894
Vacuolar area of secondary lamellae (VASL)	1.000	.885
Total gill area (TGA)	1.000	.978
Secondary lamellar area (SLA)	1.000	.953
Primary lamellar area (PLA)	1.000	.947
Interlamellar spase (ILS)	1.000	.842
Gill Ratio (GR) (GR=SLA/PLA)	1.000	.877
Intersecondary ratio of gill (ISR)	1.000	.961
Primary lamellar epithelial area (PLEA)	1.000	.873
Total mucous cells area (TMCA)	1.000	.970
Total mucous cells area over total gill area (TMCA / TGA)	1.000	.969
Secondary lamellar perimeter length (SLPL)	1.000	.960
Median of minimum Feret secondary lamellae (MedianFERETMinSL)	1.000	.941
Median of maximum Feret secondary lamellae (MedianFERETMaxSL)	1.000	.946
Mucous cell number in PLEA	1.000	.938

Mucous cells area in PLEA	1.000	.973
(MCA-PLEA)/PLEA	1.000	.941
Mucous cell number in secondary lamellar area	1.000	.961
Mucous cells area of secondary lamellar area	1.000	.967
Mucous cells area of secondary lamellar area over with secondary lamellar area	1.000	.962
Total mucous cells number (TMCN)	1.000	.959
Total mucous cells number corrected with total gill area (TMCN / TGA)	1.000	.879
Median of secondary lamellar length (MedianSLL)	1.000	.960
Secondary lamellar perimeter length over secondary lamellar area (SLP/SLA)	1.000	.869
Secondary lamellar perimeter length over mean secondary lamellar length (SLP/MeanSLL)	1.000	.821

The first 'Component' has the largest eigenvalue and represents the most variance. The first component explains nearly 24% of the variation between individuals. The first two 'components' combined explain 40% ('Cumulative %') of the variation between individuals between them.

The rotated component matrices (Table 3.5) were used to compare the relationship of the variables extracted from Principal Components 1 and 3. The first component is highly correlated with TGA, SLA, TMCA, TMCA/TGA, SLPL, MedianFERETMaxSL, MCA-PLEA, MCN-SLA, MCA-SLA, MCA-SLA/SLA, TMCN, TMCN/TGA and MedianSLL. but of those, TMCA, TMCN, TMCA/TGA, MCN-SLA, MCA-SLA provide the greatest explanatory power. The second component correlates more with SLPL, GR, MedianFERETMaxSL. It is highly correlated with inter SLPL. Plotting of components 1 and 2 from the PCA analysis discriminates pre-trial control group (black dots) from other time points as illustrated in the scatter plot in Figure 3.18. The differential location / position of individual time points compared to pre-trial control group are individually illustrated in Figure 3.19 B-F.

Table 3.5 Component matrices generated from PCA analysis of measured morphometric variable. The parameters indicate greater explanatory power is shaded in grey

Morphometric parameters	Component									
	1	2	3	4	5	6	7	8	9	10
Weight	.234	.330	.143	-.226	.631	-.417	.035	.406	.064	.048
Length	.083	.303	.110	-.059	.355	-.405	.035	.522	.310	.345
K factor	.283	.198	.101	-.283	.605	-.211	.017	.056	-.241	-.307
VAPL	-.214	-.178	.698	.174	-.037	-.002	.012	-.139	.509	-.141
VASL	-.106	.102	.502	.270	-.176	-.076	-.150	.049	.647	-.242
TGA	.563	-.017	.775	-.023	-.028	-.027	.152	-.122	-.087	.110
SLA	.698	.312	.567	-.018	-.119	-.027	-.126	.026	-.089	.086
PLA	.261	-.335	.744	-.019	.073	-.018	.377	-.228	-.055	.098
ILS	.089	.456	-.344	.122	.226	.014	.552	-.208	.158	.264
GR	.277	.592	-.227	-.002	-.226	-.006	-.535	.247	.009	-.011
ISR	-.421	.111	-.630	.108	.233	.064	.478	-.164	.173	.139
PLEA	.329	-.343	.729	.101	.065	-.047	.262	-.163	-.052	.020
TMCA	.909	-.332	-.161	.004	.037	.032	-.045	-.005	.022	.049
TMCA/TGA	.810	-.395	-.371	.025	.045	.035	-.080	.021	.094	-.029
SLPL	.557	.706	.030	.141	-.306	.104	.038	.040	.000	.154
MedianFERETMinSL	.126	.386	.220	.331	.514	.427	-.312	-.210	-.007	.172
MedianFERETMaxSL	.532	.630	.002	-.235	-.336	-.208	.194	-.117	-.003	-.059
MCNPLEA	.434	-.245	-.211	.700	.011	-.383	-.007	-.059	-.057	-.042
MCAPLEA	.511	-.259	-.186	.649	.034	-.400	-.045	-.108	-.112	.004
MCAPLEA_PLEA	.423	-.179	-.347	.661	.015	-.386	-.115	-.094	-.037	-.018
MCNSLA	.804	-.291	-.147	-.331	.045	.266	.052	.041	.144	.001
MCASLA	.857	-.280	-.109	-.287	.029	.218	-.033	.042	.076	.056
MCASLASLA	.712	-.443	-.270	-.322	.056	.247	.047	.021	.122	-.014
TMCN	.876	-.351	-.211	-.022	.044	.087	.043	.014	.104	-.015
TMCNTGA	.684	-.375	-.462	.021	.054	.092	-.003	.045	.181	-.101
MedianSLL	.529	.793	-.027	.121	-.123	.049	.094	-.053	.007	-.081
SLPL/SLA	-.398	.273	-.704	.173	-.109	.166	.225	.005	.133	.049
SLPL/MedianSLL	-.028	-.387	.146	.091	-.476	.065	-.162	.202	-.025	.586

The PCA analysis indicated a distinct pattern of relevant time points. The 0 h.p.e. shows that the pre-trial control fish are homogeneously scattered, but a gradual movement of the other timepoints. Initially, the 4 h.p.e group was seen to move away from control group (black dots). The highest negative values in the PCA were seen for ISR, SLPL_SLA, PAPL and VASL with values for 4 d.p.e timepoint moving in a left direction. However by 24 h.p.e (green rhombuses) the values had moved further, towards the left, however, they appeared to be less scattered. Then at the end of the trial period, the values acquired their original position seen with pre-trial controls. As shown by univariate analysis values, d.p.e appeared to be the breakeven point for ISR and SLPL/SLA (their highest values), and the mean value of each parameter started decreasing after this time. In contrast to the previous time points, the 7 d.p.e moved towards the controls at 0 h.p.e.

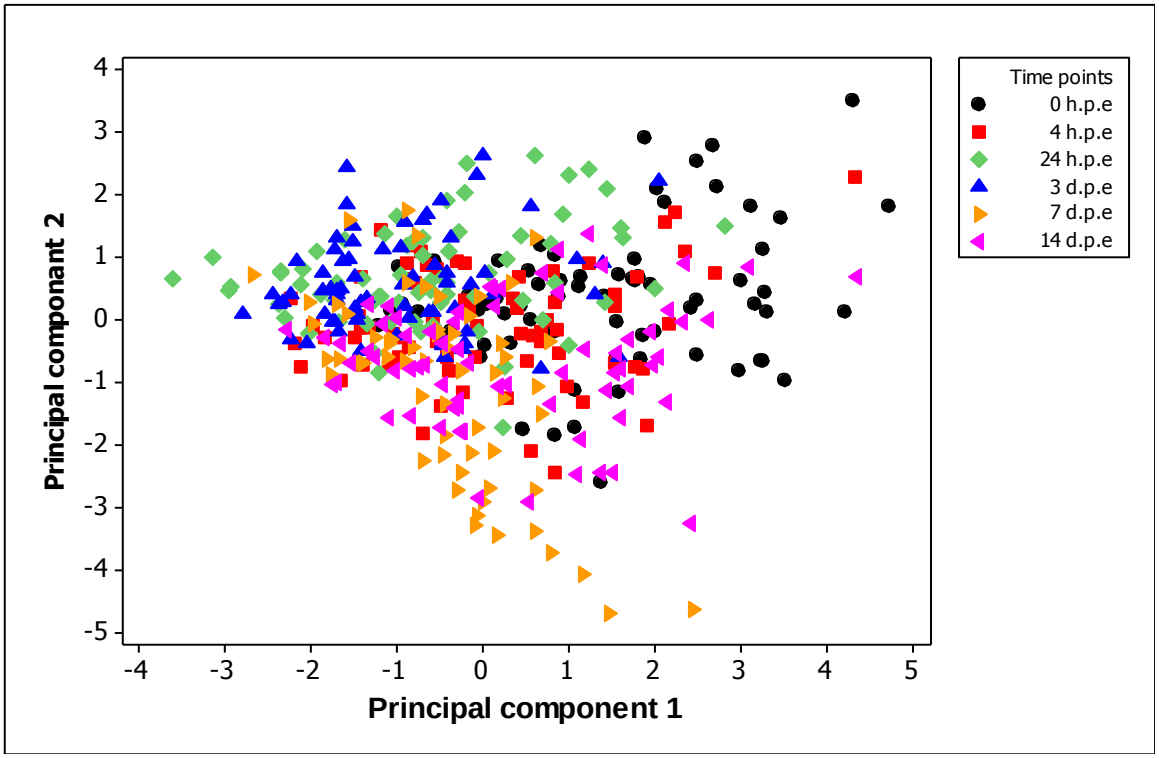

Figure 3.18. A scatter plot generated from PCA analysis, plotting principal component 1 and 2 and showing clear clustering of subsamples of fish belong to different groupings.

By 14 d.p.e. (purple colour triangles) the values seems to be closer to the controls, indicating that some of the fish were showing signs of recovery indicated by their distribution amongst the controls values represented by the black dots

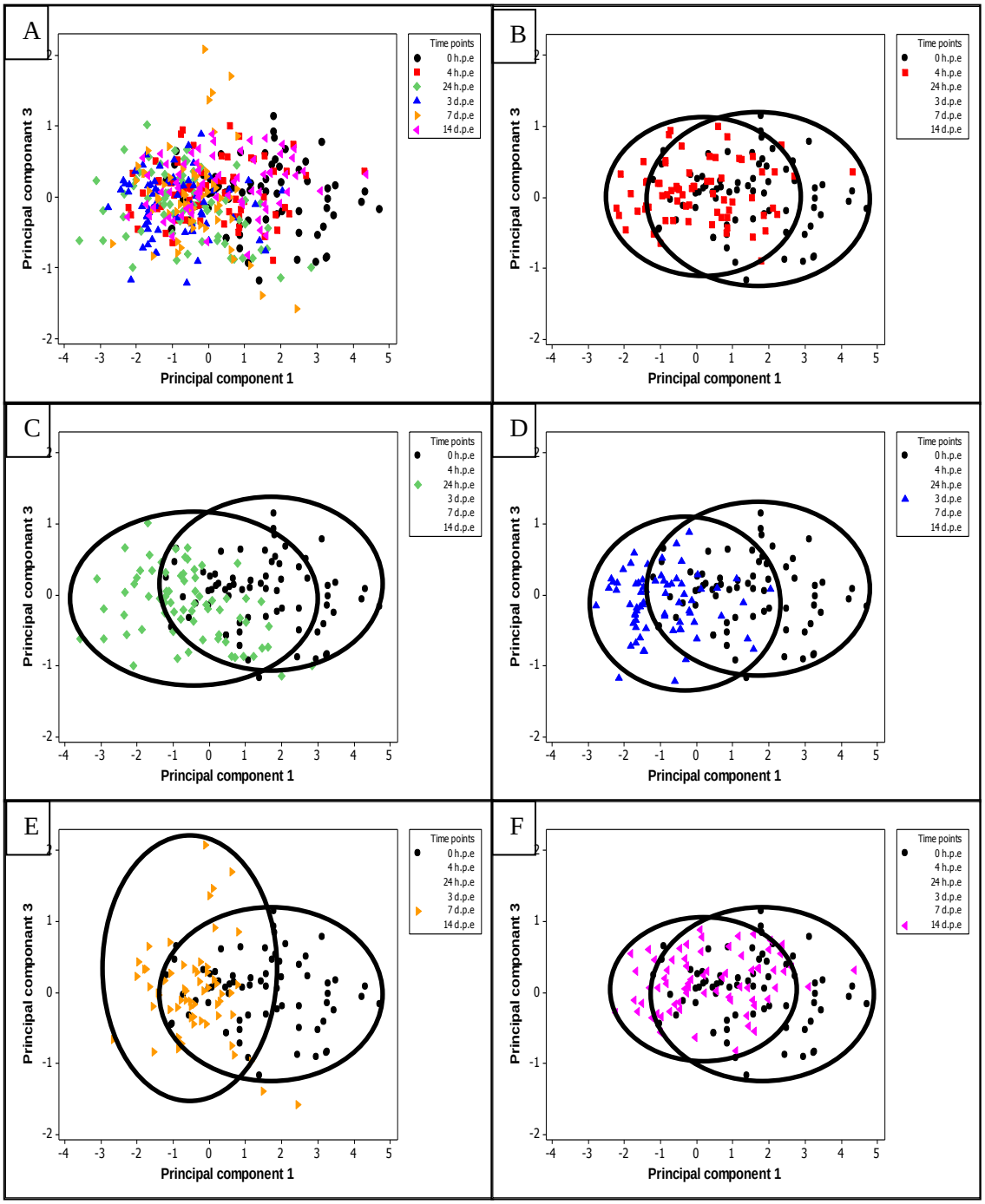

Figure3.19. Classification of subsamples of fish belonging to different time points using new variables PC1 and PC2. (A) All six sampling points, (B) Control versus 4 h.p.e., (C) control versus 12 h.p.e., (D) control versus 3 d.p.e., (E) control versus 7 d.p.e., (F) control versus 14 d.p.e.

3.3.3 **Discussion**

The objective of the present study was to evaluate the histopathological / morphometric changes seen in Atlantic salmon gills after exposure to a therapeutic dose of H_2O_2. The histological evaluation found that most lesions previously described after H_2O_2 treatment (Mallatt 1985; Kiemer and Black, 1997) were present in the gills collected during the current study *i.e.* hyperplasia and hypertrophy of cells, epithelial cell lifting, congested blood cells in the lamellae, mucus hypersecretion, mucous cell hyperplasia, hyperplasia and hypertrophy of chloride cells, damage or necrosis of chloride cells, dilation or constriction of lamellar blood sinus and leukocyte infiltration into gill epithelium. However, more acute and severe lesions such as oedema and necrosis of the epithelium and rupture of the lamellae epithelium were not noted. The histopathological changes observed were quantitatively evaluated by developing a new gill scoring system for H_2O_2 treated gills of Atlantic salmon. This scoring system is based on the previous gill scoring systems carried out by Kiemer and Black (1997). In their experiment, a grading system was introduced in order to quantify the gill histopathological response, which was found to be highly correlated with level of exposure and the degree of the damage. The histomorphometric assessment made during the present trial was performed using whole slide imaging and virtual microscopy, followed by image processing and analysis. This provides an advance on conventional histopathology evaluation techniques and can help to increase consistency and objectivity as well as providing data suitable for statistical analysis.

The results obtained from the gill scoring system, based on the morphometric changes described in Table 3.1, *i.e.* significant and non-significant differences, agreed with the morphometric changes identified through GIA analysis.

The sequence of events occurring in the gills immediately after H_2O_2 treatment includes a rapid response, reflecting sudden changes of key gill morphometric parameters *e.g.* reduction of the TGA, SLPL and MeanSLL. Changes in all the secondary lamellae associated morphometric parameters tend to reflect a reduction in the size of the gill surface area. Changes in the primary lamellae associated gill morphometric parameters also play a supportive role in reducing their tissue area indicated by a reduction in the PLEA and the PLA. The reduction of the total gill area appears to be first line of defence in the gills, irrespective of the type of harmful irritant substances encountered (Mallatt 1985). Furthermore, from the review by Mullatt, which included more than 150 papers describing various types of chemical treatment on fish that have an effect on the gills, most of them reported that gill changes were a common occurrence and non-specific in nature. Recently, Henrikson *et al.* (2014) revealed that when gills were exposed to H_2O_2 alone or alongside bacterial pathogens or were pre-treated with H_2O_2 followed by bacterial challenge, the former had an impact on gill morphology. For example, infection with *Flavobacterium psychrophilum* was found to intensify the damage and delay the healing process of the gills. Furthermore, previous studies which focused on the initial stage of acute phase response found it to be characterised by elevated stress indicators and physiological parameters, and indicated that the fish was not fully recovered until at least 24 h.p.e. Previous work on other fish species (sea bass, *Dicentrachus labrax* and sea bream, *Sparus aurata*) indicates full recovery between 24 h and 7 d.p.e (Tort *et al.,* 2003) and further suggests that the acute effects of H_2O_2 baths

are less harmful to the fish than the effects of persistent chronic exposure (Mansell *et al.,* 2005).

During the present study it was obvious that after 24 h.p.e fish started to gradually recover, returning to their original state around 7 d.p.e. It was further illustrated by PCA that by 7 d.p.e. the morphometric changes in the gill tended to start return to pre-treatment values. Although this seems to be the outcome during experimental or culture conditions, in natural environments fish have more choice to the environmental factors they are exposed to such as water salinity, water temperature and dissolved oxygen content. Thus, they tend to show a modification in their behavioural and tend to migrate away from the hazard in order to find more favourable conditions. It has been hypothesized that the effects of H_2O_2 is more intense for fish in freshwater than in sea water due to the differences in the hardness of the water (Powell and Perry, 1997). The effect of H_2O_2 exposure on gill morphology was studied in walleye, *Stizostedion vitreum*, with increased lamellar fusion and lamellar oedema evident.

It would appear that fish was undergoing an acute stress response show alteration in hormone levels, changing blood ion concentrations and variation in blood parameters including haematocrit values (Tort *et al.,* 2003). In addition to body homeostatic changes, gill morphometric changes characterised by a reduction in the gill surface area can temporary impair the gas exchange much needed for managing successful acute stress response. After this short period of acute stress, fish gradually recover to pre-treatment status. Most of the gill parameters identified through the GIA tool showed this gradual move towards their initial pre-treatment state at later timepoints *e.g.* 7 d.p.e., although it is clear that even by 14 d.p.e. full recovery was not achieved in most individuals.

The response of the fish during the first 6 h.p.e. could be crucial for maintaining homeostasis, while coping with acute stress conditions. Roque *et al.,* (2010) found that, when sea bass were exposed to a H_2O_2 dose of 50 ppm for 1 hour, increased plasma glucose and lactate levels of treated fish were 1.5 or 1.4 fold higher than the respective control fish. Other authors have also shown that typical stress responses include plasma glucose and lactate responses (Lowe-Jinde and Niimi, 1984; Hontela *et al.,* 1997; Santos and Pacheco, 1996). Moreover, stress responses have adaptive value since they increase the availability of energy substrates necessary for the maintenance of homeostasis, including regaining the multifunctional capacity of the gills. This sudden energy mobilisation could benefit the gill remodelling, morphometric adaptation and later healing of functional tissues (Donaldson *et al.,* 1984). After a 24 h recovery period, glucose and lactate values were seen to decrease to similar or lower values than seen in control fish. The present study revealed that the morphometric parameters measured reflect a pattern of reduction of TGA until 24 h.p.e. where the value is equal to the value representing 3 d.p.e., speculating that there might be further lower value point between these two timepoints. The plasma glucose concentration has been shown to be elevated in Atlantic salmon in the first 24 h.p.e with H_2O_2 treatment (Bowers *et al.,* 2002). It was also found that Atlantic salmon exposed to H_2O_2 had elevated blood cortisol that remained between 6 and 12 h.p.e., and subsequently returned to the resting state by 24 h.p.e. (Bowers *et al.,* 2002). There are several reports in the literature regarding acute phase response in relation to plasma and blood chemistry in different species including significant alterations in plasma ion concentrations such as sodium, magnesium and calcium found in sea bass (Roque *et al.,* 2010) and Atlantic salmon (Bowers *et al.,* 2002). Further, exposure to H_2O_2 may elicit disturbances in acid-base

balance, oxygen and carbon dioxide transport and also transport of ions, which reflect alterations in gas exchange (Tort *et al.*, 2003).

During the initial stress period some fish species show an increase in their haematocrit values and total plasma protein concentration, which may be due to the increased demand of oxygen supply to the major organs in response to higher metabolic demand, which is needed for oxidative phosphorylation, as described by Sepulveda *et al.*,. (2004) in largemouth bass, *Micropterus salmoides floridanus*, under stress conditions. Although the present study did not attempt to measure any of these plasma indicators, the observed patterns of gill morphometric change supports a correlation with lowered capacity for gas exchange resulting from a reduction in gill respiratory surface area as indicated by changes in the SLPL. Due to the reduced respiratory surface area of the fish gill, secondary compensatory mechanisms may be brought into play such as elevated haematocrit to increase the oxygen supply to major organs in response to their higher metabolic demand (Cnaani *et al.*, 2004). Powell and Perry (1997) explained that the increase in haematocrit value in rainbow trout, *Oncorhynchus mykiss*, exposed to H_2O_2 may be due to an elevation of catecholamine levels, produced during a stress response. The increase in haematocrit value probably results from β-adrenergic activation of Na+/H+ exchange, resulting in cell swelling and hence a reduced mean cell haemoglobin concentration but also from α-adrenergic splenic contraction. Also there are suggestions of changes in the fish's lymphatic system, possibly releasing extra blood into the central circulation and hence reducing haematocrit values (Olson, 1996). However, as a result of H_2O_2 exposure, elevated haemoglobin has also been suggested to represent a strategy for increasing the oxygen carrying capacity of blood during periods of high energy demand (Montero *et al.*, 1999). In contrast, Powell and Perry

(1997) reported that increased haemoglobin in rainbow trout exposed to H_2O_2 might be due to a reduction in the level of oxygen specifically bound to haemoglobin.

One of the key effects of H_2O_2 treatment on salmonid gills is the rapid change in mucous cell morphology and abundance. Roberts and Powell, (2003) found that after treatment with H_2O_2 or challenge with AGD or both, changes in the morphometry of mucous cells occurred *i.e.* mucous cells hyperplasia and hypertrophy. The role of mucus in ionic regulation by fish is uncertain (Zuchelkowski *et al.,* 1985; Shephard, 1994), however, its role in disease through host pathogen interactions has been well characterised in mammalian systems (Jones and Reid, 1978; Verdugo, 1990). Roberts and Powell, (2002) indicated that gill mucous cell abundance / morphology and the thickness of the mucus layer are important for efficient ion regulation during disease progression. In comparison to previous studies on rainbow trout, Atlantic salmon have a greater short-term ionic regulatory capacity, which may become a crucial factor relevant to acute gill response. It has been suggested that branchial mucus impairs CO_2 excretion without hindering oxygen uptake across the gills (Powell and Perry, 1999), leading to subsequent respiratory acidosis that occurs with AGD (Ferguson *et al.,* 1992; Powell *et al.*, 2000). It was hypothesised that AGD affected fish would have an ionic regulatory dysfunction reflected by variations in whole body net ionic fluxes compared to control fish, and that this could be correlated with gill mucous cell conformation. This proven close relationship of ion regulation and gill histomorphometry could generate importance of measuring morphometric parameters of Atlantic salmon gills reflecting ion regulatory status of the gills.

Quantification of mucous cell populations through histochemistry is a widely used method for pathological assessment in disease conditions (Jones and Reid, 1978; Ferguson *et al.*, 1992). In the present study a set of morphometric parameters associated with mucous cell histochemistry were evaluated over seven days following treatment with H_2O_2. The TMCA and TMCN values were significantly decreased at one or more time points until 7 d.p.e., then increased again by 14 d.p.e., corresponding to previous studies showing recovery and healing by this point. The pattern of mucous cell change previously mentioned have been standardised and confirmed from TMCA\TGA and TMCN\TGA values, which were proven to be independent of the changes in gill area. In contrast, parameters like MCN-PLEA and MCA-PLEA showed significant change, reaching their highest levels at 4 h.p.e., possibly due to an acute stress response, and resulting in increased production of mucous as a first line of defence.

The GIA tool produces a number of indices developed by combining primary measured variables *e.g.* ILS, ISR and GR. The TGA, which was the mean value of cumulative area of interest (AOI) originally consists of PLA and SLA (PLA=PLEA + central venous sinus; CVS). Due to the high number of variables\parameters measured, it is useful to synthesise new indices like ISR and GR to evaluate the changes in gill morphometry. During analysis ISR (ISR=ILS\SLA) was shown to be increased until 3 d.p.e., which was due to an increase in ILS and reduced SLA by shrinking of the TGA.

Almost all the parameters measured were imported into multivariate analysis and from this key variables were selected for a gill health index for Atlantic salmon. The scatter plot generated by PCA showed a distinct pattern, grouping individual fish into their relevant time points. The pre-trial control fish were considered to have a pathophysiologically normal gill structure. All the morphometric parameters measured

at the various time points were compared to the pre-trial control group, which show clear clustering in the PCA indicating separation of fish into their relevant time points. The red colour square designating the 4 h.p.e. group (in Figure 3.18 and 3.19) can be seen to be placed away from control group (indicated by black dots), reflecting a biological change in response to H_2O_2 treatment by alterations in gill morphology. In the component matrices generated from the PCA carried out on the measured morphometric variables revealed that PC1 had the highest negative values for ISR, SLPL_SLA, PAPL and VASL accordingly. The highest negative values tended to be seen by a move of the 4 d.p.e group in a more left direction. As time passed, values moved further to the left indicating an increase in the changes within the gill. Compared to 4 h.p.e, the parameters measured at 24 h.p.e show a more homogeneous response driven by PC1, evidenced by the same morphometric parameters mentioned above. Considering the time scale for the gills response, the response observed at 24 h.p.e indicated an acute response. However few fish were close to the 4 h.p.e or control suggesting minimal variation from the control. This is the actual response to be expected in a population. As shown by the univariate analysis on the morphometric data measured, 3 d.p.e. appears to reflect the breakeven point in the gill response *i.e.* ISR and SLPL_SLA were highest at 3 d.p.e. and then started decreasing thereafter. In contrast to previous time points, 7 d.p.e reflect that individual fish were starting to recover, indicated by values moving back toward the control fish values, with PC1 having large negative values scattered between individual fish reflecting signs of recovery. Values seen at 14 d.p.e indicated by the purple colour triangles, were distributed amongst controls values, indicating that some fish had already recovered.

In conclusion, the application of GIA to analyse the response of Atlantic salmon gill to H_2O_2 treatment has been able to identify and quantify morphometric changes in gill

structure, which can be correlated to histopathology / gill plasticity previously reported in the literature. Demonstration of the success of this technology indicates that it may provide a useful tool for evaluating changes occurring in response to disease or environmental factors and can assist in our understanding of the role of gills in maintaining / regaining homeostasis. In particular, this technology, as it matures, may be capable of picking up early changes, which can provide warnings of harmful agents or pathogenesis.

CHAPTER 4

THE EFFECTS OF TEMPERATURE ON GILL IMMUNITY AND MORPHOLOGY IN ATLANTIC SALMON FED WITH DIFFERENT FUNCTIONAL FEEDS

4.1 Introduction

4.1.1 The effects of water temperature on gill physiology

Most mammals and birds are homoeothermic endotherms that maintain a relatively constant temperature as a result of the metabolic heat that they generate. Fish, reptiles and amphibians are mainly poikilotherms, and cannot regulate their body temperature, so their body temperature fluctuates with that of their surrounding environment. Fish are classified as ectothermic animals because their body temperature is largely determined through heat exchange with the surrounding environment, usually water. Most ectotherms have a low metabolic rate and as a result do not generate sufficient internal heat to balance the heat loss to the environment. The internal heat they produce tends to be continuously lost through their gills, because of the circulation of blood through this organ and its high surface area. They do not produce or retain sufficient metabolic heat to raise their body temperature above ambient water temperature, so they use behavioural means to regulate their body temperature, by changing their habitat for more favourable environmental conditions (Reynolds *et al.,* 1976; Grans *et al.,* 2012; Boltana *et al.,* 2013).

The metabolic activity and morphology of fish gills adapt in response to adverse environmental conditions and it is the plasticity of the gill that allows morphological changes to take place, thereby helping the gill to rapidly adjust to changing environmental conditions, such as temperature. Changing environmental temperature

has been used as a model system to examine gill plasticity in crucian carp (*Carassius carassius*) (Sollid *et al.,* 2003). It has been shown that the secondary lamellae of crucian carp gills initially have a sausage-like appearance when kept at temperature lower than 20 °C in aerated water. They subsequently retracted when the fish are moved into water with less O_2 saturation (6-8 %) while being maintained at the same temperature (*i.e.* 20 °C), however within a few days this contraction reverses and protruding lamellae are seen. The plasticity of the gill is clearly evident when the fish are moved back into relative cold normoxic water for a week, with their gill filaments once again adapting a sausage-like morphology.

Work by Sollid *et al.,* (2003) showed that the lamellae of crucian carp gills are embedded within a cell mass referred to as the inter-lamellar cell mass (ILCM). During exposure to normoxic cold water the inter-lamellar space is filled through hyperplasia within the ILCM (Figure 4.1). The restructuring of the lamellar morphology is associated with an increased rate of apoptosis referred to as programme cell death, combined with supressed mitosis, and completion of this transformation normally takes place within 3 to 7 days. The ILCM appears to be made up primarily of undifferentiated cells, but numerous superficial osmoregulatory ionocytes are also located in this region, and do not appear to be involved in the hypoxia-induced apoptosis (Figure 4.2). This gill epithelium is less leaky when the lamellae are seen protruding from the gill filament (Mitrovic *et al.,* 2009). This decreased permeability may reduce the ion fluxes associated with the increased gill surface area.

The trade-off between osmoregulation and other necessary gill functions including respiration that results from gill remodelling is referred to as the "osmo-respiratory compromise" (Ramos *et al.,* 2013; Matey *et al.,* 2011). According to Nilsson (1986) and

Gonzalez and McDonald (1992), fish have to balance ion regulation through an energetically expensive process of ion pumping, and suggested that an increase in the size of the respiratory surface area helps with this process. In salmon this increase has been associated with hyperplasia and hypertrophy of the respiratory ionocytes termed mitochondria rich cells (MRC). It is estimated that the cost of ion and acid base regulation accounts for more than 10 % of the total energy budget of the fish (Boeuf and Payan, 2001).

The osmo-respiratory compromise has been well documented in rainbow trout (*Oncorhynchus mykiss*), and it has been shown that exercise and hypoxia can lead to an increase in functional respiratory surface area due to an increase in the number of perfused lamellae, resulting in increased or decreased water uptake and loss of ions into the water (Wood and Randall 1973; Matey *et al.,* 2011). O_2 and CO_2 can easily pass through the lipid membrane by simple diffusion, driven by the partial pressure gradients elicited by counter-current flow between the bloods in the gills and water over the gills. Experiments conducted by Endeward *et al.,* (2008), Carbely and Agre (2009) and Perry *et al.,* (2010b) showed that CO_2 moves through Rhesus (Rh) proteins and aquaporins. However, some evidence has shown that the major route for CO_2 efflux is by direct diffusion through the cell membranes, or by movement between the cells.

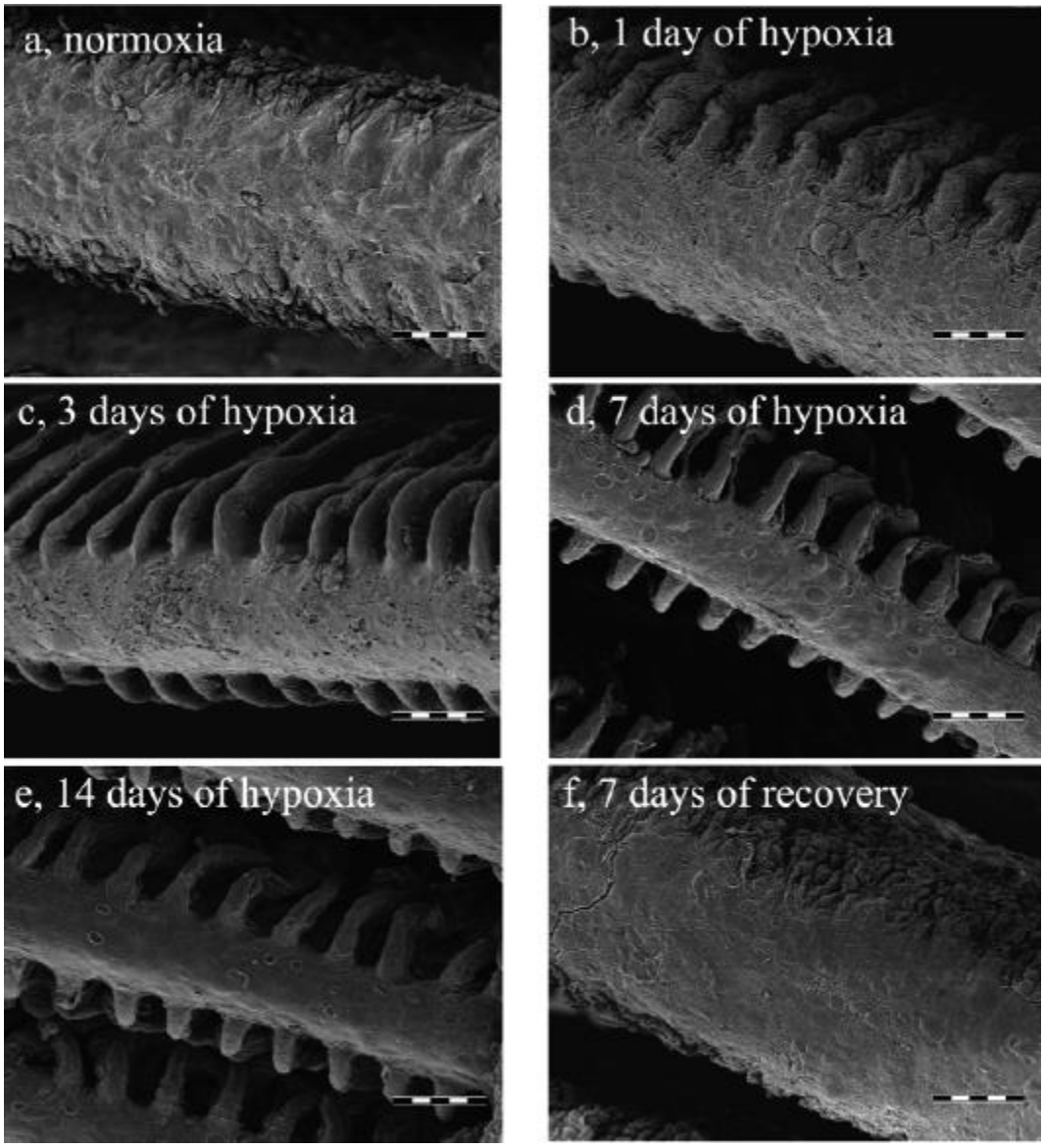

Figure 4.1 A scanning electron micrographs from the 2nd gill arch of crucian carp kept in normoxic or hypoxic water: (a) In normoxia, the gill filaments have no protruding lamellae; (b) The morphology has already changed after 1 day of hypoxia exposure ($0.75\pm0.15 \cdot mg \cdot O_2 \cdot L^{-1}$); (c, d). The change progresses for up to 7·days in hypoxia, but (e) there were no further changes with subsequent exposure; (f) When the fish were moved to normoxic water, the morphological changes were reversed within 7 days. Scale bar, 50 mm (Sollid *et al.*, 2003)

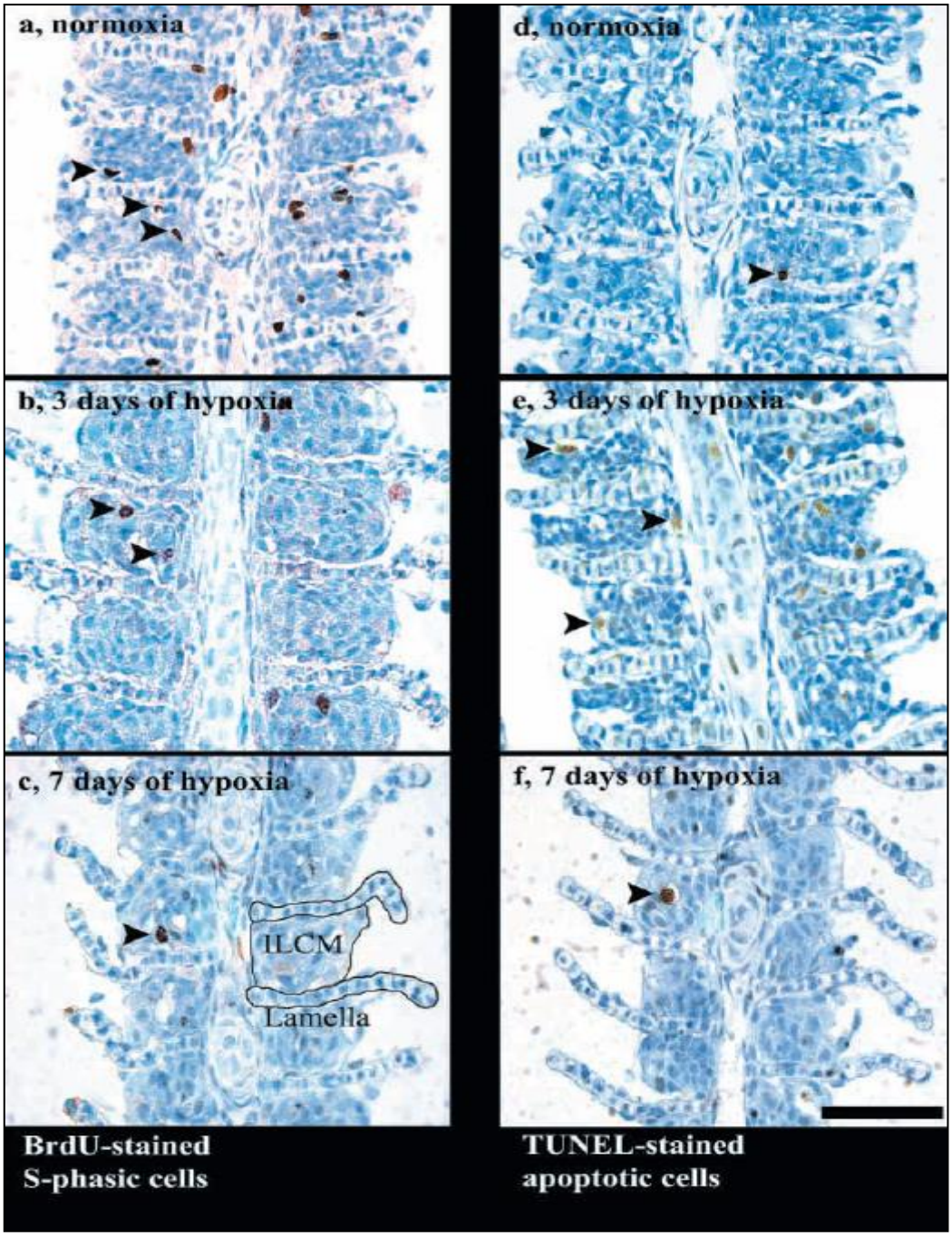

Figure 4.2 Light micrographs of gills stained for (a–c) S-phase cells (BrdU) and (d–f) apoptotic cells (TUNEL). Picture series starts with normoxia (a, d), 3·days of hypoxia (b,e) and 7·days of hypoxia (c,f). Arrows point out some of the stained cells seen on the micrographs. ILCM, interlamellar cell mass. Scale bar, 50·mm. (Sollid *et al.*, 2003)

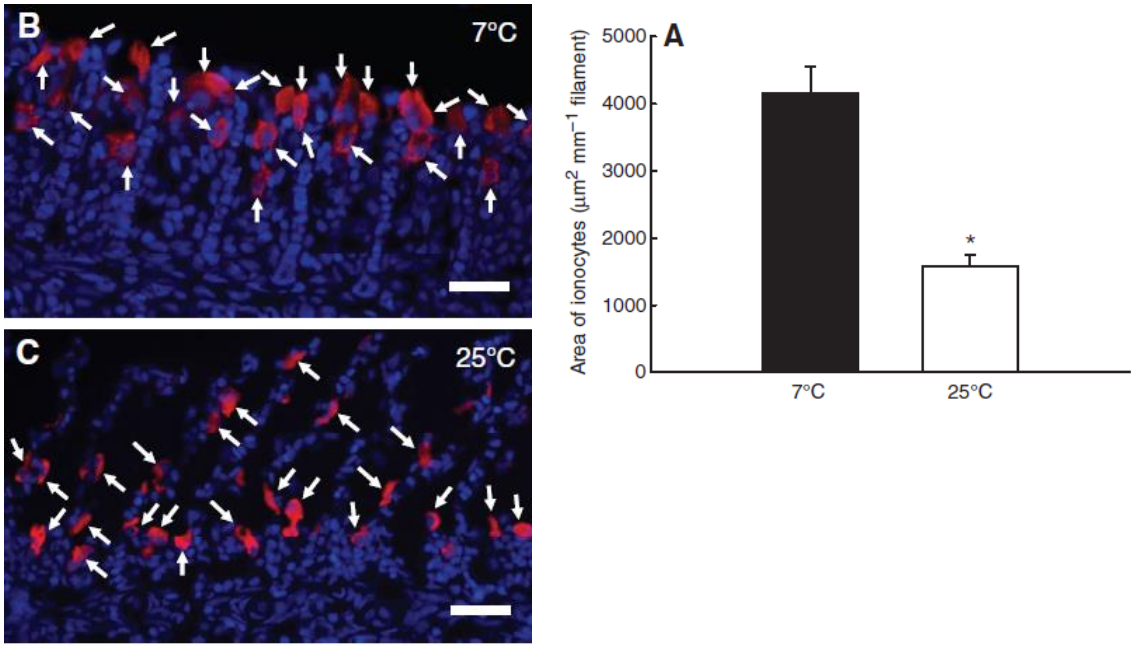

Figure 4.3 The effects of acclimation temperature on the surface area of ionocytes (as determined by Na+/K+-ATPase immunofluorescence) and their distribution in goldfish (*Carassius auratus*). (A) The surface area of ionocytes was significantly decreased (indicated by asterisk) in fish acclimated to 25 °C (N=6) when compared with fish kept at 7 °C (N=6); data are presented as means ± 1 s.e.m. (B, C). Representative light micrographs illustrate that the decrease in ionocyte (arrows) surface area in fish acclimated to 25 °C was a result of decreased numbers and sizes of individual cells. Note that the ionocytes were confined to the outer edge of the ILCM in the fish acclimated to 7 °C; scale bars, 20 μm. Sections were labelled with DAPI-containing mounting media to show cell nuclei (blue) (Mitrovic and Perry, 2009).

The molecular signals and underlying mechanisms involved in gill remodelling are not well understood. Recent studies have focused on the transcription factor, hypoxia inducible factor 1-alpha (HIF-1α), which seems to be the master switch for many hypoxia-induced changes in animals as well as fish. Recent evidence has suggested an increase in levels of HIF-1α transcript and protein expression levels in crucian carp exposed to hypoxia, which can initiate the cellular changes seen in the ILCM (Mitrovic *et al.*, 2009). Furthermore, decreased levels of HIF-1α transcripts and protein expression have been observed during decreasing temperature under normoxic conditions, when ILCM morphology is maintained. It has been reported that inducible nitric oxide synthase (iNOS), an enzyme induced by HIF-1α and known to be involved in apoptosis, is unaffected by hypoxia in crucian carp (Nilsson, 2007). Further work is

needed to establish whether similar mechanisms of gill remodelling exist in other fish species including Atlantic salmon and rainbow trout. New techniques, including the robust GIA tool discussed in Chapter 2, are potentially very useful for quantifying morphometric changes in the gills, which can then be compared to existing morphometric parameters published in the literature.

4.1.2 **The effect of temperature on teleost immunity**

Temperature is defined as a measurement of the average kinetic energy or heat content within a substance or system. In relation to fish, their whole body is usually subject to fluctuations in the water temperature of their environment. Bly and Clem (1992) and subsequently Morvan (1997) published reviews on the effects of temperature on the adaptive and innate immune responses of fish. They also concluded that immuno-competence, defined as the fish's ability to function adaptively when facing pathogen or parasitic challenges, can be severely affected by low environmental temperature, making them more prone to increased disease susceptibility. A good example of this is the fish's response to spring viraemia of carp (*Cyprinus carpio*), which occurs at low environmental temperatures (Baudouy *et al.,* 1967). In general, fish are immunosuppressed at lower water temperatures (Bly and Clem, 1992), due to a reduced T-helper cell response.

This thermo-sensitivity of the fish's immune system has been extensively studied in relation to lower environmental temperature. However, not a great deal of attention has been given to changes that occur at higher temperature, although interest in this has increased more recently due to increasing water temperature as a result of climate change (Portner and Peck, 2010, Callaway *et al.,* 2012). Due to the recent advances in

fish immunology, special attention has been given to mucosal immunity and their role of mucus in helping the fish to combat aquatic pathogens, including bacteria and viruses (Esteban, 2012).

It is worth considering the underlying mechanisms involved in immune modulation in teleosts, with regards to environmental water temperature changing over the course of the year due to seasonality, as well as daily changes (*i.e.* diurnal temperature changes), causing fluctuations in water oxygen levels throughout the day (Avtalion *et al.,* 1973; Braganza *et al.,* 2004).

The effect of temperature on antibody responses in fish has been extensively studied in a variety of different fish species (Avtalion 1969; Avtalion *et al.,* 1970; Rijkers and Frederix-Wolters, 1980; Bly and Clem, 1992). Both primary and secondary antibody responses were examined after injecting carp intraperitoneally with bovine serum albumin (BSA). The results suggested that the primary antibody response is suppressed at lower temperature, but that the secondary antibody response can be elicited at low temperature if immunological memory has been established at a high temperature (Avtalin *et al.,* 1972). Further studies by Rijkers *et al.* (1980), showed that lower temperature resulted in a delay in the peak primary antibody response, but did not affect the magnitude of the primary response obtained. The mechanism of this immune modulation of humoral adaptive response could be governed by one or more of the thermo-sensitive steps involved. One suggestion is that temperature can influence discrete events during the maturation and/or co-operation of immune competent cells (Cone and Marchalonis, 1972; Avtalion *et al.,* 1973). This has been shown using catfish (*Ictalurus punctatus*) as a model fish, with reduced concanavalin (Con A) and phytohaemagglutinin (PHA) which activated lympho-proliferation obtained at lower

temperatures (<22 °C) (Cunchens and Clem, 1977). Similar temperature effects were observed on specific cytotoxicity of carp kidney lymphocytes against tri-nitrophenyl (TNP) in TNP-modified autologous cells (Verlhac *et al.,* 1990). The work published by Weiss and Avtalion (1977), indicated that antibody production against a hapten was normally supressed at lower temperatures if pre-immunisation of the carrier molecule was performed at high temperature. Furthermore, Avtalion *et al.,* (1977), suggested that the low temperature sensitive step of antibody production was as a result of reduced T-helper function. To confirm this, Clem *et al.,* (1991) conducted a series of experiments in vitro using leukocytes isolated from channel catfish. They initially showed that low temperature negatively affected the lympho-proliferation of T cells in the presence of Con A, while B cell-stimulation by lipopolysaccharide (LPS) was not affected by low temperature. Also mixed leukocyte reactions, mediated by T lymphocytes, were also sensitive to low temperature (Millar *et al.,* 1986). Millar and Clem (1984) conducted an experiment using both thymus dependent (TD) and thymus independent (TI) hapten carrier conjugates to discriminate between lymphocyte function at different water temperatures. It was concluded that only the generation of T-helper cells were affected by decreasing environmental temperature, but not the T memory cells or B cell responses. Suppression of primary T cell responses at low temperature was previously shown not to be due to a lack in ability to process TD antigens by antigen presenting cells (APC) (Vallejo *et al.,* 1992) or to produce interleukin-1 (IL-1) (Bly and Clem, 1992). According to above findings it is clear that defined subsets of immune cells are affected by low temperature leading to the immune suppression seen in teleost fish.

As suggested above, lower environmental temperature adversely affects not only humoral immune response, but also cellular specific immune response in various fish species. Temperatures that give rise to an effective immune response, and temperatures

resulting in immunosuppression are categorised immunologically as ‘permissive’ and ‘non permissive’ temperatures respectively, which vary according to the fish species *e.g.* the permissive temperature for salmonid is 4 °C and above, 14 °C for carp and 22 °C for catfish (Bly and Clem, 1992).

The thermo-sensitive effect on T-helper cell activation and proliferation in response to stimulation with Con A has been studied in catfish using sudden changes of culture temperature in vitro (Clem *et al.,* 1984). It has been shown using phorbol ester ionophore stimulation that, during the first 8 h following stimulation (relatively early in the cell activation process), T cells showed low thermo-sensitive effects, at a critical point prior to protein kinase C activation, (Ellsaesser *et al.,* 1988: Lin *et al.,* 1992). The T cell receptor CD3 trans membrane signalling/G protein activation were considered to be important in the process, leading to the conclusion that low temperature exerts an effect on the T cell plasma membrane. Research has focused on protein kinase C activation, and its sensitivity to temperature (Clem *et al.,* 1991; Lin *et al.,* 1992). Furthermore, it has been shown that T cells are able to patch and cap receptor–ligand complexes at low temperature to the same extent as B cells (Bly *et al.,* 1987, 1988). However, when fish were acclimatised to low temperature prior to performing in vitro assays, the T helper cell response was restored (Clem *et al.,* 1984; Millar and Clem, 1984).

Another theory for reduced cell-mediated specific immunity is the lack of homeoviscous adaptation of immune cell membranes at lower temperatures. It has been suggested that catfish T cells are unable to undergo homeoviscous adaptation at low temperature to maintain the homeostasis of the cell membrane required for normal T cell function. This has been partially shown using fluorescence polarisation studies in

catfish (Abruzzini *et al.,* 1982; Bly and Clem 1988). The process of homeoviscous adaptation of T cells is relatively slow compared to B cells, and this could be the reason for the slow onset of adaptive immunity in fish when acclimatised to low temperature. Further studies have shown that the T cells regain the homeoviscous properties of their membranes by increasing the level of supplemented oleic acid (18:1) and decreasing the level of stearic acid (18:0) (Bly *et al.,* 1986) in vitro. It was also shown that the T cell response to Con A is inhibited by adding stearic acid to the culture, but this can be increased by adding oleic acid (Bly *et al.,* 1990). They found that catfish B cells can desaturate stearic acid to oleic acid, while T cells are unable to do this. This suggests that homeoviscous adaptation of lymphocyte plasma membranes, through changing their fatty acid composition, is an important aspect of teleost immunity, although it does not fully explain what caused immunomodulation at low temperature.

Plasma membrane cell receptors, comprising proteins and glucocides, are involved in a number of signal transduction processes, which can be affected by environmental temperature change (Sharon and Lis, 1989). Le Morvan *et al.,* (1996) showed that there was no quantitative modification in the protein profile of common carp leukocyte membranes at low environmental temperature, when examined by electrophoresis and isoelectric-focusing. In contrast, glucoside components of leukocyte cell membranes seem to be thermo-sensitive, with sialic acid levels decreasing in leukocytes at lower temperature. Terminal sugar molecules present on the sialic acid or rearrangement of glycans produced by desialylation of glycol conjugates is in line with the modifications seen in the plasma membrane structure and function. It can be concluded that alterations in carbohydrate moieties present on cell membrane can change the immune response of fish at lower environmental temperature (Morvan *et al.,* 1996).

Immunomodulation due to stress caused by changing environmental water temperatures, including seasonality, has been widely studied. In carp, sudden changes in environmental temperature under experimental conditions from 20 °C to 12 °C, lead to elevated plasma cortisol levels 2 h after reducing the temperature. These results suggest that the immunomodulation occurs during the first hours following the temperature decrease, and is induced as part of the stress response, but the direct effect of immunomodulation at low temperature appears to be induced by alterations in the plasma membrane structure.

Modulation of innate immunity in fish is also known to occur due to a decrease in environmental temperature. The effect of temperature on phagocytic function has been evaluated in channel catfish, and phagocytes appeared to be more resistant to low temperature than lymphocytes (Scott *et al.,* 1985: Anisworth *et al.,* 1991). This has also been shown by Dexiand and Anisworth (1991), who found bactericidal activity to be associated with increased respiratory burst activity at lower water temperatures. Other fish species like tench (*Tinca tinca*) (Jensen *et al.,* 1986) and rainbow trout (Hardie *et al.,* 1994) also show increased effectiveness of phagocytosis at lower temperature. In channel catfish, components like opsonins, which help to increase phagocytosis, and phosphorylcholine-reactive protein (PRP) increased during the winter months despite a reduction in environmental water temperature (Szalai *et al.,* 1994). Macrophage respiratory burst activity was also seen to increase with a reduction in the experimental assay temperature (Le Morvan *et al.,* 1997).

Nonspecific cytotoxic cells (NCCs) from teleost fish are considered to be the phylogenetic precursors of mammalian natural killer cells (NKs), which lyse a wide variety of human and mice tumour target cells (Evans and McKinney, 1990). These are

commonly seen in fish during certain protozoan parasite infections (Graves *et al.*, 1985). In carp, the lytic activity mediated by NCCs against murine mastocytoma cells is thermo-sensitive, showing increased activity at low environmental temperature, possibly acting directly on the cell plasma membrane (Le Morvan *et al.*, 1996).

Complement activity in fish, combined with antibodies, helps to destroy many bacteria before they are able to establish an infection within host tissues. This has been studied in cyprinids subjected to lower environmental temperature, where it has been shown that the alternative complement pathway is still effective while in contrast the classical complement pathway is depressed (Yano *et al.*, 1984; Hayman *et al.*, 1992; Collazos *et al.*, 1994). Thus, fish appear to show a strong innate immune response during the winter months, a vital defence mechanism to compensate for an immuno-compromised adaptive immune response at lower temperature.

To date three immunoglobulin isotypes have been identified in teleost fish, *i.e.* IgM, IgD and IgT. Immunoglobulin T (functional homolog of mammalian IgA) was first discovered in rainbow trout by Hansen *et al.,* (2005), which were then confirmed to be involved in mucosal immune system of rainbow trout gut. Zhang *et al.,* (2010) established a model system that uses a gut parasite (*Ceratomyxa shasta*, a myxosporean parasite of salmonids) to induce strong IgT-specific responses in the gut (IgT+ B cells) of rainbow trout, which was later cloned and identified in Atlantic salmon (Tadiso , 2012). To date there has been limited data published relating to the effect of temperature on mucosal immunity. A few authors have described mucosal immunity as being compartmentalised into two compartments *i.e.* innate mucosal immunity and adaptive mucosal immunity (Gomez *et al.,* 2013). A comparison between the mucosal immune response of fish and mammals may lead to a better understanding of the

phylogenetic development of mucosal immunity, and an improved understanding of the selective pressures of host-pathogen interactions that have helped to shape the mucosal immune systems of both mammals and fish (Gomez *et al.*, 2013).

4.1.3 **Gill specific morphometric response to different functional diets**

There has been an increased interest in different functional feeds, enriched with feed additives, to prevent either nutritional deficiencies or improve the health status of the fish (Kiron, 2012). Gills are one of the most versatile organs in fish, and as such have a high metabolic demand because of their multifunctional nature *i.e.* osmoregulation, nitrogenous waste excretion, respiration and immune function. There is an increasing interest in making special feeds enriched with high amounts of electrolytes, anti-oxidants, with a high energy content and added immunostimulants to boost the gill health of the fish (Skretting ARC, Norway). However, the morphometric response that occurs in fish gills without normal physiological ranges in temperature, salinity and oxygen, has not been fully assessed due to a lack of tools suitable for quantifying subtle microscopic changes in the gill accurately. The study performed in this chapter used the GIA tool developed and validated in Chapter 2 to evaluate the effects of different functional feeds on gill morphology and gill immunology, in response to changing environmental temperature, using diets formulated by Skretting ARC, Norway.

4.2 Materials and Methods

4.2.1 Fish and feeds

4.2.1.1

Experiment 1 – evaluation of morphometric changes of Atlantic salmon gill reared in three different temperatures and fed with a conventional diet

A total number of 300 disease-free vaccinated Atlantic salmon parr (mean initial weight ±1 S.D. 96 ±10 g), obtained from AquaGen, Norway, were maintained at the industrial experimental research facility (ILAB, Bergen, Norway) at 10 °C for a two week acclimation period prior to starting the feeding trial. The fish were maintained in 500 L flow-through tanks with 30 randomly allocated fish per tank employed for each state studied. Fish were fed with a standard control diet (Diet A) or a test diet (Diet B). Fish were acclimated to three different water temperatures in the study; 4 °C, 10 °C and 16 °C. At the beginning of the trial, the temperature was gradually changed by 2 °C per day over a period of three days, elevating the water temperature to 16 °C or decreasing it to 4 °C. The remaining fish were held at 10 °C, which was considered to represent an optimal culture temperature. The fish held at the three temperature were fed with either Control Diet A or Test Diet B throughout the experimental period. All the experimental diets were formulated and manufactured by the Skretting ARC, Stavanger, Norway. Control diet A was a standard farm feed, while Test diet B was enriched with different feed additives, which were designed to target immune function and improve the anti-oxidant status of the fish to help combat temperature-related immunosuppression. The tanks were monitored throughout the experimental period for oxygen saturation and pH fluctuations. The oxygen saturation was maintained between 80 - 100 % in all experimental tanks throughout the experiment period. After 7 weeks, representing 2 weeks of acclimatisation and a further 5 weeks of feeding, fish were sampled, taking

gill samples for histology and for analysis of immune gene expression. Only the gills from fish fed with control Diet A were used in the gill morphometric study described in Section 4.3.1.1, sampling them according to Section 2.2.2, while fish fed with either control Diet A or test Diet B were used for the gene expression study, using gills sampled into RNAlater (Sigma) for the analysis as described in Section 2.2.8.

4.2.1.2

Experiment 2 – evaluation of morphometric changes, immune gene expression of Atlantic salmon gill reared in two different temperatures and fed with three different diets

A total of 600 disease-free, vaccinated Atlantic salmon parr (mean initial weight 230 g) obtained from AquaGen, Norway, were acclimatised for 2 weeks prior to starting the experiment. They were transferred into experimental tanks and maintained on the standard control diet (Diet A) at 8 °C. Then fish were allocated into 20 small tanks (50 fish per tank), and were gradually acclimated to two different water temperatures 4° C or 12 °C. Initial sampling of fish was carried out at day one and again after one week (two days after the temperature was adjusted from 8 °C to 4 °C or 12 °C). The two first sampling points were not examined in the work described in this chapter, but the final sampling at week 7 post temperature change, prior to termination of the trial, was analysed in order to evaluate the long-term effects of different functional feeds on the outcome for Atlantic salmon's gills exposed to different experimental temperature regimes. Duplicate tanks of fish held at each temperature were fed one of five different diets (Diets A, B, C, D and E), specially formulated for health improvements by the Skretting ARC, Stavanger, Norway. However, only fish fed diets A (control), B and D (gill health improvement) were selected for the present study. The tanks were monitored throughout the experiment for oxygen saturation and pH fluctuations. After 7 weeks (approximately 50 days) of continuous feeding, gills were sampled from all

dietary groups for the gill morphometric study and gill samples were also collected into RNAlater for immune gene expression analysis, described in Section 4.2.6.

4.2.2 **Sampling of fish**

For sampling, fish were euthanized using benzocaine (100 mg L^{-1}) in compliance with recommended guidelines established to maintain animal welfare standards of Norwegian National Legislation for Laboratory Animals. Three fish (n=3) were randomly sampled from each replicate tank at two sampling points *i.e.* at 2 weeks after having been placed on control diet A and at the end of the experiment feeding period (7 weeks in both Experiment 1 and Experiment 2). Blood samples were taken from fish prior to gill sampling and gills were freshly sampled as soon as possible into 4 % NBF for histological analysis and also 30-100 mg into ml^{-1} RNAlater for gene expression analysis. After 24 to 48 h fixation at 4 °C, RNAlater (Sigma) was removed and samples were kept at -20 °C until processed.

4.2.3 **Sample processing for histology**

Processing of samples for histology and staining with H&E or Alcian blue was carried out as previously described in Chapter 2 Section 2.2.2. A summary of the samples collected from fish in Experiment 1 and 2 is presented in Table 4.1.

4.2.4 **Light microscopy, imaging and processing**

Both darkfield and brightfield microscopes were used to evaluate the stained tissue. Light microscope images were taken with a Zeiss AxioCam MRC colour digital camera attached to an Olympus BX51TF light microscope. MRGrab version 1.0 software (Zeiss) was used to capture and save images and a slide graticule was used to calibrate

images. Furthermore scanning of differentially stained WSI and subsequent processing of images for GIA tool was performed as described in Chapter 2, Section 2.2.3.

4.2.5 Evaluation of gills using GIA tool

The GIA algorithm made (Chapter 2, section 2.2.5) which imported into KSRUN platform and used to examine 25 different histomorphometric parameters/variables with respect to temperature and diet (Chapter 2, section 2.2.6). A list of parameters examined and the analyses used are detailed in Chapter 2, Table 2.1. In addition to morphometric parameters listed in the table, fish weight, length and condition factors were also included in both univariate and multivariate analysis.

4.2.6 Gene expression analysis

In Experiment 1 expression levels of IgM, IgT, membrane immunoglobulin M (mIgM), membrane immunoglobulin T (mIgT) and polymeric immunoglobulin receptor R pIgRL were analysed, while in Experiment 2 expression levels of interleukin one beta (IL-1β), interleukin ten (IL-10), tumour necrosis factor alpha (TNFα), cluster of differentiation eight (CD8), cluster of differentiation four (CD4), IgM, IgT, pIgRL, mIgT and mIgM were analysed. Total RNA was extracted from samples using Tri Reagent according to the method outlined in Chapter 2 Section 2.2.8.1 and cDNA synthesis performed according to Chapter 2 Section 2.2.8.2.

4.2.6.1 Primer optimisation using conventional PCR reaction

The details of the primers including primer name used, primer sequence, fragment size, annealing temperature, gene bank accession number and source literature used for this experiment are given in Table 4.2. Before performing the assays, primers were

optimised to obtain optimum performance using both conventional PCR Chapter 2 Sections 2.2.8.3 and RT-qPCR.

Table 4.1 Details of the samples prepared for histology for the gill morphometric studies

Experiment 1

Temperature	Dietary groups	Number of fish	Subsamples per gill	Total images analysed
4 °C	A (control)	6	5 images per gill arch	30
10 °C	A (control)	6	5 images per gill arch	30
16 °C	A (control)	6	5 images per gill arch	30

Experiment 2

Temperature	Dietary groups	Tanks	Number of fish	Subsamples per gill	Total images analysed
4 °C	A,B and D	2 tanks per dietary group	N=6 (3 fish per tank)	5 images per gill	150 images (50 per dietary group)
12 °C	A,B and D	2 tanks per dietary group	N=6 (3 fish per tank)	5 images per gill	150 images (50 per dietary group)

Table 4.2 The PCR primers used to measure immunomodulation induced by diet in the in the gills of fish reared at different temperature

Transcript (Target genes)	Primer name	Primer sequence	Fragment	Tm	Accession No	Source
IL 1β	As_IL1_F As_IL1_R	AGGACAAGGACCTGCTCAACT CCGACTCCAACTCCAACACTA	72	58 °C	NM_001123582.1	Petterson *et al.*, 2008
IL 10	As_IL10_F As_IL10_R	CCTGTTGGACGAAGGCATTCTAC AACTTCAGGATGCTGTCCATAGC	75	58 °C	GI 121053631 (EF 165029.1)	Hølvold (2007)
TNFα	As_TNF_F As_TNF_F	CGTGGTGTCAGCATGGAAGA AGTATCTCCAGTTGAGGCTCCATT	64	58 °C	NM001123590	Fredriksen *et al.*,, 2011,
CD8β	As_CD8_F As_CD8_R	GGAGGCCAGGAGTTCTTCTC GGCTTGGGCTTCGTGACA	70	58 °C	NM_001123584.1	Hølvold (2007)
CD4	As_CD4_F As_CD4_F	TGACACCCTGAAGAGAAGTATTCGT GTTGACCTCCTGACCTAGAAAGG	88	58 °C	NM_001171848.1	Hølvold (2007)
IgM	As_IgM_F As_IgM_F	TGAGGAGAACTGTGGGCTACACT TGTTAATGACCACTGAATGTGCAT	69	58 °C	GI-2182101	Tadiso *et al.*,2011
IgT	As_IgT_F As_IgT_R	CAACACTGACTGGAACAACAAGGT CGTCAGCGGTTCTGTTTTGGA	97	58 °C	HQ379938.1	Tadiso *et al.*,2011
mIgM	As_mIgM_F As_mIgM_R	GGTCCTTGGTAAAGAAACCCTACAA CTGCATGGACAGTCAGTCAACAC	67	58 °C	Y12457.1	Tadiso *et al.*,,2011
mIgT	As_mIgT_F As_mIgT_F	GAATGTTTGGGACACGGAAG TCACATATCTTGACATGAGTTACCC	124	58 °C	GQ907004.1	(New design)
pIgRL	As_pIgRL_F As_pIgRL_R	CAAAGTATCCGTGGACCTCACA CCCCCCTCCTCACCAGATA	84	60 °C	HM452379.1	T.M. Tadiso *et al.*,,2011
		Reference genes				
ELF1	As_ELF1_F As_ELF1_R	CTGCCCCTCCAGGACGTTTACAA CACCGGGCATAGCCGATTCC	175	58 °C	NM_001123629.1	Morais *et al.*,(2009)
Bactin	As_ βactin_F As_ βactin_R	ACTGGGACGACATGGAGAAG GGGGTGTTGAAGGTCTCAAA	157	58 °C	NM_001123525.1	Herath *et al.*, (2010)
Cofilin2	As_ Cofilin2_F As_ Cofilin2_R	AGCCTATGACCAACCCACTG TGTTCACAGCTCGTTTACCG	224	58 °C	BT 125570.1	Morais *et al.* (2009)

4.2.6.2 Primer optimisation using RT-qPCR in Realplex Eppendorf platform

Once primers were able to produce a reliable PCR product, they were then were tested for its efficiency using an Eppendorf real time thermal cycler platform (Eppendorf UK Limited, Eppendorf House, Gateway 1000 Whittle Way Arlington Business Park Stevenage, UK) prior to use in the assays. Briefly cDNA pools were prepared by mixing the 1 µL of cDNA from all samples of the experiment (pooled cDNA). Serial dilutions were made for standard curve preparations. From each cDNA dilution 5 µL were aliquoted in triplicate into 96 well clear PCR plates (STAR lab, UK) and master-mix, made by combining 1 µL of forward and reverse primers (10 pmol μL^{-1}), 3µL nuclease free water PCR grade water and 10 µL of absolute qPCR SYBR Green Mix (Thermo Scientific UK) was added prior to performing quantitative real time RT-PCR using a Eppendorf Mastercycler® ep realplex (Eppendorf, UK) programmed for an initial enzyme activation step at 95 °C for 15 min, followed by 40 cycles 15 s at 95 °C, 15 s at the specific primer pair annealing Tm (Table 4.2) and 15 s at 72 °C. After the amplification phase, a melting curve of 0.5 °C increments from 75 °C to 90 °C was performed according to manufacturing instructions to confirm amplification of single products by one distinct peak over the thresholds, and sizes were visually confirmed by agarose gel electrophoresis.

4.2.6.3 Reverse Transcription Quantitative Polymerase Chain Reaction (RT-qPCR) in Realplex Eppendorf platform

The cDNA from control and test sample groups were all diluted in nuclease-free water at a 1:20. The qPCR analysis for each sample was carried out in duplicates which compliant with MIQE guidelines published by Bustin *et al.,* 2010, in an Eppendorf thermal cycler (Thistle Scientific, UK). The qPCR reaction comprised 5 µL of 1:20

diluted cDNA, 1 µL of each primer (20mM) and 10 µL of AbsoluteTM qPCR SYBR® Green mix with magnesium concentration (Thermo Scientific, UK) in final volume of 20 µL. All amplification reactions were carried out with a systematic negative control non template control (NTC), containing no cDNA and no reverse transcriptase enzyme (RT minus) and serial dilution of cDNA to extrapolate reaction efficiency (E) of the assay. The qPCR assay was performed using same amplifications profiles used for primer optimisation as described in Section 4.2.6.2. Melting curve of each sample was checked manually to determine the specificity of the reaction and to identify unspecific PCR products below or above the chosen temperature, *e.g.* to eliminate primer dimers, to ensure accurate quantification of target and reference genes. The size of the product obtained was checked using agarose gel electrophoresis for a selection of the samples.

4.2.6.4 Gene expression analysis using GenEx software

GenEx Enterprise software (Version 5.4.3) is a commercially available software tool (www.multid.se) to quantify gene expression data. This software allows multiple data analysis taking into account the variance (sample to sample and between plates) within the data set. The main data analysis steps used with this software are summarised in Figure 4.4. Briefly, data analysis was carried out after quality control and pre-processing of data. Initially one of the reference genes, ELF1 (or reference gene index consisting of ELF1, β Actin and Cofilin) was used as internal reference gene/genes. If the samples were spread over more than one plate for a particular gene, the efficiency correction was performed using the value obtained from standard curve on the relevant plate (efficiency <1). Expression values of the target genes were normalised with three reference genes (reference gene index) by dividing the expression values of particular target gene by geometric means of three reference genes as a standard protocol after

testing a series of different methods. This software is comprised of two different options; (i) pre-examination of behaviour of reference genes throughout the sampling points, and (ii) across different organs if used more than one organ. This gives the option to choose the most stable reference gene/genes, which were least regulated in particular experiment (*e.g.* for this experiment) and suitable for normalisation. During the analysis, all the options were tested to examine the accuracy of the standard protocol including normalisation using all three reference genes.

4.2.7 **Statistical analysis**

Statistical differences between groups were performed using GenEx (www.multid.se), Minitab and SPSS software. The normalised mean gene expression values, calibrated against relevant control groups, were examined for normality and homogeneity of variance. When normality and homogeneity were achieved a parametric GLM was employed. Where these assumptions were not met, a non-parametric equivalent for ANOVA, Kruskal-Wallis tests was employed. The post-hoc tests, Tukey HSD and Mann-Whitney U Test were employed for GLM and non-parametric ANOVA respectively.

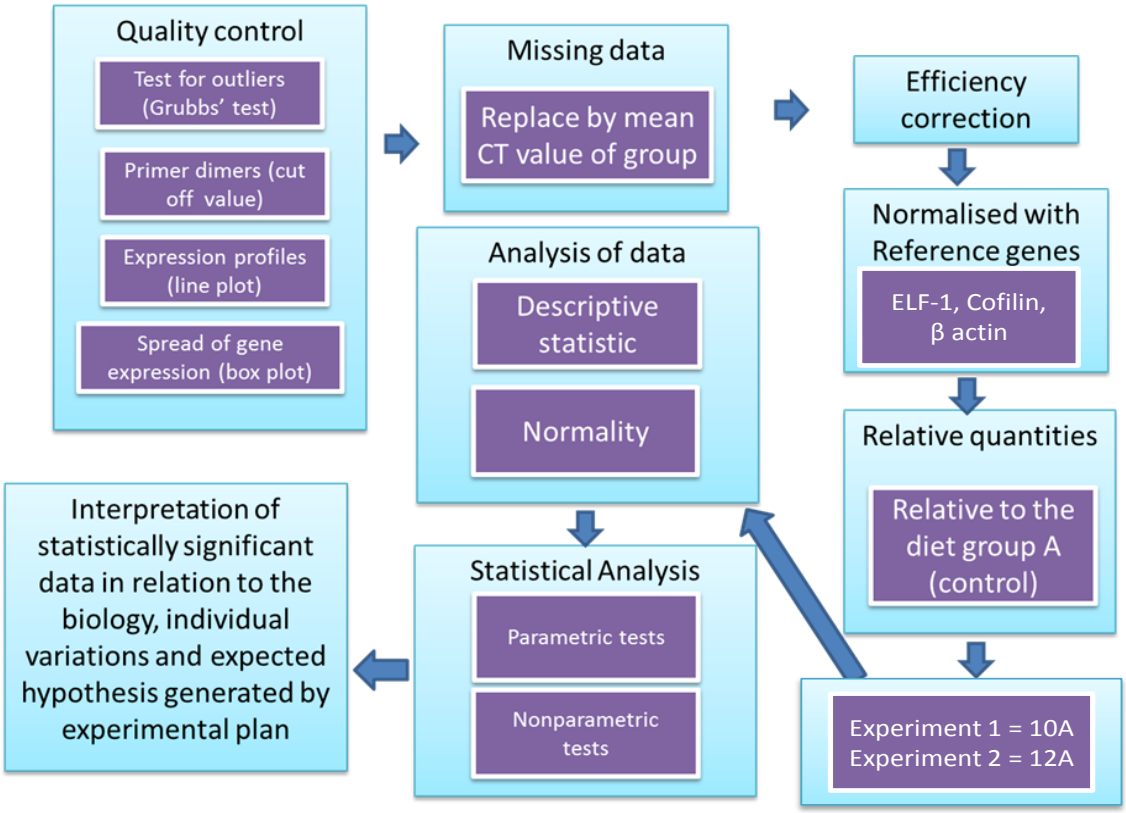

Figure 4.4 Flow chart to show different steps of data processing in GenEx Enterprise software, which included a step of quality assurance, replacement of missing data to fulfil the requirement of balance ANOVA (GLM). Most suitable and recommended normalisation was achieved by using reference gene index.

4.3 Results

4.3.1 Experiment 1 - evaluation of morphometric changes of Atlantic salmon gill reared at three different temperatures and fed a conventional salmon diet

The fish reared at 10 °C were used as the control group in Experiment 1 and were compared to the groups reared at 4 °C or 16 °C. The weights and the lengths of fish maintained at 4 °C were significantly lower than those of control fish reared at 10 °C ($p<0.05$) (Figure 4.5; Table 4.3). The fish maintained at high temperature were also significantly higher ($p<0.05$) than those control fish reared at 10 °C. The condition factor (K) was not significantly different ($p<0.05$) between the groups ($p>0.05$).

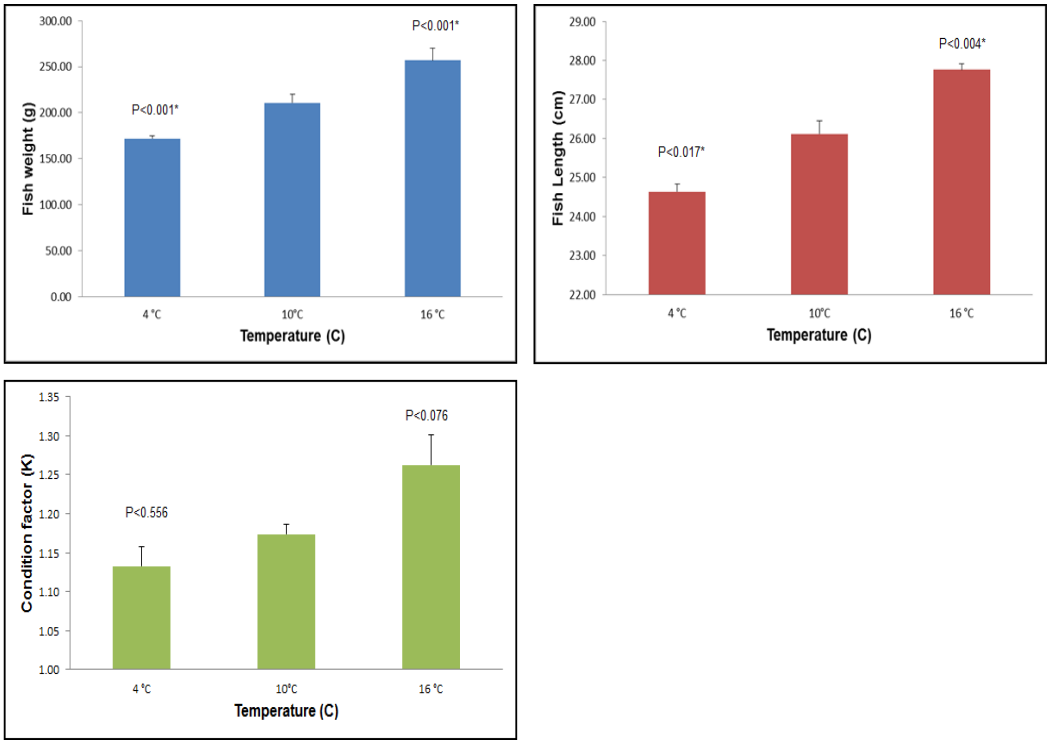

Figure 4.5 Growth performances (fish weight, fish length and condition factor) of fish from experiment 1, reared at three different temperatures. *indicates significant difference compared to the control group (10 ºC) when $p<0.05$. Error bars indicate ±SEM. N= 11.

4.3.1.1 Histology

Gills were sampled from fish reared at the three different experimental temperatures. In Experiment 1, after 12 weeks of continuous feeding with control Diet A or test Diet B, only the gills from fish fed the control diet were evaluated here. Gill sections were examined using conventional histological methods after staining them with Alcian blue and counter staining with haematoxylin. The gills were screened for any visible morphological differences that were evident between the experimental groups. The histomorphometric changes seen were not very pronounced, appearing generalised and of low magnitude with multifocal or diffuse changes throughout the gill section (Figure 4.6). In certain areas of the gill, such as the primary and secondary lamellae, increased cellularity was present (Figure 4.6A), the thick arrows indicates areas of high cellularity within the primary lamellar area). In general, fish reared at 4 °C exhibited increased cellularity within the interlamellar area of their primary lamellae and at the distal extremity of the secondary lamellae (Figure 4.6 A), compared to fish reared at 10 °C (Figure 4.6 B). However fish reared at 16 °C had a lower degree of increased cellularity in interlamellar area of primary lamellae, but less pronounced increased cellularity in the secondary lamellar area (Figure 4.6 C). The mucous cell number appeared to differ in the gills of fish maintained at 4 °C (Figure 4.6 A) or 16 °C (Figure 4.6 C) compared to the group maintained at 10 °C (Figure 4.6 B), with more mucous cells (hyperplasia of mucous cell) evident in the 4 °C group (Figure 4.6 A). As well as the mucous cell number changing, the size of the mucous cells also appeared to change (hypertrophy of mucous cell). The mean size of the mucous cells in fish reared at low temperature (4 °C) was seen to be higher relative to the fish reared at the high temperature (16 °C). However, it was very difficult to accurately quantify mucous cell size and number using

conventional light microscopy, and therefore GIA was applied to better quantify the gill associated morphometric changes in the experimental fish.

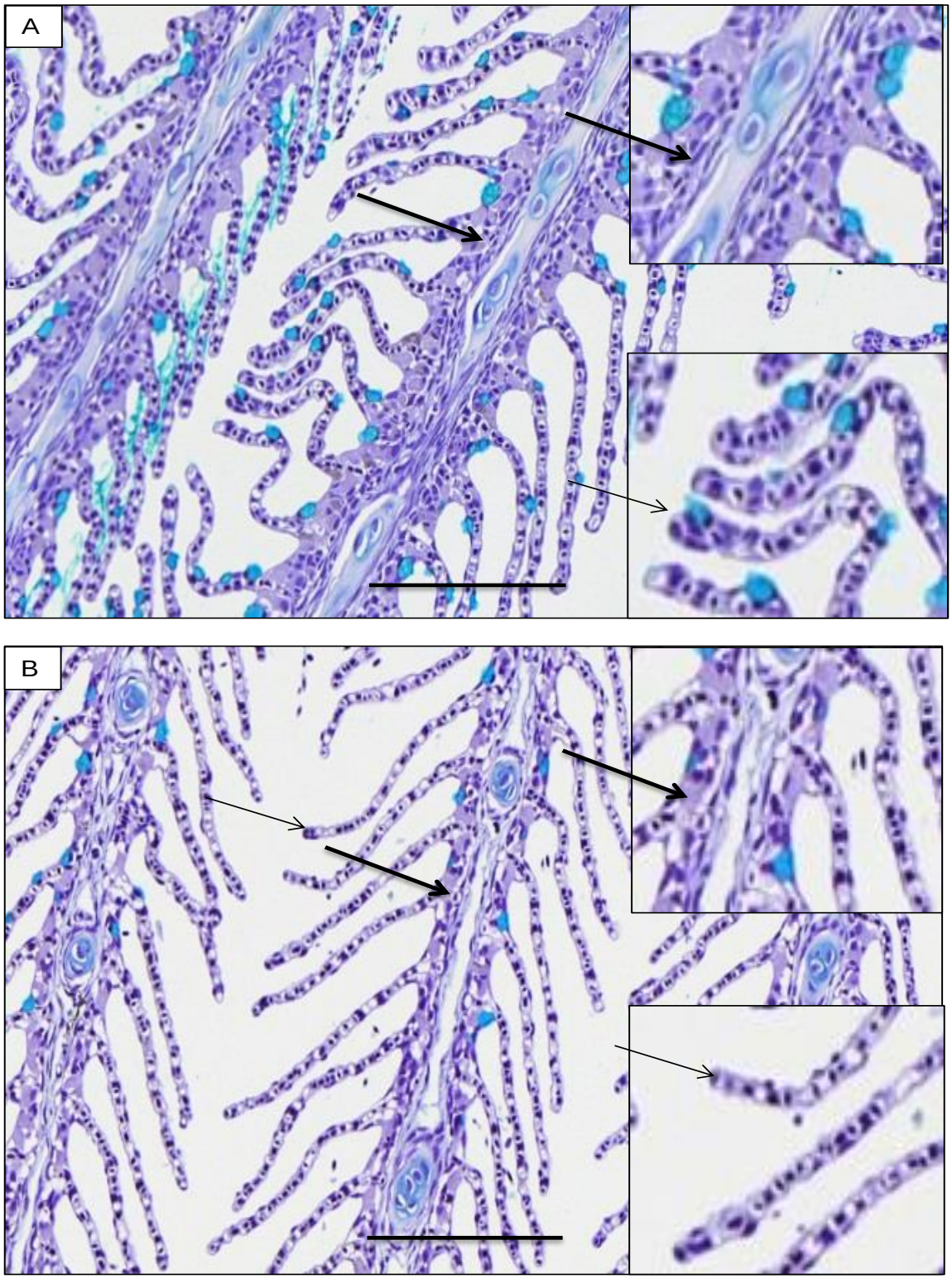

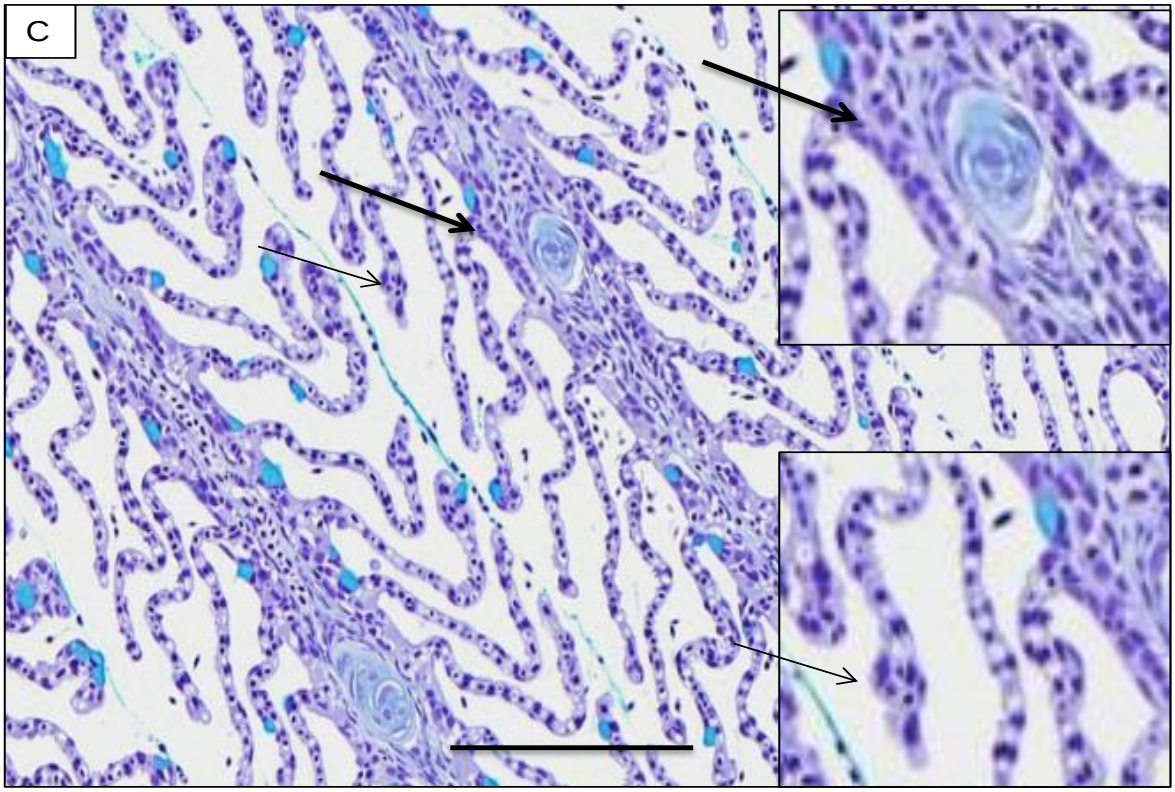

Figure 4.6 Representative gill micrographs of gill sections from fish maintained in Experiment 1, stained with Alcian blue and haematoxylin, (A) fish at 4 °C, (B) fish at 10 °C, (C) fish at 16 °C. All fish were fed with control diet (Diet A). The upper small box shows primary lamellar area displaying different magnitudes of cellularity, while the lower small box shows the distal end of the secondary lamellae at approximately twice the magnification (with arrows indicating the region selected within the gill section). The mucous cells are stained light blue and nuclei are stained dark blue. Scale bars 50 µm.

4.3.1.2 Morphometric analysis

(a) Univariate analysis of morphometric data, General Linear Model (GLM)

The GIA tool developed in Chapter 2 was used to examine changes occurring in the gill as a result of the fish being maintained at different temperatures in both Experiment 1 and Experiment 2. It was used to quantify any changes compared to the control group, and to compare these changes relative to those observed using conventional histology. In Experiment 1, the morphometric data were used to examine the effect of temperature on the plasticity of Atlantic salmon gill using data from fish fed a standard commercial

diet. Most of the morphometric parameters measured during Experiment 1 appeared significantly different between the temperature groups, namely the TGA, PLA, PLEA, ILS, MedianFERETMinSL, and the SLPL/SLA.

The parameters describing different areas for elements of the Atlantic salmon gill that were significantly different between both the temperature groups relative to the control group *i.e.* TGA, SLA and PLA are shown in Figure 4.7. Most of the morphometric parameters relating to mucous cell histochemistry were significantly changed due to temperature. The TMCA/TGA was significantly different between the 4 °C and the 16 °C groups, but not compared to the control group at 10 °C.

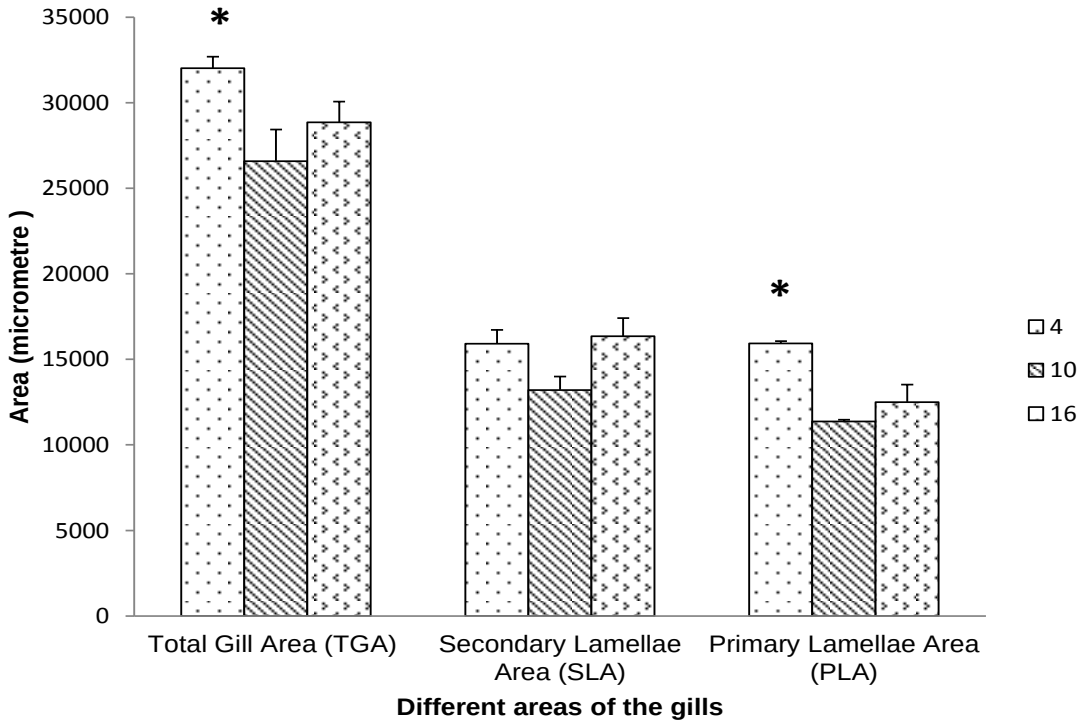

Figure 4.7 Changes in gill area parameters at different rearing temperatures (4, 10 and 16 °C). All fish were fed with control Diet A. (n=6, significance between temperature groups were indicated by * when $p < 0.05$).

Table 4.3 Univariate statistical analysis of morphometric data generated from gill sections taken from fish held at different experimental water temperatures (4, 10 and 16 °C) in Experiment 1. General Linear Model (GLM) performed using SPSS statistical software.

Gill parameter/indices	GLM (p< 0.05)	4 °C				16 °C			
		Mean	SE	SD	P value	Mean	SE	SD	P value
Weight	0.004*	172.08	4.50	11.02	0.025*	246.08	18.11	44.37	0.001*
Length	0.008*	24.80	0.10	0.24	0.023*	26.67	0.56	1.37	0.004*
CF	0.060	1.16	0.03	0.07	0.874	1.29	0.06	0.14	0.076
Total Gill Area (TGA)	0.035*	32016.33	674.04	1651.06	0.028*	28866.42	1195.64	2928.72	0.463
Secondary Lamellar Area (SLA)	0.051	15915.33	803.67	1968.57	0.114	16353.14	1059.43	2595.07	0.061
Primary lamellar area (PLA)	0.001*	15943.39	120.06	294.10	0.001*	12513.28	1004.26	2459.93	0.381
Interlamellar Spase (ILS)	0.036*	16699.68	860.64	2108.14	0.108	21264.46	511.77	1253.58	0.840
Gill Ratio (SGA/PGA= GR)	0.061	0.98	0.10	0.25	0.241	1.38	0.15	0.37	0.667
Inter-Secondary Ratio (ISR)	0.063	1.07	0.07	0.18	0.054	1.27	0.13	0.32	0.281
Primary Lamellar Epithelial Area (PLEA)	0.001*	9190.78	502.77	1231.53	0.013*	6201.72	325.45	797.18	0.314
Total Mucous Cells Area (TMCA)	0.200	548.85	104.75	256.58	0.055	418.55	83.10	203.55	0.125
TMCA / TGA	0.023*	0.02	0.00	0.01	0.078	0.01	0.00	0.01	0.077
Secondary lamellar perimeter length (SLPL)	0.086	3465.20	179.74	440.26	0.998	4021.98	217.02	531.58	0.133
Median secondary FERETMIN (MedianFERETMinSL)	0.002*	32.97	1.17	2.86	1.000	42.78	2.60	6.36	0.032*

MCN_PLEA	0.001*	4.60	0.46	1.12	0.001*	2.20	0.40	0.99	0.914
Mucous cells Area of primary lamellar epithelial area (MCA-PLEA)	0.001*	271.12	38.49	8886.73	0.021*	110.38	20.07	49.16	1.000
(MCA-PLEA)/PLEA	0.004*	0.03	0.00	0.01	0.027*	0.02	0.00	0.01	0.434
MCN-SLA	0.014*	6.13	1.32	3.24	0.074	6.40	1.16	2.85	0.035*
Mucous cells area of secondary lamellar area (MCA-SLA)	0.029*	277.84	68.49	167.76	0.107	308.17	70.05	171.58	0.070
(MCA-SLA)/SLA	0.034*	0.02	0.00	0.01	0.158	0.02	0.00	0.01	0.038*
Total mucous cells number (TMCN)	0.008*	10.73	1.74	4.25	0.030*	8.60	1.44	3.54	0.065
TMCN / TGA	0.014*	0.00	0.00	0.00	0.062	0.00	0.00	0.00	0.054
Median SLL	0.201	136.25	8.69	21.28	0.803	148.04	7.31	17.90	0.184
SLP/SLA	0.001*	0.22	0.01	0.01	0.001*	0.25	0.01	0.02	0.168
SLP/Median SLL	0.242	25.54	0.67	0.93	0.472	27.16	0.67	1.38	0.861

GLM was used to compare the means of temperature groups as the main subject effect (fish fed with control diet A only were analysed). The post hoc test were performed using Tukey'HSD and significant were indicated * when the $p < 0.05$. Bold letters indicate the gill parameters which were significantly different to the control group (10 °C).

Almost all the parameters related to mucous cell morphology and numbers in the primary lamellae were significantly different in the low temperature group compared to the control group including MCN-PLEA, MCA-PLEA, and MCA-PLEA/PLEA. The parameters associated with mucous cell morphology and numbers in the secondary lamellae were also significantly different between the high temperature group (16 °C) and the control group at 10°C. The TMCA, TMCN, were significantly different compared to TGA between the fish groups at low temperature (4 °C) and the high temperature group (16 °C), but both were not significantly different to the control group at 10°C. Overall the mucous cell parameters associated with the primary lamellae were significantly changed in the gills of fish at the low temperature.

(b) Multivariate analysis of morphometric data

Principal Component Analysis (PCA)

Multivariate analysis of the morphometric data from Experiment 1 was performed using PCA, which allows exploration of the relationship between variables. In this experiment, 28 morphometric variables and indices were initially measured. The 'Cumulative % column' gives the percentage of variance accounted for by the first 10 components. The cumulative percentage for the first two principal components is standing for 58 %, with the sum of the percentage of variance being 37 % for the first principal component and 21 % for the second principal component. The second column of the values shows the extracted components, which explained nearly 90% of the variability in the original ten variables (Table 4.4).

Table 4.4 Total variance of extracted first 10 principal components in Experiment 1

Total Variance Explained						
	Initial Eigenvalues			Extraction Sums of Squared Loadings		
Component	Total	% of Variance	Cumulative %	Total	% of Variance	Cumulative %
1	12.6	37.0	37.0	12.6	37.0	37.0
2	7.3	21.6	58.6	7.3	21.6	58.6
3	3.4	10.1	68.7	3.4	10.1	68.7
4	2.7	8.0	76.6	2.7	8.0	76.6
5	2.1	6.1	82.8	2.1	6.1	82.8
6	1.5	4.5	87.3	1.5	4.5	87.3
7	1.1	3.2	90.5	1.1	3.2	90.5
8	0.9	2.6	93.1			
9	0.8	2.3	95.0			
10	0.5	1.5	96.9			

The rotated component matrices were used to compare the relationship of the variables extracted from Principal Components 1 and 2. The first component is highly correlated with TMCA, TMCN, TMCN/TGA and (MCA-PLEA)/PLEA, but of these, TMCA and TMCN appear the better representatives because they are less correlated with the other two components. The second component correlates more with GR, SLPL and mean secondary lamellar length MSLL. It is highly correlated with inter secondary ratio of the gill.

A plot of factor scores 1 and 2 (Principal Component 1 and 2) showed that the response of Atlantic salmon gills reared at the lower temperature (4 °C) was clearly clustered away from the other two temperature groups. All groups clustered separately with minimal overlap (Figure 4.8). Another prominent feature was that individuals within the 10 °C group (control group) were more closely clustered (related) compared to both lower and higher temperature groups.

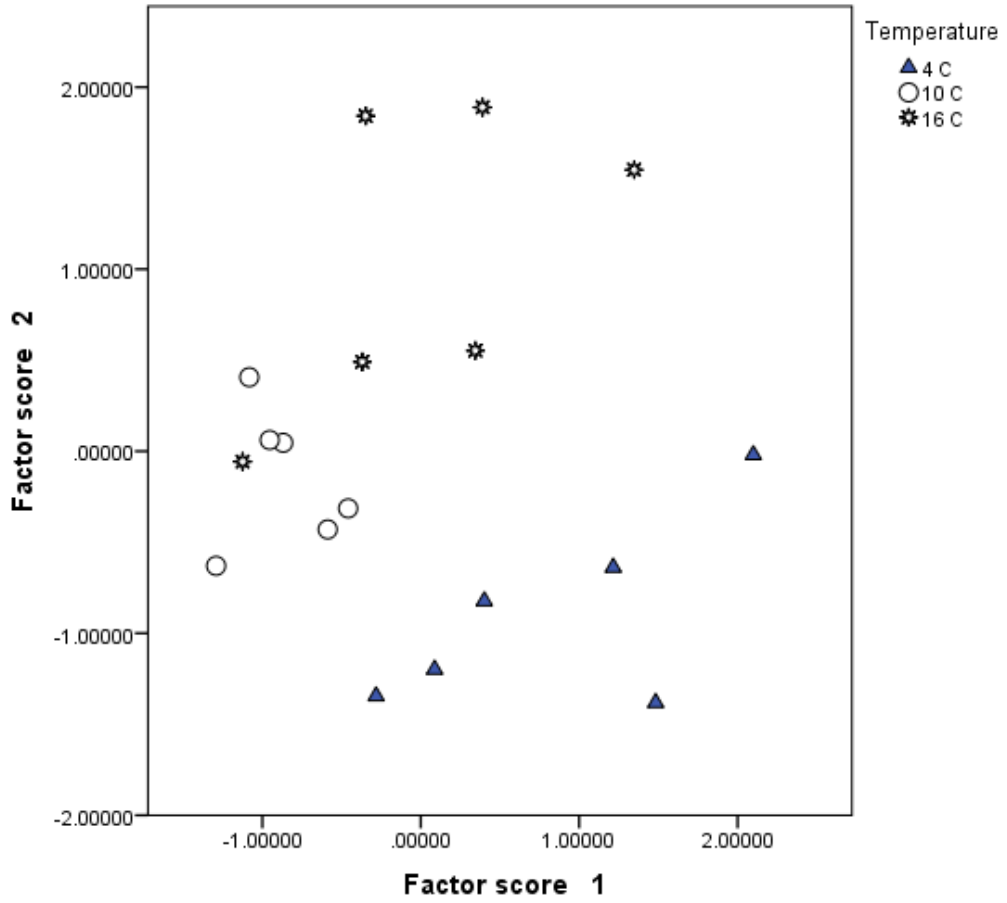

Figure 4.8 Score plot of first two principal components (factors) from Experiment 1 showing clear differentiation of individuals from different temperature regimes. n = 6 per state.

Discriminant function analysis (DFA)

The idea of the discriminant analysis of morphometric data from Experiment 1 was to provide a set of weightings that allows individuals from different temperature regimes to be distinguished. These weighting can be used to assign unknown individuals to a group to provide a probability of them belonging to each of the possible temperature groups. The discriminant analysis of temperature versus measured variables generated the following results. After subtracting group means, TMCA, TMCA/TGA, MCA-PLA, TMCN, and TMCN/TGA were highly correlated with other predictors *i.e.* TGA, SLA, SGA/PGA, TMCA), TMCA / TGA, SLPL, MedianFERETMaxSL, MCN-PLEA,

MCA-PLA, (MCA-PLEA/PLEA, TMCN, TMCN / TGA. The classification summary (Table 4.5) shows the true groups and the calculated group allocation for each individual. Members from all groups, 1(4 °C), 2 (10 °C), 3 (16 °C) were correctly assigned giving an allocation accuracy of 100 %.

Table 4.5 Summary of classification of discriminant analysis for morphometric data generated from experiment 1

Group	**4 °C**	**10 °C**	**16 °C**
N	**6**	**6**	**6**
Summary of classification		True groups	
Put into groups	4 °C	10 °C	16 °C
4 °C	6	0	0
10 °C	0	6	0
16 °C	0	0	6
total number	6	6	6
Number correct	6	6	6
Proportion	100 %	100 %	100 %
N= 18	N correct = 18		Proportion = 100 %
Squared distance between groups	4 °C	10 °C	16 °C
4 °C	0.001	53.505	33.991
10 °C	53.505	0.001	351.535
16 °C	433.991	351.535	0.001

4.3.1.3 Gene expression analysis

(a) Univariate analysis of gene expression data, General Linear Model (GLM)

The expression of a number of target immune genes (*i.e.* IgM, IgT, mIgM, mIgT, pIgR) were examined in the gills of Atlantic salmon fed either control Diet A and test Diet B in Experiment 1 using a relative RT-qPCR. The expression values obtained were subjected to statistical analysis using SPSS and Minitab statistical software. Both diet (control Diet A and test Diet B) and temperature were considered as fixed factors, in a

model examining 'diet, temperature, diet*temperature (interaction effect)'. Mean gene expression which was normalised to geometric mean of reference gene index, then relatively quantified to the control diet group at 10 °C (A10). The initial test performed to observe normality and homogeneity of variance on target genes showed $p>0.05$, indicating that gene expression data was normally distributed and homogeneous across the groups. GLM was applied to examine differences between different temperatures and dietary groups in terms of gene expression.

The normalised expression pattern of IgT was significantly different between fish fed control Diet A and test Diet B, but no statistically significant difference was observed in the mean expression of IgT between different diets at the same temperature. As shown in Figure 4.9, mean expression of IgT in the gills of Atlantic salmon at 16 °C (fed the control diet) was significantly higher than expression at 4 °C. The gills from fish fed with Diet B had higher levels of IgM, IgT, mIgM and mIgT expression at 16 °C compared to the same dietary fish at 4° °C and 10°° C.

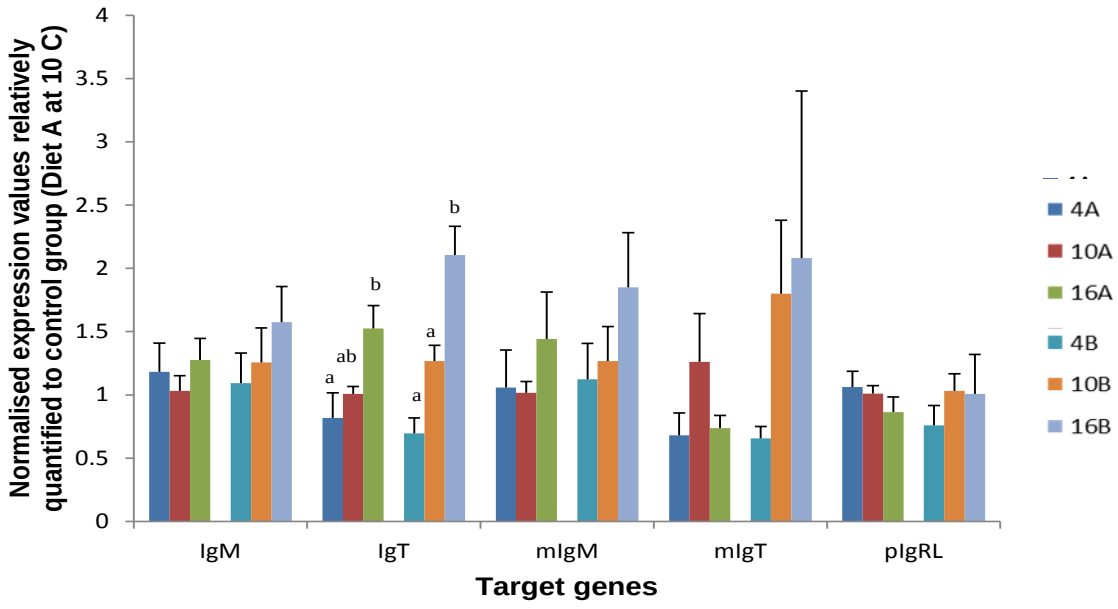

Figure 4.9 Levels of gene expression in gills sampled from Atlantic salmon in Experiment 1 maintained at three different temperatures (4, 10 and 16 °C) and fed two different diets (control

diet A and test diet B). Different colours indicate the groups of fish. Normalised expression values are compared to the control group (Diet A at 10°C). Unlabelled groups are not significantly different between states. Groups labelled with different letters are significantly different ($p < 0.05$) for selected target genes. N=6, bars represent normalised expression values ± SE).

(b) Multivariate analysis of gene expression data

Principal Component Analysis (PCA)

Principal Component Analysis was performed on gene expression data from Experiment 1. Data were continuous and normally distributed after the fourth root transformation (X^0.25). The results of the PCA are described in Table 4.6 with values for five principal components shown.

Table 4.6 Total variance of extracted first 10 principal components in Experiment 1

Total Variance Explained						
	Initial Eigenvalues			Extraction Sums of Squared Loadings		
Component	Total	% of Variance	Cumulative %	Total	% of Variance	Cumulative %
1	2.335	46.693	46.693	1.900	38.002	38.002
2	1.053	21.067	67.760	1.488	29.758	67.760
3	0.794	15.878	83.638			
4	0.502	10.048	93.685			
5	0.316	6.315	100.00			

Distribution of different groups among principal component 1 and 2 are illustrated in Figure 4.10. The degree of separation was prominent between groups A10 and B16. No clear demarcation or clustering effect was observed among other groups.

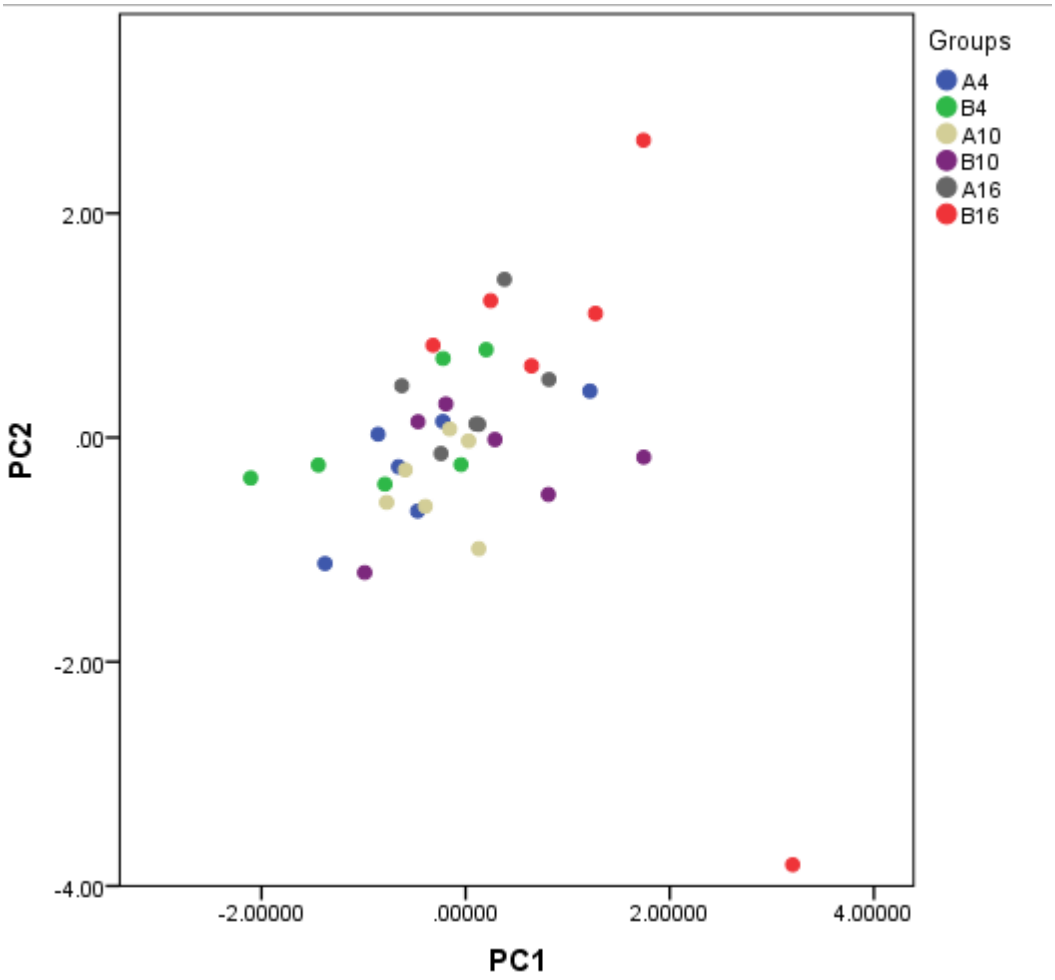

Figure 4.10 The scatter plot of PC1 and PC2 generated from the gene expression data in Experiment 1. Individuals are assigned to their relevant sub group representing temperature and diet. Groups colour coded by temperature (4, 10 and 16 °C) and by diet (Control Diet A and Test Diet B).

4.4

Experiment 2 - evaluation of morphometric changes, immune gene expression of Atlantic salmon gill reared in two different temperatures and fed with three different diets

The fish in Experiment 2 were fed three different functional diets (A, B and D) and maintained at two different temperatures 4 ° C or 12 °C (control group). The groups of experimental fish were subsequently referred to as A4, A12, B4, B12, D4 and D12. Comparisons were made between fish fed Diet B and D relative to the control feed at 12 °C (A12). The weight and the length of fish at 4 °C were significantly lower than those

reared at the higher temperature of 12 °C. The condition factor (CF) was not significantly different between temperatures.

4.4.1.1 Histology

Atlantic salmon gills, obtained from fish fed three different diets (Diet A, B and D) and reared at two different experimental temperatures (4 °C and 12 °C), were examined using conventional histology. In fish fed with same diet but reared at different temperature, histomorphological differences were evident including increased cellularity in both primary lamellae and secondary lamellar areas (Figure 4.10). Hyperplasia and hypertrophy of gill cells, also known as clubbing, were observed at the distal extremity of the secondary lamellae. This was more pronounced in fish fed with Diet B than fish fed with Diet A or D, (see inserts/magnified box in Figure 4.11 A and B). No obvious difference was seen in gills obtained from fish from the three different diets reared at same temperature.

Mucous cell numbers in primary lamellae and secondary lamellae also appeared higher in the low temperature group (4 °C) compared to the higher temperature group (12 °C), especially in fish fed with Diet B (Figure 4.11 A). Fish reared at 12 °C appeared to have increased their secondary lamellar length (Figure 4.11 B). Further analysis on these samples was performed using GIA to establish whether morphological changes were evident (significant) in the groups reared at the low and high temperature and fed with different diets.

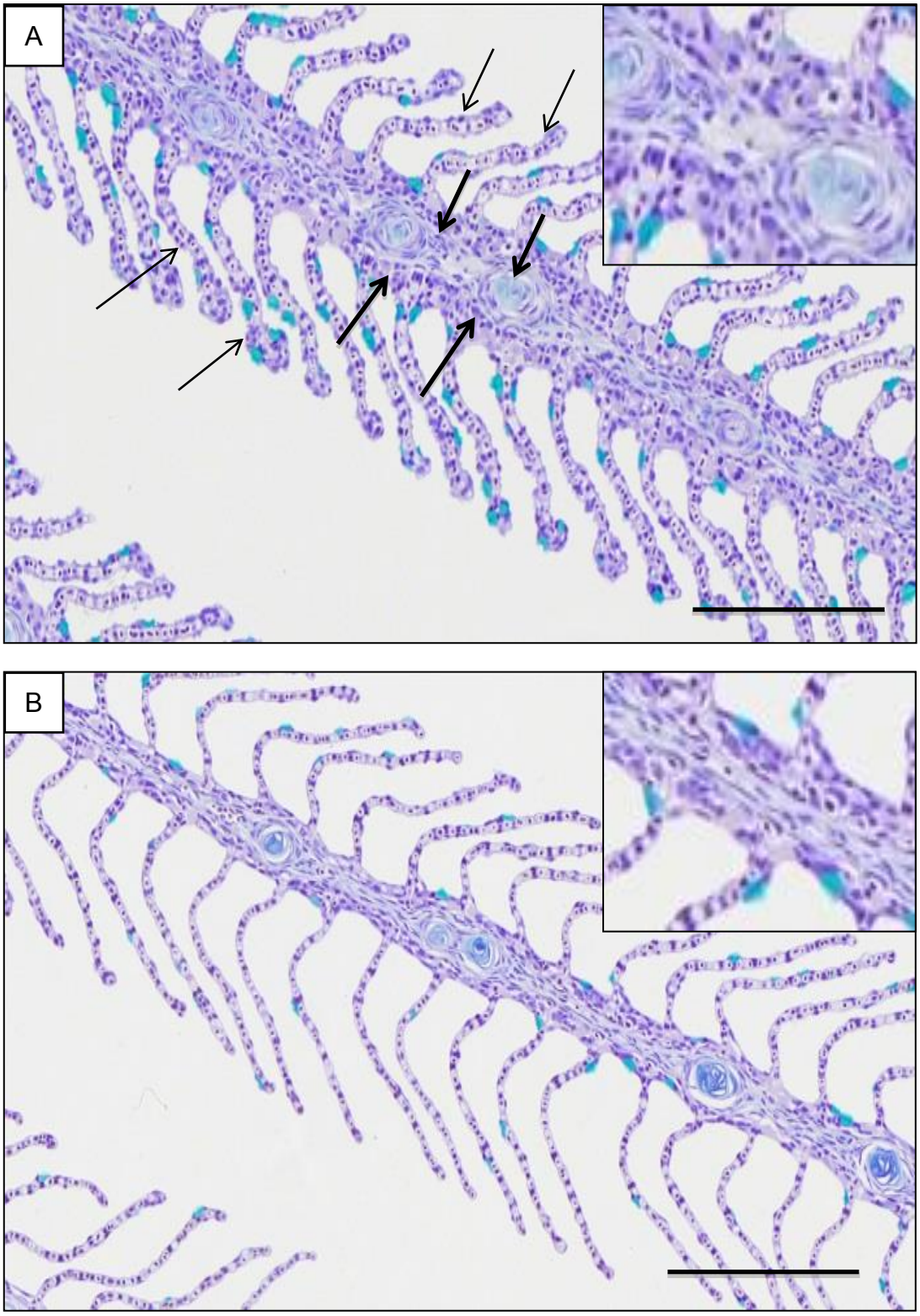

Figure 4.11 Representative gill micrographs from Experiment 2, stained with Alcian blue and haematoxylin. (A) Fish at 4 °C fed with diet B, (B) Fish at 12 °C fed with diet B. The mucous cells were stained light blue with Alcian blue and nuclei were stained purple-blue with haematoxylin. The small insert at twice the magnification of the original shows the prominent cellularity in the primary lamellar area. Scale bar 50 μm

4.4.1.2 Morphometric analysis

(a) Univariate analysis of morphometric data, General Linear Model (GLM)

The differences in the gill parameters between the groups were identified using a GLM in Minitab statistical software (Minitab, UK). Analysis of Variance (ANOVA) was conducted using temperature and diet as fixed factors. The interactions between these two factors were also analysed using a mixed model consisting of temperature, diet and interaction between temperature and diet (Temperature*Diet) (Table 4.7).

The experimental water temperatures, 4 °C and 12 °C significantly affected gill morphology (Table 4.7). Further analyses were carried out using post hoc tests on dietary groups (A, B and D) only. Significant differences were observed between means of 18 out of 28 morphometric parameters measured between fish held at 4 °C and 12 °C. Gill histomorphometric parameters varying significantly between the two temperatures, are presented in Table 4.7.Many of the morphometric parameters analysed coincide with parameters that are known to be involved in gill plasticity, with the shape of the gill being found to differ significantly between the groups maintained at the different temperatures, but not between the dietary groups.

As shown in Figure 4.12, four major gill morphometric parameters representing areas of different gill elements, including PLA, SLA, PLEA and TGA, were significantly different between the two different rearing temperatures. Out of those four morphometric parameters, TGA, PLA and EAPL only showed differences across temperature groups. SLA showed significant differences between feed types at particular temperatures

Table 4.7 Univariate analysis of morphometric data generated from gill sections taken from fish held at different water temperatures (4 and 12oC) in Experiment 2. The General Linear Model (GLM) was performed using Minitab statistical software

Variable	General Linear Model (GLM)			Diet			Temperature		Groups					
	Diet	Temperature	Diet*Temp	A	B	D	4°C	12°C	A4	A12	B4	B12	D4	D12
Vacuolar Area of Primary Lamellae (VLPL)	0.786	0.001*	0.280	A	a	a	a	b	a	b	ab	ab	ab	b
Vacuolar Area of Secondary Lamellae	0.258	0.012*	0.253	A	a	a	a	b	a	a	a	a	a	a
Total Gill Area (TGA)	0.425	0.001*	0.492	A	a	a	a	b	a	b	a	b	a	b
Secondary Lamellar Area (SLA)	0.112	0.001*	0.539	A	a	a	a	b	a	cd	ab	bcd	abc	d
Primary Lamellar Area (PLA)	0.854	0.001*	0.358	A	a	a	a	b	a	b	a	b	a	b
Interlamellar Spase (ILS)	0.674	0.017*	0.337	A	a	a	b	a	a	a	a	a	a	a
Gill Ratio (SLA/PLA)	0.083	0.002*	0.127	A	a	a	b	a	b	ab	ab	a	b	ab
Inter-Secondary Ratio (ISR)	0.273	0.001*	0.862	A	a	a	b	a	c	ab	c	ab	bc	a
Primary Lamellar Epithelial Area (PLEA)	0.576	0.001*	0.609	A	a	a	a	b	a	b	a	b	a	b
Total Mucous Cell Area (TMCA)	0.085	0.001*	0.045*	A	a	a	a	b	ab	c	a	c	bc	c
TMCA of TGA	0.151	0.001*	0.030*	A	a	a	a	b	ab	b	a	b	b	b
Mucous Cell Number of PLEA	0.192	0.024*	0.359	A	a	a	a	b	a	a	a	a	a	a
Mucous Cell Area of PLA	0.278	0.002*	0.404	A	a	a	a	b	ab	ab	a	ab	ab	b
MCA of PLEA / PLEA	0.325	0.514	0.523	A	a	a	a	a	a	a	a	a	a	a
MCN of SLA	0.337	0.001*	0.065	A	a	a	a	b	ab	c	a	c	abc	bc
Mucous Cell Area of SLA	0.096	0.001*	0.019*	A	a	a	a	b	ab	c	a	c	bc	c
MCA of SLA / SLA	0.261	0.001*	0.006*	A	a	a	a	b	ab	bc	a	c	bc	bc
Total Mucous Cell Number	0.142	0.001*	0.065	A	a	a	a	b	a	b	a	b	ab	b
TMCN of TGA	0.456	0.070	0.089	A	a	a	a	a	a	a	a	a	a	a
Mean Secondary Lamellar Length	0.384	0.098	0.114	A	a	a	a	a	a	a	a	a	a	a
Standard Deviation of SLL	0.644	0.214	0.387	A	a	a	a	a	a	a	a	a	a	a
Median SLL	0.387	0.148	0.201	A	a	a	a	a	a	a	a	a	a	a
SLPL / MeanSFL	0.540	0.132	0.988	A	a	a	a	a	a	a	a	a	a	a
SLPL / SLEA	0.070	0.001*	0.928	A	a	a	b	a	b	a	b	a	b	a

GLM was used to compare diets (A, B and D) and temperatures (4 °C and 12 °C) and the interaction between them (diet*temperature). Post hoc tests were performed to see the multiple comparisons on different dietary groups in different temperatures using Tukey'HSD and significance indicated * when $p < 0.05$. Bold letters indicate the gill parameters which were significantly different between groups. Means that do not share a letter are significantly different as indicated separately for diet, temperature and diet*temperature.

A)

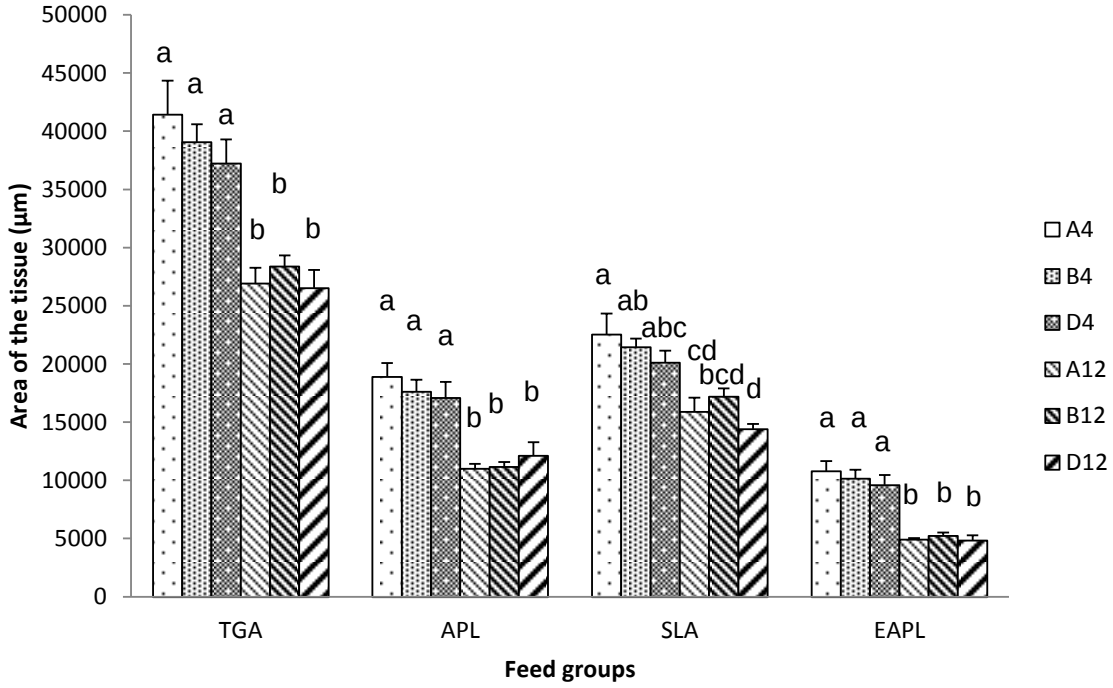

Figure 4.12 Changes in different gill area parameters at different rearing temperatures (4 and 12 °C). The fish were fed with three different diets (control diet A, B and D). (n=6, significance between temperature groups indicated by * when p< 0.05. The graph indicates individual morphometric parameters at the different combination of temperature and diet. Means that do not share a letter are significantly different as indicated separately for diet, temperature and diet*temperature.

The parameters related to mucous cell morphology, TMCA, TMCA/TGA, MCA-SLA and (MCA-SLA)/SLA was shown to have a significant interaction between temperature and dietary groups. The interactions (effect of a one factor on other factor) can be visualised in interaction plots. In those plots, parallel lines indicate no interaction. The greater the difference in the slope between the lines, the higher is the degree of interaction. GLM was used to determine if the interaction was statistically significant ($p< 0.05$). Significant interactions between diet and the temperature were assessed using profile plots of the main effect and mean plots (Figure 4.13).The interaction plot for MCA-SLA/SLA showed a significant interaction between different dietary groups (A, B and D) and temperature. The results of Experiment 2 showed significant interactions

between the dietary groups and temperature with respect to important gill parameters, such as TMCA, TMCA/TGA, MCA-SLA and MCA-SLA/SLA. The interaction plot for (MCA-SLA)/SLA showed a significant interaction between different dietary groups (A, B and D) vs temperature.

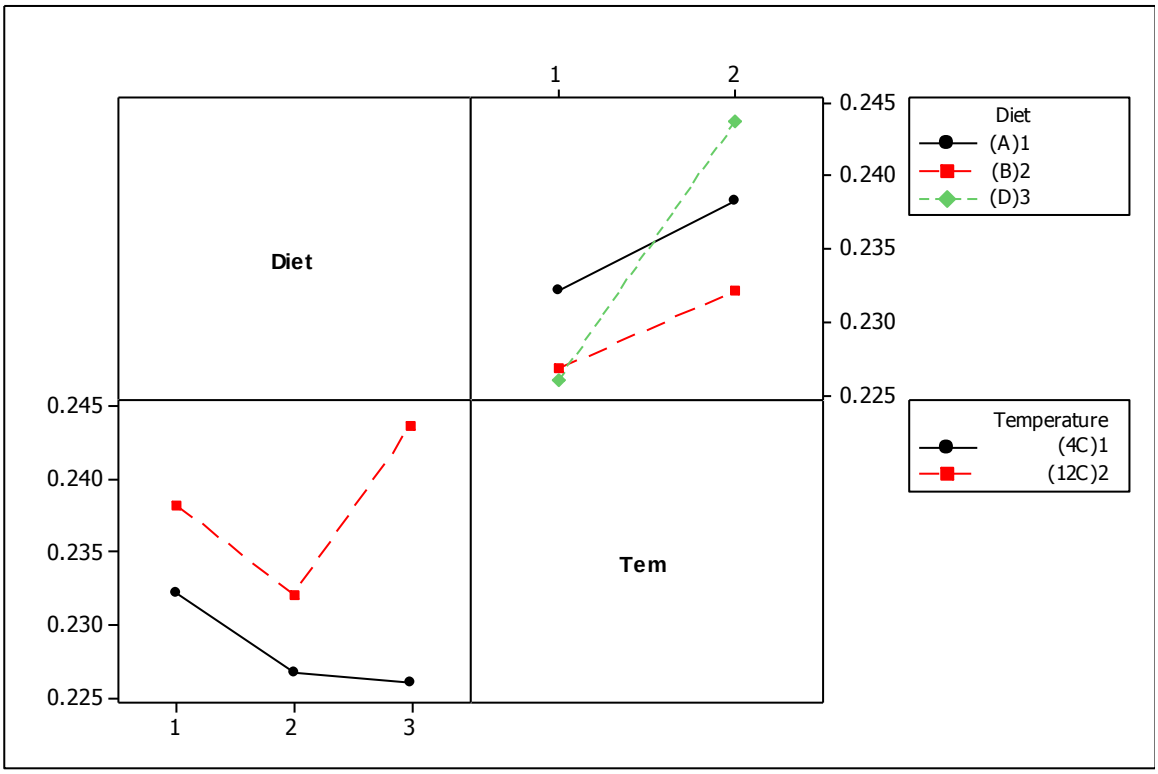

Figure 4.13 Interaction plots for mucous cell area of secondary lamellar area secondary lamellar area compared to secondary lamellar area

(b) Multivariate analysis of morphometric data

Principal Component Analysis (PCA)

In principal component analysis (morphometric data of Experiment 2), the first component (PC1) accounted for 42 % and the second (PC2) for 18 % of the morphometric variations between groups in the gills. The first 5 variables were above 1 (which is the cut-off usually used by SPSS statistical software) and the cumulative variability of 85 % between group variability.

The direction of loading for variables in terms of the first two principal components is shown in Figure 4.13. Visual examination of the measured variables shows that they are clearly clustered into three different directions. This separation of direction makes it possible to distinguish the most important set of morphometric gill parameters changed due to a thermal effect on gill morphology.

Using the first principal component, as new dependent variable, GLM was performed to distinguish any significant variability among groups (diet and temperature) as well as interaction between diet and temperature (Table 4.8). There was a significant ($p<0.05$) variability among temperature groups, but no significance observed with diet. However there was a significant difference observed in term of interactions between diet and temperature.

Table 4.8 Analysis of variance for principal component 1 (GLM). The significance is indicated by * when $p< 0.05$.

Source	DF	Seq SS	Adj SS	Adj MS	F	P
Diet	2	17.597	17.597	8.799	2.15	0.134*
Temperature	1	318.824	318.824	318.824	77.87	0.001*
Diet*Temperature	2	23.742	23.742	11.871	2.90	0.071*
Error	30	122.830	122.830	4.094		
Total	35	482.993				

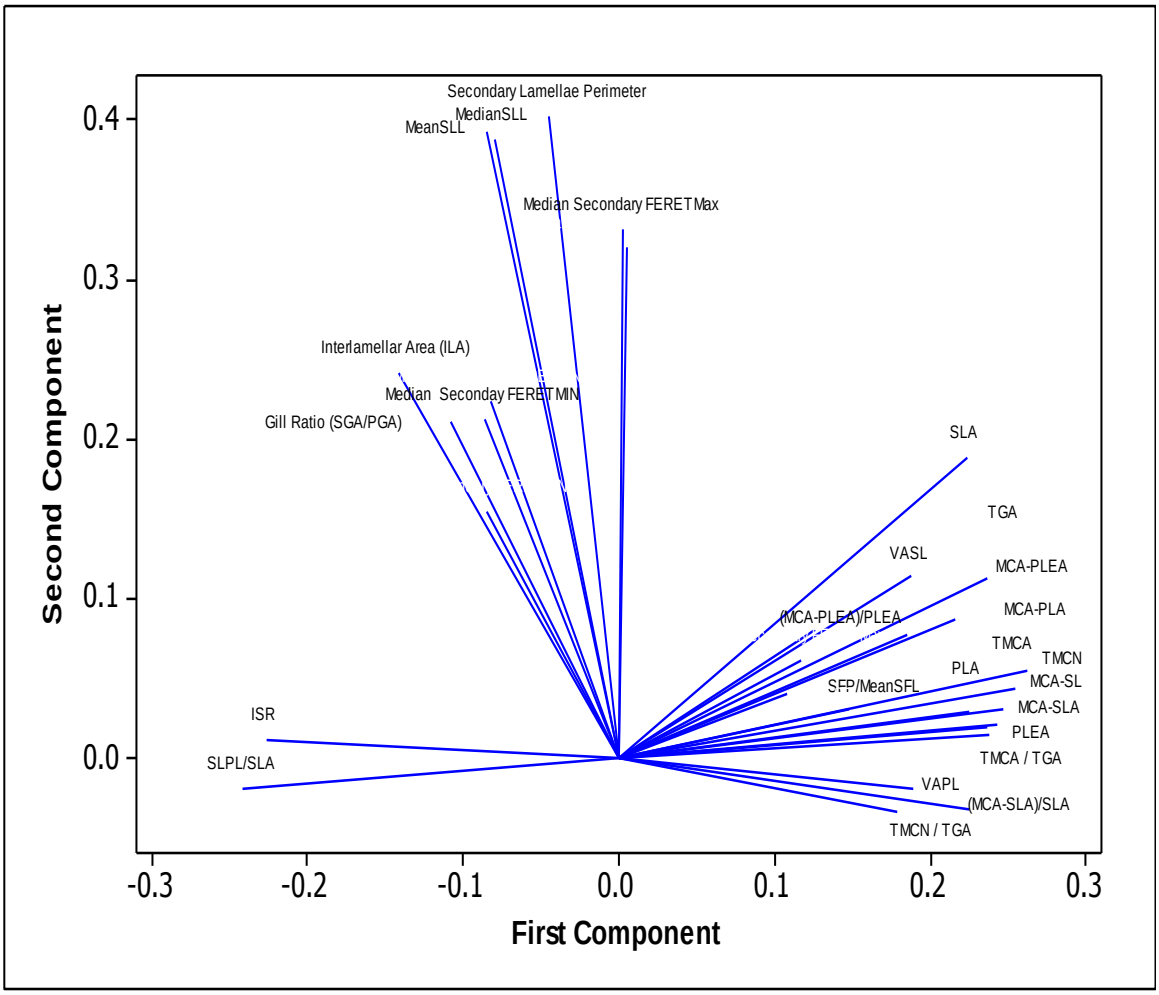

Figure 4.14 Loading plot of measured morphometric variables for gill parameters and indices analysed from Experiment 2 morphometric data. Numbers 1, 2 and 3 indicate three different clustered groups of variables: 1. Secondary lamella-associated direct gill measurements including indices like GR; 2. Gill indices made from combining two gill parameters *e.g.*, ISR and SLPL compared to SLA; 3. All other gill parameters.

Visual examination of the scatter plots generated from PC1 and PC2 revealed a clear differentiation between the groups (Figure 4.15).The morphology of the gills were undistinguishable at 12 °C between the three dietary groups (Figure 4.16 A), while fish reared at 4 °C showed some degree of separation *i.e.* between dietary group B and D (Figure 4.16 B). More distinct differentiation was evident when the same dietary group was examined across two different temperatures, however (Figure 4.16 C, D and E).

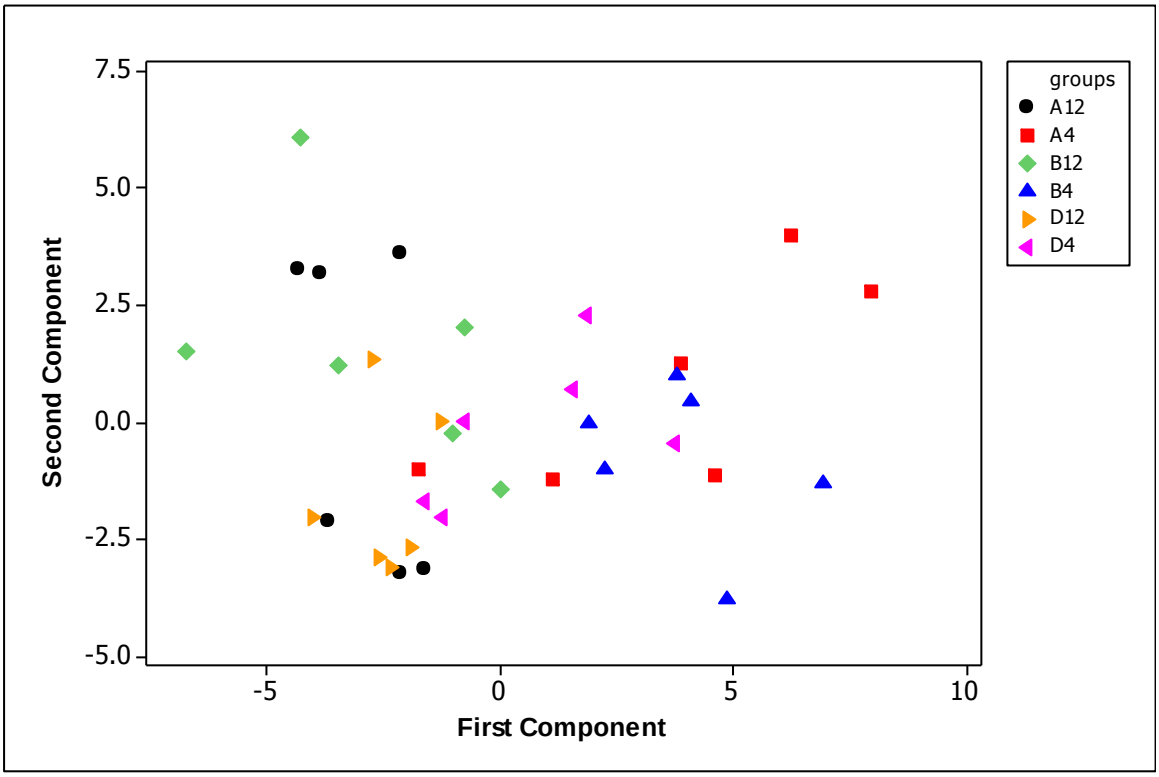

Figure 4.15 Plot of first and second principal components for variables relating to gill morphology, showing clear differentiation between fish maintained at different temperatures and those fed a particular diet at specific temperatures.

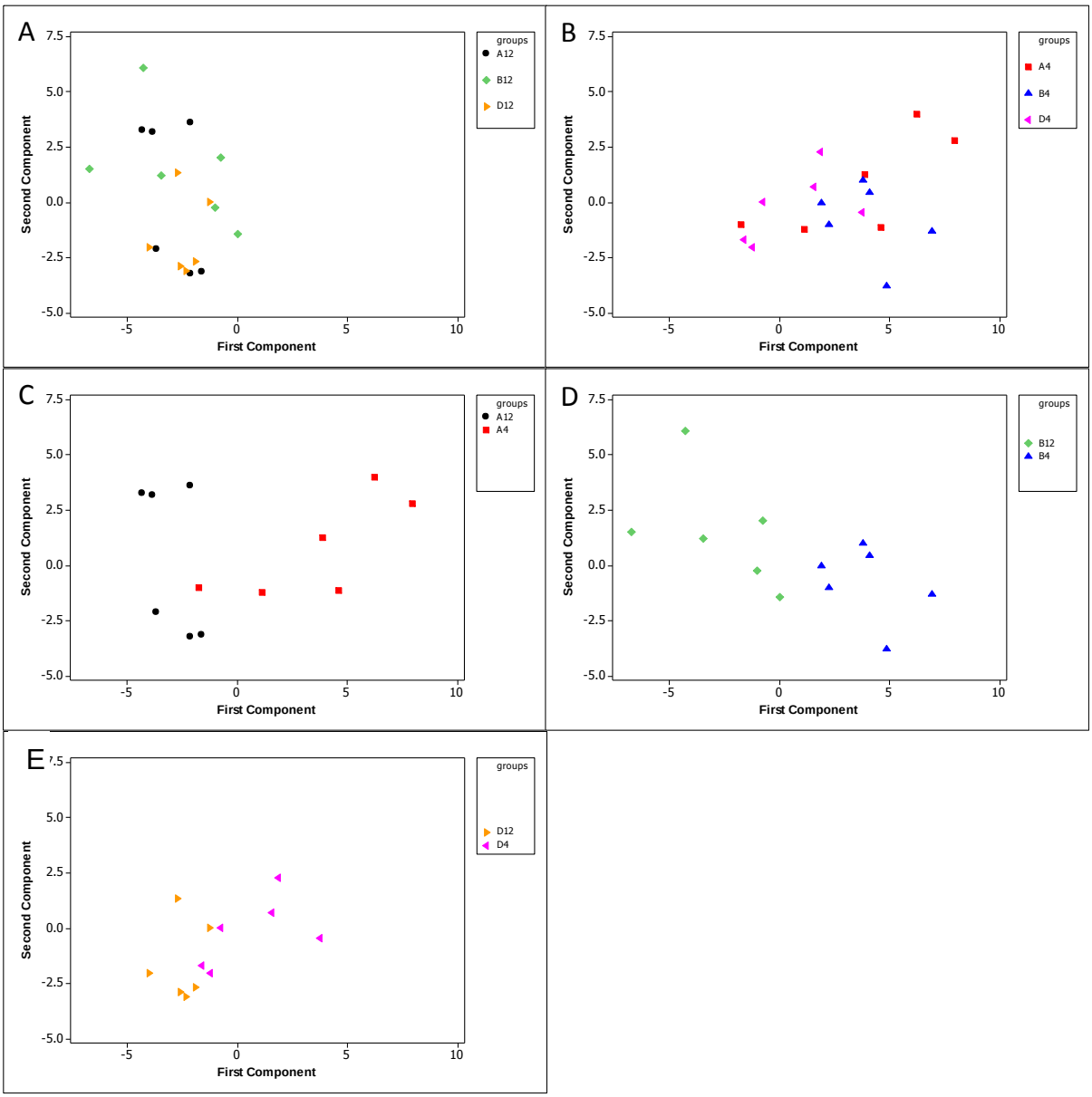

Figure 4.16 Classification of individuals belonging to different dietary groups A, B and D at two different temperatures (4°C and 12° C) by new variables/principal components. Groups are indicated as corresponding letters for dietary groups followed by temperature (A4, A12, B4, B12, D4 and D12).

4.4.1.3 Gene expression analysis

(a) Univariate analysis of gene expression data, General Linear Model (GLM)

In addition to morphometric analysis of the gills, mucosal and systemic immune responses were evaluated using RT-qPCR, to examine the effects of diet and

temperature (12 °C Figure 4.17a and 4 °C Figure 4.17b) on the expression of genes IL-1, IL-10, TNF, CD8, CD4, IgM, IgT, pIgRL, mIgT and mIgM.

The relative expression of TNFα significantly increased in Diet D at 12 °C compared to the control diet at the same temperature ($p < 0.05$, $n = 6$) (Table 4.9). At 4 °C relative expression of IgT significantly increased in the group of fish fed diet D, compared to fish fed diets B and A (Table 4.9). However, the expressions of the remaining genes were not significantly altered in the different temperature groups or the dietary groups.

Table 4.9 Analysis of TNF α expression in response to diet and temperature using a general linear model (GLM). Significance has indicated as * when $p< 0.05$.

Source	**DF**	**SeqSS**	**Adj SS**	**Adj MS**	**F**	**P**
Diet	2	0.88338	0.88338	0.44169	12.12	0.001*
Temperature	1	1.03696	1.03696	1.03696	28.46	0.001*
Diet*Temperature	2	0.62063	0.62063	0.31032	8.52	0.001*
Error	30	1.09298	1.09298	0.03643		
Total	35	3.63396				

Table 4.10 Analysis of IgT expression in response to diet and temperature using a general linear model (GLM). Significance has indicated as * when $p< 0.05$.

Source	DF	SeqSS	Adj SS	Adj MS	F	P
Diet	2	0.0698	0.0698	0.0349	0.30	0.741
Temperature	1	0.9292	0.9292	0.9292	8.05	0.008*
Diet*Temperature	2	1.6241	1.6241	0.8121	7.04	0.003*
Error	30	3.4618	3.4618	0.1154		
Total	35	6.0850				

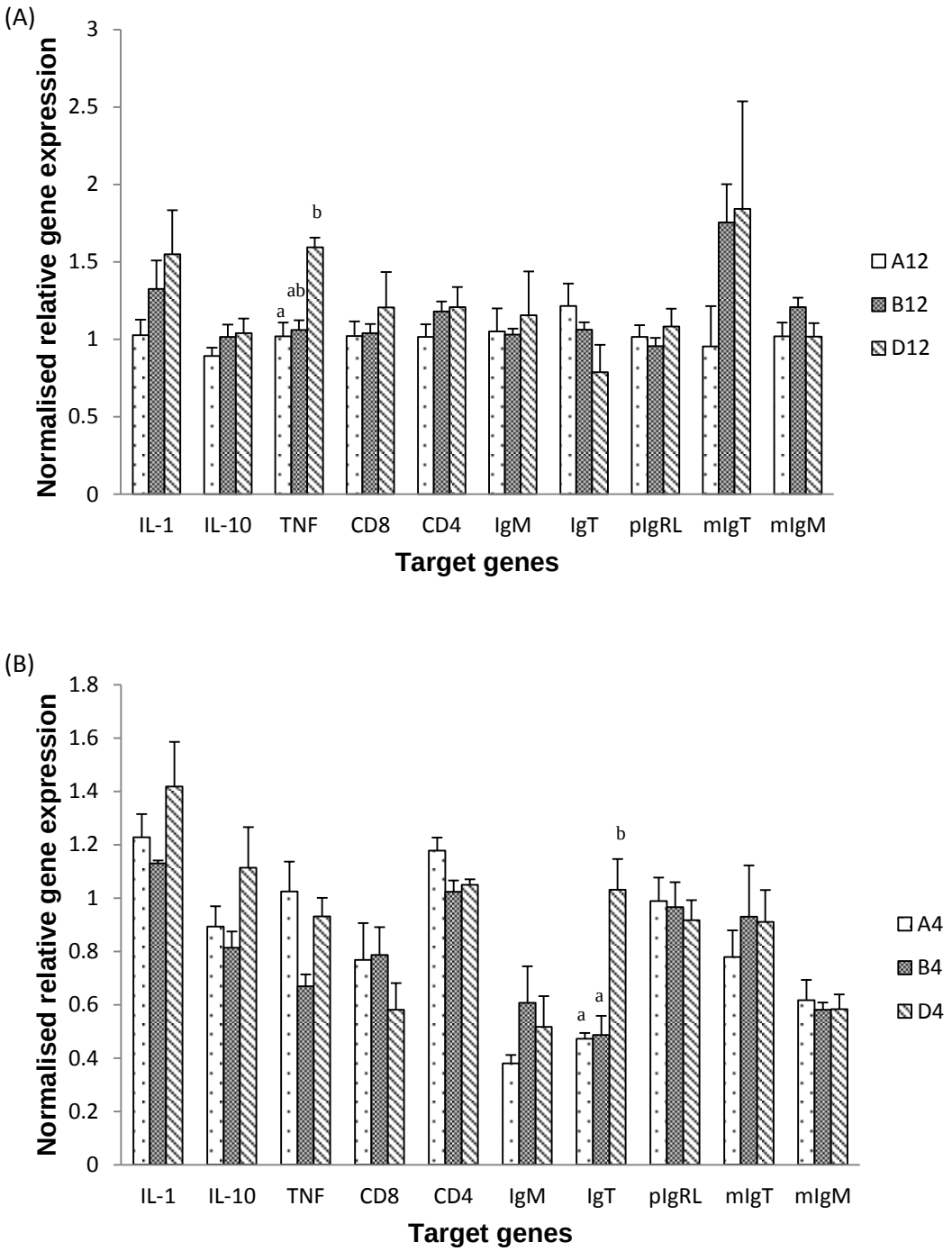

Figure 4.17 Relative expression of immune genes in Experiment 2 in the gills of fish fed Diets A, B and D when maintained at (A) 12oC or (B) 4oC). Means that do not share a letter are significantly different as indicated at $p<0.05$, n=6.

(b) Multivariate analysis of gene expression data

Principal Component Analysis (PCA)

After analysis of variance of individual measured variables between different states, an alternative approach was used to analyse the relative expression of the target genes using multivariate statistical analysis (PCA) as described above. The scree plot showed that the first 4 principal components were above the cut off value set by SPSS (IBM, UK) statistical software. The first component accounted for 36 % and second for 12% of gene expression variation among the samples. The loading plot of measured variables (measured target immune genes) in Figure 4.18 illustrates different dimensions leading to three distinct directional clusters. The IL-1 gene, encoding for a pro-inflammatory cytokine, was separated from other targets.

The plotting of PC1 and PC2, as shown in Figure 4.18, shows a low but discernible degree of separation between dietary groups at each temperature (Fig 4.4 19 A & B). Clear separation of each diet at different temperatures is seen for all diets (Fig 4.19 C, D & E)

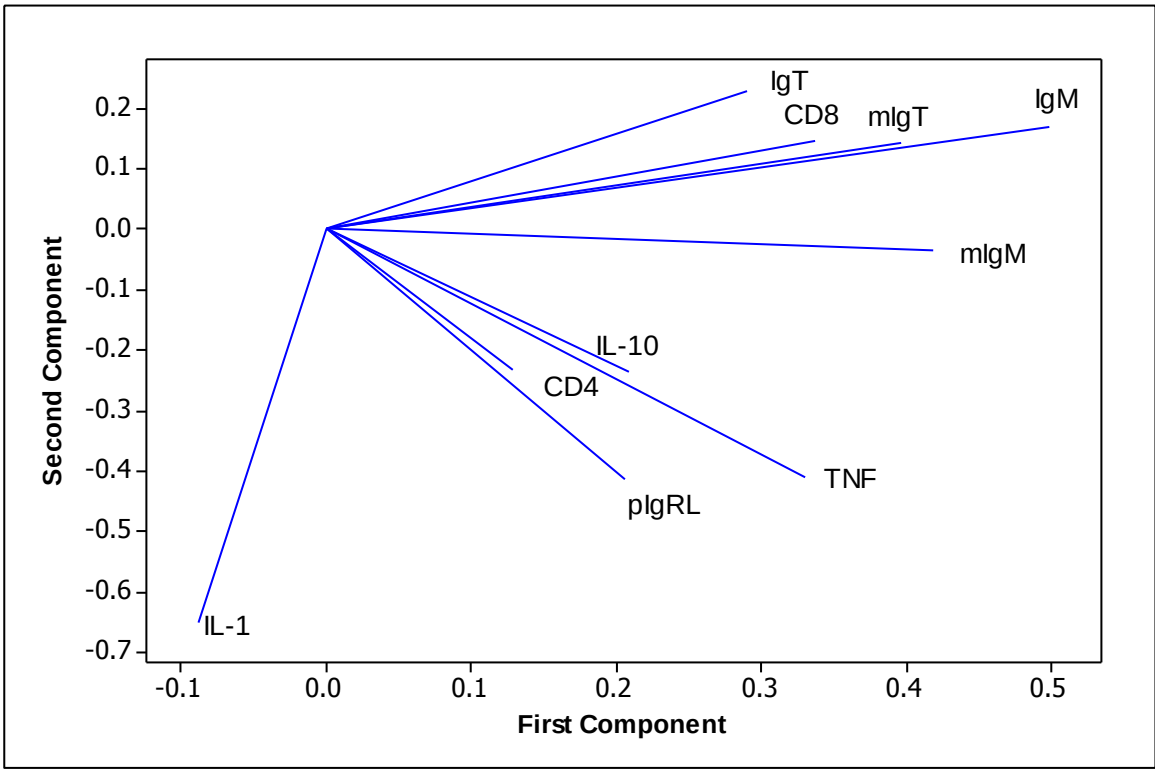

Figure 4.18 Loading plot of measured variables *i.e.* measured 10 target genes. Loading plot of measured target genes shows three distinct directional clusters

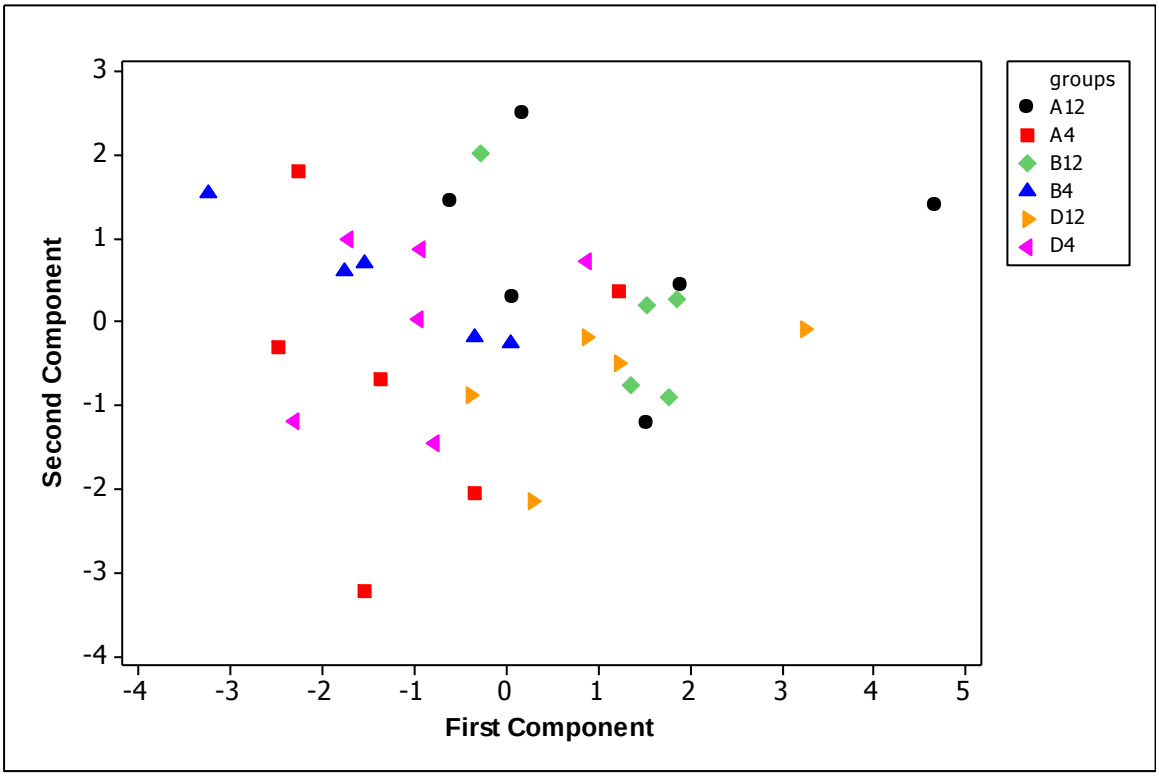

Figure 4.19 Classification of individuals belonging to different dietary groups at different temperatures by plotting PC1 and PC2 (new variables/components).

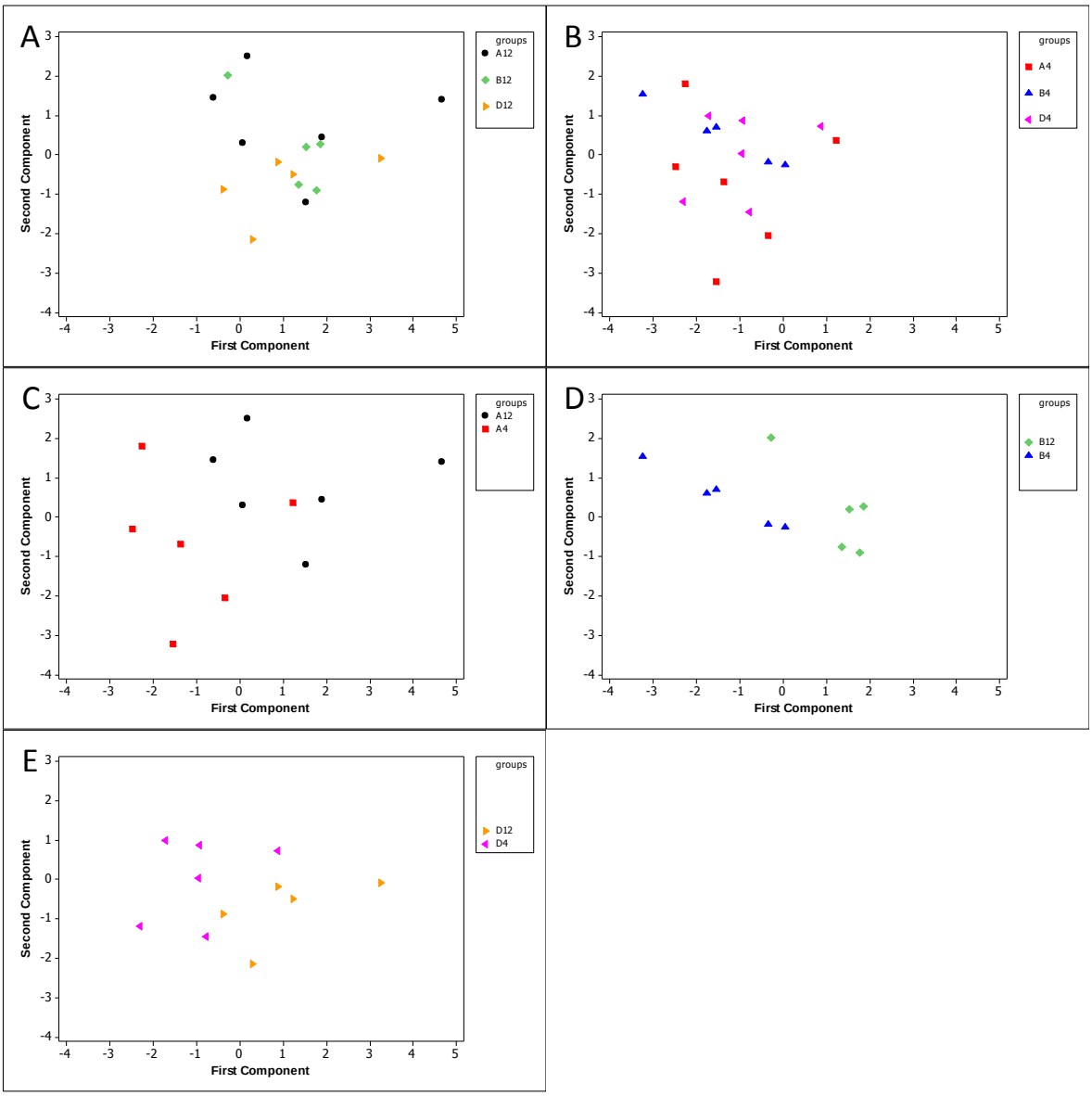

Figure 4.20 Classification of individuals belonging to different dietary groups (A, B and D) by new variables (principal components) at 12^0 C and 4^0 C (Score plots, A and B).

Classification of individuals belonging to individual dietary groups at different temperatures (at 4°C and 12°C) by new variables component 1 and 2 (Score plots, C, D and E)

4.4.1.4 PCA Analysis of combined morphometric and gene expression data of Experiment 2

The analysis of Experimental 2 data using PCA was performed after combining the morphometric and gene expression data. Loading plot of measured variables *i.e.* measured morphometric and target immune gene data from Experiment 2, illustrated a unique direction of each variable accounted in various different scale. The large set of variables generated more power to see synergistic effect of both morphometric and gene expression data on clustering individuals into their groups. Combining the effects of large variable sets helped to generate a PCA with better clustering of individuals, with groups clearly separated (Figure 4.21).

The loading plot of measured variables indicated the directional orientation of morphometric and gene expression variables (Figure 4.22). The gene expression variables compared to morphometric variables showed shorter distances from the centre indicating less contribution to the total outcome where oriented in the same direction as some of morphometric measurements (SLPL/SLA, ISR), although TNFα showed a strong contribution having longest distance from the centre. Out of the morphometric variables, the longest distances from the centre were represented by SLPL, MedianSLL, SLA and TGA. The indices that were strongly represented (Figure 4.22) were identified as SLPL/SLEA, ISR and ILS. (New variables/components).

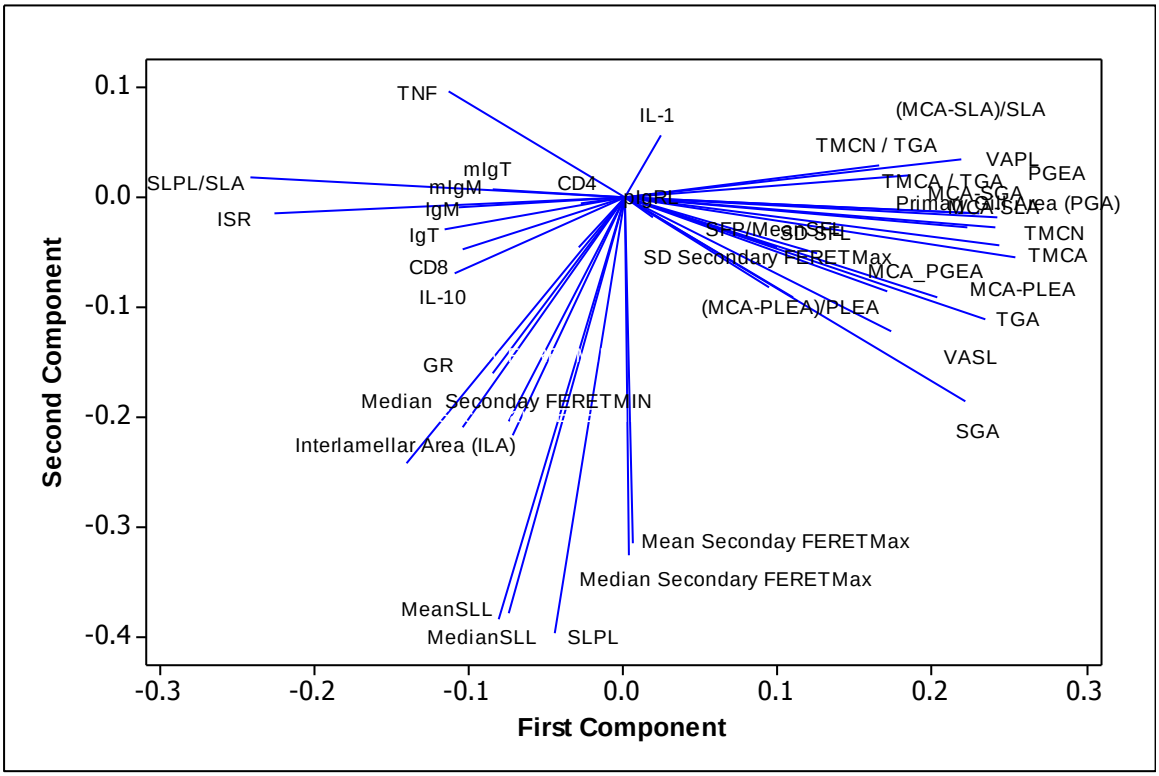

Figure 4.21 Loading plot of measured variables *i.e.* measured morphometric and target immune gene data from experiment 2.

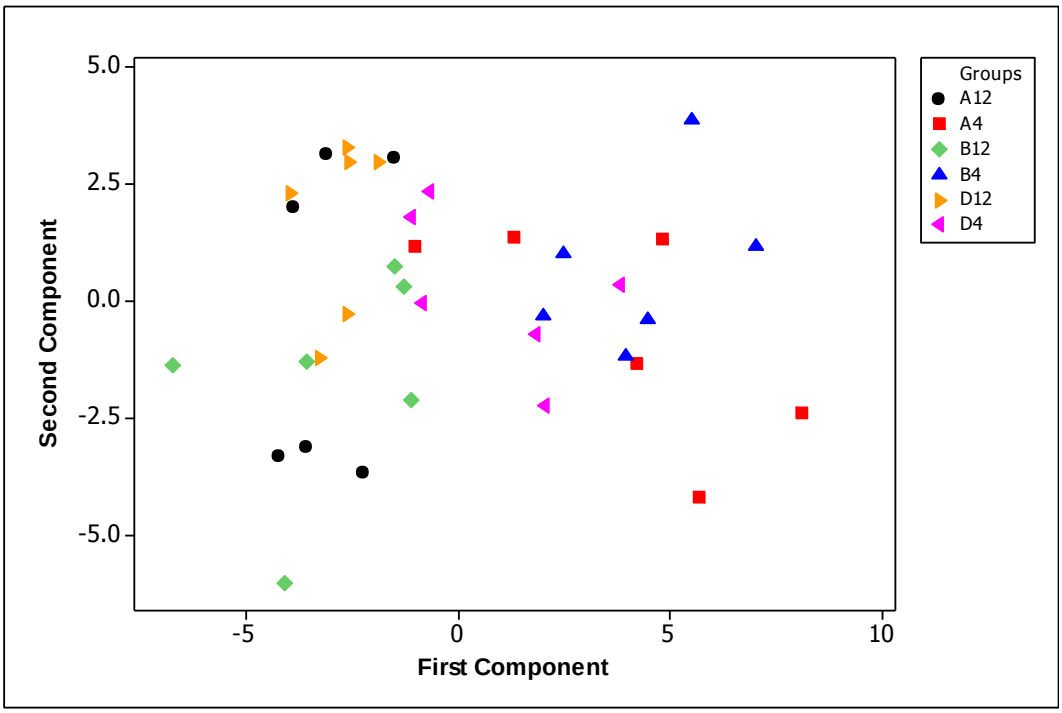

Figure 4.22 Classification of individuals belonging to different dietary groups based on morphometric and gene expression data at different temperatures by plotting PC1 and PC2

The results after combining morphometric and gene expression analysis shown that degree of separation between temperature groups was improved and better clustering was observed (Figure 4.23 Graphs C, D and E).

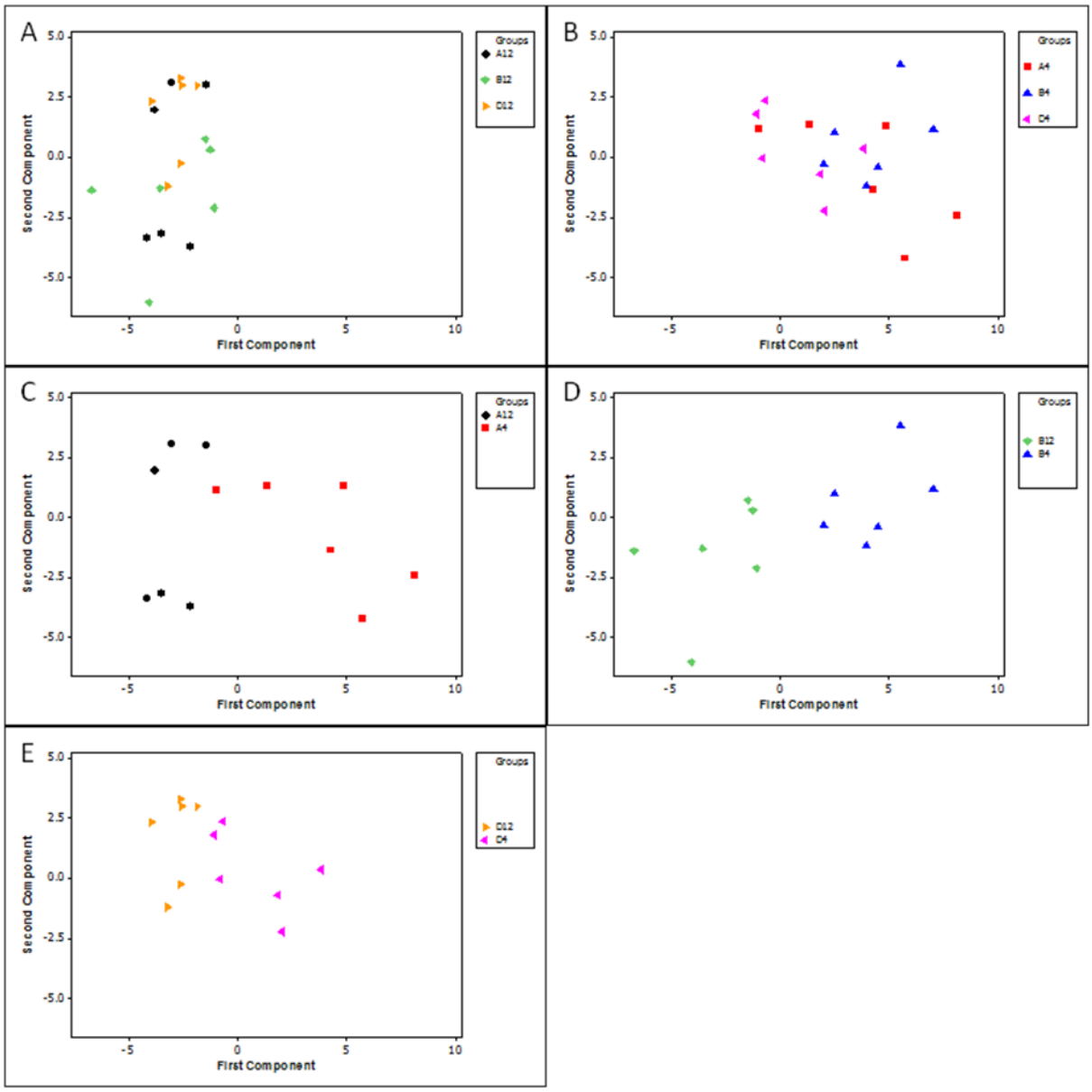

Figure 4.23 PCA classification of individuals belonging to different dietary groups classified by new variables (principal component 1 and 2). Score plots A and B: all diets at two different temperatures (A = 12 °C and B = 4 °C). Score plots D, C & E: Grouping of individuals belonging to the same dietary group at different temperatures. Data were generated from both morphometric and gene expression values from Experiment 2.

4.5 **Discussion**

The fish gill has been shown to have an extraordinary ability to reversibly remodel their gill morphology (Nilsson, 2007), and this was also confirmed in the present study. The gill of Atlantic salmon shows a significant degree of plasticity against both external and internal stimuli *i.e.* temperature and functional feeds respectively. This plasticity reflects the ability of the gill to maintain homeostasis. Similar gill remodelling has also been seen in other salmonids species and anabantoids during exposure to aluminium and/or acid water (Nilsson *et al.,* 2012). It is evident that the gills of Atlantic salmon can respond by dramatically altering their lamellar surface area *i.e.* changes in the SLPL in order to maximise the respiratory capacity of the gill (Sollid *et al.*, 2003). This has also been shown to occur in cyprinid fishes and eels (Nilsson, 2007, Nilsson *et al*., 2012).

In Experiment 1, histomorphometric analysis was performed on Atlantic salmon gills from fish fed with a conventional salmon diet exposed to two temperatures extremes *i.e.* 4 °C and 16 °C compared to a control temperature of 10 °C, to explore the mechanisms underlying gill plasticity. Conventional histological assessment made using H&E and PAS/Alcian Blue, showed subtle morphological changes in the PLA, specifically with increased cellularity in the PLEA, indicating the histomorphometric changes similar to those seen in other fish species (Perry and Gilmour, 2010).

The mechanisms governing gill plasticity have been investigated in model fish species such as crucian carp (*Carassius carassius*) (Sollid *et al.,* 2003) and goldfish (*Carassius auratus*) (Sollid *et al.,* 2005a). The ILCM has been identified as an important region of the gills for influencing these changes, with increased cellularity observed even at the very early stage in these morphological changes. Atlantic salmon are known to alter

their gill morphology to a certain extent at low temperatures (Perry and Gilmour, 2010). In Experiment 1, changes in the morphometric parameters of the gill were measured using the GIA tool, with significant changes noted in TGA, PLA, PLEA, MCN-PLEA, MCA-PLEA, TMCN and SLPL/SLA ($p<0.05$) relative to the control group, highlighting the effect of temperature on structural morphology of the gill. It would appear that the ILCM seems to play a major role in gill plasticity (Sollid *et al.*, 2003), and this was confirmed using the GIA tool in which parameters associated with primary (filament) and secondary lamellae (lamellae) were significantly altered in the test groups compared to control group. The interlamellar cell mass (ILCM), corresponding to PLA and PLEA in the GIA tool, was also significantly changed. In addition, the ILS, which reflects the approximate space between two secondary lamellae (measured in cross section), becomes smaller as a result of the increase in the ILCM.

Atlantic salmon is recognised as a hypoxia sensitive species, with their haemoglobin having less capacity to carry oxygen (Perry and Gilmour, 2010). Among all the parameters tested using the GIA tool, the parameter associated with the functional respiratory surface area (also referred to as the SLPL) was not changed in fish at the lower temperature (4 °C) compared to fish at 10 °C. The SLPL is expected to be higher in fish maintained at higher temperatures compared to those at lower temperatures (generally higher temperature has relative low dissolved oxygen than low temperature). In contrast to what we expected, due to the fact that both 10 °C and 4 °C do not cause hypoxia but later could have comparatively higher availability of oxygen for respiration. However as a result low temperature body metabolism tent to slow down but could possibly be due to the mechanism of ‘osmo-respiratory compromise’ where reservation of energy was become the priority due to poikilothermic nature. By keeping an approximately constant SLPL, and by altering other associated morphometric

parameters, would allow fish to rearrange their homeostasis keeping metabolic cost to a minimum.

The gill epithelium is less leaky when the lamellae are seen protruding from the gill filament (Mitrovic *et al.*, 2009). The constant size of the SLPL helps to maintain the optimal ion regulatory surface area, helping to lower the metabolic cost. It is estimated that the cost of ion and acid base regulation accounts for more than 10 % of the total energy budget of the fish (Boeuf and Payan, 2001). Further investigations, such as quantifying the ion-regulatory capacity of the gill, by measuring $Na^+ K^+$ ATPase activity (NKA activity) are also warranted. It is worth mentioning that this osmo-respiratory leads to a decrease in other highly metabolically demanding activities, such as swimming, to preserve energy (Beitinger and Fitzpatrick 1979).

Fish would naturally move from an unfavourable temperature to a more favourable temperature (Boltana *et al.*, 2013), but in the present study fish were confined to tanks, which means that the only way to compensate for changes in water temperature is by altering their organ structure *e.g.* gill plasticity or physiological response such as alterations in metabolic activity, nitrogenous waste excretion and acid base balance. At higher temperatures (*i.e.* 16 °C) compared to the control temperature of 10 °C, fish displayed a significant increase in their growth and an increase in mucous cell associated morphometric parameters such as MCN-SLA and MCA-SLA/SLA. In contrast, at 4 °C, both of these parameters were unchanged compared to the control group, although the increase in SLA was almost significant ($p< 0.051$) and in favour of keeping constant SLPL.

In multivariate PCA analysis of the data derived from the GIA tool, three distinct groups were observed in the scatterplot generated from PC1 and PC2. The fish in the

control group were located close to each other reflecting minimal difference in their biological response. In contrast, fish from the high and low temperatures groups (*i.e.* 4 °C and 16 °C) were generally located away from each other suggesting differences in their response to the different temperatures, although one fish from lower temperature group was situated with the control group, showing no obvious difference to the control group as assessed by the morphological analysis of GIA tool. Furthermore, the fish in the 4°C group showed higher positive values in the component matrixes for PC1 and higher negative values for PC2, representing changes in PLA and PLEA that were previously evident during conventional histological examination with increased cellularity in these areas. The other GIA morphometric parameters that were significantly changed at lower temperature (4 °C) were TGA, MCN-PLEA, MCA-PLEA and MCA-PLEA/PLEA. The second multivariate analysis technique used, discriminant function analysis (DFA), was able to distinguish between the weights of individual fish held at the three different temperatures with high accuracy, discriminating them into the three different groups. Collectively all of the techniques used to analyse the morphometric data collected in Experiment 1 support gill histomorphometric change that reflect changes in gill plasticity.

The second experiment involved feeding fish with specialised diets with altered micro-nutrients with the aim of improving the robustness of the gills by altering the integrity of the physical membranes and the gill immune response. The fish used for this experiment were reared at two different temperatures, 4 °C (test) and 12 °C (control) and fed with 3 different functional feeds (A, B and D), which gave rise to six groups (A4, A12, B4, B12, D4 and D12). Conventional histological examination was performed on the gills prior to analysing them with the GIA tool, which revealed observable morphological differences between the gills of the two different groups

regardless of the functional feed type fed, suggesting that temperature does affect the pathophysiology of fish gills. The results of this experiment were similar to those of the previous experiment, confirming that gill plasticity is temperature dependent. The parameters that were significantly different between the groups included PLA, SLA, PLEA, ILS, TGA, TMCA, TMCA/TGA, MCA-SLA, MCA-SLA/SLA, TMCN, MCN-PLEA, MCN-SLA and SLPL/SLA. Of these parameters TMCA, TMCA/TGA, TMCN, TMCN/TGA, which are associated with mucous cells, were found to be significantly different between fish fed the different diets at the same temperature, suggesting possible effects of the diets on mucous cells in the gill. The mechanism for these dietary alterations are not very well described, but there are a few recent publications indicated that dietary manipulation can alter the mucous cell quantity and composition (Pittman *et al.*, 2011, 2013). The composition of diet is an integral part in providing the essential building blocks for mucosal cell turnover (Pittman *et al.*, 2011, 2013). Furthermore Provan *et al.*, (2013) published a comprehensive study reflecting how functional feeds reduced sea lice infection (*Lepeophtheirus salmonis*), such as those containing immunostimulants or ingredients that alter the protein composition in the epidermal mucus of Atlantic salmon. The mucus of fish is known to have antimicrobial and anti-parasitic properties that reduce the pathogen burden to the host through several different mechanisms, including direct killing of bacteria by antimicrobial peptides (Ellis, 2001) and the physical removal of pathogens by continuous production of mucus lubricating the skin, making it less favourable for pathogen attachment (Dalmo *et al.*, 1997).

This study supported recent ideas of using functional feeds in commercial aquaculture to improve the immune response and disease resistance of fish by manipulating the macro and micronutrient composition of diets to enhance fish health (Waagbo, 2006). These types of diets are manufactured with the aim of enhancing immune function and

the physiology of the fish in order to overcome stressful conditions experienced by cultured fish under farming conditions such as grading, vaccination, and transportation. In general, those feeds are enriched with different micro ingredients such as essential amino acids, trace minerals, vitamins E and C and immunostimulants (*e.g.* β glucans). The strengthening of the innate immune system at the mucosal level plays an important role in the natural defence mechanisms of the fish, in turn enabling the reduction of chemotherapeutic usage.

Evaluation of gene expression by RT-qPCR is considered to be a reliable method for elucidating the molecular basis for a number of pathophysiological conditions related to fish biology and immunity (Giulietti *et al.*, 2001; Bustin *et al*., 2010). In Experiment 1, fish reared at different experimental temperatures (*i.e.* 4 °C, 10 °C and 16 °C) showed differential IgT expression at the different temperatures studied supporting the observation of an increased immune response at higher temperatures and a decreased immune response at lower temperatures as explaned by Bly and Clem (1992). The changes seen in mucosal associated immunoglobulin IgT (Hansen *et al.*, 2005: Tadiso *et al.*, 2011a; Zhang *et al.*, 2011), in response to temperature is interesting and warrants further investigation to confirm its relationship in the immune status of fish at the different environmental temperatures.

Several studies have examined the cellular and molecular composition of mucosal surfaces in salmonids (Niklasson *et al*., 2011), carp (Rombout *et al.*, 2008), cod (Rajan *et al.*, 2011), and flounder (Palaksha *et al.*, 2008). In farmed fish, pathogens that are capable of causing widespread mortality can enter through gut, gills and skin and therefore fish are under a high infectious pressure, similar to terrestrial vertebrates. Niklasson *et al.*, (2011) recently demonstrated that hypoxia induced intestinal barrier

disruption could lead to an increase in mucosal immunity due to the disturbance of the integrity of this barrier. The association between increas temperature in summer and enteritis in Tasmanian aquaculture (Battaglene *et al.*, 2008) also suggests that temperature and hypoxia can lead to mucosal barrier disruption. In worst case scenario, similar to gut, the disruption of mucosal barrier integrity of the gill can lead to an influx of common pathogens from the environment, stimulating mucosal immune parameters such as IgT. The oxidative stress caused by a high level of free radicals could also lead to membrane damage of cells in the gills, mostly to epithelial cells (Machlin and Bendich, 1987).

The gene expression results in Experiment 2 illustrate the effects of diets on various physiological parameters including the immune response. The significant increase seen in IgT transcripts in fish fed Diet D at 4 °C compared to Diet A and B suggests that at low temperature Diet D may have a positive effect on mucosal immunity. Diet D may potentially be beneficial to the fish when exposed to winter temperatures, when the innate immune parameters are compromised such as the alternative complement pathway and the adaptive cellular and humoral response (Le Morvan *et al.*, 1998). Fish fed Diet D at 12 °C also showed a significant increase in TNFα transcripts, a pro-inflammatory cytokine involved in mediating the inflammatory response by enhancing neutrophil migration and macrophage respiratory burst activity, inducing apoptosis and enhanced neuroendocrine activity, as well as playing a role in chronic inflammation and activation of the adaptive immune system (Bayne and Gerwick, 2001; Pasare and Medzhitov, 2004). The results of the study suggest that Diet D has a positive effect on favouring/promoting inflammation, which is important as a first line of defence against pathogens and is involved in linking the innate and the adaptive immune responses. To validate the link between the histomorphometrical and immunological results obtained

in this study, the signatures relating to other metabolic parameters need be checked and it would be useful to perform global gene expression analysis (*e.g.* microarray or RNAseq) to understand the fuller picture .

The approach of using multivariate analysis of variance (principle component analysis PCA) on both morphometric data and gene expression data provided a better understanding of how fish adapt to different rearing temperatures, represented here by low and high permissible temperatures for Atlantic salmon of 4 °C and 16°C respectively. The scatter plots generated from Experiment 1 and 2, with prominent clusters relating to different temperature groups, suggest their significant difference in biological response, and the relationship with altered histomorphometric parameters. The PCA has been successfully used previously to evaluate the respiratory function of carp in relation to different coping styles (Jenjan *et al.,* 2013). Even though individual fish clustered into different temperature groups, within same group they were somewhat scattered possibly due to the differences in the pattern of response of individual fish. In both experiments, it was obvious that the control groups showed a tight correlation amongst individuals. When the same technique was applied to the gene expression data from Experiment 1, individual fish were shown to cluster in groups similar to what was observed in the PCA analysis for the GIA data, helping to validate the results obtained from morphometric analysis.

The application of PCA for the morphometric data in Experiment 2 was shifted to right of the scatter plot generated by PC1 and PC2, regardless of the feed type administered. The loading plot generated to measure morphometric variables showed that the general movement of data in a right direction was mainly manifested by mucous cell associated morphometric parameters *e.g.* TMCA, TMCA/TGA, MCN-PLEA, MCA-PLA, MCN-

SLA, MCA-SLA, MCA-SLA/SLA, TMCN, and TMCN/TGA. Out of those parameters TMCA, TMCA/TGA, MCA-SLA and MCA-SLA/SLA were associated with further groupings of the fish into dietary groups. Thus moving in a right direction was much greater in dietary groups A4>B4>D4, indicating that dietary group D4 had a biological position closest to control group 12A.

In conclusion, this work explored further research on the use of functional feeds for targeted improvement of salmon health during adverse environmental conditions in terms of maintaining an adequate immune response. We have successfully applied PCA for identifying biologically related groups and for understanding the underlying pathophysiological changes that are strategically mitigated by nutritional modification through functional feeds. Both conventional histology and, to a greater degree the novel GIA tool, were able to detect subtle changes in gill morphology associated with different rearing temperatures, supporting the versatility and plastic nature of the gill. More precise interpretation of the increased gill cellularity seen during conventional histology has been confirmed using the GIA tool. This has minimised the time taken to examine a large number of sections *i.e.* large number of fish from a population for screening, and quantifying changes observed during conventional histology. The GIA tool can be used to detect the changes in a relatively small number of sections with a quantitative interpretation of the morphology compared to the qualitative assessment of conventional histology. This technology would be an ideal tool to support the histopathologist, in term of identifying and interpreting subtle histopathological changes associated with early stage changes of gill disease.

CHAPTER 5

IMMUNE RESPONSE OF THE ATLANTIC SALMON (SALMO SALAR) GILL FOLLOWING VACCINATION AND EXPERIMENTAL INFECTION WITH *AEROMONAS SALMONICIDA* SUBSP. *SALMONICIDA*

5.1 Introduction

Commercial fish farming became highly intensified through optimisation of farming practices. Although intensified farming increases commercial fish production, it has also lead industry to face many challenges induced by various stresses and diseases. At present, vaccination is used as the main method for controlling some infectious diseases (Brudeseth *et al.,* 2013).

The use of vaccines for disease prevention in aquaculture has expanded rapidly in recent years, both with regard to the number of fish species and the number of microbial diseases addressed (Hastein Gudding, 2005). Aquatic vaccines are available in more than 40 countries for more than 17 different species of fish and protect against more than 22 different bacterial diseases and 6 different viral diseases (Brudeseth *et al.,* 2013). Compared to other livestock, most bacterial vaccines produced for aquaculture are inactivated whole cell bacterial products, and the application of modern recombinant vaccine technology is still limited. In marine fish species vaccination is performed by immersion or injection. Usually, salmonid fish are immunised with multivalent vaccines by intraperitoneal (i.p.) injection. Injection vaccination is the most popular method of application and automated vaccination machines are beginning to be introduced for this purpose. Although side effects are often reported with injectable adjuvanted vaccines (Midtlyng *et al.,* 1996), they are still popular due to the long

lasting and high level of protection they elicit. Orally administered fish vaccines are also commercially available.

Aeromonas salmonicida subsp. *salmonicida*, is a common pathogen in aquaculture that successfully controlled with commercial vaccines. This bacterium, first recognised as a fish pathogen in 1900, has been extensively studied ever since (Janda and Abbott, 2010). It is a Gram-negative, fermentative, non-motile rod, which causes severe systemic disease in fish belonging to families *Anaoplomidae*, *Salmonidae* and *Cyprinidae* (Austin and Austin 2007). In salmonids, *A. salmonicida* subsp. *salmonicida* causes 'classical furunculosis', which is characterised by severe acute haemorrhagic septicaemia, followed by death as a result of septicaemia causing circulatory shock (Vanden Bergh and Frey, 2013). In chronic infections, the disease is characterised by large furuncles (boils) on the flank of fish, giving rise to high mortalities (Ferguson, 2006, Bruno *et al.*, 2013). Internally, an enlarged spleen, pale liver, engorged inflamed blood vessels in the intestine and sometimes liquefied kidneys can be seen.

The virulence determinants of *A. salmonicida* can be divided into exotoxins, endotoxins, adhesion proteins and a type III secretory system (T3SS). The exotoxins and endotoxins are generally secreted into the extracellular environment. The outer surface layer (S-layer, comprising A protein), which is part of the bacterial envelope, helps confer virulence by promoting adhesion of the pathogen to host cell membranes and also increases resistance to protease digestion (Gardũno *et al.*, 1997). The type IV pili are also known to be involved in adhesion to host cell membranes (Gardũno *et al.*, 1997). The T3SS, a novel, complex virulence determinant, was also shown to be involved in disease pathogenesis (Burr *et al*., 2005; Vanden Bergh and Frey, 2013).

Under laboratory conditions, *A. salmonicida* grow as rough, smooth or G-phase colonies between 15 and 25 °C on tryptone soya agar (TSA) or brain heart infusion agar (BHIA) (Austin and Austin, 2007), and may produce characteristic brown pigment on agar. For isolation of the bacterium from clinical material, it is recommended that the initial incubation be carried out for 24 to 48 h at 22 °C in TSB, followed by subsequent culturing on Brilliant blue agar (BBA) (Austin and Austin, 2007). While classical bacteriological isolation still remains the gold standard, antibody-based detection *e.g.* latex agglutination and enzyme linked immunosorbent assays (ELISA) and molecular methods such as polymerase chain reaction (PCR), are also routinely used to identify *A. salmonicida*.

Furunculosis was a major economic threat to a growing aquaculture industry in the early 1990s, and efforts were made to develop effective control measures for the disease including good management practices (*e.g.* improved water quality management, better stocking densities, disinfections and controlled fish movements), selective breeding, improved diets, application of immunostimulants and antimicrobial peptides, and most importantly the use of effective vaccines.

Vaccine research for furunculosis, together with other fish diseases, began in 1942 pioneered by Duff (Lillehauge, 1997), using suspensions of formalin killed whole-cell bacteria to vaccinate fish orally with a certain degree of success. Later injection (Adams *et al.,* 1988) and immersion vaccination (Rodgers, 1990) were used with improved success. A commercial vaccine for furunculosis became available in the late 1980s (Lillehauge, 1997), and during the last two decades furunculosis has been successfully controlled using oil adjuvanted injection vaccines (Romstad *et al.,* 2013).

The protection induced by vaccination in fish is mainly assessed by measuring survival of vaccinated fish compared to non-vaccinated fish after subsequent infection with the pathogen (Anon, 2006). An alternative method is being explored using serology to measure a specific serum antibody response induced by vaccination, which correlates with protection, thus removing the need to perform an experimental challenge (Romstad *et al.*, 2013). Although both of these methods can provide valuable information, neither explains the mechanisms and pathways responsible for inducing protection. Recently the cloning of fish immune-related genes has allowed the expression of genes to be studied in relation to evaluating mechanisms of protection (Mulder *et al.*, 2007; Fast *et al.*, 2007, Harun *et al.*, 2011).

A study was performed here with the aim of improving our understanding of the immune response elicited locally in the gill of Atlantic salmon compared to the systemic immunity elicited in kidney and spleen of the fish following vaccination and experimental infection with *A. salmonicida*. This bacterium was chosen as the model pathogen for this study because of the knowledge that is available relating to both the host's response to the pathogen and its response to vaccination, but little is known of the response of gills to vaccination or challenge. The main aims of this study was to assess the immune response in the gills of Atlantic salmon in comparison to their kidney and spleen following vaccination with a furunculosis vaccine by i.p. injection and also to investigate how these responses reflect the level of protection elicited during subsequent infection with *A. salmonicida*.

5.2 Materials and Methods

5.2.1 Fish

The samples collected for this work originated from a larger experiment performed in the Aquatic Vaccine Unit, IoA, University of Stirling, on a DEFRA-funded project to develop serology protocols to evaluate batch potency testing for furunculosis vaccines. Unvaccinated Atlantic salmon (*Salmo salar* L.) parr (n = 1080), average weight 20 g, were obtained from the Niall Bromage Research Facility, University of Stirling, Stirling, UK, and were transported to the Aquaculture Research Facility (ARF), at IoA, University of Stirling and held for a 2 week quarantine period followed by routine health investigation to rule out common fish pathogens. Details described here only refer to the samples used in the present study and not to the larger study where various vaccine doses were used. After the 2 week quarantine period, fish were randomly allocated into experimental tanks (100 L) maintained in a freshwater flow through system at 15±1°C. An overview of the experimental design is shown in Figure 5.1 and consisted of four tanks with 35 fish per tank for post-vaccination sampling (Group 1), four tanks with 15 fish per tank to establish relative percentage survival at 60% mortality by experimental infection after post-vaccination (Group 2) and eight tanks with 20 fish in each (Groups 3 and 4) to sample for immune gene analysis in experimental infection of *A. salmonicida* post-vaccination. Further details relating to the vaccination and infection can be found in Sections 5.2.2 and Figure 5.2 and Sections 5.5.3 and Figure 5.3 respectively. Fish were-fed twice a day with a commercial diet at 1 % of their total body weight and were acclimatised to their rearing conditions for 7 days prior to starting the experiment.

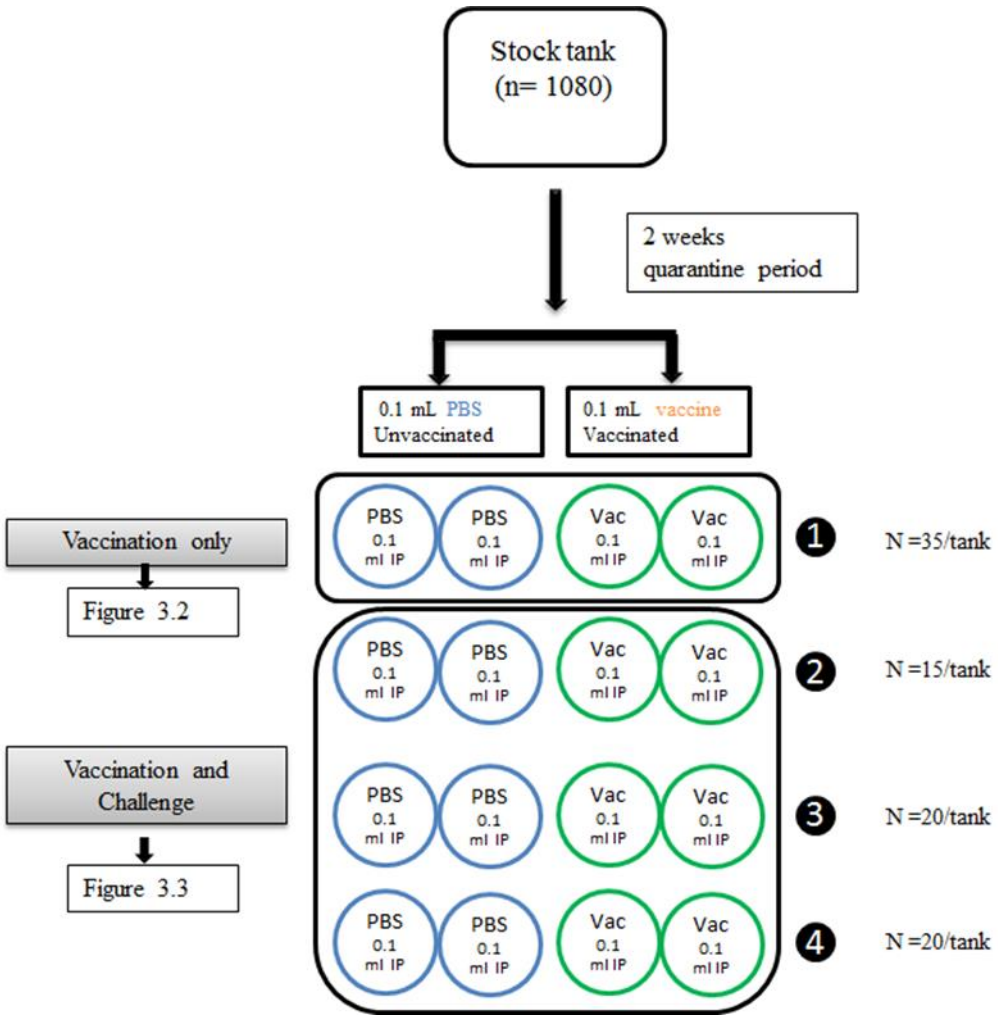

Figure 5.1 Overview of experimental plan of *Aeromonas salmonicida* vaccination and challenge trial performed on Atlantic salmon. Four sets of duplicate tanks of fish were used and first four tanks (n-35/tank) were vaccinated with a commercial furunculosis vaccine (0.1 ml) eight tanks of fish were injected with 0.1 ml of PBS. Please note that 1080 fish were used for full experiment

5.2.2 **Vaccination**

Fish in duplicate tanks from all four groups shown in Figure 5.2 were injected intraperitoneally (i.p.) with 0.1 ml of AquaVac™ FNM Plus, a commercial *A salmonicida* emulsion injection vaccine supplied by MSD Animal Health (Milton Keynes, Bucks, UK). The fish in remaining replicate tanks of all four groups were injected i.p. with 0.1 ml phosphate buffered saline (PBS) as controls. Fish were anesthetised with 100 mg L^{-1} benzocaine (Sigma, UK) before injection and observed for recovery prior to moving them back into experimental tanks. Fish were closely monitored twice a day during a 59 day experimental period following vaccination (*i.e.* approximately 885 degree days). Two tanks per group with 35 fish were used for sample collection for gene expression. These groups were referred to as vaccinated or unvaccinated respectively. The samples were collected at 0, 12, 24 and 59 d.p.v. to monitor their immune gene response. Here gills were analysed for 12 and 24 d.p.v. only.

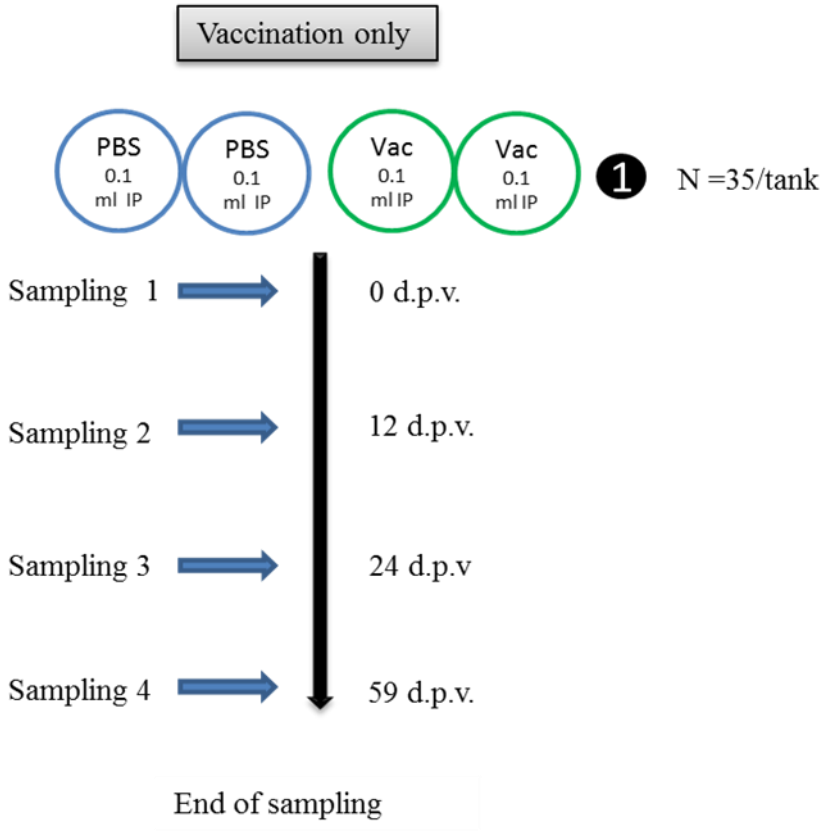

Figure 5.2 After the vaccination, four fish per tank were sampled for gill, head kidney and spleen from Group 1 at 12, 24, and 59 days post vaccination (d.p.v.).

5.2.3 **Experimental infection of fish with *A. salmonicida* after vaccination**

A virulent strain of *A. salmonicida* (Hooke), kindly supplied by Dr. Dawn Austin, Heriot Watt University, Edinburgh, UK, was used to experimentally infect fish. A pre-challenge experiment was carried out to determine a 70 % infective dose for the challenge experiment.

The fish that had been vaccinated with AquaVac™ FNM Plus (vaccinated) or injected with PBS (controls) in Group 2, 3 and 4 (Figure 5.3), were moved into challenge suite in order to performed challenge experiment at the end of the vaccination period *i.e.* 60 d.p.v. All vaccinated and control fish from Group 2 (15 fish/tank) were injected with 0.1 ml containing 10^8 ml *A. salmonicida* sub species *salmonicida* i.p and used to measure mortalities. Two of the tanks contained 20 fish vaccinated and 20 fish unvaccinated (Group 3) were infected with *A. salmonicida* at the same infective dose. The remained two tanks of 20 fish of vaccinated and unvaccinated (Group 4) were injected with 0.1 ml PBS as controls (*i.e.* mock challenge).These four groups are referred to as vaccinated infected/challenged (thereafter vaccinated challenged), vaccinated uninfected/unchallenged (thereafter vaccinated), unvaccinated infected (fish which died within 4 days were not included in the analysis) and unvaccinated uninfected (thereafter unvaccinated) (Table 5.1). Those groups were samples for sequential gene expression in gill head kidney and spleen after post challenged (Figure 5.3). All three were monitored 4 times a day throughout the experimental period.

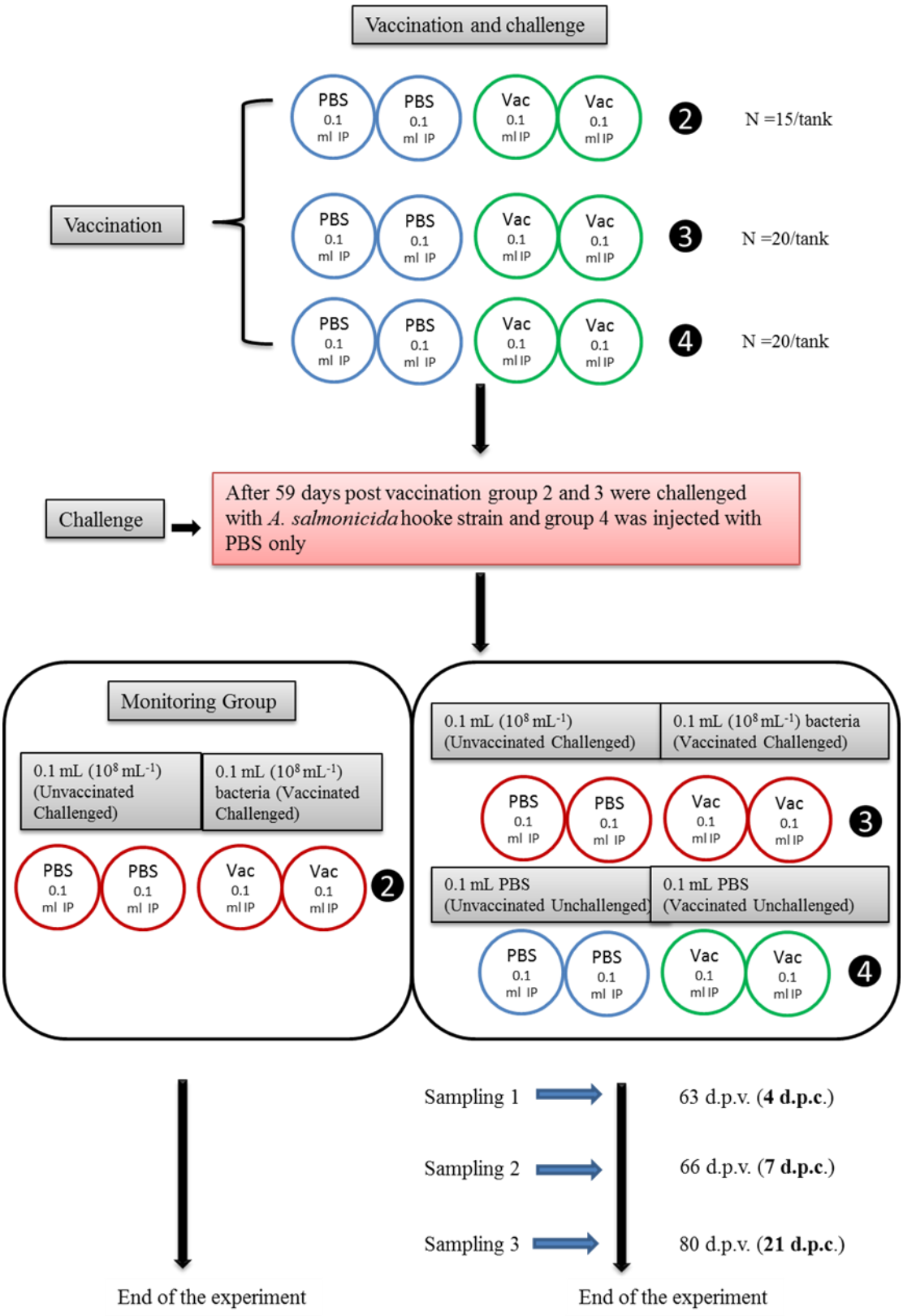

Figure 5.3 Layout of challenge experiment. At 59 d.p.v Group 3 (n= 20/tank)) was challenged with a virulent strain of *A. salmonicida* Hooke strain and group 4 (n=20/tank) was kept as unchallenged (but second PBS injection was given). The samples (8 fish/tank/organ; gill, head kidney and spleen) were collected from group 3 and 4, at 4, 7 and 21 d.p.c analysed for immune gene expression. The group 2 (n=15/tank) was monitored for mortality count.

Table 5.1 Final experimental groups and nomenclature. The colour code indicates the identity of relevant groups in bar graphs

Groups	Purpose	Vaccination	Challenge	Designated group	Thereafter
Group ❶	Vaccination study only	First duplicate tanks were vaccinated	Unchallenged	Vaccinated group	Vaccinated group
	Vaccination study only	Second duplicate tanks were PBS injected	Unchallenged	Unvaccinated group	Unvaccinated group
Group ❷	Monitoring group of challenge study	First duplicate tanks were vaccinated	After 59 d.p. v. challenged with *A. salmonicida* Hooke strain	Vaccinated challenged	Vaccinated challenged (Figure 5.5 vaccinated)
	Monitoring group of challenged study	Second duplicate tanks were PBS injected	After 59 d.p. v. challenged with *A. salmonicida* Hooke strain	Unvaccinated challenged	Unvaccinated challenged (Figure 5.5 unvaccinated)
Group ❸	For sampling of challenged study	First duplicate tanks were vaccinated	After 59 d.p. v. challenged with *A. salmonicida* Hooke strain	Vaccinated challenged	Vaccinated challenged group
	For sampling of challenged study	Second duplicate tanks were PBS injected	After 59 d.p. v. challenged with *A. salmonicida* Hooke strain	Unvaccinated challenged	Did not used for analysis (fish died after 4 days)
Group ❹	For sampling of challenged study	First duplicate tanks were vaccinated	Unchallenged	Vaccinated unchallenged	Vaccinated group
	For sampling of challenged study	Second duplicate tanks were PBS injected	Unchallenged	Unvaccinated unchallenged	Unvaccinated group

5.2.4 **Sampling of fish post-vaccination and post-infection**

Blood and tissues (*i.e.* gills, skin, spleen and head kidney) were taken from two fish from each tank on Day 0 (D0) before vaccination to confirm their disease free status by routine bacteriological invstigations. Gill, head kidney and spleen were sampled from vaccinated fish (4 fish per tank) at 12 and 24 day post-vaccination (d.p.v) for gene expression analysis (Figure 5.2). The vaccinated/challenged fish (4 fish per tank) from Group 3 and 4 were sampled at 4, 7, and 21 days post-challenge (d.p.c.) for gene expression analysis (*i.e.* gill, head kidney and spleen) and histology (*i.e.* gill, head kidney and spleen) (Figure 5.2). All fish were bled from the caudal vein using a 1 ml syringe fixed with 23 G needle prior to sampling.

Tissues (gill, head kidney and the spleen) were fixed in RNAlater (Sigma) for gene expression analysis and in buffered RNAse and DNAse-free paraformaldehyde (4 % w/v) for histological and immunohistochemical analysis. In addition, a loopful of kidney from both anterior and posterior kidney from dead or moribund fish from Group B was also sampled for bacteriology to confirm *A. salmonicida* as the causative agent for mortality. The kidney tissue was cultured on tryptone soya agar (TSA) at 22 ^{o}C. After 24-48 h incubation, from the plates that colonies were developed, a colony was sub-cultured on to fresh TSA plate using a sterile platinum loop. For confirmatory diagnosis, Gram stain and immune florescent antibody test (IFAT) using an anti-*A. salmonicida* monoclonal antibody were performed on bacterial smears prepared on glass slides from plates sub-cultured.

5.2.5 **Histology**

5.2.5.1 Sample processing for histology

An automated Shandon Excelsior Enclosed Tissue Processor (Thermo Scientific, UK) was used to process the samples. All tissues were trimmed, cassetted and separated into hard tissues (gills) and soft tissues (head kidney and spleen) prior to processing. The processed tissues were then embedded in Moulton paraffin wax (Sigma, UK) in Leica Histoembedder and wax dispenser EG1160, GmbH. The wax blocks were carefully trimmed to expose tissue, and then 5 μm thick paraffin sections were cut using a Shandon Finesse® microtome (Thermo Scientific, Waltham, MA, U.S.A.) and carefully layered onto a water bath maintained at 54^{o}C. The sections were then placed on positively charged white frosted glass microscope slides (Solmedia Ltd, Shrewsbury, UK). Prior to staining, sections were transferred into slide holders and kept in a drying cabinet maintained at 60°C for 1 h.

5.2.5.2 Haematoxylin and eosin staining

The 5 μm thick paraffin wax sections were stained with H&E as described in Chapter 2, section 2.2.2.1. Briefly, slides were pre-incubated at 60°C for 1 h before being de-paraffinised through two xylene baths for 5 min each, then transferred into absolute alcohol for 2 min before being placed into methylated spirits for 1.5 min. Slides were then washed in running tap water before placing in them in haematoxylin Z for 5 min and again washing them in tap water until clear (30 sec to 1 min) before 3 quick dips in 1 % acid alcohol. Slides were then washed in tap water and Scott's tap water substitute for 1 min then brought back into water before placing them in eosin for 5 min. Slides were then given a quick wash in tap water before placing them in to methylated spirit

for 30 sec. Stained slides were dehydrated through an ethanol series before clearing through xylene and mounting using Pertex (Cellpath, UK).

5.2.5.3 PAS and Alcian blue staining

The 5 μm thick paraffin wax sections were pre-incubated at 60° C in an oven before being deparaffinised in two consecutive xylene baths for 5 min each time. They were transferred into alcohol for 2 min before placing them in methylated spirit for 1.5 min and washed in tap water for 30 sec to 1 min. Slides were then placed in a 1 % Alcian blue solution (Alcian blue, Sigma) dissolved in 3 % acetic acid (pH 2.5) for 10 min. When Alcian blue was used without combining it with periodic acid Schiff's reagent (Sigma, UK), slides were placed in Alcian blue for a further 30 min. Once slides were stained with Alcian Blue, they were washed in tap water and then incubated in distilled water for 30 min. Slides were then transferred into 1 % aqueous periodic acid for 5 min and rinsed well in distilled water. Slides were transferred in to Schiff's reagent for 15 min and wash in running tap water 5 min before counter stain with Mayer's haematoxylin for 2 min. After washing under running tap water for 2 min, two quick dips in 1 % acid alcohol was performed and then rinsed in alcohol for dehydration and clearing through xylene before cover slipping with Pertex (Cellpath, UK).

5.2.6 **Immunohistochemistry**

The majority of IHC procedures were performed in the Aquatic Vaccine Unit, IoA, University of Stirling. On occasions when the procedure could not be optimised, slides were sent to the Veterinary Diagnostics Services, University of Glasgow (*e.g.* staining of CD3 on gill tissues).

For all IHC assays, 5μm tissues sections on PolyFrost Lysine coated adhesive frosted slides (Solmedia, UK) were used to ensure that the tissue was firmly attached to the

slide, to avoid detachment during heat induced antigen retrieval methods. Slides were de-waxed using two rinses of 100 % xylene for 5 min each, and rehydrated through an ethanol series (100 %, 95 %, 70 % and 50 % ethanol) and finally placed in distilled water. Tissue sections were subjected either to enzymatic antigen retrieval or heat induced antigen retrieval as indicated.

For enzymatic antigen retrieval, Uni-Trieve (Innovax, 1099 Essex Ave, Richmond, CA; a mild temperature induced universal retrieval solution) was used at 65 to 70 ^{o} C for 30 min using a simple water bath. The slides were placed in the solution and incubated in a water bath. In addition to the above, a low pH (pH 6) antigen retrieval buffer (0.001 M sodium citrate solution) was also used (Koppang *et al.,* 2010). Deparafinised tissue sections (on poly A lysine coated slides, Solmedia, UK) were placed in a Pyrex beaker containing 300 ml of sodium citrate solution. The beaker was then covered with perforated cling film and microwaved at 850 W for 15 min or covered with foil and autoclaved at 121° C for 15-20 min (Astell, swiftlock compact 23, Astell Scientific Ltd). The sections were allowed to cool to room temperature before starting the procedure.

Following antigen retrieval, gill sections were pre-treated with 3% (v/v) hydrogen peroxide in distilled water, methanol, TBS or PBS for 10-20 min to quench endogenous peroxidase activity. When commercial kits were used blocking reagents within the kit were used (*e.g.* Endogenous Enzyme block from Dako, EnVisionTM + Dual link System-HRP). The sections were washed three times in TBS (50mM Tris, 150mM NaCl, pH 7.6) prior to blocking for 30 min with 10 % (v/v) goat serum in TBS. This blocked nonspecific binding reducing backgrounds levels. The sections were then incubated with the concentrations of primary antibodies shown in Table 5.2 in TBS for

2 h at room temperature (9-12 °C) or overnight at 4° C. The next day slides were washed 3 times in TBS and incubated with 1/200 anti-mouse biotin conjugated (Sigma, UK) or anti rabbit biotin conjugated (Sigma, UK) in TBS for 30 min at room temperature for amplified reactions (which enhanced the affinity and opportunity for detection technology as shown in Table 5.2). The sections were washed as previously described using PBS for the last wash, then 1/200 Streptavidin-Horseradish Peroxidase (Vector Labs, Peterborough, England) in PBS was added for 30 min. After 3 washes in PBS, sections were incubated with VIP substrate kit (Vector Labs, cat no 5400), or Nova red (Vector labs, cat no 4600) according to the manufacturers' instructions or DAB respectively. The sections were counterstained with different counter stains including haematoxylin for 1 to 2 min with VIP kit and DAB, and methyl green (Vector Labs) for 5 min at 60°C with Nova Red, and rinsed in running tap water or distilled water, then dehydrated in an ethanol series and permanently mounted with VectaMount (Vector Labs), or Citifluor (Agar Scientific Ltd, Essex, England).

During optimising of the IHC protocols, several commercial substrate kits and detection systems were tested both on gill and gut tissues. In general, sections were first tested using unamplified methods. In some instances the sensitivity of the assay had to be improved by using amplified reactions. The controls of each experimental assay included a negative control without primary antibody (commercial or purified from cell culture supernatant), and when the supernatant was used as primary antibody the negative controls were replaced by serum from the same animal that the primary antibody was raised in. The different targets and detection kits and appropriate substrate kits used are summarised in Table 5.2.

5.2.7 **Laser scanning confocal microscopy (LSCM)**

The fluorogenic detection of target antigens using unamplified and amplified reactions was performed by confocal laser scanning microscopy (Leica TCS SP2 AOBS laser scanning confocal microscope coupled to an inverted Leica DMIRE2 microscope equipped with a HC PL APO 20× objective to confirm tissue localisation of *A. salmonicida* antigens in infected tissues. During the IHC and confocal microscopy procedures, the same primary antibodies were used, but the secondary antibodies were replaced with fluorescent conjugated antibodies (either FITC or Texas red) anti mouse or anti rabbit antibodies, respectively. In addition, the cytoplasm was counter stained with phallodium (a green fluorescent dye with a wave length of 620 nm) and cell nuclei were stained with 4',6-diamidino-2-phenylindole (DAPI) in the same sections to achieve better contrast.

5.2.8 **Gene expression analysis**

Total RNA was extracted from samples (head kidney, spleen and gill) using TriReagent according to the manufacturer's instructions as described in Chapter 2, 2.2.8. Total RNA extracted was was dissolved in RNAse/DNAse free water for at least 1 h at 4°C prior to quantifying the amount of RNA present using Nanodrop1000® spectrophotometer. Total RNA extracted from head kidney, spleen and gill was reverse transcribed using high capacity cDNA reverse transcription (RT) kit as described in Chapter 2.2.8.2. The primers used in this experiment are summarised in the Table 5.3 including the primer name used, primer sequence, fragment size, annealing temperature, gene bank accession number and source literature. All primers were tested for efficiency using an Eppendorf Master cycler® ep-realplex real time thermal cycler

platform following the method described in Chapter 4, Section 2.6.2 prior to use in the assays. Reverse Transcription Quantitative Polymerase Chain Reaction (RT-qPCR) was performed, following the same protocol described in Chapter 4, Section 4.2.6.3, according to MIQE guidelines published. The qPCR analysis for each sample was carried out in duplicate. Briefly, the master mix for qRT-PCR was comprised of AbsoluteTM qPCR SYBR® Green mix 10 µL, 5 µL of 1:20 diluted cDNA and 1 µL of each primer (20mM) in final volume of 20 µL. All amplification reactions were carried out with a systematic negative control non template control (NTC), containing no cDNA and no reverse transcriptase enzyme (RT minus) and serial dilution of cDNA to extrapolate reaction efficiency (E) of the assay.

Table 5.2 Immunohistochemistry targets, primary and secondary antibodies, reagents used in the IHC procedures and resulting staining obtained following IHC

Target antigen	Primary antibody	Secondary antibody	Detection methods	Result
CD3 cell receptors (marker for T cells)	anti-Human CD3 polyclonal antibody	Goat anti-mouse HRP conjugate	DAB+ Chromogen	All types of T cells stained dark brown in colour
Eosinophilic Granular Cells (EGC) as a nonspecific marker for inflammatory reactions	Anti- Caspase 3 (Promega and Millipore, UK)	Goat anti-mouse HRP conjugate	DAB+Chromogen	EGC stained dark brown in colour at low magnification. At higher magnification the EGCs stained brown with a granular appearance.
LPS of A salmonicida as a marker for detection of pathogen	Anti -*A. salmonicida* monoclonal antibody (9F7**)	Anti-mouse IgG HRP conjugate (for amplified reactions anti-mouse IgG biotin conjugate was used first followed by streptavidin-HRP conjugate)	DAB+Chromogen or RED substrate kit for peroxidase (NovaRED Peroxidase Substrate Kit,SK4800, Vector lab, Petersburg, UK)	*A. salmonicida* stained brown in colour (DAB) or red in colour (NovaRED Peroxidase Substrate Kit, Vector lab, SK 4800)
B cells Secretory IgM and transmembrane IgM	Anti-trout IgM *	Anti-mouse IgG HRP conjugate (for amplified reactions anti-mouse IgG biotin conjugate was used first followed by, streptavidin-HRP conjugate)	DAB+Chromogen	Could not be optimised
Immunoglobulin T (marker for mucosal immunoglobulin)	Anti-trout IgT*	Anti-mouse IgG HRP conjugate (for amplified reactions anti-mouse IgG biotin conjugate was used first followed by, streptavidin-HRP conjugate)	DAB+Chromogen	Could not be optimised

*Commercially available antibodies (Aquatic Diagnostics Limited, Stirling, UK), **available from the Aquatic Vaccine Unit, University of Stirling, UK

Table 5.3 The qPCR primers used to measure changes in the gills of fish following vaccination and challenge

Transcript (Target genes)	Primer name	Primer sequence	Fragment	Tm	Accession No	Source
IL 1β	As_IL1_F As_IL1_R	AGGACAAGGACCTGCTCAACT CCGACTCCAACTCCAACACTA	72	58°c	NM_001123582.1	Petterson *et al.*, 2008
IFNγ	As_IFN_F As_IFN_R	CGTGTATCGGAGTATCTTCAACCA CTCCTGAACCTTCCCCTTGAG	94	58°c	AY795563.1	Hølvold, 2007
IgM	As_IgM_F As_IgM_F	TGAGGAGAACTGTGGGCTACACT TGTTAATGACCACTGAATGTGCAT	69	58°c	GI-2182101	Tadiso *et al.*, 2011
IgT	As_IgT_F As_IgT_R	CAACACTGACTGGAACAACAAGGT CGTCAGCGGTTCTGTTTTGGA	97	58°c	HQ379938.1	Tadiso *et al,*, 2011
Reference genes						
ELF1	As_ELF1_F As_ELF1_R	CTGCCCCTCCAGGACGTTTACAA CACCGGGCATAGCCGATTCC	175	58°c	NM_001123629.1	Morais *et al.*, (2009)
Bactin	As_ βactin_F As_ βactin_R	ACTGGGACGACATGGAGAAG GGGGTGTTGAAGGTCTCAAA	157	58°c	NM_001123525.1	Herath *et al.*, (2010)
Cofilin2	As_ Cofilin2_F As_ Cofilin2_R	AGCCTATGACCAACCCACTG TGTTCACAGCTCGTTTACCG	224	58°c	BT 125570.1	Morais *et al.*, (2009)

The qPCR profiles were set to an initial enzyme activation step of 95 °C for 15 min, followed by 40 cycle comprised of 15 sec of melting at 95 °C, 15 sec gene specific primer pair annealing at the specific annealing temperature of each primer and 15 sec extension at 72 °C. The unspecific PCR products melt below the chosen temperature, *e.g.* primer dimers are eliminated, so the nonspecific fluorescence signal ensures accurate quantification of target genes as well as the reference genes. The size of the product obtained was determined using agarose gel electrophoresis.

5.2.8.1 Analysis of gene expression

GenEx Enterprise software (Version 5.4.3) software tool (www.multid.se) was used to quantify gene expression data. This software allows multiple data analysis taking into account the variance (sample to sample and between plates) within the data set. Similarly to Chapter 4 section 2.6.4, quality control and pre-processing of data was performed with in this software are summarised in Figure 5.4. Initially one of the reference genes, ELF1 (or reference gene index consisting of ELF1, beta actin and cofilin) was used as internal reference gene/genes prior to data analysis. The normalised relative gene expression of vaccinated and vaccinated challenged fish were then calibrated to unvaccinated (*i.e* unvaccinated unchallenged) fish, which allow to compare relative gene expression of each target gene across the time points.

The normalised mean gene expression values, calibrated against relevant control groups, were examined for normality and homogeneity of variance. Statistical differences between groups were performed using GenEx (www.multid.se), Minitab and SPSS software. When normality and homogeneity were achieved a parametric GLM was employed. Where these assumptions were not met, a non-parametric equivalent for ANOVA, Kruskal-Wallis tests was employed. The post-hoc tests, Tukey

HSD and Mann-Whitney U Test were employed for GLM and non-parametric ANOVA respectively.

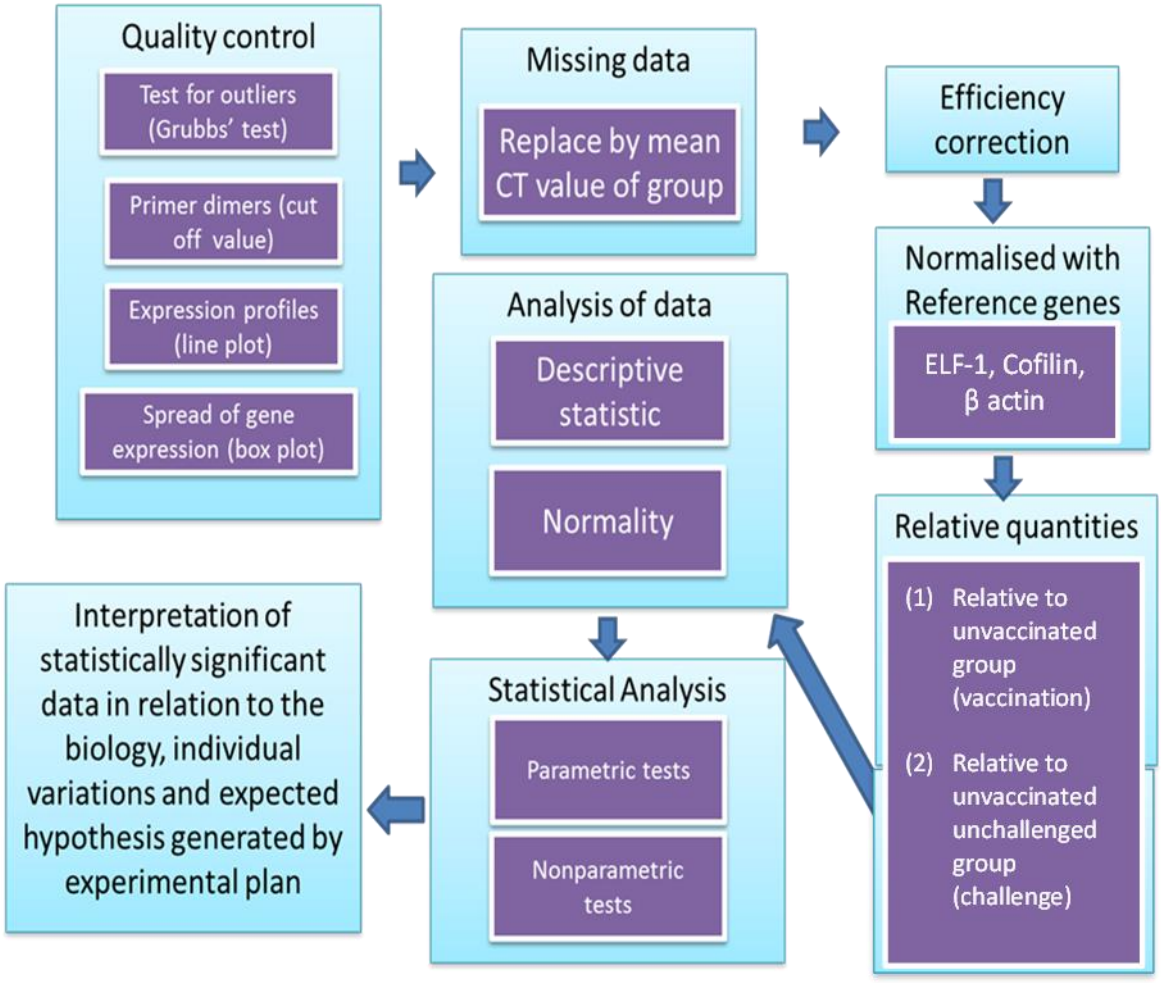

Figure 5.4 Flow chart of different steps of data processing in GenEx Enterprise software which included a step of quality assurance, replacement of missing data to fulfil the requirement of balance ANOVA (GLM). Most suitable and recommended normalisation was achieved by using the reference gene index.

5.3 **Results**

5.3.1 **Mortality curve and cause of death**

The un-vaccinated fish (*i.e.* PBS-injected), challenged with *A. salmonicida*, started to die from 2 d.p.i , with most mortalities occurring by 4 d.p,i. (> 80 % mortality; Figure 5.5) and reach 100 % mortality by 15 d.p.i. In contrast, at the end of the challenge

period (21 d.p.i.), only 20 % mortality had been observed in vaccinated challenged fish, dying between 3 and 8 d.p.i (Figure 5.5). It was confirmed that fish had died from an *A. salmonicida* infection using Gram stain and IFAT.

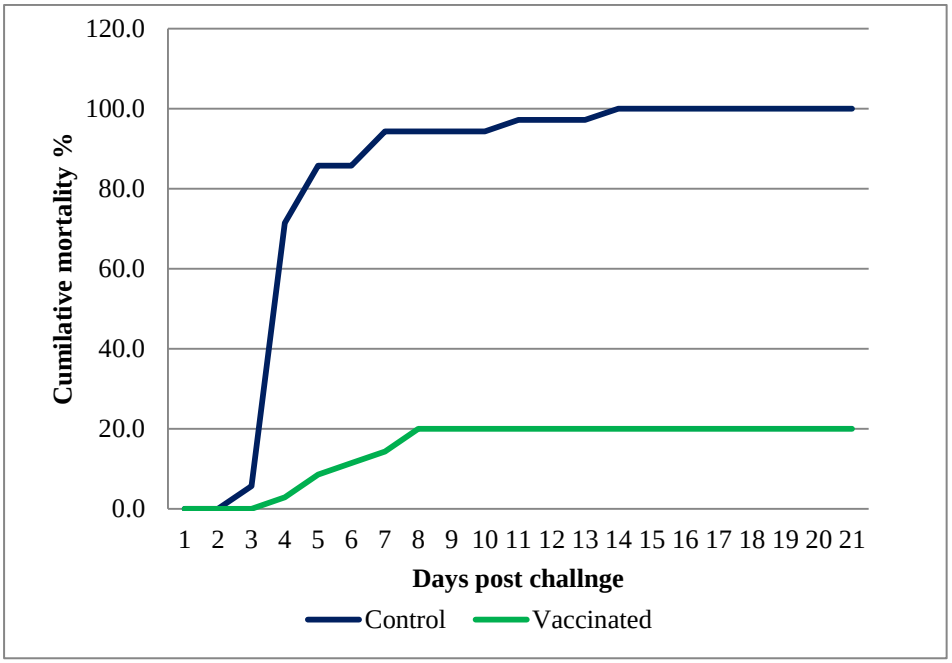

Figure 5.5 Cumulative mortality of Atlantic salmon (duplicate tanks) injected with 0.1 ml PBS ml or 0.1 ml commercial furunculosis vaccine following challenge with *Aeromonas salmonicida*. The relative percentage survival (RPS) of vaccinated fish was 80 %.

5.3.2 **Histology and immunohistochemistry**

The histological investigations of H & E stained transverse sections of the gill were carried out on a computer screen using digital images generated from WSI technology, as described in Chapter 2, Section 2.2.3. No observable histological changes were noted in the gills of uninfected fish. Bacterial colonies were noted in the central venous sinuses and distal marginal channel of the gill. A small lymphoid aggregation located in the distal end of interbrachial septum, known as intraepithelial lymphoid tissue (ILT) was observed in the tissue sections (Figure 5.6). A large number of lymphoid cells were predominant in this region and featured round nuclei and a high cytoplasm/nucleus

ratio, and this cellular structure formed a dense tissue exposed to the lumen of the brachial chamber covering the epithelium (forming an epitheliod capsule), with numerous mucous cells on the mucosal surface (Figure 5.6). No bacterial colonies nor any histological changes were noted compared to control fish in this area.

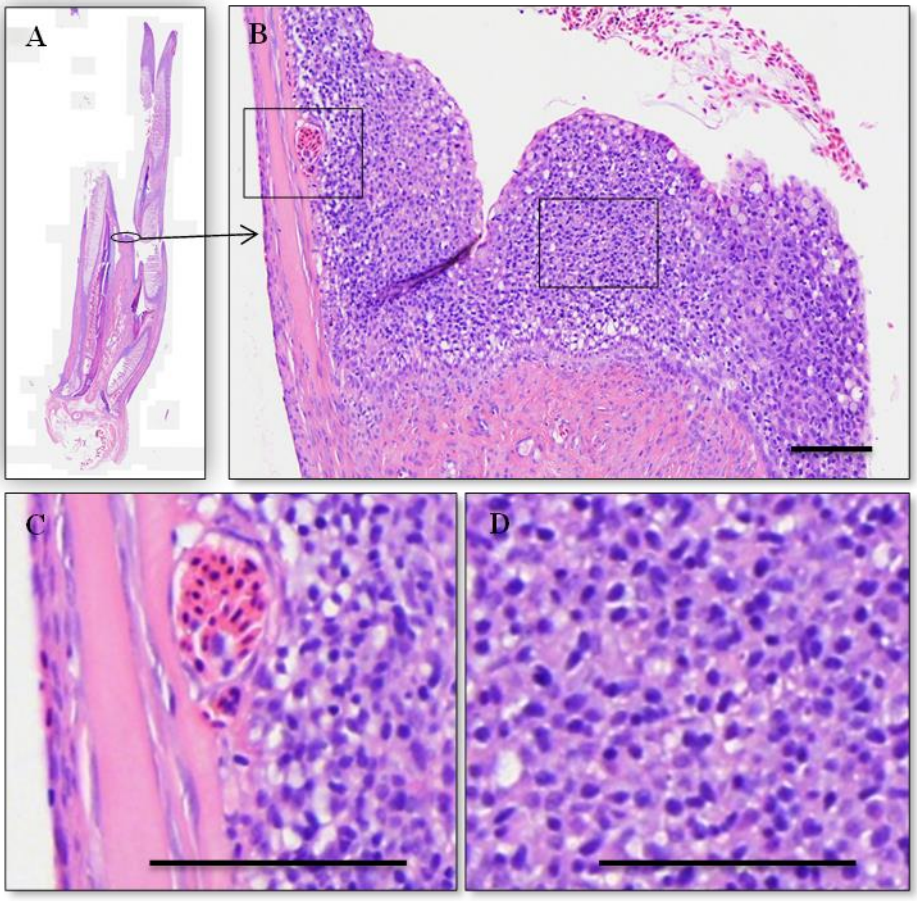

Figure 5.6 Intraepithelial Lymphoid Tissue (ILT) in the gills. (A) digitally scanned high resolution whole slide image of transversely sectioned Atlantic salmon gill. (B) enlarged image of lymphoid cell aggregation of ILT in the gills. (C) high magnification of highlighted area (left) in B representing closely associated blood vessels, (D) high magnification of highlighted area (right) in B of lymphoid aggregation mostly filled with a homogeneous set of lymphocytes.

Immunohistochemistry was performed to confirm the presence of *A. salmonicida* using mouse monoclonal antibody 9F7 directed against the LPS of *A. salmonicida*. No specific staining was observed in the unchallenged fish. Within the gills of infected fish, no histological changes were apparent, however, samples were positive for *A. salmonicida* by IHC (data not shown). Specific staining for *A. salmonicida* was

observed scattered as patches in the renal parenchyma and in some instances bacteria stained as large patches in and around areas of tissue damage (Figure 5.7 B – D). In addition, severe multifocal interstitial necrosis (hematopoietic tissue necrosis) and tubular degeneration was present in the renal tissue (Figure 5.7 D). The density of melanomacraphage centres (MMC) also appeared to be increased in the renal tissue.

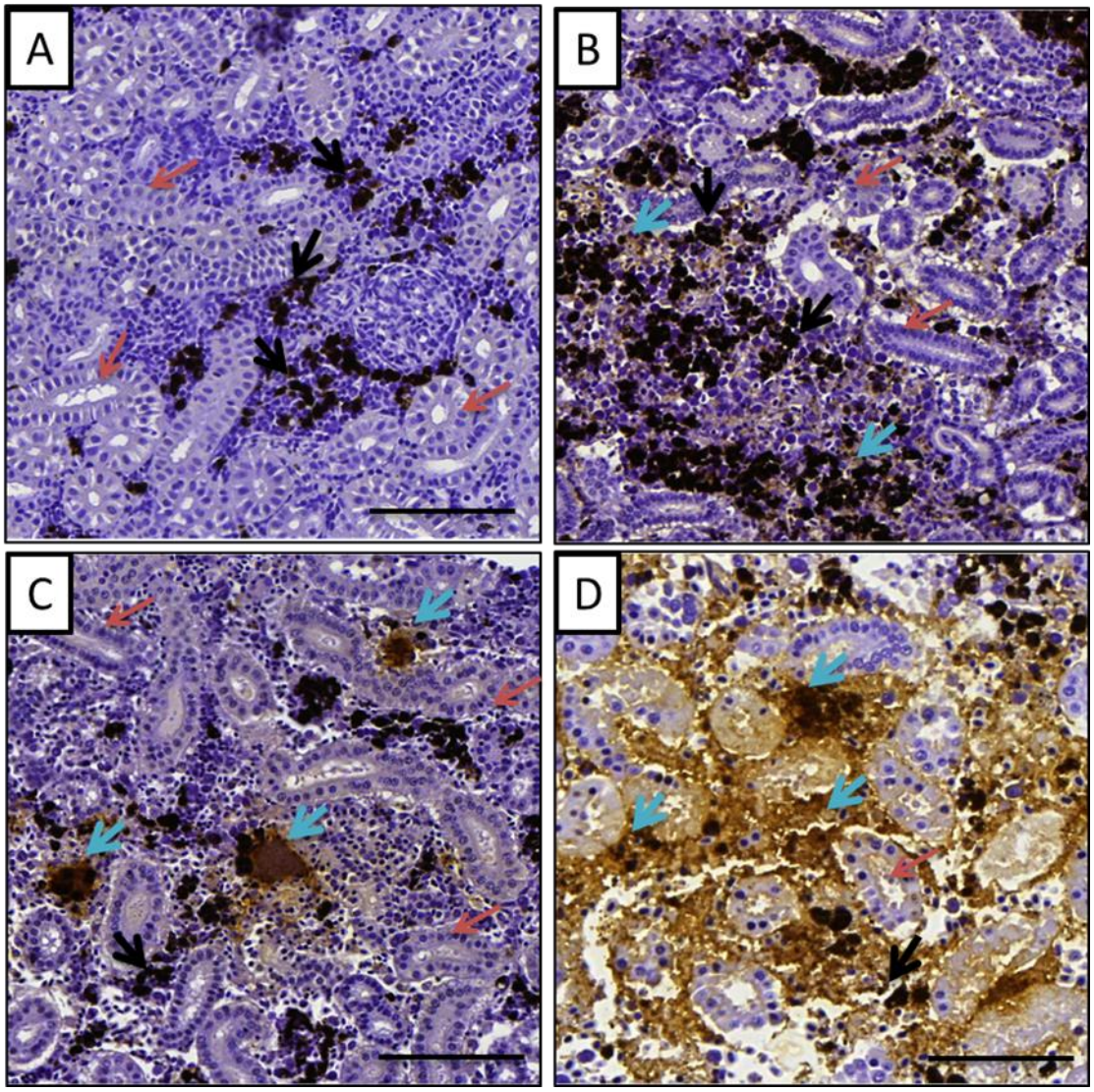

Figure 5.7 Atlantic salmon posterior kidney from (A) control (unvaccinated unchallenged) fish (7 d.p.c.) (B) unvaccinated challenged fish at 4 d.p.c. (C) lower magnification and (D) high magnification IHC positive tissue from moribund fish sacrificed at 4 d.p.c. Note bacterial colonisation in interstitial paranchyma (blue arrow), sever diffuse degeneration of kidney tubules and necrosis loss of interstitial tissues (D). Short black thick arrow heads indicate melanomacrophage centres (MMC) aggregated between renal interstitial tissues. Thin brown arrows indicate that different types of crossed sectioned tubules. Scale bar A, B, C 100µm and D 25 µm

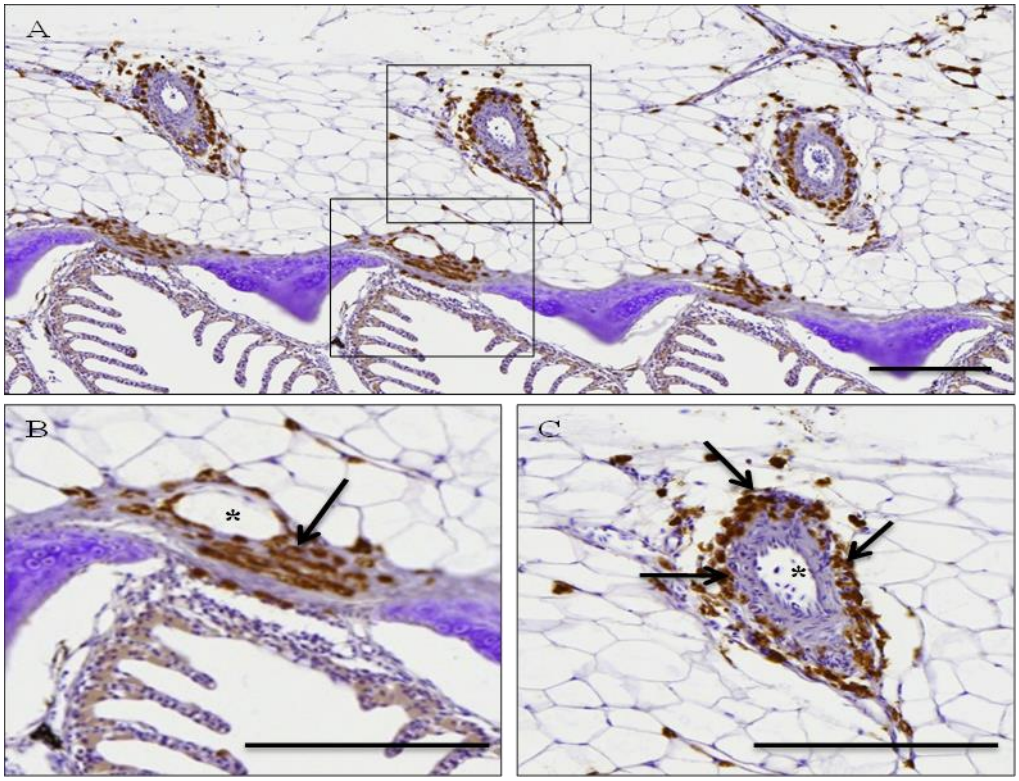

Figure 5.8 Atlantic salmon gills enriched with eosinophilic granular cells (EGC) in vaccinated challenged fish. (A) EGC stained with anti-caspase 3 polyclonal antibody using immunohistochemistry on *A. salmonicida* infected gills (4 d.p.c.). (B) EGC located around veins (please note the lumen is labelled with * and thin walls around the lumen) and (C) high magnification of presence of EGC around arteries (afferent) (please note the lumen is labelled with * and thick walls around the lumen). Scale bar 200 µm.

Gills cells positively stained with human CD3 MAb were aggregated at the distal end of the primary lamella, on the primary lamella and also on the secondary lamellae (Figure 5.9). The numbers of CD3 positive cells appeared to be higher in the vaccinated and challenged fish than in control group (observation data). Although CD3 staining was able to specifically stain cell cytoplasm of a population of cells in the gills, on some occasions, in some gills non-specific staining (Figure 5.13) was also noted, especially in the cartilage and some times in the primary and secondary lamellar epithelia. The IHC

protocols performed to identify the cells that produced the major immunoglobulins using anti-trout IgM and anti-trout IgT were unsuccessful.

5.3.3 **Laser scanning confocal microscopy (LSCM)**

Under laser scanning confocal microscopy, cytoplasmic granules of EGCs stained with anti-caspase 3 polyclonal antibody and FITC staining appeared green were scattered around the blood vessels of the gills (Figure 5.10 A and B). In challenged fish, application of anti-*A. salmonicida* LPS monoclonal antibody (9F7) and anti-mouse HRP conjugated with texas red showed bacteria as red clumps in the gills (Figure 5.10 C) and the EGCs were much more dispersed and located closely to the bacterial clumps. In the kidney large patches of bacteria were observed dispersed in the renal interstitial tissues (Figure 5.10 D). The kidney tubules were severely damaged however no bacteria were visible inside the tubules.

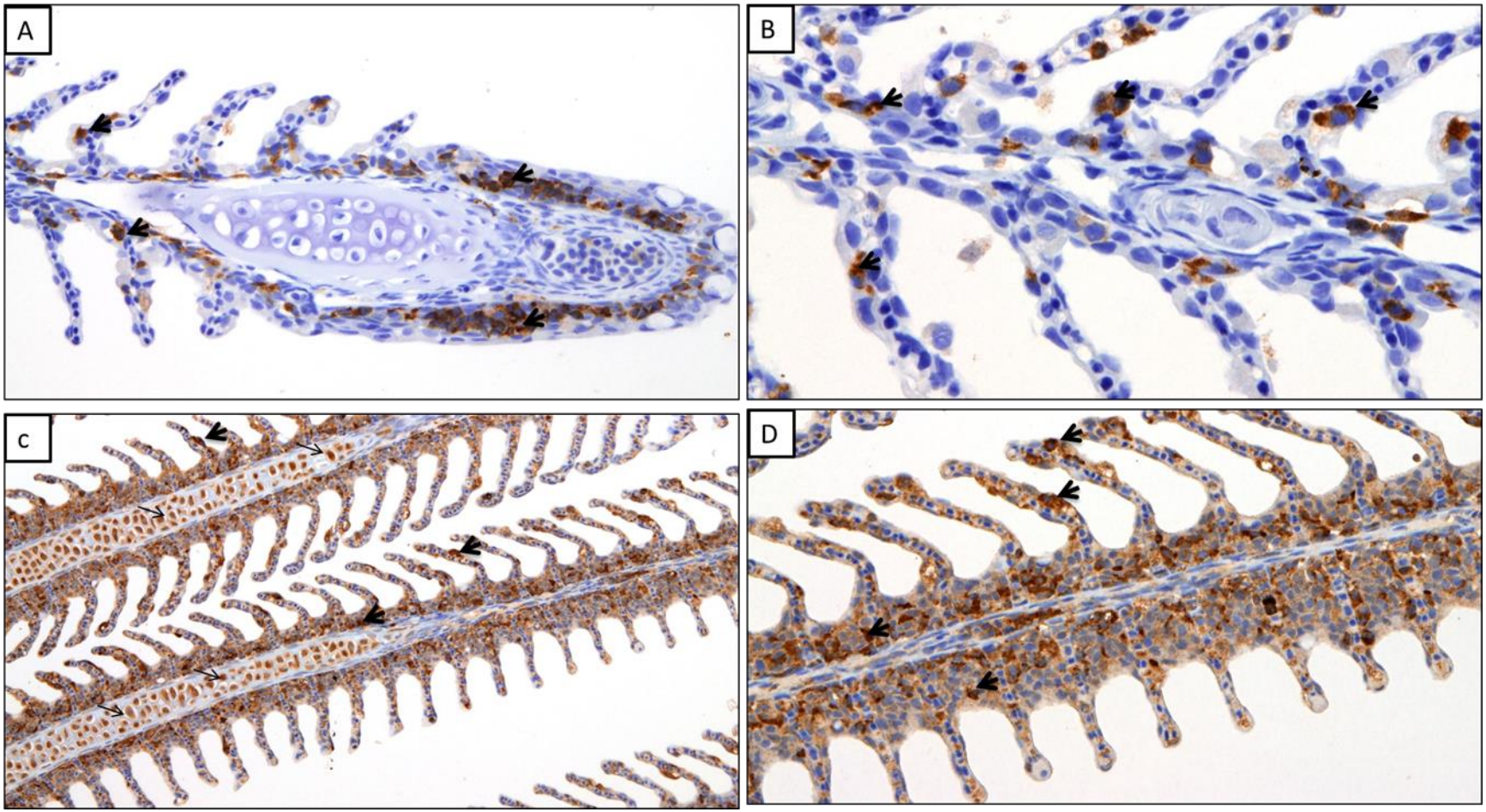

Figure 5.9 Immunohistochemstry staining of gill of Atlantic salmon vaccinated with *A. salmonicida* stained with CD3 monoclonal antibody. Cytoplasm of CD 3 positive cells (T lymphocytes) stained intensely dark (black arrow) found at (A) distal end of the primary lamellae (B) mid region of the primary lamellae, however, in some instances non-specific staining was also encountered in (C) chondrocytes of the primary lamellae and (D) epithelium of primary and secondary lamellae noted as light brown staining. 100µm.

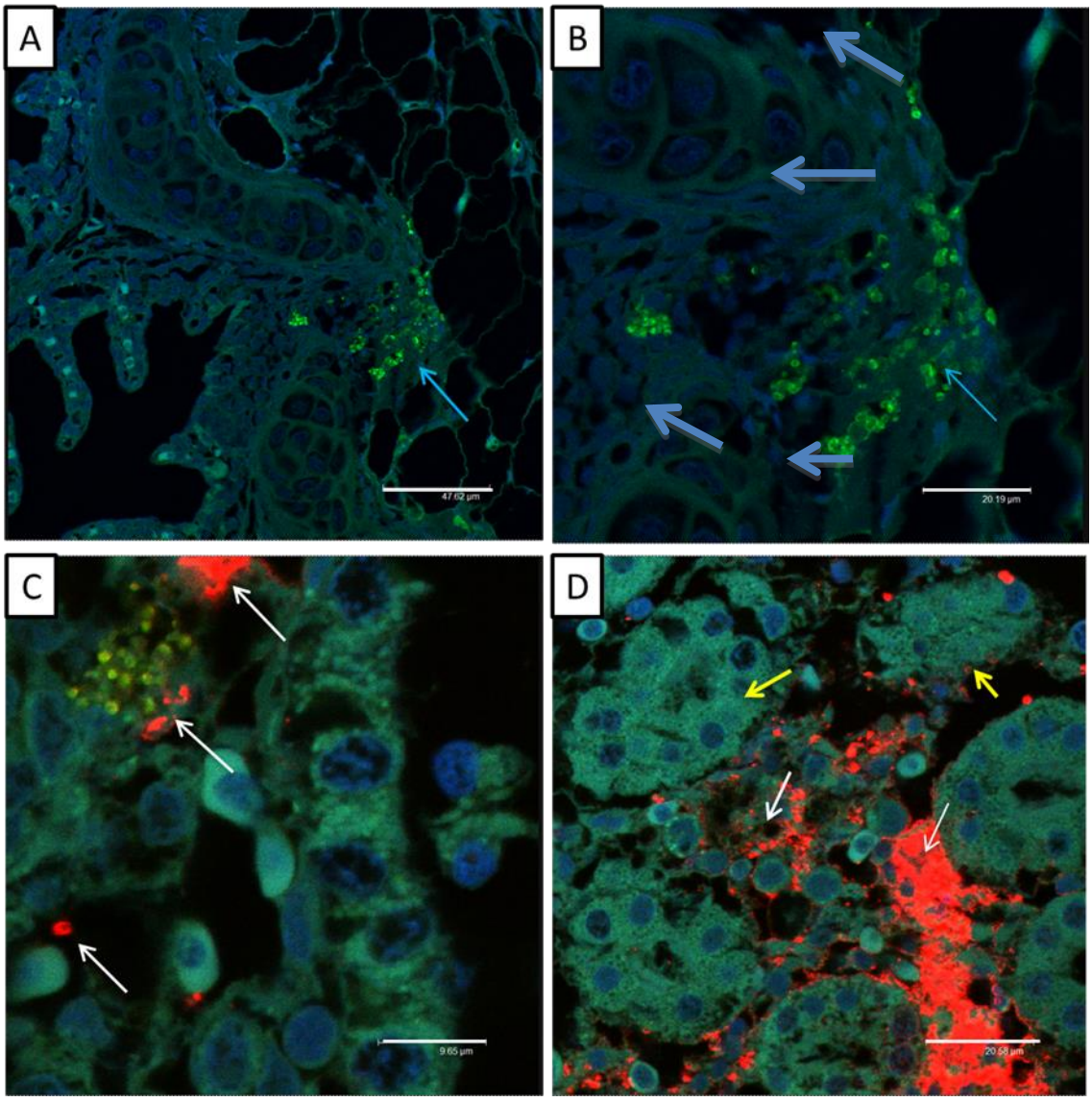

Figure 5.10 Laser scanning confocal micrographs Atlantic salmon gill (A) low magnification (B) high magnification showing eosinophilic granular cells (EGCs) which stained green (blue arrow) with anti-caspase 3 polyclonal antibody and FITC and *A. salmonicida*-infected moribund fish (C) gills and (D) posterior kidney at 7 days post infection confirming the presence of bacteria which stained red with anti-*A. salmonicida* monoclonal antibody 9F7 and Texas red (white arrow). The renal tubules (yellow arrow) are distorted. Scale bar indicates (A) 50 µm, (B) & (D) 20 µm. (D) 10 µm.

5.3.4 Gene expression analysis results

5.3.4.1 Normalised immune gene expression of head kidney, spleen and gill, during *A. salmonicida* infection post-vaccination

The Cp values obtained for each gene (IgM and IgT) in head kidney, spleen and gills, were normalised to the reference genes ELF1, cofilin and actin (reference gene index), and their expression compared between vaccinated and unvaccinated fish at each time point. The normalised mean gene expression was not significantly different over time in the unvaccinated group. The normalised mean IgM expression was significantly higher in the kidney of vaccinated fish compared with unvaccinated fish at 12 d.p.v. By 24 d.p.v., and these levels had returned to similar levels expressed to those in the unvaccinated fish (Figure 5.11 A). In contrast, the normalised mean IgM expression in the spleen of vaccinated fish was significantly increased over time from 12 to 24 d.p.v., and was significantly different to the control group at 24 d.p.v. (Figure 5.11 B). In the gills, the normalised mean gene expression for IgM in vaccinated fish compared to the PBS-injected control group was higher on both 12 and 24 d.p.v. post-vaccination; however, it was only significantly different at 12 d.p.v. (Figure 5.11 C).

The normalised mean IgT expression in the head kidney appeared to be significantly lower in vaccinated fish compared to unvaccinated fish at both sampling points, and was statistically significant between vaccinated and unvaccinated fish on 12 d.p.v and over time (Figure 3.12 A). In contrast, the normalised mean IgT expression in the spleen of vaccinated fish significantly increased over time from 12 to 24 d.p.v., and was significantly higher in the vaccinated group compared to unvaccinated group by 24 d.p.v (Figure 5.12 B). In gills at 12 d.p.v., the normalised mean expression of IgT was significantly higher in the vaccinated fish compared to control fish, and this level

decreased overtime in the vaccinated fish from 12-24 d.p.v. to levels similar to those in the unvaccinated fish (Figure 5.12 C).

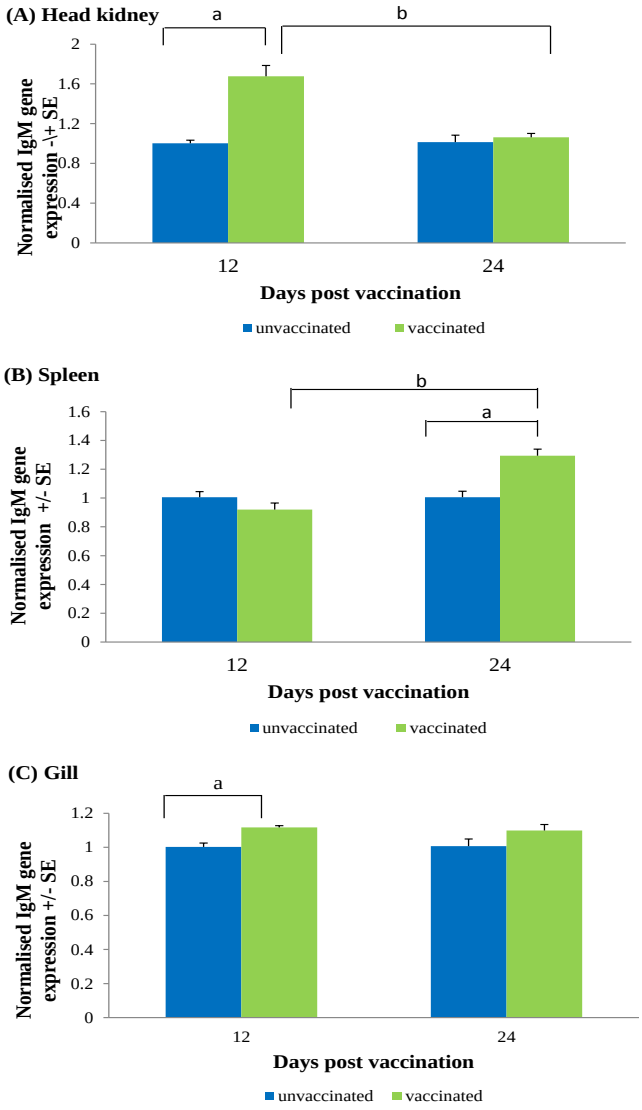

Figure 5.11 The SYBR green real time PCR results for IgM gene expression in head kidney (A), spleen (B) and gill (C) in Atlantic salmon vaccinated with *Aeromonas salmonicida*. The mean IgM expression of vaccinated fish (blue) (n=8) and unvaccinated (green) fish (n=8) sampled at Day 12 and 24 post vaccination were normalised to reference gene index (ELF1, cofilin, actin) +/- SE. The significance difference ($P \leq 0.05$) is marked between groups (a) and between time points for vaccinated fish (b) and for unvaccinated fish (c).

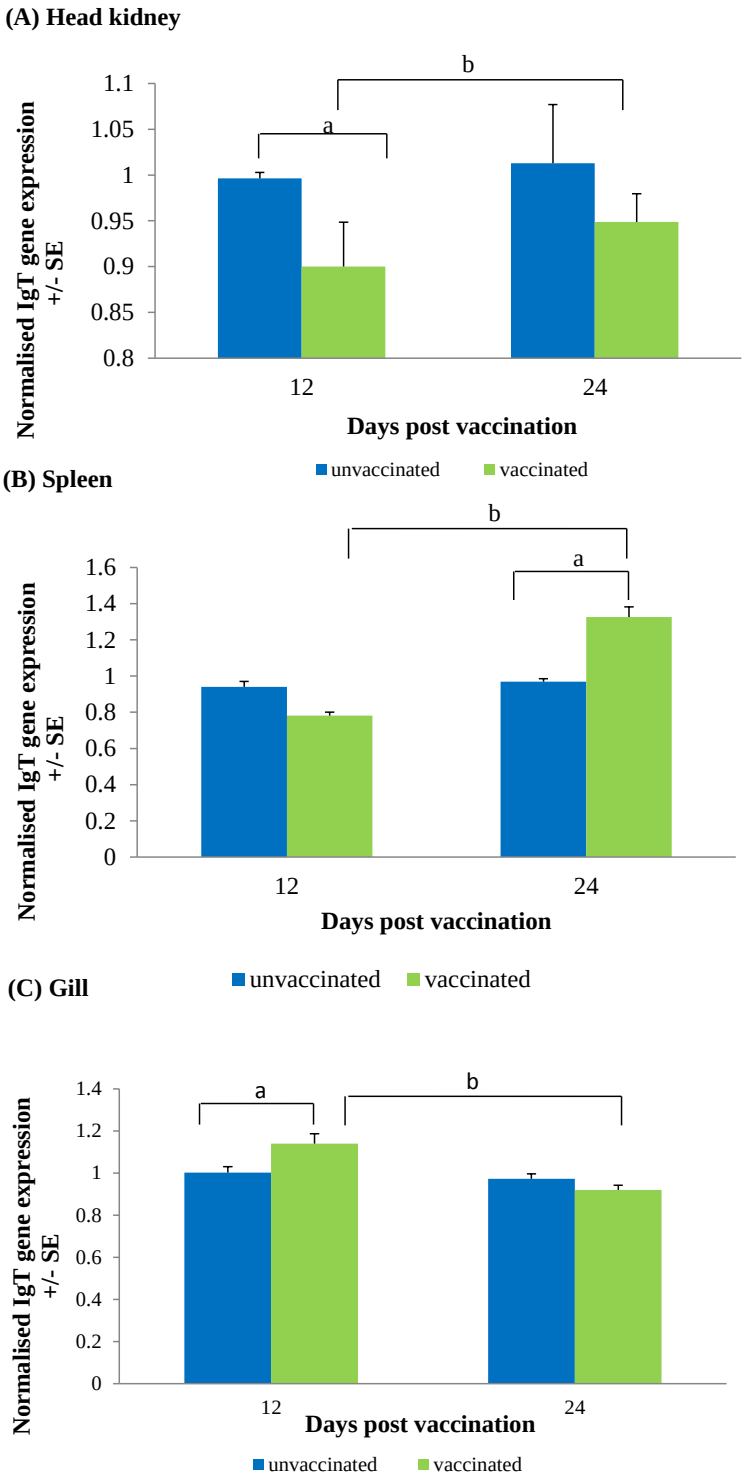

Figure 5.12 The SYBR green real time PCR results for IgT gene expression in head kidney (A), spleen (B) and gill (C) in Atlantic salmon vaccinated with *Aeromonas salmonicida*. The mean IgT expression of vaccinated fish (blue) (n=8) and unvaccinated (green) fish (n=8) sampled at Day 12 and 24 post vaccination were normalised to reference gene index (ELF1, cofilin, actin). The significance difference ($P \leq 0.05$) is marked between groups (a) and between time points for vaccinated fish (b) and for unvaccinated fish (c).

5.3.4.2 . Normalised immune gene expression of head kidney, spleen and gill of vaccinated and unvaccinated fish following challenge with *A. salmonicida*

After 59 days post-vaccination the fish from Group 3 were challenged with a virulent strain of *A. salmonicida* (Hooke). The samples were collected and gene expression analyses were performed using quantitative RT-PCR to detect IL-1β, IFNγ, IgM and IgT.

5.3.4.3 IL-1β

On 4 days post-challenge (d.p.c.), the normalised mean IL-1β expression in the vaccinated challenged group appeared significantly higher in all three tissues examined, compared to the control group (*i.e.* unvaccinated/unchallenged= unvaccinated) (Figure 5.13 A-C). In kidney, on both 7 and 21 d.p.c., the normalised IL-1β expression in both the vaccinated unchallenged (vaccinated) fish and vaccinated challenged fish were high compared to the unvaccinated group (Figure 5.13 A). Furthermore, in the kidney, the normalised IL-1β expression in the vaccinated fish was significantly increased over time from 4 to 7 d.p.c., while levels in the vaccinated/challenged group did not change (Figure 5.17 A). In the spleen, at 7 d.p.c. the Ct values for IL-1β transcripts of individual fish in the vaccinated group of fish were highly variable and this gave rise to a large standard error (Figure 5.13 A), and although this expression appeared to be lower in the vaccinated/challenged fish compared to the control group it was not statistically different possibly due to the large individual variation in expression. However, in the spleen, the normalised IL-1β expression in the vaccinated/challenged group significantly decreased over time between 4 and 7 d.p.c. and also between 4 and 21 d.p.c. (Figure 5.13 B).

Significant differences in the normalised IL-1β expression in the gills of unvaccinated fish and vaccinated/challenged fish were observed at 4 d.p.c. with the latter having

significantly higher levels of expression. Furthermore, at both 7 and 21 d.p.c., this expression appeared significantly higher in vaccinated/challenged fish compared to both vaccinated and unvaccinated fish at each time point. Moreover, IL-1β expression in the gill of vaccinated/challenged fish appeared to be higher at both 7 and 21 d.p.c compared to 4. d.p.c (Figure 5.13 C).

5.3.4.4 INF-γ

In head kidney, the expression of INF-γ was significantly lower on both 4 and 7 d.p.c. in the vaccinated/challenged group compared to both unvaccinated/unchallenged and vaccinated/unchallenged control groups (Figure 5.14 A). Although no statistical significance was noted, the INF-γ expression of kidney on Day 21 in the vaccinated/challenged group appeared higher compared to both control groups (Figure 5.14 B). In the vaccinated group, INF-γ expression increased significantly over time from 4 to 7 d.p.c. Similarly, in the head kidney of vaccinated/challenged fish, INF-γ expression increased over time and was significantly different between 4 and 21 d.p.c and between 7 and 21 d.p.c.

In the spleen, on 21 d.p.c., the normalised INF-γ expression among the three groups analysed was significant, with the expression in the vaccinated fish shown to be significantly lower than the control group, while expression was significantly higher in the vaccinated/challenged group compared to the unvaccinated group. Over time in both the vaccinated and vaccinated/ challenged groups, INF-γ expression was significantly different between 4 and 7 d.p.c and also between 4 and 21 d.p.c (Figure 5.14 B).

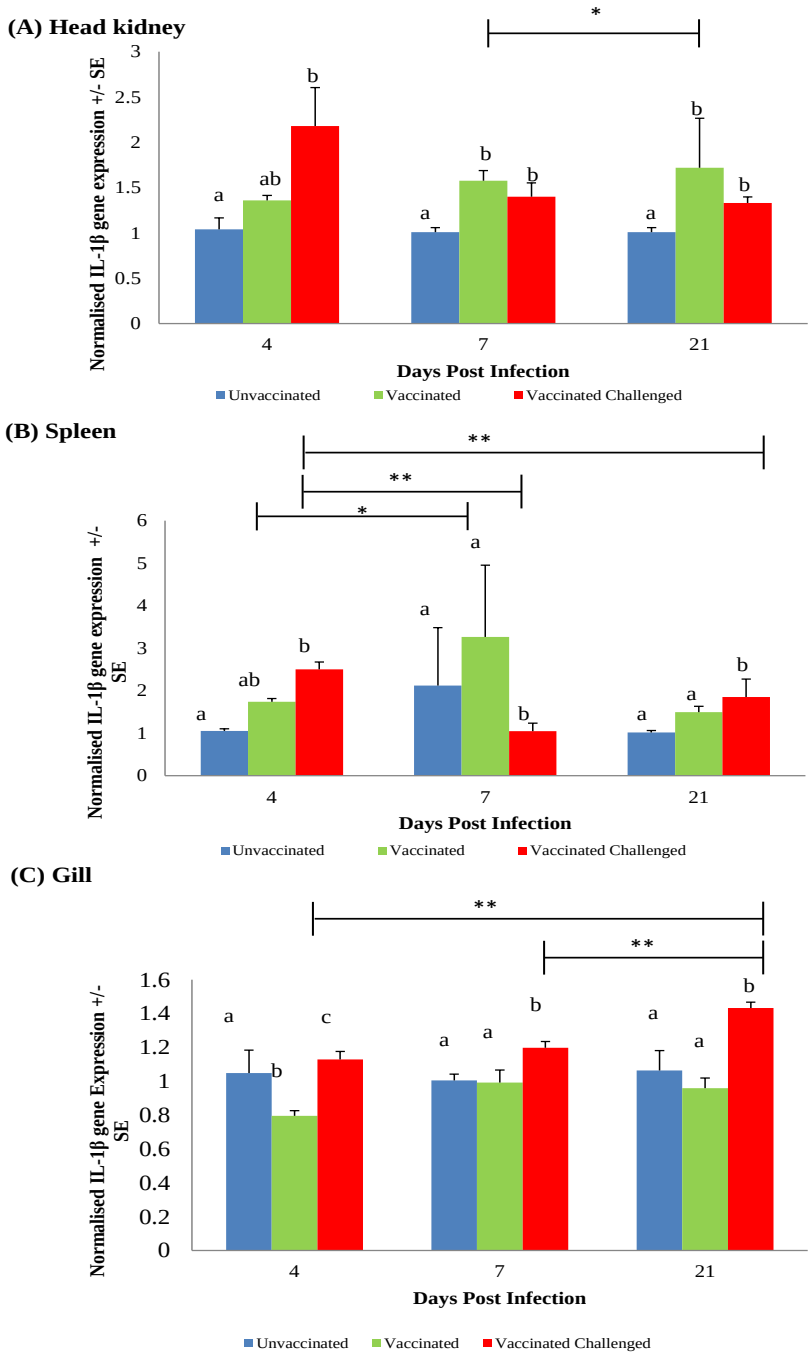

Figure 5.13 The SYBR green real time PCR results for IL-1β gene expression in head kidney (A), spleen (B) and gill (C) during vaccination and following challenge with *A. salmonicida*. The mean IL-1β expression of un-vaccinated/unchallenged fish (blue) (n=8), vaccinated/unchallenged (green) and vaccinated/challenged (red) fish (n=8) sampled at Day 4, 7 and 21 post challenged were normalised to reference gene index (ELF1, Cofilin, Actin). A different letter within individual time points indicates a significant difference between groups. at that time point. Significance differences between vaccinated unchallenged and vaccinated challenged fish at different time points is indicated with an * or ** respectively.

On Day 7, similar to IL-1β expression, INF-γ expression also showed a large individual variation especially in the vaccinated group (Figure 5.13 and Figure 5.14).

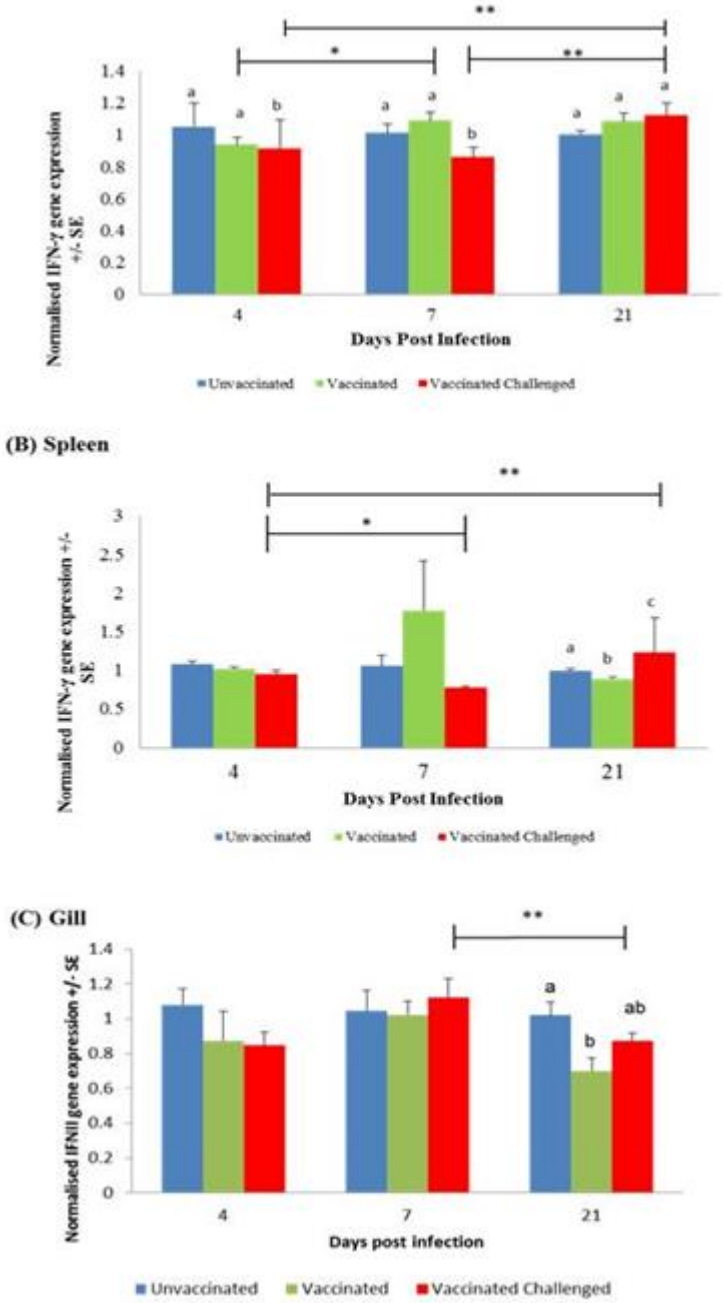

Figure 5.14 The SYBR green real time PCR results for IFN-γ gene expression in head kidney (A), spleen (B) and gill (C) during vaccination and following challenge with *A. salmonicida*. The mean IFN-γ expression of unvaccinated fish (blue) (n=8), vaccinated (green) and vaccinated/challenged (red) fish (n=8) sampled at Day 4, 7 and 21 post challenged were normalised to reference gene index (ELF1, Cofilin, Actin). A different letter within individual time points indicates a significant difference between groups at that time point. Significance differences between vaccinated unchallenged and vaccinated challenged fish at different time points is indicated with an * or ** respectively

5.3.4.5 IgM

In the head kidney, on Day 4 and Day 21, normalised IgM expression in both vaccinated and vaccinated/challenged fish were significantly higher compared to the unvaccinated control group (Figure 5.15 A). The IgM expression appeared to decrease significantly in both groups from 4 to 7 d.p.c and then increased significantly over time from 7 to 21 d.p.c (Figure 5.15 A). The relative IgM expression was significantly higher in both groups of fish at 21 d,p.c. than 4 d.p.c. (Figure 5.15 A).

In the spleen on 4 d.p.c., the normalised IgM expression in the vaccinated/challenged was lower than measured in the control groups (unvaccinated and vaccinated) and it appeared to be significantly different from the unvaccinated group (Figure 5.15 B). In contrast, on 21 d.p.c, IgM expression in both vaccinated and vaccinated/challenged group was found to be significantly higher than the unvaccinated/unchallenged group (Figure 5.15 B). The IgM expression, in both vaccinated and vaccinated challenged groups was steadily increased over time with IgM expression appearing to be significantly different between all three time points, except in the vaccinated group between 4 and 7 d.p.c. In gills, IgM expression was significantly higher in the vaccinated challenged group compared to the unvaccinated group at all three time points measured, and also between vaccinated and unvaccinated groups on 21 d.p.c. As with the spleen, IgM expression appeared to be steadily increased over time in both vaccinated and vaccinated/challenged groups, although no statistically significant differences were observed during the time course.

5.3.4.6 IgT

Among all three tissues and all three groups examined, IgT expression was found to be only significantly different between unvaccinated and vaccinated challenged groups in

the gill on 4 d.p.c (Figure 5.16. C). However, in the kidney of vaccinated fish, IgT expression appeared

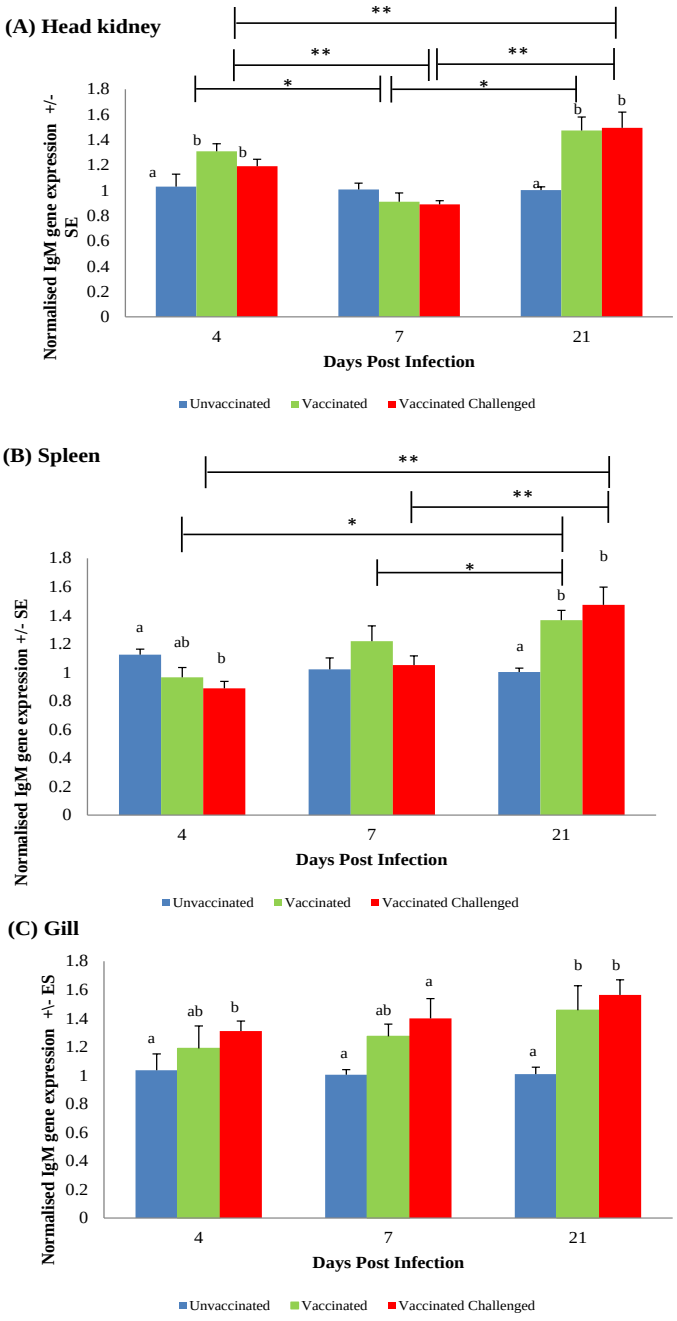

Figure 5.15 The SYBR green real time PCR results for IgM gene expression in head kidney (A), spleen (B) and gill (C) during vaccination and following challenge with *A. salmonicida*. The mean IgM expression of un-vaccinated/unchallenged fish (blue) (n=8), vaccinated/unchallenged (green) and vaccinated/challenged (red) fish (n=8) sampled at Day 4, 7 and 21 post challenged were normalised to reference gene index (ELF1, Cofilin, Actin). A different letter within individual time points indicates a significant difference between groups at that time point. Significance differences between vaccinated unchallenged and vaccinated challenged fish at different time points is indicated with an * or ** respectively.

significantly increased between 4 and 21 d.p.c and also between 7 and 21 d.p.c. Furthermore, in all three tissues of vaccinated challenged fish that were analysed, IgT expression showed an increasing trend between 4 and 7 d.p.c and became significantly higher in the gill on 7 d.p.c. compared to 4 d.p.c, while IgT expression in the gill of vaccinated challenged fish was significantly different between 4 d.p.c and 21 d.p.c. No statistical differences were seen in the spleen between either groups examined or between time points for normalised expression of IgT.

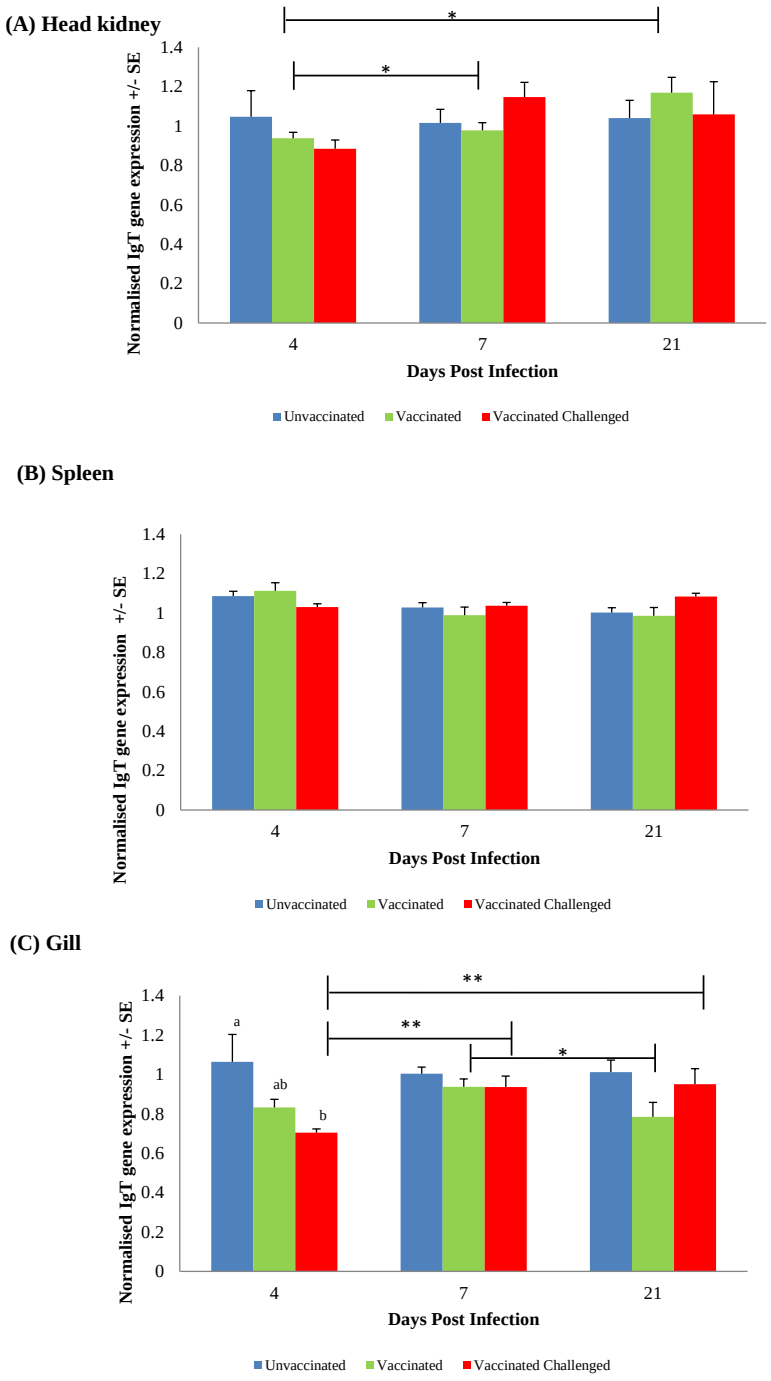

Figure 5.16 The SYBR green real time PCR results for IgT gene expression in head kidney (A), spleen (B) and gill (C) during vaccination and following challenge with *A. salmonicida*. The mean IgT expression of un-vaccinated/unchallenged fish (blue) (n=8), vaccinated/unchallenged (green) and vaccinated/challenged (red) fish (n=8) sampled at Day 4, 7 and 21 post challenged were normalised to reference gene index (ELF1, Cofilin, Actin). A different letter within individual time points indicates a significant difference between groups. at that time point. Significance differences between vaccinated unchallenged and vaccinated challenged fish at different time points is indicated with an * or ** respectively

5.4 **Discussion**

The aim of this study was to compare the immune response elicited in the head kidney and spleen of Atlantic salmon after vaccination with a commercial *A. salmonicida* vaccine compared to that measured in the gills of the fish, and also to investigate how the immune response of these fish reacts to infection with *A. salmonicida* subsp. *salmonicida*, especially the mucosal immune response of the gills despite administration of the pathogen by injection. Although pathogen challenge via i.p. injection does not represent a natural route of infection, this is the standard method of vaccine efficacy testing/batch potency testing for *A. salmonicida* at present (Villumsen and Raida, 2013).

The experimental design consisted of an initial group of Atlantic salmon parr vaccinated with a commercial oil adjuvanted, monovalent *A. salmonicida* vaccine administered by i.p. injection, formulated with two formalin inactivated *A. salmonicida* isolates MT004 and MT423 (http://www.msd-animal health.co.uk). Fish were challenged 59 d.p.v vaccination with a virulent strain of *A. salmonicida* (Hooke). Immunohistochemistry, laser scanning confocal microscopy (LSCM) and quantitative RT-PCR were used to evaluate the pathophysiological changes in Atlantic salmon immune organs (head kidney, spleen and gills) occurring at both the cellular and tissue levels in response to the vaccination and also in response to experimental infection, administered by i.p. injection.

The natural portal of entry for *A. salmonicida* in fish appears to be through abraded skin, gills and the intestine (Farto *et al.*, 2011), although any trauma to the epithelial barrier is likely to facilitate bacterial attachment and penetration into the host tissues and so as to gain access to nutrients through cytolysis at these sites, ensuring

establishment of a systemic infection. Of the various challenge routes available for experimental infection with *A. salmonicida,* (*i.e.* bath, co-habitation and oral intubation, i.p. injection was chosen as the route of infection in the present study over other routes of infection. This route of infection allows an equal dose of pathogen to be administered to each fish, which is the normal way of assessing the immune response of fish to the vaccine (Harun *et al.,* 2011). There is currently no commercial bath vaccine available for *A. salmonicida,* a route which may be important for inducing a mucosal immune response in the gill of vaccinated fish. Furthermore, to observe the level of protection induced by the vaccine, infection with *A. salmonicida* was performed by injecting a relatively high level of bacteria ($1x10^8$ c.f.u./ml/fish) i.p. (which was determined by pre-challenge experiment), and this produced a level of mortalities of > 80 % in unvaccinated fish, causing an acute infection with fish starting to die between 3-5 d.p.c,, while the RPS value was 80 %.

The *A. salmonicida* isolate used in vaccine efficacy testing (Vivas *et al.,* 2004) was the Hooke isolate, which was first isolated from a trout farm in England, and is considered to be highly virulent and was used as the challenge isolate in the current study. The results of the challenge following vaccination were in accordance with that recommended in the technical specifications provided by the manufacture, where the RPS in vaccinated fish was greater than 60% (RPS60) and mortality in control fish higher than 80%. The vaccination period prior to challenge was 885 degree days (59 d.p.v.) to ensure optimal immune induction by the vaccine. The minimum recommended period for this by the vaccine producer was 400 degree days. At the time of vaccination, the weight of the fish was greater than the minimum size recommended for vaccinated (*i.e.* 25 g) and water temperature was maintained at15±1ºC to facilitate faster and optimum immune induction.

Colonisation and persistence of bacteria in host tissues may be related to the interactions between different host factors and bacterial virulence factors (Casadevall and Pirofski, 1999; Casadevall and Pirofski, 2003). During acute stages of *A. salmonicida* infection, bacterial colonises can be found in abundance in the spleen, liver, heart and head kidney (Burr *et al.,* 2005), and during chronic stages of infection bacteria are mostly found in skeletal and cardiac muscle (Farto *et al.,* 2011). The type III secretion system (T3SS) appears to have a direct involvement in the pathogenesis of *A. salmonicida*, and can suppress the host's immune response during the initial stage of infection (Vanden Bergh and Frey, 2013). The inactivation of the T3SS by marker-replacement mutagenesis of the ascV gene, (encoding an inner-membrane component of the type III secretion system) has been shown to attenuate the virulence of *A. salmonicida* by being more readily phagocytised by rainbow trout peripheral blood leukocytes, while wild-type *A. salmonicida* appears more resistant to phagocytosis (Burr *et al.,* 2005). Virulent T3SS+ strain 01-B526 was found to depress B and T lymphocyte proliferation in head kidney during the first 3 d.p.c. (Dautremepuits *et al.,* 2006). Thus, the immunosuppressive action of T3SS helps bacteria to disseminate through the body hiding from fish's immune system. In the present study, bacteria were observed in the kidney of infected fish as early as 4 d.p.c. using IHC. The challenge was undertaken by i.p. injection, which by passes the natural defence barriers offered by the skin, gill and gut, and facilitates the rapid entry of the pathogen into the kidney. Even though it is known that injury to the mucous membrane assists in the development of an *A. salmonicida* infection, there is little information available on the colonisation of *A. salmonicida* on mucosal surfaces other than the gut (Mulder *et al.,* 2007). However, in the present study, under bright field and confocal laser scanning microscope, specific *A. salmonicida* immunostaining was observed in the central venous sinuses and distal

marginal channel of the gill as early as 4 d.p.c. These observations were similar to the histopathology changes in the central venous sinuses observed during natural infections (Ferguson, 2006; Bruno *et al.,* 2013). This is indicative of gills have been exposed to bacteria either through the blood stream as a result of systemic infection or from re-entering into the gills from the surrounding water.

The presence of gill specific lymphoid tissue, possibly involved in eliciting both a local and a systemic immune response (Haugarvoll *et al.*, 2008; Koppang *et al.*, 2010) were clearly noted in the present study, however no histological or IHC staining differences were noted between vaccinated, unvaccinated or vaccinated challenged fish in the tissue architecture of these lymphoid cells. Attempts to stain IgM and IgT secreting cells with IHC were unsuccessful; therefore interpretation of the immune aggregates in relation to *A. salmonicida* infection cannot be fully elucidated. The presence of *A. salmonicida* was seen in the peripheral vasculature in the gill under confocal microscopy. The formation of perivascular cuffing by EGCs, evidenced by anti-casapse 3 IHC staining, appeared interesting and a recent review article on mast cells (EGC) by Sfacteria *et al.,*.(2014) suggested the wider functionality linking different immune compartments in lower vertebrates like fish. The absence of any pathology in the gill, confinement of bacteria in the vasculature, but not in the gill epithelium, together with the arrangement of EGCs suggests a possible role for EGC in preventing pathogen entry into the tissue from the vasculature in the gill, Furthermore, strong CD3 signals in the gill of challenged fish suggest, an immune primed status of these cells in the gill.

Differential regulation of gene expression is one of the most important biological processes that determine the functional protein signatures of cells (Vogel and Marcotte, 2012). Real-time quantitative RT-PCR represents one of the most powerful

molecular technologies for the detection of trace amounts of mRNA, and this is widely used to study differential expression of immune genes (Heid *et al.,* 1996; Lockey, 1998). The quality of the mRNA and suitability of reference genes affects results obtained (Dheda *et al.,* 2004). Vandesompele *et al.* (2002) outlined a robust and innovative strategy to identify the most stably expressed (*i.e.* least regulated) reference gene(s) in a given set of tissues (*e.g.* gill, head kidney and spleen) from the same species (*e.g.* Atlantic salmon), and also to determine the minimum number of genes required to calculate a reliable normalization factor. They highlighted that for normalization of data in comparison to the use of multiple genes (reference gene index consists of three reference genes), the conventional way of using a single gene could lead to relatively large errors in a significant proportion of samples tested in various human tissues. Furthermore, the geometric mean of multiple reference genes were tested and validated as an accurate normalization factor for a particular tissue (gills) specified within a particular experiment prior to data analysis. The normalisation of target genes with reference genes is essential for relative quantification of RT-qPCR data (Pfaffl *et al.,* 2002; Radonić *et al.,* 2005). With the introduction of this new analysis protocol for fish research, initially reference genes were ranked in order to find out which gene(s) were least regulated at particular time points (*e.g.* 4 d.p.c.) as well as over the time points (*e.g.* 4, 7 and 21 d.p.c.) using the existing software geNorm (Vandesompele *et al.,* 2002), Normfinder (Andersen *et al.,* 2004) (MOMA, Department of Molecular Medicine, Aarhus University Hospital, Denmark) and RefFinder (a user-friendly web-based comprehensive tool developed for evaluating and screening reference genes from extensive experimental datasets). It integrates the currently available major computational programs geNorm, Normfinder, BestKeeper, and the comparative ΔΔCt method, to compare and rank the tested candidate reference genes

(http://www.leonxie.com/referencegene.php). After considering all these factors, GenEx software (Version 5.4.3) (http://www.multid.se), a modern comprehensive qPCR data analysis programme (http://genex.gene-quantification.info/), which is designed to minimise the variations within and between assays, was employed to assess RT-qPCR data. This software tool, which includes both Genorm and Normfinder, allows the comparison of multiple reference genes and selection of the best fit of the data set to ensure accurate quantification of mRNA expression at different time points for a particular tissue. For the data analysis in GenEx, three reference genes, Beta actin, Cofilin and ELF1a (referred to as a reference gene index) was used to normalise the gene expression data of the selected target genes (*i.e.* IgM, IgT, IL-1β, and IFNγ) in the present study. The recent publication on inflammatory and immune gene expression in Atlantic salmon gills infected with AGD, used two reference genes for normalisation that was the geometric mean of the two reference genes EF1-a and b-actin (Pennacchi *et al.*, 2014)

To date, three major immunoglobulin (Ig) isotypes have been characterised in teleost fish *i.e.* IgM, IgD, and IgT/IgZ. Here IgM and IgT were evaluated in Atlantic salmon vaccinated with a commercial *A. salmonicida* vaccine and also in fish subsequently challenged with the bacterium in order to examine the transcriptional response (mRNA) of antibody mediated immunity to vaccination and infection. The total IgM transcripts in immune organs and the gills were measured. To measure IgM transcript levels, including membrane and secreted forms of IgM, a gene specific primer designed to amplify both mIgM and sIgM of immunoglobulin H chain (Tadiso, 2012) was used here in SYBR green RT-qPCR assays.

Head kidney and spleen of rainbow trout contains multiple, developmentally diverse and tissue-specific B cell populations including antigen presenting cells (Zwollo *et al.,* 2008). The anterior kidney is morphologically and functionally similar to mammalian bone marrow, acting as a major haematopoietic organ and also as a major site of antibody production. In fish in a resting stage (*i.e.* not undergoing an infection), the highest expression of the different Igs were found in head kidney followed by spleen (Stenvik and Jorgensen, 2000; Stenvik *et al.*, 2001; Hirono *et al.*, 2003; Hansen *et al.,* 2005; Saha *et al.,* 2005; Tian *et al.,* 2009). The thymus has lower levels of Ig transcripts than head kidney and spleen. The head kidney immune cells are mainly comprised of developing B and Ig-secreting B cells, with a few resting, mature B cells. In contrast, the spleen and peripheral blood contains mostly resting B cells and they lack secreted Ig. Upon LPS stimulation, (mimicking a Gram negative bacterial infection) the great majority of splenic B cells become strongly activated and start producing serum IgM (Zwollo *et al.,* 2008). In the present experiment, the significantly high level of IgM transcripts detected in the kidney of i.p. vaccinated compared to unvaccinated fish (naïve fish) at 12 and 24 d.p.v., indicates that these early transcripts may result in IgM antibodies in the head kidney. In contrast, in the spleen, IgM transcripts of vaccinated fish were significantly increased over time from 12 to 24 d.p.v becoming significantly higher in the vaccinated group compared to the control group, further explaining the spleen's inherent trend of activation of IgM production upon pathogen or mitogen stimuli (Zwollo *et al.,,* 2008). Furthermore, increased IgM expression in the spleen over time may be partly due to the mobilisation of B cells clones from the head kidney after stimulation with a bacterial antigen *e.g. Aeromonas salmonicida* LPS (Zwollo *et al.,* 2008). Continuous production of IgM transcripts in the spleen further explains the role that spleen plays as a secondary lymphoid organ. This

observation may also help to verify the ability of B cells encountered in spleen or kidney to differentiate into antibody secreting cells (ASC) in event of contact with a specific target (Ye *et al.,* 2011) such as *A. salmonicida* in the present experiment, where the commercial vaccine (AquaVac™ FNM Plus) resulted in a significant increase in serum immunoglobulin IgM after 6 weeks post vaccination (ELISA results not presented in this thesis).

Teleost IgM found in serum and/or mucus, is a tetramer composed of four monomers (Bromage *et al.,* 2006). The IgM heavy chain (H chain) possesses four constant heavy chain domains, μ1-μ4, with these C domains encoding sites for the binding of effector cells (Stafford *et al.,* 2006; Nayak *et al.,* 2010), cytotoxic cells (Shen *et al.,* 2003) or molecules such as complement (Magnadottir *et al.,* 1995). Mucosal IgM plays a direct role in neutralising bacteria, as well as combining with complement and red blood cells eliciting haemagglutination (Ourth and Wilson, 1982), which could explain the presence of bacteria as aggregates in the distal marginal channel detected by IHC. In response to the pathogen IgM antibodies can be produced locally within the mucosa (Zhao *et al.,* 2008; Findlay *et al.,* 2013). In fish, the production of antibodies and their localization appears to depend on the route of immunization. For example, vaccination with *Vibrio harveyi*, immersion compared to i.p. or oral vaccination, stimulates higher specific antibody titres in the mucosal tissues (Zu *et al.,* 2009), whereas i.p. injection produced a higher levels of IgM in the systemic circulation, and compared to oral stimulation, increased the level of ASCs in the head kidney and blood. The high level of IgM transcripts observed in the gill 12 d.p.c. may be a result of antigen stimulation of gill-associated immune tissues or increased levels of B cells in the gill vasculature and the route of stimulation, with the latter perhaps making the most significant contribution for the IgM response in the gill. The gill is a complex organ,

which contains a considerable amount of blood even after bleeding the fish from the caudal vein before sampling. Residue blood may explain some of the gene expression results obtained from the gills.

IgT is another immunoglobulin isotype found in head kidney and spleen of fish (Tadiso *et al.,* 2011b). The abundance of IgT transcripts in mucosal tissues (skin and hind gut) of healthy fish is relatively weak (Tadiso *et al.,* 2012). However, during the first few days post-infection with salmon louse (*Lepeophtheirus salmonis*) (*i.e.* 3-15 d.p.c.) (Tadiso *et al.,* 2011a) in salmon and ciliated parasite Ichthyophtirius multifiliis (Xu *et al.,* 2013) in trout, the levels of IgT transcripts increased in the skin indicating production of IgT transcripts following a parasitic infestation supporting the hypothesis that IgT is the signature molecule involved in mucosal immunity (Sunyer *et al.,* 2009). Most recently, the immune response of the Atlantic salmon gill was evaluated against viral infections (ISA) in both normal gill tissue as well as laser micro-dissected ILT compared to mid kidney (Austbo *et al.,* 2014). A strong innate response was observed in gills of all three tissues examined regardless of the presence of virus. A small delayed increase in IgT transcripts, exclusively in the ILT, could indicate that this tissue has a role as a secondary lymphoid organ with clonal expansion of IgT expressing B-cells. There are other mucosal markers, including lysozyme, mucus and IgM suggested in previous literature (Salinas *et al.,* 2011).

In the present experiment, a significant rise of IgT transcripts over time in both the head kidney and the spleen suggests the possible production of new B cells in response to vaccination, with mobilization of them into gill giving a significantly high transcriptional abundance of IgT in gill. This also suggested the importance of IgT as a

mucosal immune signature, and especially when it should be noted that the route of administration was by i.p. injection.

Both pro-inflammatory cytokines (*e.g.* IL-1β, IL-6, and IL-8, TNFα) and cytokines related to adaptive immunity (*e.g.* IFNγ, IL-10, TGFβ) are important cellular mediators that are partly influenced by the establishment of an *A. salmonicida* infection (Bergh and Fery, 2014). Many of the effector roles of IL-1β are mediated and influenced by the up- or down- expression of other cytokines and chemokine genes (Dinarello ,1997). IL-1β is one of the earliest expressed pro-inflammatory cytokines and enables organisms to respond promptly to infection by inducing a cascade of reactions leading to inflammation. In spleen, at early time points, the expression of IL-1β between individual fish in the vaccinated/unchallenged (vaccinated) group was highly variable and this could be a response to the injection itself (acute stress response to i.p injection) rather than a specific response to vaccination. In contrast to the decrease in IL-1β expression observed in the spleen and the kidney, high and constant expression of IL-1β in the vaccinated/challenged group suggest that gills act as a pro-inflammatory organ. This immune priming may help protect surviving fish from subsequent infection. For example, an increased resistance to *Aeromonas hydrophila*, administered by i.p. injection, primed IL-1β expression in infected fish (Kono *et al.*, 2002).

IFNγ is a strong activator of macrophages and the key cytokine of type 1 T helper (Th1) cell immune responses during infections with intracellular pathogens, autoimmune diseases and anti-tumour defence (Bogdan *et al.*, 2004). IFNγ is not expressed constitutively in vitro in head kidney cells from rainbow trout, but is inducible by PHA or poly (I:C). In vivo expression of IFNγ is observed in the head kidney and spleen after i.p. injection of poly I:C (Zou *et al.*, 1999). During the initial stage of *A. salmonicida*

infection, the T3SS of the bacteria can highjack the immune response in a IL-10 dependent manner and also activate suppressor regulatory T lymphocytes (Treg) during the first days of the infection (Bergh and Fery, 2014).This immune evasion mechanism helps bacteria colonise immune organs, especially head kidney. The low level INFγ expression noted in the vaccinated/challenged group compared to control groups detected at early time points could be a possible consequence of such initial immune suppression. Although the host is able to gradually recover immunoproliferation activation of T cytotoxic responses, such as INFγ expression, represses the T3SS system so as establish a specific immune response to *A. salmonicida*, and this may have given rise to significant elevation of INF expression both in head kidney and spleen in the surviving fish in the present experiment. The significant elevation in expression of INFγ noted in the head kidney of vaccinated/unchallenged (vaccinated) fish suggests that the injection could enhance INFγ as a non-specific immune response.

In conclusion, this study provides an insight into the protective mechanisms of *A. salmonicida* during vaccination and challenge, using routes of administration currently used for efficacy testing commercial *A. salmonicida* vaccines in Atlantic salmon. It was clear that different tissues have different responses towards vaccination and subsequent infection by the pathogen. As evidenced by the gene expression analysis performed, head kidney and spleen play a critical role in eliciting immune protection. Furthermore, there is an apparent cellular response to *A. salmonicida* in the gills of Atlantic salmon, evidenced from the differential expression of numerous cytokines. Further work is needed to determine the function of these pro-inflammatory cytokine in gills during *A. salmonicida* infection, to provide further understanding of the protective mechanism involved in terms of eventual survival or recovery of the fish from *A. salmonicida* infection.

CHAPTER 6

FINAL DISCUSSION AND CONCLUSIONS

Recent statistics from the world food and agriculture organisation (FAO, 2011) have identified aquaculture as a fast-growing food production sector that is capable of providing high quality protein and is much favoured over land based protein producing sectors due to low carbon emissions. The global demand for farmed Atlantic salmon has also increased recently (FAO, 2013; Munro and Wallace 2013), leading to a rapid intensification of the salmon farming industry, based on the use of sophisticated culture technologies *e.g.* improved storm-proof containment systems, genetically improved disease resistant strains of salmon with reduced morbidity and mortality (Aquagen, Norway) and improved fish vaccines to reduce chemical and antibiotic use (Torrissen *et al.,* 2011). With the increased incidence of disease, including viral (Murray, 2013) and bacterial diseases (Toranzo *et al.,* 2005), derived in part from intensification, monitoring and management of health has become a critical issue for the sustainable growth of the industry. Newly emerged gill-associated pathologies such as AGD and PGI have exposed the salmon farming industry in Scotland and Ireland to a range of new challenges (Mitchell and Rodger, 2011). The complexity and multifactorial aetiology of gill disease, coupled with deleterious effects from the changing environment, makes disease diagnosis and intervention extremely complicated (Anon, 2013). One of the key methods to mitigate the effects of disease is the identification of early warning signs, which can be assisted by the development of sensitive health monitoring tools that are able to help identify and quantify gill responses to various factors including pathogens, salinity change, fluctuation of dissolve oxygen and changes in water temperature. In order to address the need for new tools, a novel computer based image analysis system (GIA) was developed through the research

described in this thesis in a joint venture between IoA, University of Stirling and Skretting ARC, Norway. The findings presented here could prove highly beneficial to the global salmon farming industry in terms of the concerted effort to improve gill health.

Over the last decade, improvements in modern computer-assisted technologies associated with biomedical sciences have made customised digital image analysis into a practical research tool that allows quantification of a broad range of histomorphometric changes in different human and terrestrial animal tissues (Doube *et al.,* 2010). This technology has several advantages including rapid, accurate diagnosis and the potential for interpretation with minimal human intervention, high throughput and user friendliness, compared to traditional conventional histopathology based disease diagnosis (Wilbur *et al.,* 2009). Digital image analysis has been previously attempted in fish research *e.g.* quantification of gaping, bruising and blood spots in salmon fillets (Balaban *et al.,* 2011), evaluation of vaccinated farmed Atlantic salmon for spinal and skull deformities (Berg *et al.,* 2012), determination of fat and connective tissue in salmon muscle (Borderías *et al.,* 1999; Stien *et al.,* 2007), application of automated image analysis to quantify colour and composition of rainbow trout cutlets (Stien *et al.,* 2007), morphometric discrimination of parasite taxonomy in fish including *Gyrodactylus salaris* Malmberg (Monogenea) (Shinn *et al.,* 2001) and parasite enumeration for *Benedenia* and *Zeuxapta* in Australian aquaculture (Whittington *et al.,* 2011). However, these advanced techniques appear to have been under-utilised for assessment of fish health due to initial cost and lack of expertise knowledge . The development of the novel GIA tool described in this thesis, in parallel to an investigation conducted on gut health (Silva, 2014), demonstrates the feasibility of employing digital pathology and image analysis to monitor the gill health status of

salmon. In both instances, the tools developed were targeted specifically to screen for subtle changes occurring during preclinical stages in Atlantic salmon gills and gut in response to functional feeds and different environmental management changes.

This thesis comprises a number of research chapters that describe the development of the GIA pipeline and then its application to a range of questions regarding gill pathology / plasticity in response to specific disease or environmental cues.

In Chapter 2, a comprehensive description of the development of the high-throughput GIA tool and evaluation of its use for quantitative assessment of Atlantic salmon gill histomorphometric changes in response to different functional feeds was provided. To achieve this, a range of modern technologies and approaches including digital histology (Bandyopadhyay, 2011), WSI technology, histomorphology (Diamond *et al.,* 2004; Al-Hezaimi *et al.,* 2012) and CAD systems (Gurcan *et al.,* 2009; Marrocco *et al.,* 2010) were successfully incorporated. Specific attention was paid to obtaining high quality histology sections of the gills, which is the most important prerequisite for successful deployment of gill image analysis technologies. In general fish undergo post-mortem changes rapidly after death and therefore timing of sampling is an important factor that details should have been requested. The orientation of gill lamellae, the successful production of histology sections without artefacts, and the development of consistent staining protocols were further key elements in producing quality sections suitable for GIA tool analysis.

During the development of the GIA tool, many of the parameters measured were based on a set of well-defined morphometric parameters of the gill that have been used previously by histopathologists and fish biologists in the fish health community (comprising 25 different features) (Mallatt, 1985; Ferguson, 2006; Roberts and Rodger ,

2012). The nomenclature for the tool was also adopted from descriptions used in primary references (Mallatt, 1985; Evans *et al.,* 2005) and standardised nomenclature (Ferguson, 2006; Roberts and Rodger, 2012). The successes of the GIA tool and relevance of the selected morphometric indices were evaluated through a set of gill samples obtained from a feeding trial (Chapter 2), which consisted of three different diets (*i.e.* A-conventional salmon feed, B-25 % soya bean replacement C-enriched with immunostimulants). The results of this evaluation highlighted the fact that functional feeds could alter gill histomorphology and, to our knowledge, with the first attempt to evaluate the effects of functional feeds using digital image analysis. This study showed that the GIA tool could detect subtle changes in gill histomorphology as shown by significantly altered VASL and TGA in the gills of fish fed functional feed compared to a control diet. The results of this study revealed that the sensitivity of the tool was considerably higher than that of routine histology. While univariate analysis revealed only a few significantly altered parameters, application of multivariate PCA analysis was able to reveal clear differences between the control diet and one of the functional feeds, this being statistically supported by a Kruskal-Wallis ANOVA and *post-hoc* analysis. This underlined the power achievable by use of multivariate analyses in combination with image analysis.

In Chapter 3, the GIA tool was employed to evaluate the alteration of gill morphology over time in response to a therapeutic dose of H_2O_2. This study has current relevance to the salmon farming industry, as H_2O_2 is used as the treatment of choice for AGD in Scotland and Norway, due to the logistical difficulties with use of freshwater as a recommended treatment (Powell and Kristensen, 2014; Adams *et al.,* 2012). Our experiment examined the changes of gill morphology after H_2O_2 bath treatment over a time course, from which it was shown that the GIA tool was able to discriminate

histomorphometric changes during acute and chronic responses of the gills. In examination of the changes that occurred after treatment, the most striking finding was a significant reduction in size denoted by low SLPL, SLA, PLEA, and PLA of the gills exposed to H_2O_2 compared to pre-trial control at 4 hours post exposure. This change was regarded as reflecting a peracute response and this may in turn help fish to minimise further contact with H_2O_2. This response is a histological reflection of the 'fight or flight' response, which is recognized as the first stage of a general adaptation that regulates a stress response among vertebrates and other organisms (Gozhenko *et al.,* 2009). It is possible to monitor this acute stress response by looking for elevated glucose levels in the blood of the fish or high cortisol levels as a result of mobilisation of glycogen reserves as demonstrated by Bowers *et al.,* (2002). In terms of treatment, Adams *et al.,*. (2012) demonstrated the successful application of H_2O_2 to treat Atlantic salmon affected with AGD. They reported significant differences in the percentage of filaments affected with hyperplastic lesions, measured by routine histology and changes in plasma osmolality between groups immediately after post-bath treatment. It would be appropriate to apply the GIA tool to explore similar experiments in order to compare healthy versus pathogen-affected salmon gills exposed to therapeutic doses of H_2O_2 to elucidate how disease affects the capacity of fish gills to respond. Future studies on the application of the GIA might involve field-based various environmental factors, before, during and after H_2O_2 treatment.

Chapter 3 demonstrated significant changes in the measured morphometric parameters by GLM analysis. The significant parameters indicated that Atlantic salmon gills exposed to H_2O_2 reflect a wide response of histomorphometric changes. In terms of understanding fish biology and individual variation, however, each time point should ideally be compared with parallel untreated control fish. Unfortunately, this experiment

lacked a set of untreated control tanks, which could provide fish of comparable size for parallel sampling over the duration if the experiment. However, multivariate PCA nevertheless generated clear clustering at the successive time points away from the initial control fish population and showed that fish had moved back to the position of the control fish population by 14 d.p.e. These analyses further outlined the strength of combining the image analysis pipeline with a subsequent multivariate analysis approach.

In Chapter 4, the GIA tool was used to assess the effect of temperature on feed performance (Chapter 4 Experiment 1) and gill performance with respect to different functional feeds fed to fish at different temperatures (Chapter 4 Experiment 2). The work presented successfully quantified histomorphometric alterations by applying the GIA tool, enabling classification of fish into the groups fed with different functional feeds, with this being further supported by statistical analysis (as shown in interaction plots generated from GLM analysis of morphometric data) and immune gene expression analysis using RT-qPCR. The results of the first experiment showed that temperature (4, 10 and 16°C) significantly influenced histomorphometry and plasticity of the gill of Atlantic salmon. Complementary results were also generated by analysing skin samples from the same experiment, which similarly showed histomorphometric changes in epidermal thickness measured by quantitative histology (Jensen *et al.*, 2014). The majority of quantitative histology associated morphometric parameters were changed significantly at the lower temperature (4°C) compared to control temperature of 10 °C, but rarely at the high temperature (16^{o}C) compared to the control temperature. The 10° C group was chosen as the nominal control in this experiment as it is more comparable to ambient sea water temperature in Norway and Scotland. In the second experiment three functional feeds (A, B and D) were tested across two different

temperatures (4°C and 12°C). The results of the second experiment showed that the fish fed the same feed in different temperatures gave different gill histomorphometric responses, eventually elicited from a combination of temperature and feed used to distinguish between the different ingredients of the feed (*e.g.* vitamin E, nucleotides). During this study PCA analysis clearly clustered individuals into their relevant sub groups (*e.g.* A4 or A12) reflecting their biological difference generated as result of a combination of feed and temperature, measured by the GIA tool. During the PCA analysis, GLM was performed on first principle component to see any direct effect of diet on fish gill histomorphology. In parallel to the histomorphometric study, immune related transcripts were evaluated to understand the underlying pathophysiological conditions of the gills. The relative expression of TNFα significantly increased in Diet D at 12°C compared to the control diet at the same temperature ($p < 0.05$, $n = 6$). At 4°C relative expression of IgT significantly increased in the group of fish fed diet D, compared to fish fed diets B and A which reflects immunomodulation by functional feeds at low temperature. During the above study the application of the GIA tool and gene expression analysis allowed examination of the effects of functional feed on the pathophysiology of the gill.

During the last five years, considerable attention has been paid to understanding the mucosal health of different fish species; carp (Rombout *et al.*, 1986, 1989), rainbow trout (Zhang *et al.*, 2011), Atlantic salmon (Tadiso *et al.*, 2011b). The mucosal surfaces (skin, gills and gut) are regarded as providing an important first line of defence against aquatic pathogens, continuously interacting with the microbiota and ambient conditions of the surrounding environment more so than do those of their terrestrial counterparts (Rombout *et al.*, 2014). The results from the second experiment described in Chapter 2 suggested that both feed and temperature effects interact with each other to influence

histomorphometric changes seen in the gills. Studies on modulation of gill-associated mucosal immunity in response to immunostimulants (Bridle *et al.,* 2003) and in response to pathogens (Bridle *et al.,* 2006; Pennacchi *et al.,* 2014) are becoming more widely available in the recent literature, however, the effects of functional feeds on mucosal immunity of the gill are not well studied and this remains an important area to be explored. Furthermore, a snap-shot of immune-related genes found them to be significantly affected by use of different functional feeds, warranting future in-depth studies on overall gene regulation of the gills in response to functional diets. Collectively, these approaches can be used to help formulate different functional feeds to obtain maximum health benefits and possibly be used to examine interactions with the effects of environmental change in order to assist management interventions to allow minimisation of stress.

Recent research by Niklasson *et al* (2011) found that simulation of mucosal immunity in response to hypoxia induced breakdown of gut integrity at high temperature (16°C) in Atlantic salmon held in farm cages during adverse weather conditions. Similar observations were made by Sundh *et al.,* (2010), who revealed that adverse environmental conditions (low water flow, low DO levels at low and high temperature that can occur in sea cages). They found that primary and secondary stress responses were elicited in the affected post-smolt Atlantic salmon, with the intestinal barrier function being significantly affected by prolonged hypoxic stress even when no primary stress response was observed. This suggested that intestinal barrier function is a good experimental marker (welfare indicator) for evaluation of chronic stress. Although there has been minimal equivalent discussion in regards to the gill, the results presented suggest that gills are also sensitive to changes in environmental temperature, warranting further study of the association between gill mucosal integrity and farm conditions. It is

suggested that the GIA pipeline could provide an appropriate tool for assessing such interactions.

Chapter 5 examined responses of the gill to pathogen challenge in vaccinated fish. This work set out to explore the host response in Atlantic salmon gill following vaccination and pathogen challenge using *Aeromonas salmonicida* subsp. *salmonicida* as a model pathogen. The *A. salmonicida* vaccine is one of the most successful commercial vaccines and has been suggested to provide cross-protection to other bacterial infections (Romstad *et al.*, 2013, 2014). The samples for the present study were derived from a separate large-scale research project that evaluated 'Development of an *in vitro* method to test batch potency testing for *A. salmonicida* subsp. *salmonicida*'. The original aim of the work presented in Chapter 5 was to characterise the host response in Atlantic salmon parr gills, in terms of vaccination and of post-vaccination pathogen challenge, using both immune gene expression analysis and histomorphometric analysis using the GIA tool. However, the latter could not be conducted as planned due to technical problems in automated slide scanning (due to the specific slides employed) and the tight time constraints of the project. The effect of a commercial vaccine against *A. salmonicida* subsp. *salmonicida* on Atlantic salmon gills was evaluated for immunologically important transcripts (IL-1β, IgM and IgT) in comparison to expression in the other main lymphoid organs *i.e.* head kidney and spleen. The challenge study carried out after 59 d.p.v., using a virulent strain of the bacterium, revealed that significant differential gene expression could be detected in all three organs. In gills, a significant increase in expression of gene transcripts, including immune genes, was noted suggesting that the gill might be a useful tissue for sampling and routine evaluation during vaccine / host-pathogen interaction studies. The immune response of the gill towards pathogen challenge is relatively well characterised for

Atlantic salmon affected with AGD, where it has been explored using various methods including microarray (Morrison *et al.,* 2006), RT-qPCR (Wynne *et al.,* 2008; Bridle *et al.,* 2006), *in situ* hybridisation (Young *et al.,* 2007), IHC (Morrison and Norwak, 2008) and proteomics (Valdenegro-Vega *et al.,* 2014).

From previous gene expression studies it has been found that the gill is capable of eliciting a potent immune response (Fast *et al.,* 2007; Rebl *et al.,* 2014) and the application of standardised RT-qPCR based methods to evaluate gene expression in the gills has been an important component of the work described in this thesis. The most popular and reliable RT-qPCR technique (Bustin and Nolan, 2004) has been used successfully to evaluate pathophysiological alteration in mRNA levels in the various experiments conducted in this thesis. In the past, the majority of gene expression studies have used single reference genes, which were obtained from previous publications regardless of comparability of the current experiment and type of treatment (Jorgensen *et al.,* 2008). In Chapter 2, while establishing the protocol, only one reference gene, β actin, was used during the first set of RT-qPCR assays, however, in Chapter 4 and 5 a larger number of reference genes (three reference genes later referred as reference gene index) was used for normalisation of the target gene / genes (Vandesompelle *et al.,* 2002). For data analysis the initial software used, REST version 2009 and REST384 (Pfaffl *et al.,* 2002) were replaced by GenEx (genex.gene-quantification.info), which has integrated statistical analysis functions as well as using multiple reference genes for normalisation and being equipped with different calibrators for various approaches to relative quantification.

Recent research on gill immunity in pathogen challenges (*e.g.* ISAV infection on Atlantic salmon gills) has highlighted the importance of the interbranchial lymphoid

tissue (ILT) compared to normal gill tissue from routine sampling, with the data generated from these studies by laser micro-dissection in particular (Aas *et al.,* 2014). The results suggested that the ILT acted as a reservoir for T-cells and performed important immune regulatory functions, mainly strong innate responses and delayed increase of IgT transcripts (Austbo *et al.,* 2014). In general, the best way of eliciting mucosal immunity and the recommended route for pathogen challenge is immersion or bath treatment / challenge (Rombout *et al.,* 2014). However, the present study had to adhere to the i.p. route as it was the recommended method for vaccine efficacy testing for *A. salmonicida* vaccination trials. The results obtained using an i.p. route showed that Atlantic salmon gill was still stimulated from i.p injection. According the findings of earlier chapters, the Atlantic salmon gill can be modulated in terms of immune response by a range of external factors such as environmental temperature. However, in term of maximising immune modulation (*i.e.* immune stimulation), when salmon are exposed to unfavourable environmental conditions, these might be mitigated by combining vaccination and functional feed strategies although the immune interactions between these approaches need further research. Although it was not possible to study morphometric changes in the gill using GIA in the present study, the GIA tool is likely to prove a useful tool for elucidating gill responses to commercial vaccination.

One of the most significant achievements of the work presented in this thesis was the productive combination of a range of different approaches for the assessment of gill response to a range of environmental and pathogenic factors. The work presented has combined a digital image analysis pipeline with conventional histological observation and has used RT-qPCR to provide supporting measurements of gene expression. Additional power has been provided by the use of a range of multivariate data

exploration and analysis techniques, which have allowed a range of different indicators of gill state to be analysed together.

One of the available semi-quantitative gill scoring system studies, only that of Mitchell *et al.*,. (2012) comprises a large-scale field based investigation, which can be widely applied to quantification of gill pathologies around the world. A recent attempt has also been made by Mona Gjessing (2014, Norwegian School of Veterinary Science, unpublished data) to improve semi-quantitative scoring on gill pathologies. The GIA pipeline developed in this study and successfully evaluated for research purposes can provide a powerful tool for future aquaculture health assessment, particularly in its ability to detect subtle changes that could potentially be used as early warning system for disease / pathology in farmed Atlantic salmon. The ability to detect and quantify change in tissues also provides the opportunity for such tools to supplement traditional histopathology, improve training of observational skills and give more capacity to undertake quantitative of large-scale field study samples. Additional power is provided by the combination of image analysis with gene expression analysis and multivariate data exploration and analysis techniques. The final validation of the usefulness of such approaches is their adoption by the commercial sector, and following the work presented in this thesis these methods are currently being applied and developed further.

REFERENCES

Aas, I. B., Austbo, L., Konig, M., Syed, M., Falk, K., Hordvik, I. & Koppang, E.O. (2014). Transcriptional characterization of the T cell population within the calmonid interbranchial lymphoid tissue, *Journal of Immunology,* vol. 193, pp. 3463-3469.

Abbas, A. K., Lichtman, A. H., & Pober, J. S., (2006). Cellular and molecular immunology. 7th edition , W. B. Saunders Company USA.

Abel, P. (1974). Toxicity of synthetic detergents to fish and aquatic invertebrates, *Journal of Fish Biology,* vol. 6, no. 3, pp. 279-298.

Abel, P. & Skidmore, J. (1975). Toxic effects of an anionic detergent on the gills of rainbow trout, *Water Research.* vol. 9, no. 8, pp. 759-765.

Abel, P. (1976). Toxic action of several lethal concentrations of an anionic detergent on the gills of the brown trout (*Salmo trutta* L.). *Journal of Fish Biology,* vol. 9, no. 5, pp. 441-446.

Abel, P. 1987. Evaluating the effects of pollution on natural marine ecosystems: some outstanding problems of biological surveillance techniques. FAO Fisheries Report (FAO).

Abruzzini, A.F., Ingram, L.O. & Clem, L.W. (1982). Temperature-mediated processes in teleost immunity: homeoviscous adaptation in teleost lymphocytes. *Proceedings of the Society for Experimental Biology and Medicine,* vol. 169, no. 1, pp. 12-18.

Adams, A., Auchinachie, N., Bundy, A., Tatner, M.F. & Horne, M. (1988). The potency of adjuvanted injected vaccines in rainbow trout (*Salmo gairdneri* Richardson) and bath vaccines in Atlantic salmon (*Salmo salar* L.) against furunculosis. *Aquaculture,* vol. 69, no. 1, pp. 15-26.

Adams, M. & Nowak, B. (2001). Distribution and structure of lesions in the gills of Atlantic salmon, *Salmo salar* L., affected with amoebic gill disease, *Journal of Fish Diseases,* vol. 24, no. 9, pp. 535-542.

Adams, M. & Nowak, B. (2003). Amoebic gill disease: sequential pathology in cultured Atlantic salmon, *Salmo salar* L., *Journal of Fish Diseases,* vol. 26, no. 10, pp. 601-614.

Adams, M., Villavedra, M. & Nowak, B. (2008). An opportunistic detection of amoebic gill disease in blue warehou, *Seriolella brama Günther*, collected from an Atlantic salmon, *Salmo salar* L., production cage in south eastern Tasmania, *Journal of Fish Diseases,* vol. 31, no. 9, pp. 713-717.

Adams, M.B., Crosbie, P.B. & Nowak, B.F. (2012). Preliminary success using hydrogen peroxide to treat Atlantic salmon, *Salmo salar* L., affected with experimentally induced amoebic gill disease (AGD), *Journal of Fish Diseases,* vol. 35, no. 11, pp. 839-848.

Agius, C. & Roberts, R. (2003). Melano-macrophage centers and their role in fish pathology, *Journal of Fish Diseases,* vol. 26, no. 9, pp. 499-509.

Ainsworth, A.J., Dexiang, C., Waterstrat, P. & Greenway, T. (1991). Effect of temperature on the immune system of channel catfish (*Ictalurus punctatus*). Leucocyte distribution and phagocyte function in the anterior kidney at 10°C, *Comparative Biochemistry and Physiology Part A: Physiology,* vol. 100, no. 4, pp. 907-912.

Alderman, D. & Hastings, T. (1998). Antibiotic use in aquaculture: development of antibiotic resistance–potential for consumer health risks, *International Journal of Food Science & Technology,* vol. 33, no. 2, pp. 139-155.

Alejo, A. & Tafalla, C. (2011). Chemokines in teleost fish species, *Developmental & Comparative Immunology,* vol. 35, no. 12, pp. 1215-1222.

Alexander, J.B. & Ingram, G.A. (1992). Noncellular nonspecific defense mechanisms of fish, *Annual Review of Fish Diseases,* vol. 2, pp. 249-279.

Al-Hezaimi, K., Al-Askar, M., Al-Fahad, H., Al-Rasheed, A., Al-Sourani, N., Griffin, T., O'Neill, R. & Javed, F. (2012). Effect of enamel matrix derivative protein on the healing of standardized epithelial wounds: a histomorphometric analysis. *International wound journal,* vol. 9, no. 4, pp. 436-441.

Alvarez-Pellitero, P. (2008). Fish immunity and parasite infections: from innate immunity to immunoprophylactic prospects, *Veterinary Immunology and Immunopathology,* vol. 126, no. 3, pp. 171-198.

Ángeles Esteban, M. (2012). An overview of the immunological defenses in fish skin, *International Scholarly Research Notices,* vol. (2012).

Anon. (2006). Responsible use of vaccines and vaccination in fish production. NOAH Compendium of Data Sheets for Animal Medicines, published by NOAH and online at http://www.noahcompendium.co.uk

Anon, (2010). FAO, Population Division of the Department of Economic and Social Affairs of the United Nations, Secretariat, World Population Prospects: The 2010 Revision.

Anon. (2013). Kontali Analyse AS, Industriveien 18, NO-6517 Kristiansund N, Tlf. +47 71 68 33 00, Fax +47 71 68 33 01 • Epost: mail@kontali.no.

Anon. (2013). Marine Institute. GILPAT: An Investigation into Gill Pathologies in Marine Reared Finfish. Marine Research Sub-Programme (NDP 2007-'13),PBA/AF/08/002 (01).

Anon. (2014). FAO, The state of World Fisheries and Aquaculture 2014. Rome. 223pp

Aoki, T. (1992). Chemotherapy and drug resistance in fish farms in Japan, *Diseases in Asian Aquaculture,* vol. 1, pp. 519-529.

Aoki, T., Takano, T., Santos, M.D., Kondo, H. & Hirono, I. (2008). Molecular innate immunity in teleost fish: review and future perspectives, *5th World Fisheries Congress,* pp. 263

Aranishi, F. & Mano, N. (2000). Antibacterial cathepsins in different types of ambicoloured Japanese flounder skin, *Fish & Shellfish Immunology,* vol. 10, no. 1, pp. 87-89.

Arason, G. (1996). Lectin as defence molecules in vertebrates and invertebrates. *Fish and Shellfish Immunology,* vol. 6, pp. 277-289

Arndt, R.E. & Wagner, E.J. (1997). The toxicity of hydrogen peroxide to rainbow trout *Oncorhynchus mykiss* and Cutthroat trout *Oncorhynchus clarki* fry and fingerlings, *Journal of the World Aquaculture Society,* vol. 28, no. 2, pp. 150-157.

Au, D. (2004). The application of histo-cytopathological biomarkers in marine pollution monitoring: a review, *Marine pollution bulletin,* vol. 48, no. 9, pp. 817-834.

Austbø, L., Aas, I.B., König, M., Weli, S.C., Syed, M., Falk, K. & Koppang, E.O. (2014). Transcriptional response of immune genes in gills and the interbranchial lymphoid tissue of Atlantic salmon challenged with infectious salmon anaemia virus, *Developmental & Comparative Immunology,* vol. 45, no. 1, pp. 107-114.

Austin, B. & Austin, D.A. (2007). *Bacterial fish pathogens: disease of farmed and wild fish,* Springer, Praxis Publishing Limited, Chichester, UK.

Austin, B. & Brunt, J. (2009). The use of probiotics in aquaculture, *Aquaculture Microbiology and Biotechnology,* vol. 1, pp. 185-207.

Avtalion, R.R. (1969). Temperature effect on antibody production and immunological memory, in carp (*Cyprinus carpio*) immunized against bovine serum albumin (BSA), *Immunology,* vol. 17, no. 6, pp. 927-931.

Avtalion, R., Wojdani, A., Malik, Z., Shahrabani, R. & Duczyminer, M. (1973). Influence of environmental temperature on the immune response in fish, In *Current Topics in Microbiology and Immunology/Ergebnisse der Mikrobiologie und Immunitätsforschung* Springer, pp. 1-35.

Avtalion, R.R. & Shahrabani, R. (1975). Studies on phagocytosis in fish. In vitro uptake and killing of living *Staphylococcus aureus* by peripheral leucocytes of carp (*Cyprinus carpio*), *Immunology,* vol. 29, no. 6, pp. 1181-1187.

Avtalion, R., Malik, Z., Lefler, E. & Katz, E. (1970). Temperature effect on immune resistance of fish to pathogens, *Bamidgeh,* vol. 22, pp. 33-38.

Avtalion, R.R. & Milgrom, L. (1976). Regulatory effect of temperature and antigen upon immunity in ectothermic vertebrates. Influence of hapten density on the immunological and serological properties of penicilloyl-carrier conjugates, *Immunology,* vol. 31, no. 4, pp. 589-594.

Avtalion, R.R. & Clem, L.W. (1981). Environmental control of the immune response in fish, *Critical Reviews in Environmental Science and Technology,* vol. 11, no. 2, pp. 163-188.

Baeverfjord, G. & Krogdahl, Å. (1996). Development and regression of soybean meal induced enteritis in Atlantic salmon, *Salmo salar* L., distal intestine: a comparison with the intestines of fasted fish, *Journal of Fish Diseases,* vol. 19, no. 5, pp. 375-387.

Bailey, J. (2014). Looking for sustainable solutions in salmon aquaculture, *Nordic Journal of Applied Ethics,* vol. 1, no. 1, pp 22-40.

Bailly, Y., Dunel-Erb, S. & Laurent, P. (1992). The neuroepithelial cells of the fish gill filament: Indolamine-immunocytochemistry and innervation, *The Anatomical Record,* vol. 233, no. 1, pp. 143-161.

Balaban, M.O., Ünal Şengör, G.F., Soriano, M.G. & Ruiz, E.G. (2011). Quantification of gaping, bruising, and blood spots in salmon fillets using image analysis, *Journal of Food Science,* vol. 76, no. 3, pp. E291-E297.

Balfry, S.K. & Higgs, D.A. (2001). Influence of dietary lipid composition on the immune system and disease resistance of finfish, In *Nutrition and fish health, eds* Carl D Webster, Chhorn Lim:CRC Press, pp. 213-234.

Bandyopadhyay, S.K. (2011). Digital Pathology: An Electronic Environment for Performing Pathologic Analyses from image, *International Journal of Computer Sciences and Technology,* vol. 1, no. 3, pp. 127-130.

Battaglene, S., Hobday, A., Carter, C., Lyne, V. & Nowak, B. (2008). Preparing for climate change: information needs for an aquaculture industry, *Skretting Australasian Aquaculture,* pp. 1.

Baxter, E.J., Rodger, H.D., McAllen, R. & Doyle, T.K. (2011). Gill disorders in marine-farmed salmon: investigating the role of hydrozoan jellyfish, *Aquaculture Environment Interaction,* vol. 1, pp. 245-257.

Bayne, C.J. & Gerwick, L. (2001). The acute phase response and innate immunity of fish, *Developmental & Comparative Immunology,* vol. 25, no. 8, pp. 725-743.

Beitinger, T.L. & Fitzpatrick, L.C. (1979). Physiological and ecological correlates of preferred temperature in fish, *American Zoologist,* vol. 19, no. 1, pp. 319-329.

Belsare, A. & Mushrif, M. (2012). Histopathological image analysis using image processing techniques: An overview, *Signal & Image Processing: An International Journal (SIPIJ)* vol. 3, pp. 23-36.

Berg, A., Yurtseva, A., Hansen, T., Lajus, D. & Fjelldal, P. (2012). Vaccinated farmed Atlantic salmon are susceptible to spinal and skull deformities, *Journal of Applied Ichthyology,* vol. 28, no. 3, pp. 446-452.

Bermingham, M. & Mulcahy, M. (2006). Microfauna associated with amoebic gill disease in sea-farmed Atlantic salmon, *Salmo salar* L., smolts, *Journal of Fish Diseases,* vol. 29, no. 8, pp. 455-465.

Bernoth, E. (1997). Furunculosis: the history of the disease and of disease research, In:*Furunculosis: Multidisciplinary Fish Diseases Research*, eds. Eva-Maria Bernoth, Anthony E. Ellis, Paul J. Midtlyng, Gilles Olivier and Peter Smith, Elsevier Science Publishing co. Inc, Academic Press: San Diago, USA. pp 1-20.

Bernoth, E., Ellis, A.E., Midtlyng, P.J., Olivier, G. & Smith, P. (1997). *Furunculosis: multidisciplinary fish disease research,* Academic Press: San Diago, USA

Bhattacharjee, S., Mukherjee, J., Nag, S., Maitra, I.K. & Bandyopadhyay, S.K. (2014). Review on histopathological slide analysis using Digital Microscopy, *International Journal of Advanced Science & Technology*, vol. 62. pp 65-96.

Biering, E., Villoing, S., Sommerset, I. & Christie, K.E. (2005). Update on viral vaccines for fish, *Developments in Biologicals*, vol. 121, pp. 97-113.

Black, E., Whyth, J., Bagshaw, J. & Ginther, N. (1991). The effects of algae *Heterosigma akashiwo* on juvenile *Oncorhynchus tshawytscha* and its implications for fish culture, *Journal of Applied Ichthyology*, vol. 7, no. 3, pp. 168-175.

Bly, J.E., Cuchens, M.A. & Clem, L.W. (1986). Temperature-mediated processes in teleost immunity: binding and mitogenic properties of concanavalin A with channel catfish lymphocytes, *Immunology*, vol. 58, no. 3, pp. 523-526.

Bly, J., Buttke, T., Cuchens, M. & Clem, L. (1987). Temperature-mediated processes in teleost immunity: the effects of temperature on membrane immunoglobulin capping on channel catfish B lymphocytes, *Comparative Biochemistry and Physiology Part A: Physiology*, vol. 88, no. 1, pp. 65-70.

Bly, J., Cuchens, M. & Clem, L. (1988). Temperature mediated processes in teleost immunity: differential abilities of channel catfish T and B lymphocytes to cap membrane antigen, *Comparative Biochemistry and Physiology Part A: Physiology*, vol. 90, no. 1, pp. 103-107.

Bly, J.E., Buttke, T. & Clem, L. (1990). Differential effects of temperature and exogenous fatty acids on mitogen-induced proliferation in channel catfish T and B lymphocytes, *Comparative Biochemistry and Physiology Part A: Physiology*, vol. 95, no. 3, pp. 417-424.

Bly, J.E. & Clem, L.W. (1992). Temperature and teleost immune functions, *Fish & Shellfish Immunology*, vol. 2, no. 3, pp. 159-171.

Boehm, T. & Bleul, C.C. (2007). The evolutionary history of lymphoid organs, *Nature Immunology*, vol. 8, no. 2, pp. 131-135.

Boeuf, G. & Payan, P. (2001). How should salinity influence fish growth? *Comparative Biochemistry and Physiology Part C: Toxicology & Pharmacology*, vol. 130, no. 4, pp. 411-423.

Bogdan, C., Mattner, J. & Schleicher, U. (2004). The role of type I interferons in non-viral infections, *Immunological Reviews*, vol. 202, no. 1, pp. 33-48.

Bols, N.C.; Brubacher, J.L.; Ganassin, R.C. & Lee, L.E.J. (2001). Ecotoxicology and innate immunity in fish. *Developmental and Comparative Immunology*, Vol. 25, pp. 853-873

Boltana, S., Rey, S., Roher, N., Vargas, R., Huerta, M., Huntingford, F.A., Goetz, F.W., Moore, J., Garcia-Valtanen, P., Estepa, A. & Mackenzie, S. (2013). Behavioral fever is a synergic signal amplifying the innate immune response, *Proceedings: Biological sciences / The Royal Society*, vol. 280, no. 1766, pp. 20131381.

Bone, Q. & Moore, R. (2008). *Biology of fishes*, Taylor & Francis, New York, USA.

Booth, J.H. (1979). Circulation in trout gills: the relationship between branchial perfusion and the width of the lamellar blood space, *Canadian Journal of Zoology*, vol. 57, no. 11, pp. 2183-2185.

Borderías, A.J., Gomez-Guillen, M., Hurtado, O. & Montero, P. (1999). Use of image analysis to determine fat and connective tissue in salmon muscle, *European Food Research and Technology*, vol. 209, no. 2, pp. 104-107.

Bowden, T.J. (2008). Modulation of the immune system of fish by their environment, *Fish & Shellfish Immunology*, vol. 25, no. 4, pp. 373-383.

Bowers, J., Speare, D.J. & Burka, J.F. (2002). The effects of hydrogen peroxide on the stress response of Atlantic salmon (*Salmo salar*), *Journal of Veterinary Pharmacology and Therapeutics*, vol. 25, no. 4, pp. 311-313.

Braganza, K., Karoly, D.J. & Arblaster, J. (2004). Diurnal temperature range as an index of global climate change during the twentieth century, *Geophysical Research Letters*, vol. 31, no. 13.

Bravo, S. (2010). The reproductive output of sea lice *Caligus rogercresseyi* under controlled conditions, *Experimental Parasitology*, vol. 125, no. 1, pp. 51-54.

Bricknell, I. & Dalmo, R.A. (2005). The use of immunostimulants in fish larval aquaculture, *Fish & Shellfish Immunology,* vol. 19, no. 5, pp. 457-472.

Bridle, A., Butler, R. & Nowak, B. (2003). Immunostimulatory CpG oligodeoxynucleotides increase resistance against amoebic gill disease in Atlantic salmon, *Salmo salar* L., *Journal of Fish Diseases,* vol. 26, no. 6, pp. 367-371.

Bromage, E.S., Ye, J. & Kaattari, S.L. (2006). Antibody structural variation in rainbow trout fluids, *Comparative Biochemistry and Physiology Part B: Biochemistry and Molecular Biology,* vol. 143, no. 1, pp. 61-69.

Brown, S. & Jones, P. (1968). Reactions between haemin and hydrogen peroxide. Part 2.—Destructive oxidation of haemin, *Transactions of the Faraday Society,* vol. 64, pp. 994-998.

Brown, A and Zarza, C. (2012). "Travel to Europe to meet with fish health professionals from Scotland and Ireland to review and analyse recent European AGD outbreak. Dr. Alistair Brown and Dr. Carlos Zarza (Tassal Fish Health Managers)". Project no 2012/712.

Brudeseth, B.E., Wiulsrød, R., Fredriksen, B.N., Lindmo, K., Løkling, K., Bordevik, M., Steine, N., Klevan, A. & Gravningen, K. (2013). Status and future perspectives of vaccines for industrialised fin-fish farming, *Fish Shellfish Immunology*., vol, 35, no. 6, 1759-1768.

Bruno, D. & Raynard, R. (1994). Studies on the use of hydrogen peroxide as a method for the control of sea lice on Atlantic salmon, *Aquaculture International,* vol. 2, no. 1, pp. 10-18.

Bruno, D.W., Noguera, P.A. & Poppe, T.T. (2013). *Pathology and Disease Diagnosis.* In: *A Colour Atlas of Salmonid Diseases.*Springer, pp. 33-51.

Burr, S.E., Pugovkin, D., Wahli, T., Segner, H. & Frey, J. (2005). Attenuated virulence of an *Aeromonas salmonicida* subsp. *salmonicida* type III secretion mutant in a rainbow trout model, *Microbiology,* vol. 151, no. 6, pp. 2111-2118.

Burr, S. & Frey, J. (2007). Analysis of type III effector genes in typical and atypical *Aeromonas salmonicida*, *Journal of Fish Diseases,* vol. 30, no. 11, pp. 711-714.

Bustin, S.A. & Nolan, T. (2004). Pitfalls of quantitative real-time reverse-transcription polymerase chain reaction, *Journal of Biomolecular Techniques,* vol. 15, no. 3, pp. 155-166.

Bustin, S.A., Beaulieu, J., Huggett, J., Jaggi, R., Kibenge, F.S., Olsvik, P.A., Penning, L.C. & Toegel, S. (2010). MIQE precis: Practical implementation of minimum standard guidelines for fluorescence-based quantitative real-time PCR experiments, *BMC Molecular Biology,* vol. 11, no. 1, pp. 74.

Callaway, R., Shinn, A.P., Grenfell, S.E., Bron, J.E., Burnell, G., Cook, E.J., Crumlish, M., Culloty, S., Davidson, K. & Ellis, R.P. (2012). Review of climate change impacts on marine aquaculture in the UK and Ireland, *Aquatic Conservation: Marine and Freshwater Ecosystems,* vol. 22, no. 3, pp. 389-421.

Camparo, P., Egevad, L., Algaba, F., Berney, D.M., Boccon-Gibod, L., Compérat, E., Evans, A.J., Grobholz, R., Kristiansen, G. & Langner, C. (2012). Utility of whole slide imaging and virtual microscopy in prostate pathology, *Acta Pathologica, Microbiologica Et Immunologica Scandinavica,* vol. 120, no. 4, pp. 298-304.

Campos-Perez, J.J.; Ward, M.; Grabowski, P.S.; Ellis, A.E. & Secombes, C.J. (2000). The gills are an important site of iNOS expression in rainbow trout *Oncorhynchus mykiss* after challenge with the Gram-positive pathogen *Renibacterium salmoninarum*. *Immunology,* Vol. 99, pp: 153-161

Carbrey, J.M. & Agre, P. (2009). Discovery of the aquaporins and development of the field, In: *Aquaporins.* Springer, pp. 3-28.

Casadevall, A. & Pirofski, L.A. (1999). Host-pathogen interactions: redefining the basic concepts of virulence and pathogenicity, *Infection and Immunity*, vol. 67, no. 8, pp. 3703-3713.

Casadevall, A. & Pirofski, L. (2003). Microbial virulence results from the interaction between host and microorganism, *Trends in Microbiology,* vol. 11, no. 4, pp. 157-158.

Chaves-Pozo, E., Muñoz, P., López-Muñoz, A., Pelegrín, P., Ayala, A.G., Mulero, V. & Meseguer, J. (2005). Early innate immune response and redistribution of inflammatory cells in the bony fish gilthead sea bream experimentally infected with *Vibrio anguillarum*, *Cell and Tissue Research,* vol. 320, no. 1, pp. 61-68.

Christie, K., Graham, D., McLoughlin, M., Villoing, S., Todd, D. & Knappskog, D. (2007). Experimental infection of Atlantic salmon *Salmo salar* pre-smolts by ip injection with new Irish and Norwegian salmonid alphavirus (SAV) isolates: a comparative study, *Diseases of Aquatic Organisms*, vol. 75, no. 1, pp. 13.

Clem, L., Faulmann, E., Miller, N., Ellsaesser, C., Lobb, C. & Cuchens, M. (1984). Temperature-mediated processes in teleost immunity: Differential effects of *in vitr*o and *in vivo* temperatures on mitogenic responses of channel catfish lymphocytes, *Developmental & Comparative Immunology*, vol. 8, no. 2, pp. 313-322.

Clem, L.W., Miller, N.W. & Bly, J.E. (1991). Evolution of lymphocyte subpopulations, their interactions and temperature sensitivities, In *Phylogenesis of Immune Functions, eds Warr G. W. & Cohen N.* , pp. 191-213.

Cnaani, A., Tinman, S., Avidar, Y., Ron, M. & Hulata, G. (2004). Comparative study of biochemical parameters in response to stress in *Oreochromis aureus*, *O. mossambicus* and two strains of *O. niloticus*, *Aquaculture Research*, vol. 35, no. 15, pp. 1434-1440.

Collazos, M.E., Barriga, C. & Ortega, E. (1994). Optimum conditions for the activation of the alternative complement pathway of a cyprinid fish (*Tinca tinca* L.). Seasonal variations in the titers, *Fish & Shellfish Immunology*, vol. 4, no. 7, pp. 499-506.

Contador, E. (2014). *Epitheliocystis in lake trout (Salvelinus namaycush)*, MSc Thesis, University of Guelph, Guelph, Ontario, Canada.

Cooper, M.D. & Alder, M.N. (2006). The evolution of adaptive immune systems, *Cell*, vol. 124, no. 4, pp. 815-822.

Cope, O.B., Wallen, G.H. & Wood, E.M. (1970). Some chronic effects of 2, 4-D on the bluegill (*Lepomis macrochirus*), *Transactions of the American Fisheries Society*, vol. 99, no. 1, pp. 1-12.

Corbel, M. (1975). The immune response in fish: a review, *Journal of Fish Biology*, vol. 7, no. 4, pp. 539-563.

Cuchens, M.A. & Clem, L.W. (1977). Phylogeny of lymphocyte heterogeneity: II. Differential effects of temperature on fish T-like and B-like cells, *Cellular immunology*, vol. 34, no. 2, pp. 219-230.

Dalela, R.C., Bhatnagar, M.C., Tyagi, A.K. & Verma, S.R. (1979). Histological damage of gills in *Channa gachua* after acute and subacute exposure to endosulfan and rogor, *Mikroskopie*, vol. 35, no. 11-12, pp. 301-307.

Dalmo, R., Ingebrigtsen, K. & Bøgwald, J. (1997). Non-specific defence mechanisms in fish, with particular reference to the reticuloendothelial system (RES), *Journal of Fish Diseases*, vol. 20, no. 4, pp. 241-273.

Dalmo, R.A. & Bøgwald, J. (2008). ß-glucans as conductors of immune symphonies, *Fish & Shellfish Immunology*, vol. 25, no. 4, pp. 384-396.

Dannevig, B.H., Lauve, A., Press, C.M. & Landsverk, T. (1994). Receptor-mediated endocytosis and phagocytosis by rainbow trout head kidney sinusoidal cells, *Fish & Shellfish Immunology*, vol. 4, no. 1, pp. 3-18.

Da Silva, P.F. (2014). A novel image analysis approach to characterise the effects of dietary components on intestinal morphology and immune system in Atlantic salmon. PhD thesis: University of Stirling.

Daunoravicius, D., Besusparis, J., Zurauskas, E., Laurinaviciene, A., Bironaite, D., Pankuweit, S., Plancoulaine, B., Herlin, P., Bogomolovas, J., Grabauskiene, V. & Laurinavicius, A. (2014). Quantification of myocardial fibrosis by digital image analysis and interactive stereology, *Diagnostic Pathology*, vol. 9, pp. 114-1596-9-114.

Dautremepuits, C., Fortier, M., Croisetiere, S., Belhumeur, P. & Fournier, M. (2006). Modulation of juvenile brook trout (*Salvelinus fontinalis*) cellular immune system after *Aeromonas salmonicida* challenge, *Veterinary Immunology and Immunopathology*, vol. 110, no. 1, pp. 27-36.

Delannoy, C.M., Houghton, J.D., Fleming, N.E. & Ferguson, H.W. (2011). Mauve stingers (*Pelagia noctiluca*) as carriers of the bacterial fish pathogen *Tenacibaculum maritimum*, *Aquaculture*, vol. 311, no. 1, pp. 255-257.

Dexiang, C. & Ainsworth, A.J. (1991). Effect of temperature on the immune system of channel catfish (*Ictalurus punctatus*), Adaptation of anterior kidney phagocytes to 10° C, *Comparative Biochemistry and Physiology Part A: Physiology*, vol. 100, no. 4, pp. 913-918.

Dheda, K., Huggett, J.F., Bustin, S.A., Johnson, M.A., Rook, G. & Zumla, A. (2004). Validation of housekeeping genes for normalizing RNA expression in real-time PCR, *Bio Techniques,* vol. 37, pp. 112-119.

Diamond, J., Anderson, N.H., Bartels, P.H., Montironi, R. & Hamilton, P.W. (2004). The use of morphological characteristics and texture analysis in the identification of tissue composition in prostatic neoplasia, *Human Pathology,* vol. 35, no. 9, pp. 1121-1131.

Dinarello, C.A. (1997). Interleukin-1, *Cytokine & growth factor reviews,* vol. 8, no. 4, pp. 253-265.

Doñate Jimeno, C. & Mackenzie, S.A. (2008). A transcriptomic approach toward understanding PAMP-driven macrophage activation and dietary immunostimulation in fish, PhD Thesis. University of Barcelona.

Dorin, D., Sire, M. & Vernier, J. (1994), Demonstration of an antibody response of the anterior kidney following intestinal administration of a soluble protein antigen in trout, *Comparative Biochemistry and Physiology Part B: Comparative Biochemistry*, vol. 109, no. 2, pp. 499-509.

Doube, M., Kłosowski, M.M., Arganda-Carreras, I., Cordelières, F.P., Dougherty, R.P., Jackson, J.S., Schmid, B., Hutchinson, J.R. & Shefelbine, S.J. (2010). Free and extensible bone image analysis in ImageJ, *Bone,* vol. 47, no. 6, pp. 1076-1079.

Drury, R. & Wallington, E. (1980). Carleton's Histological Technique, Oxford Medical Publication.

Dunel-Erb, S., Bailly, Y. & Laurent, P. (1982). Neuroepithelial cells in fish gill primary lamellae, *Journal Applied Physiology,* vol. 53, pp. 1342-1353.

Dunel-Erb, S., Chevalier, C. & Laurent, P. (1994). Distribution of neuroepithelial cells and neurons in the trout gill filament: comparison in spring and winter, *Canadian Journal of Zoology,* vol. 72, no. 10, pp. 1794-1799.

Eaton, W. (1990). Anti-viral activity in four species of salmonids following exposure to poly inosinic: cytidylic acid. *Diseases of Aquatic Organisms,* vol. 9, no. 3, pp. 193-198.

Ebran, N., Julien, S., Orange, N., Saglio, P., Lemaître, C. & Molle, G. (1999). Pore-forming properties and antibacterial activity of proteins extracted from epidermal mucus of fish. *Comparative Biochemistry and Physiology*. Part A, *Molecular & Integrative Physiology*, Vol. 122, No. 2, pp. 181-189

Eddy, F.B. & Handy, R.D. (2012). Ecological and environmental physiology of fishes, *Ecological and Environmental Physiology,* series, 4. Oxford University Press: Oxford. ISBN 978-0-19-954095-2, pp 253.,

Ellis, A. (2001). Innate host defense mechanisms of fish against viruses and bacteria, *Developmental & Comparative Immunology,* vol. 25, no. 8, pp. 827-839.

Ellsaesser, C.F., Bly, J.E. & Clem, L. (1988). Phylogeny of lymphocyte heterogeneity: the thymus of the channel catfish, *Developmental & Comparative Immunology,* vol. 12, no. 4, pp. 787-799.

Endeward, V., Cartron, J.P., Ripoche, P. & Gros, G. (2008). RhAG protein of the Rhesus complex is a CO_2 channel in the human red cell membrane, *FASEB Journal: Official Publication of the Federation of American Societies for Experimental Biology,* vol. 22, no. 1, pp. 64-73.

Espenes, A., Press, C.M., Dannevig, B. & Landsverk, T. 1995, Immune-complex trapping in the splenic ellipsoids of rainbow trout (*Oncorhynchus mykiss*), *Cell and Tissue Research,* vol. 282, no. 1, pp. 41-48.

Evans, D.L. & McKinney, E.C. (1990). Phylogeny of cytotoxic cells, *Phylogenesis of Immune Functions, CRC Press, Boca Raton, FL,* pp. 215-239.

Evans, D.H., Piermarini, P.M. & Choe, K.P. (2005). The multifunctional fish gill: dominant site of gas exchange, osmoregulation, acid-base regulation, and excretion of nitrogenous waste, *Physiological Reviews,* vol. 85, no. 1, pp. 97-177.

Evans, D. (2006) *Gyrodactylus salaris*, Monogean salmon parasite. Retrieved January 15th 2014 from: http://www.habitas.org.uk/invasive/species.

Falk, K., Batts, W., Kvellestad, A., Kurath, G., Wiik-Nielsen, J. & Winton, J. (2008). Molecular characterisation of Atlantic salmon paramyxovirus (ASPV): a novel paramyxovirus associated with proliferative gill inflammation, *Virus Research,* vol. 133, no. 2, pp. 218-227.

Farto, R., Milton, D.L., Bermudez, M.B. & Nieto, T.P. (2011). Colonization of turbot tissues by virulent and avirulent *Aeromonas salmonicida* subsp. *salmonicida* strains during an infection, *Diseases of Aquatic Organisms,* vol. 95, no. 2, pp. 167-173.

Fast, M.D.,Sims, D.E. Burka., J.F.; Mustafa, A. & Ross, N.W. (2002). Skin morphology and humoral non-specific defence parameters of mucus and plasma in rainbow trout; coho and Atlantic salmon. *Comparative Biochemistry and Physiology*, Vol. 132, No. 3, pp. 645-57

Fast, M., Johnson, S. & Jones, S. (2007). Differential expression of the pro-inflammatory cytokines IL-1β-1, TNFα-1 and IL-8 in vaccinated pink (*Oncorhynchus gorbuscha*) and chum (*Oncorhynchus keta*) salmon juveniles, *Fish & Shellfish Immunology*, vol. 22, no. 4, pp. 403-407.

Ferguson, H., Morrison, D., Ostland, V., Lumsden, J. & Byrne, P. (1992). Responses of mucus-producing cells in gill disease of rainbow trout (*Oncorhynchus mykiss*), *Journal of Comparative Pathology,* vol. 106, no. 3, pp. 255-265.

Ferguson, H. (2006). Systemic pathology of fish: a text and atlas of normal tissue responses in teleosts, and their responses in disease*Scotian Press, , London,* vol. 17, pp. 191-214.

Ferguson, H.W., Delannoy, C.M., Hay, S., Nicolson, J., Sutherland, D. & Crumlish, M. (2010). Jellyfish as vectors of bacterial disease for farmed salmon (*Salmo salar*), *Journal of Veterinary Diagnostic Investigation,* vol. 22, no. 3, pp. 376-382.

Finn, J.P. & Nielson, N. (1971). The inflammatory response of rainbow trout, *Journal of Fish Biology,* vol. 3, no. 4, pp. 463-478.

Fischer, U., Koppang, E.O. & Nakanishi, T. (2013). Teleost T and NK cell immunity, *Fish & Shellfish Immunology*, vol. 35, no. 2, pp. 197-206.

Fischer, U., Utke, K., Somamoto, T., Kollner, B., Ototake, M., & Nakanishi, T. (2006). Cytotoxic activities of fish leucocytes. *Fish & Shellfish Immunology* vol. 20, pp. 209-226.

Fletcher, T. (1981). Non-antibody molecules and the defense mechanisms of fish. In: *Stress and fish,* ed. Pickering, A.D. Academic press London, UK. pp. 171-183.

Fletcher, T.C., Jones, R. & Reid, L. (1976), Identification of glycoproteins in goblet cells of epidermis and gill of plaice (*Pleuronectes platessa* L.), flounder (*Platichthys flesus* L.) and rainbow trout (*Salmo gairdneri* Richardson), *The Histochemical Journal,* vol. 8, no. 6, pp. 597-608.

Fónyad, L., Krenács, T., Nagy, P., Zalatnai, A., Csomor, J., Sápi, Z., Pápay, J., Schönléber, J., Diczházi, C. & Molnár, B. (2012). Validation of diagnostic accuracy using digital slides in routine histopathology, *Diagnostic Pathology,* vol. 7, pp. 35.

Fredriksen, B., Sævareid, K., McAuley, L., Lane, M., Bøgwald, J. & Dalmo, R. (2011). Early immune responses in Atlantic salmon (*Salmo salar* L.) after immunization with PLGA nanoparticles loaded with a model antigen and β-glucan, *Vaccine,* vol. 29, no. 46, pp. 8338-8349.

Gaikowski, M.P., Rach, J.J. & Ramsay, R.T. (1999). Acute toxicity of hydrogen peroxide treatments to selected life stages of cold-, cool-, and warm water fish, *Aquaculture,* vol. 178, no. 3, pp. 191-207.

Galindo-Villegas, J. & Hosokawa, H. (2004). Immunostimulants: towards temporary prevention of diseases in marine fish, *Advances en Nutricion. Acuicola VII Memorias del VII Simposium Internationale de Nutricion Acuícola,* pp. 16-19.

García-Ayala, A. & Chaves-Pozo, E. (2009). Leukocytes and cytokines present in fish testis: A review, Chapter 2, In: Fish Defenses, Volume 1: Immunology, G. Zaccone, J. Meseguer, A. García-Ayala, B.G. Kapoor (Eds.), 37-74, Science Publishers, ISBN 978-1-57808-327-5, Enfield, New Hampshire, USA.

Garduño, R.A., Kuzyk, M.A. & Kay, W.W. (1997). Structural and physiological determinants of resistance of *Aeromonas salmonicida* to reactive radicals, *Canadian Journal of Microbiology,* vol. 43, no. 11, pp. 1044-1053.

Ghaznavi, F., Evans, A., Madabhushi, A. & Feldman, M. (2013). Digital imaging in pathology: whole-slide imaging and beyond, *Annual Review of Pathology: Mechanisms of Disease,* vol. 8, pp. 331-359.

Giulietti, A., Overbergh, L., Valckx, D., Decallonne, B., Bouillon, R. & Mathieu, C. (2001). An overview of real-time quantitative PCR: applications to quantify cytokine gene expression, *Methods,* vol. 25, no. 4, pp. 386-401.

Gjessing, M., 2014. Demonstration of a novel histopathological scoring system for salmonid gills. In: The International Gill Health Initiative, 2nd meeting, 21-23 may, 2014, Oslo.

Gomez, D., Sunyer, J.O. & Salinas, I. (2013). The mucosal immune system of fish: The evolution of tolerating commensals while fighting pathogens, *Fish & Shellfish Immunology,* vol. 35, no. 6, pp. 1729-1739.

Gozhenko, A; Gurkalova, I.P.; Zukow, W. & Kwasnik, Z (2009). Pathology - Theory. medical student's Library. Radom. pp. 270–275

Gräns, A., Rosengren, M., Niklasson, L. & Axelsson, M. (2012). Behavioural fever boosts the inflammatory response in rainbow trout *Oncorhynchus mykiss*, *Journal of Fish Biology,* vol. 81, no. 3, pp. 1111-1117.

Graves, S.S., Evans, D.L. & Dawe, D.L. (1985) Mobilization and activation of nonspecific cytotoxic cells (NCC) in the channel catfish (*Ictalurus punctatus*) infected with *Ichthyophthirius multifiliis*, *Comparative Immunology, Microbiology and Infectious Diseases,* vol. 8, no. 1, pp. 43-51.

Gurcan, M.N., Boucheron, L.E., Can, A., Madabhushi, A., Rajpoot, N.M. & Yener, B. (2009). Histopathological image analysis: A review, *Biomedical Engineering, IEEE Reviews in,* vol. 2, pp. 147-171.

Hamerman, J.A., Ogasawara, K. & Lanier, L.L. (2005). NK cells in innate immunity, *Current Opinion in Immunology,* vol. 17, no. 1, pp. 29-35.

Hamuro, K., Suetake, H., Saha, N.R., Kikuchi, K. & Suzuki, Y. (2007). A teleost polymeric Ig receptor exhibiting two Ig-like domains transports tetrameric IgM into the skin. *Journal of Immunology* , vol. 178, no. 9, pp. 5682-5689.

Hansen, J.D., Landis, E.D. & Phillips, R.B. (2005). Discovery of a unique Ig heavy-chain isotype (IgT) in rainbow trout: Implications for a distinctive B cell developmental pathway in teleost fish, *Proceedings of the National Academy of Sciences of the United States of America,* vol. 102, no. 19, pp. 6919-6924.

Hanzelova, V., Kuchta, R., Scholz, T. & Shinn, A. (2005). Morphometric analysis of four species of *Eubothrium* (Cestoda: *Pseudophyllidea*) parasites of salmonid fish: An interspecific and intraspecific comparison, *Parasitology International,* vol. 54, no. 3, pp. 207-214.

Harun, N.O., Wang, T. & Secombes, C.J. (2011). Gene expression profiling in naïve and vaccinated rainbow trout after *Yersinia ruckeri* infection: Insights into the mechanisms of protection seen in vaccinated fish, *Vaccine,* vol. 29, no. 26, pp. 4388-4399.

Hastein, T. & Gudding, R. (2005). Emergency preparedness of aquatic animal diseases: Norwegian experiences, *FAO Fisheries Proceedings (FAO),* p. 79–85.

Haugarvoll, E., Bjerkås, I., Nowak, B.F., Hordvik, I. & Koppang, E.O. (2008). Identification and characterization of a novel intraepithelial lymphoid tissue in the gills of Atlantic salmon, *Journal of Anatomy,* vol. 213, no. 2, pp. 202-209.

Heid, C.A., Stevens, J., Livak, K.J. & Williams, P.M. (1996). Real time quantitative PCR, *Genome Research,* vol. 6, no. 10, pp. 986-994.

Helfman, G., Collette, B.B., Facey, D.E. & Bowen, B.W. (2009). *The Diversity of Fishes: Biology, Evolution, and Ecology*, 2nd ed. John Wiley & Sons, UK:. 736 pp

Helge Stien, L., Manne, F., Ruohonene, K., Kause, A., Rungruangsak-Torrissen, K. & Kiessling, A. (2006). Automated image analysis as a tool to quantify the colour and composition of rainbow trout (*Oncorhynchus mykiss* W.) cutlets, *Aquaculture,* vol. 261, no. 2, pp. 695-705.

Henriksen, M.M.M., Madsen, L. & Dalsgaard, I. (2013). Effect of hydrogen peroxide on immersion challenge of rainbow trout fry with *Flavobacterium psychrophilum*, *PLOS one,* vol. 8, no. 4, pp. e62590.

Henriksen, M., Kania, P., Buchmann, K. & Dalsgaard, I. (2014). Effect of hydrogen peroxide and/or *Flavobacterium psychrophilum* on the gills of rainbow trout, *Oncorhynchus mykiss* (Walbaum), *Journal of Fish Diseases* vol. 38, no. 3, pp. 259-270.

Herath, T.K. (2010). Cellular and Molecular Pathogenesis of Salmonid Alphavirus 1 in Atlantic Salmon *Salmo salar* L., PhD Thesis, Institute of aquaculture, University of Stirling.

Hirono, I., Nam, B., Enomoto, J., Uchino, K. & Aoki, T. (2003). Cloning and characterisation of a cDNA encoding Japanese flounder *Paralichthys olivaceus* IgD, *Fish & Shellfish Immunology,* vol. 15, no. 1, pp. 63-70.

Hoffmann, K. (2009). Stimulating immunity in fish and crustaceans: some light but more shadows, *AQUA Culture AsiaPasific Magazine,* vol. 3, pp. 22-25.

Hølvold, L.B. (2007). Immunostimulants connecting innate and adaptive immunity in Atlantic salmon (*Salmo salar*), MSc Thesis, Norwegian School of Fisheries Biology, University of Tromso, Norway.

Horsberg, T. (2003). Aquatic animal medicine, *Journal of Veterinary Pharmacology and Therapeutics,* vol. 26, no. 1-2, pp. 39-42.

Houston, R.D., Davey, J.W., Bishop, S.C., Lowe, N.R., Mota-Velasco, J.C., Hamilton, A., Guy, D.R., Tinch, A.E., Thomson, M.L., Blaxter, M.L., Gharbi, K., Bron, J.E. & Taggart, J.B. (2012). Characterisation of QTL-linked and genome-wide restriction site-associated DNA (RAD) markers in farmed Atlantic salmon, *BMC Genomics,* vol. 13, pp. 244-2164-13-244.

Hughes, G., Perry, S. & Brown, V. (1979). A morphometric study of effects of nickel, chromium and cadmium on the secondary lamellae of rainbow trout gills, *Water Research,* vol. 13, no. 7, pp. 665-679.

Hughes, G. & Wright, D. (1970). A comparative study of the ultrastructure of the water-blood pathway in the secondary lamellae of teleost and elasmobranch fishes—benthic forms, *Zeitschrift für Zellforschung und mikroskopische Anatomie,* vol. 104, no. 4, pp. 478-493.

Janda, J.M. & Abbott, S.L. (2010). The genus *Aeromonas*: taxonomy, pathogenicity, and infection, *Clinical microbiology reviews,* vol. 23, no. 1, pp. 35-73.

Jensen, L.B., Boltana, S., Obach, A., McGurk, C., Waagbo, R. & MacKenzie, S. (2014). Investigating the underlying mechanisms of temperature-related skin diseases in Atlantic salmon, *Salmo salar* L., as measured by quantitative histology, skin transcriptomics and composition, *Journal of Fish Diseases,* doi:10.1111/jfd.12314..

Jerald Ainsworth, A. & Dexiang, C. (1990). Differences in the phagocytosis of four bacteria by channel catfish neutrophils, *Developmental & Comparative Immunology,* vol. 14, no. 2, pp. 201-209.

Jimeno, C.D., (2008). A transcriptomic approach toward understanding PAMP-driven macrophage activation and dietary immunostimulant in fish. PhD Thesis, pp 1-222, *Departament de Biologia Cellular, Fisiologia i Immunologia, Facultat de Ciències, Universitat Autòmona de Barcelona, Barcelona, Spain*

Johnson, S., Constible, J. & Richard, J. (1993). Laboratory investigations on the efficacy of hydrogen peroxide against the salmon louse *Lepeophtheirus salmonis* and its toxicological and histopathological effects on Atlantic salmon *Salmo salar* and chinook salmon *Oncorhynchus tshawytscha*, *Diseases of Aquatic Organisms,* vol. 17, no. 3, pp. 197-204.

Jokumsen, A. & Svendsen, L.M. (2010). *Farming of freshwater rainbow trout in Denmark,* DTU Aqua. Institut for Akvatiske Ressourcer.

Jones, R. and Reid, L. (1978). Secretory cells and their glycoproteins in health and diseases. *British Medical Bulletin,* vol. 34, no. 1, pp. 9-16.

Jones, S.R.M. (2001). The occurrence and mechanisms of innate immunity against parasites in fish. Developmental and Comparative Immunology, Vol. 25, pp. 841-852.

Joosten, P., Kruijer, W. & Rombout, J. (1996). Anal immunisation of carp and rainbow trout with different fractions of a *Vibrio anguillarum* bacterin, *Fish & Shellfish Immunology,* vol. 6, no. 8, pp. 541-551.

Jørgensen, J.B., Lunde, H., Jensen, L. Whitehead, A.S. & Robertsen, B. (2000). Serum amyloid A transcription in Atlantic salmon (*Salmo salar* L.) hepatocytes is enhanced by stimulation with macrophage factors, recombinant human IL-1β, IL-6 and TNFα or bacterial lipopolysaccharide, *Developmental & Comparative Immunology,* vol. 24, no. 6, pp. 553-563.

Jørgensen, S.M., Castro, V., Krasnov, A., Torgersen, J., Timmerhaus, G., Hevrøy, E.M., Hansen, T.J., Susort, S., Breck, O. & Takle, H. (2014). Cardiac responses to elevated seawater temperature in Atlantic salmon, *BMC physiology,* vol. 14, no. 1, pp. 2.

Kaattari, S.L. (1994). Development of a piscine paradigm of immunological memory, *Fish & Shellfish Immunology,* vol. 4, no. 6, pp. 447-457.

Kaattari, S.L., Piganell J.D. The specific immune system: humoral defense. In: Iwama, G., Nakanishi, T. (Eds.). The Fish Immune System. Academic press, NewYork, pp. 1996; pp. 207-254.

Kawai, T. & Akira, S. (2005). Pathogen recognition with Toll-like receptors, *Current Opinion in Immunology,* vol. 17, no. 4, pp. 338-344.

Kiemer, M.C. & Black, K.D. (1997). The effects of hydrogen peroxide on the gill tissues of Atlantic salmon, *Salmo solar* L., *Aquaculture,* vol. 153, no. 3, pp. 181-189.

Kiron, V. (2012). Fish immune system and its nutritional modulation for preventive health care, *Animal Feed Science and Technology,* vol. 173, no. 1, pp. 111-133.

Kitani, A. & Xu, L. (2008). Regulatory T cells and the induction of IL-17, *Mucosal immunology,* vol. 1, pp. S43-S46.

Knudsen, D., Urán, P., Arnous, A., Koppe, W. & Frøkiær, H. (2007). Saponin-containing sub fractions of soybean molasses induce enteritis in the distal intestine of Atlantic salmon, *Journal of Agricultural and Food Chemistry,* vol. 55, no. 6, pp. 2261-2267.

Kono, T., Fujiki, K., Nakao, M., Yano, T., Endo, M. & Sakai, M. (2002). The immune responses of common carp, *Cyprinus carpio* L., injected with carp interleukin-1 β gene, *Journal of Interferon & Cytokine Research,* vol. 22, no. 4, pp. 413-419.

Koppang, E.O., Fischer, U., Moore, L., Tranulis, M.A., Dijkstra, J.M., Köllner, B., Aune, L., Jirillo, E. & Hordvik, I. (2010). Salmonid T cells assemble in the thymus, spleen and in novel interbranchial lymphoid tissue, *Journal of Anatomy,* vol. 217, no. 6, pp. 728-739.

Krkošek, M., Connors, B.M., Ford, H., Peacock, S., Mages, P., Ford, J.S., Morton, A., Volpe, J.P., Hilborn, R. & Dill, L.M. (2011). Fish farms, parasites, and predators: implications for salmon population dynamics, *Ecological Applications,* vol. 21, no. 3, pp. 897-914.

Kvellestad, A., Falk, K., Nygaard, S.M., Flesja, K. & Holm, J.A. (2005). Atlantic salmon paramyxovirus (ASPV) infection contributes to proliferative gill inflammation (PGI) in sea-water-reared *Salmo salar*, *Diseases of Aquatic Organisms,* vol. 67, pp. 47.

Kvellestad, A., Dannevig, B.H. & Falk, K. (2003). Isolation and partial characterization of a novel paramyxovirus from the gills of diseased seawater-reared Atlantic salmon (*Salmo salar* L), *The Journal of General Virology,* vol. 84, no.8, pp. 2179-2189.

Le Morvan, C., Deschaux, P. & Troutaud, D. (1996). Effects and mechanisms of environmental temperature on carp (*Cyprinus carpio*) anti-DNP antibody response and non-specific cytotoxic cell activity: A kinetic study, *Developmental & Comparative Immunology,* vol. 20, no. 5, pp. 331-340.

Le Morvan, C., Cleton, P., Deschaus, P. & Trountaud, D. (1997). Effects of environmental temperature on macrophage activities in carp, *Fish & Shellfish Immunology,* vol. 7, no. 3, pp. 209-212.

Le Morvan, C., Troutaud, D. & Deschaux, P. (1998). Differential effects of temperature on specific and nonspecific immune defenses in fish, *The Journal of experimental biology,* vol. 201, no. Pt 2, pp. 165-168.

Li, J., Barreda, D.R., Zhang, Y., Boshra, H., Gelman, A.E., LaPatra, S., Tort, L. & Sunyer, J.O. (2006). B lymphocytes from early vertebrates have potent phagocytic and microbicidal abilities, *Nature Immunology*, vol. 7, no. 10, pp. 1116-1124.

Lillehaug, A. (1997). Vaccination strategies in seawater cage culture of salmonids, *Developments in Biological Standardization*, vol. 90, pp. 401-408.

Loukas, C., Kostopoulos, S., Tanoglidi, A., Glotsos, D., Sfikas, C. & Cavouras, D. (2013). Breast cancer characterization based on image classification of tissue sections visualized under low magnification, *Computational and Mathematical Methods in Medicine*, vol. 2013, Article ID 829461,doi:10.1155/2013/829461.

Lockey C, Otto E, Long Z (1998). Real-time fluorescence detection of a single DNA molecule. *Biotechniques* 24: 744–746.

Lowe-Jinde, L. & Niimi, A. (1984). Short-term and long-term effects of cadmium on glycogen reserves and liver size in rainbow trout (*Salmo gairdneri* Richardson), *Archives of Environmental Contamination and Toxicology*, vol. 13, no. 6, pp. 759-764.

Machlin, L.J. & Bendich, A. (1987). Free radical tissue damage: protective role of antioxidant nutrients, *FASEB journal : official publication of the Federation of American Societies for Experimental Biology*, vol. 1, no. 6, pp. 441-445.

Macice, A. M., Singma H. T., and Fletcheb. 1 975. Studies on the cytolytis: effects of seastar (*Marthsterias ghaciall*) saponins and synthetic surfactants in the plaice *Pleuro~ctespkatessa Biology*, vol. 29: 367-314.

Madabhushi, A. (2009). Digital pathology image analysis: opportunities and challenges, *Imaging in Medicine*, vol. 1, no. 1, pp. 7-10.

Magnadóttir, B., Gudmundsdóttir, S. & Gudmundsdottir, B. (1995). Study of the humoral response of Atlantic salmon (*Salmo salar* L.), naturally infected with *Aeromonas salmonicida* ssp. achromogenes, *Veterinary Immunology and Immunopathology*, vol. 49, no. 1, pp. 127-142.

Magnadóttir, B. (2006). Innate immunity of fish (overview), *Fish & Shellfish Immunology*, vol. 20, no. 2, pp. 137-151.

Magnadottir, B. (2010). Immunological control of fish diseases, *Marine Biotechnology*, vol. 12, no. 4, pp. 361-379.

Maina, J. (2002). Structure, function and evolution of the gas exchangers: comparative perspectives, *Journal of Anatomy*, vol. 201, no. 4, pp. 281-304.

Maina, J.N. (1991). A morphometric analysis of chloride cells in the gills of the teleosts *Oreochromis alcalicus* and *Oreochromis niloticus* and a description of presumptive urea-excreting cells in *O. alcalicus*, *Journal of Anatomy*, vol. 175, pp. 131-145.

Maina, J.N. & West, J.B. (2005). Thin and strong! The bioengineering dilemma in the structural and functional design of the blood-gas barrier, *Physiological Reviews*, vol. 85, no. 3, pp. 811-844.

Mallatt, J. (1985) Fish gill structural changes induced by toxicants and other irritants: a statistical review, *Canadian Journal of Fisheries and Aquatic Sciences*, vol. 42, no. 4, pp. 630-648.

Mallet, R.T., Squires, J.E., Bhatia, S. & Sun, J. (2002). Pyruvate restores contractile function and antioxidant defenses of hydrogen peroxide-challenged myocardium, *Journal of Molecular and Cellular Cardiology*, vol. 34, no. 9, pp. 1173-1184.

Malmstrøm, M., Jentoft, S., Gregers, T.F. & Jakobsen, K.S. (2013). Correction: unraveling the evolution of the Atlantic cod's (*Gadus morhua* L.) alternative immune strategy, *PloS one*, vol. 8, no. 10.

Manning, M.J. (1994). Fishes. In: Immunology: A Comparative Approach, R.J. Turner (Ed.), 69-100, John Wiley & Sons Ltd., ISBN 0471944009, Chichester, UK

Mansell, B., Powell, M., Ernst, I. & Nowak, B.F. (2005). Effects of the gill monogenean *Zeuxapta seriolae* (Meserve, 1938) and treatment with hydrogen peroxide on pathophysiology of kingfish, *Seriola lalandi* Valenciennes, 1833, *Journal of Fish Diseases*, vol. 28, no. 5, pp. 253-262.

Maplajacn., L., and Singh J. J.(1 973). Water pollution in relation to the biology of fishes. In: Histopathologicd changes induced by synthetic indetergents in the gills of Heteropneustes fossilis (Bloch). Wm. Syrnp. Envkon. Poll. 18-25.

Marcos-López, M., Mitchell, S. & Rodger, H. (2014). Pathology and mortality associated with the mauve stinger jellyfish *Pelagia noctiluca* in farmed Atlantic salmon *Salmo salar* L., *Journal of Fish Diseases, (In press).*

Marrocco, C., Molinara, M., D'Elia, C. & Tortorella, F. (2010). A computer-aided detection system for clustered microcalcifications, *Artificial Intelligence in Medicine,* vol. 50, no. 1, pp. 23-32.

Martin, S.A., Douglas, A., Houlihan, D.F. & Secombes, C.J. (2010). Starvation alters the liver transcriptome of the innate immune response in Atlantic salmon (*Salmo salar*), *BMC Genomics,* vol. 11, pp. 418-2164-11-418.

Martinez-Rubio, L., Morais, S., Evensen, Ø., Wadsworth, S., Ruohonen, K., Vecino, J.L., Bell, J.G. & Tocher, D.R. (2012). Functional feeds reduce heart inflammation and pathology in Atlantic salmon (*Salmo salar* L.) following experimental challenge with Atlantic salmon reovirus (ASRV), *PloS one,* vol. 7, no. 11, pp. e40266.

Martinez-Rubio, L., Wadsworth, S., González Vecino, J.L., Bell, J.G. & Tocher, D.R. (2013a). Effect of dietary digestible energy content on expression of genes of lipid metabolism and LC-PUFA biosynthesis in liver of Atlantic salmon (*Salmo salar* L.), *Aquaculture,* vol. 384, pp. 94-103.

Martinez-Rubio, L., Morais, S., Evensen, Ø., Wadsworth, S., Vecino, J.G., Ruohonen, K., Bell, J.G. & Tocher, D.R. (2013b). Effect of functional feeds on fatty acid and eicosanoid metabolism in liver and head kidney of Atlantic salmon (*Salmo salar* L.) with experimentally induced Heart and Skeletal Muscle Inflammation. *Fish & Shellfish Immunology,* vol. 34, no. 6, pp. 1533-1545.

Martinez-Rubio, L., Evensen, O., Krasnov, A., Jorgensen, S.M., Wadsworth, S., Ruohonen, K., Vecino, J.L. & Tocher, D.R. (2014). Effects of functional feeds on the lipid composition, transcriptomic responses and pathology in heart of Atlantic salmon (*Salmo salar* L.) before and after experimental challenge with Piscine Myocarditis Virus (PMCV), *BMC Genomics,* vol. 15, pp. 462-2164-15-462.

Matey, V., Iftikar, F.I., De Boeck, G., Scott, G.R., Sloman, K.A., Almeida-Val, V.M., Val, A.L. & Wood, C.M. (2011). Gill morphology and acute hypoxia: responses of mitochondria-rich, pavement, and mucous cells in the Amazonian oscar (*Astronotus ocellatus*) and the rainbow trout (*Oncorhynchus mykiss*), two species with very different approaches to the osmo-respiratory compromise, *Canadian Journal of Zoology,* vol. 89, no. 4, pp. 307-324.

Matthews, C.G., Richards, R.H., Shinn, A.P. & Cox, D.I. (2013). Gill pathology in Scottish farmed Atlantic salmon, *Salmo salar* L., associated with the microsporidian *Desmozoon lepeophtherii* Freeman et Sommerville (2009). *Journal of Fish Diseases,* vol. 36, no. 10, pp. 861-869.

Mencarelli, R., Marcolongo, A. & Gasparetto, A. (2008). Organizational model for a telepathology system, *Diagnostic Pathology,* vol. 3, no. 1, pp. S7.

Meseguer, J., López-Ruiz, A. & Garcí-Ayala, A. 1995, Reticulo-endothelial stroma of the head-kidney from the seawater teleost gilthead seabream (*Sparus aurata* L.): An ultrastructural and cytochemical study, *The Anatomical Record,* vol. 241, no. 3, pp. 303-309.

Midtlyng, P., Reitan, L. & Speilberg, L. (1996). Experimental studies on the efficacy and side-effects of intraperitoneal vaccination of Atlantic salmon (*Salmo salar* L.) against furunculosis, *Fish & Shellfish Immunology,* vol. 6, no. 5, pp. 335-350.

Miller, K.M., Teffer, A., Tucker, S., Li, S., Schulze, A.D., Trudel, M., Juanes, F., Tabata, A., Kaukinen, K.H. & Ginther, N.G. (2014). Infectious disease, shifting climates, and opportunistic predators: cumulative factors potentially impacting wild salmon declines, *Evolutionary Applications,* vol;7, no 7, pp.812-55

Mitchell, S.O., Baxter, E.J. & Rodger, H.D. (2011). Gill pathology in farmed salmon associated with the jellyfish *Aurelia aurita*, *The Veterinary record,* vol. 169, no. 23, pp. 609.

Mitchell, S. & Rodger, H. (2011). A review of infectious gill disease in marine salmonid fish, *Journal of Fish Diseases,* vol. 34, no. 6, pp. 411-432.

Mitchell, S.O., Baxter, E.J., Holland, C. & Rodger, H.D. (2012). Development of a novel histopathological gill scoring protocol for assessment of gill health during a longitudinal study in

marine-farmed Atlantic salmon (*Salmo salar*). *Aquaculture International*, vol. 20, no. 5, pp. 813-825.

Mitrovic, D., Dymowska, A., Nilsson, G.E. & Perry, S.F. (2009). Physiological consequences of gill remodeling in goldfish (*Carassius auratus*) during exposure to long-term hypoxia, *American Journal of Physiology.Regulatory, integrative and comparative physiology*, vol. 297, no. 1, pp. R224-34.

Mitrovic, D. & Perry, S.F. (2009). The effects of thermally induced gill remodeling on ionocyte distribution and branchial chloride fluxes in goldfish (*Carassius auratus*), *The Journal of Experimental Biology*, vol. 212, no. Pt 6, pp. 843-852.

Morais, S., Monroig, O., Zheng, X., Leaver, M.J., Tocher, D.R. (2009). Highly unsaturated fatty acid synthesis in Atlantic salmon: characterisation of ELOVL5- and ELOVL2-like elongases. *Marine Biotechnology* 11, 627–639.

Montalto, M., D'onofrio, F., Gallo, A., Cazzato, A. & Gasbarrini, G. (2009). Intestinal microbiota and its functions, *Digestive and Liver Disease Supplements*, vol. 3, no. 2, pp. 30-34.

Montero, D., Marrero, M., Izquierdo, M., Robaina, L., Vergara, J. & Tort, L. (1999). Effect of vitamin E and C dietary supplementation on some immune parameters of gilthead sea bream (*Sparus aurata*) juveniles subjected to crowding stress, *Aquaculture*, vol. 171, no. 3, pp. 269-278.

Moon, J.Y., Hong, Y., Kong, H.J., Kim, D., Kim, Y., Kim, W., Ji, Y.J., An, C.M. & Nam, B. (2014). A cDNA microarray analysis to identify genes involved in the acute-phase response pathway of the olive flounder after infection with *Edwardsiella tarda*, *Veterinary Immunology and Immunopathology*, vol. 161, no. 1, pp. 49-56.

Moore, J.D.; Ototake, M. & Nakanishi, T. (1998). Particulate antigen uptake during immersion immunisation of fish: The effectiveness of prolonged exposure and the roles of skin and gill. *Fish and Shellfish Immunology*, Vol. 8, pp. 393-407

Morera, D. & MacKenzie, S.A. (2011). Is there a direct role for erythrocytes in the immune response, *Veterinary Research*, vol. 42, no. 1, pp. 89.

Morera, D., Roher, N., Ribas, L., Balasch, J.C., Doñate, C., Callol, A., Boltaña, S., Roberts, S., Goetz, G. & Goetz, F.W. (2011). RNA-Seq reveals an integrated immune response in nucleated erythrocytes, *PloS one*, vol. 6, no. 10, pp. e26998.

Morganm and Tovelli P. W. A (1973). The structure of the gill of the trout, *Salmo gairdneri* (Richardson). *Journal of Anatamy*. 142: 147-162..

Morrison, R.N., Cooper, G.A., Koop, B.F., Rise, M.L., Bridle, A.R., Adams, M.B. & Nowak, B.F. (2006). Transcriptome profiling the gills of amoebic gill disease (AGD)-affected Atlantic salmon (*Salmo salar* L.): a role for tumor suppressor p53 in AGD pathogenesis? *Physiological Genomics*, vol. 26, no. 1, pp. 15-34.

Morrison, R. & Nowak, B. (2008). Immunohistochemical detection of anterior gradient-2 in the gills of amoebic gill disease-affected Atlantic salmon, *Salmo salar* L., *Journal of Fish Diseases*, vol. 31, no. 9, pp. 699-705.

Mulder, I., Wadsworth, S. & Secombes, C. (2007). Cytokine expression in the intestine of rainbow trout (*Oncorhynchus mykiss*) during infection with *Aeromonas salmonicida*, *Fish & Shellfish Immunology*, vol. 23, no. 4, pp. 747-759.

Mulero, I., Sepulcre, M.P., Meseguer, J., Garcia-Ayala, A. & Mulero, V. (2007). Histamine is stored in mast cells of most evolutionarily advanced fish and regulates the fish inflammatory response, *Proceedings of the National Academy of Sciences of the United States of America*, vol. 104, no. 49, pp. 19434-19439.

Munday, B., Zilberg, D. & Findlay, V. (2001). Gill disease of marine fish caused by infection with *Neoparamoeba pemaquidensis*, *Journal of Fish Diseases*, vol. 24, no. 9, pp. 497-507.

Murray, A.G. (2013). Epidemiology of the spread of viral diseases under aquaculture, *Current Opinion in Virology*, vol. 3, no. 1, pp. 74-78.

Nakayama, I., Matsumura, T., Kamataki, A., Uzuki, M., Saito, K., Hobbs, J., Akasaka, T. & Sawai, T. (2012). Development of a teledermatopathology consultation system using virtual slides, *Diagnostic Patholology*, vol. 7, pp. 177.

Nardocci, G., Navarro, C., Cortés, P.P., Imarai, M., Montoya, M., Valenzuela, B., Jara, P., Acuña-Castillo, C. & Fernández, R. (2014). Neuroendocrine mechanisms for immune system regulation during stress in fish, *Fish & Shellfish Immunology*, vol. 40, no. 2, pp. 531-538.

National Research Council, 2011. *Nutrient Requirements of Fish and Shrimp*. Washington, DC: The National Academies Press, ISBN: 978-0-309-16338-5.

Nayak, S. (2010). Probiotics and immunity: a fish perspective, *Fish & Shellfish Immunology*, vol. 29, no. 1, pp. 2-14.

Nelson, J. (1994). *Fishes of the World*. 4th Edi Hoboken: John Wiley & Sons, *USA*.

Niklasson, L., Sundh, H., Fridell, F., Taranger, G. & Sundell, K. (2011). Disturbance of the intestinal mucosal immune system of farmed Atlantic salmon (*Salmo salar*), in response to long-term hypoxic conditions, *Fish & Shellfish Immunology*, vol. 31, no. 6, pp. 1072-1080.

Nilsson, S. (1986). Control of gill blood flow, In Nilsson, S., Holmgren, S. (eds) *Fish Physiology: Recent Advances*, Croon Helm, Springer,London , pp. 86-101.

Nilsson, G.E. (2007). Gill remodeling in fish-a new fashion or an ancient secret ? *The Journal of Experimental Biology*, vol. 210, no. Pt 14, pp. 2403-2409.

Nilsson, G.E., Dymowska, A. & Stecyk, J.A. (2012). New insights into the plasticity of gill structure, *Respiratory Physiology & Neurobiology*, vol. 184, no. 3, pp. 214-222.

Nowak, B. & LaPatra, S. (2006). Epitheliocystis in fish, *Journal of Fish Diseases*, vol. 29, no. 10, pp. 573-588.

Nylund, A., Watanabe, K., Nylund, S., Karlsen, M., Saether, P., Arnesen, C. & Karlsbakk, E. (2008). Morphogenesis of salmonid gill poxvirus associated with proliferative gill disease in farmed Atlantic salmon (*Salmo salar*) in Norway, *Archives of Virology*, vol. 153, no. 7, pp. 1299-1309.

O'Connor, J., Neumann, D. & Sherk Jr, J. (1977). Sub-lethal effects of suspended sediments on estuarine fish. *Fort* Belvoir: Coastal Engineering Research Center; Springfield, https://archive.org/details/sublethaleffects00ocon.

Oliva-Teles, A. (2012). Nutrition and health of aquaculture fish, *Journal of Fish Diseases*, vol. 35, no. 2, pp. 83-108.

Olson, K.R. (1996). Scanning electron microscopy of the fish gill. In: Dutta, HM and JSD Mushi, eds. *Fish Morphology: horizons of new research.* Lebanon: Science Publishers, pp. 31-45.

Olson, K.R. (1991). Vasculature of the fish gill: anatomical correlates of physiological functions, *Journal of Electron Microscopy Technique*, vol. 19, no. 4, pp. 389-405.

Olson, K.R. (2002). Vascular anatomy of the fish gill, *Journal of Experimental Zoology*, vol. 293, no. 3, pp. 214-231.

Olson, K.R. (2011). Hydrogen sulfide is an oxygen sensor in the carotid body, *Respiratory Physiology & Neurobiology*, vol. 179, no. 2, pp. 103-110.

Ostrander, G.K. (2000). *The laboratory fish*, Elsevier, USA.

Ourth, D.D. & Wilson, E.A. (1982). Bactericidal serum response of the channel catfish against Gram-negative bacteria, *Developmental & Comparative Immunology*, vol. 6, no. 3, pp. 579-583.

Palaksha, K., Shin, G., Kim, Y. & Jung, T. (2008). Evaluation of non-specific immune components from the skin mucus of olive flounder (*Paralichthys olivaceus*), *Fish & Shellfish Immunology*, vol. 24, no. 4, pp. 479-488.

Parimi, V., Eisengart, L.J. & Yang, X.J. (2014). Automated detection and quantification of prostate cancer in needle biopsies by gigital image analysis, *Open Journal of Pathology*, vol. 4, pp 138-150.

Passer, B.J., Chen, C.H., Miller, N.W. & Cooper, M.D. (1996). Identification of AT lineage antigen in the catfish, *Developmental & Comparative Immunology*, vol. 20, no. 6, pp. 441-450.

Pasare, C. & Medzhitov, R. (2004). Toll-like receptors: linking innate and adaptive immunity, *Microbes and Infection*, vol. 6, no. 15, pp. 1382-1387.

Pedersen, L., Pedersen, P.B., Nielsen, J.L. & Nielsen, P.H. (2010). Long term/low dose formalin exposure to small-scale recirculation aquaculture systems, *Aquacultural Engineering*, vol. 42, no. 1, pp. 1-7.

Pennacchi, Y., Leef, M.J., Crosbie, P.B., Nowak, B.F. & Bridle, A.R. (2014). Evidence of immune and inflammatory processes in the gills of AGD-affected Atlantic salmon, *Salmo salar* L, *Fish & Shellfish Immunology*, vol. 36, no. 2, pp. 563-570.

Perry, S.F. & Tufts, B. (1998). Carbon dioxide transport and excretion. In: *FishRerespiration.*San Diago, California: Academic Press, pp 229-273.

Perry, S. & Gilmour, K. (2010). Oxygen uptake and transport in water breathers, *Respiratory physiology of vertebrates.Life with and without oxygen. Cambridge University Press, Cambridge*,pp. 49-94.

Pettersen, E.F., Ingerslev, H., Stavang, V., Egenberg, M. & Wergeland, H.I. (2008). A highly phagocytic cell line TO from Atlantic salmon is CD83 positive and M-CSFR negative, indicating a dendritic-like cell type, *Fish & Shellfish Immunology*, vol. 25, no. 6, pp. 809-819.

Peyghan, R. & Powell, M. (2006). Histopathological study of gills in experimentally amoebic gill disease (AGD) infected Atlantic salmon, *Salmo salar*, L., *Iranian Journal of Veterinary Research*, vol. 7, no. 4, pp. 8-13.

Pfaffl, M.W. (2001). A new mathematical model for relative quantification in real-time RT-PCR. *Nucleic Acids Research*, vol. 29, no. 9, pp. e45.

Pfaffl, M.W. Horgan, G.W. & Dempfle, L. (2002). Relative expression software tool (REST) for group-wise comparison and statistical analysis of relative expression results in real-time PCR, *Nucleic acids research*, vol. 30, no. 9, pp. e36.

Picchietti, S., Guerra, L., Bertoni, F., Randelli, E., Belardinelli, M.C., Buonocore, F., Fausto, A.M., Rombout, J., Scapigliati, G. & Abelli, L. (2011). Intestinal T cells of *Dicentrarchus labrax* (L.): gene expression and functional studies, *Fish & Shellfish Immunology*, vol. 30, no. 2, pp. 609-617.

Pinkney, A.E., Wright, D.A., Jepson, M.A. & Towle, D.W. (1989). Effects of tributyltin compounds on ionic regulation and gill ATPase activity in estuarine fish, *Comparative Biochemistry and Physiology Part C: Comparative Pharmacology*, vol. 92, no. 1, pp. 125-129.

Pisam M. (1981). Membranous systems in the chloride cell of teleostean fish gill: their modifications in response to the salinity of the environment. *The Anatomical Record*, Vo. 200: 401–414.

Pisam, M. Caroff, A. & Rambourg, A. (1987). Two types of chloride cells in the gill epithelium of a freshwater-adapted euryhaline fish: *Lebistes reticulatus*: their modifications during adaptation to saltwater, *American Journal of Anatomy*, vol. 179, no. 1, pp. 40-50.

Pisam, M., Prunet, P., Boeuf, G. & Jrambourg, A. (1988). Ultrastructural features of chloride cells in the gill epithelium of the Atlantic salmon, *Salmo salar*, and their modifications during smoltification, *American Journal of Anatomy*, vol. 183, no. 3, pp. 235-244.

Pittman, K., Sourd, P., Ravnøy, B., Espeland, Ø., Fiksdal, I., Oen, T., Pittman, A., Redmond, K. & Sweetman, J. (2011). Novel method for quantifying salmonid mucous cells, *Journal of Fish Diseases*, vol. 34, no. 12, pp. 931-936.

Pittman, K., Pittman, A., Karlson, S., Cieplinska, T., Sourd, P., Redmond, K., Ravnøy, B. & Sweetman, E. (2013). Body site matters: an evaluation and application of a novel histological methodology on the quantification of mucous cells in the skin of Atlantic salmon, *Salmo salar* L., *Journal of Fish Diseases*, vol. 36, no. 2, pp. 115-127.

Pörtner, H. & Peck, M. (2010). Climate change effects on fishes and fisheries: towards a cause-and-effect understanding, *Journal of Fish Biology*, vol. 77, no. 8, pp. 1745-1779.

Powell, M.D. & Perry, S.F. (1997). Respiratory and acid-base pathophysiology of hydrogen peroxide in rainbow trout (*Oncorhynchus mykiss* Walbaum), *Aquatic Toxicology*, vol. 37, no. 2, pp. 99-112.

Powell, M.D. & Perry, S.F. (1999). Cardio-respiratory effects of chloramine-T exposure in rainbow trout, *Experimental Biology Online*, vol. 4, no. 5, pp. 1-59.

Powell, M.D. & Kristensen, T. (2014). Freshwater treatment of amoebic gill disease and sea-lice in seawater salmon production: considerations of water chemistry and fish welfare, Norwegian Institute for Water Research. REPORT SNO 6632-2014.

Powell, M., Fisk, D. & Nowak, B. (2000). Effects of graded hypoxia on Atlantic salmon infected with amoebic gill disease, *Journal of Fish Biology*, vol. 57, no. 4, pp. 1047-1057.

Pratap, H. & Wendelaar Bonga, S. (1993). Effect of ambient and dietary cadmium on pavement cells, chloride cells, and Na/K-ATPase activity in the gills of the freshwater teleost *Oreochromis mossambicus* at normal and high calcium levels in the ambient water, *Aquatic Toxicology*, vol. 26, no. 1, pp. 133-149.

Press, C.M. & Evensen, Ø. (1999). The morphology of the immune system in teleost fishes, *Fish & Shellfish Immunology*, vol. 9, no. 4, pp. 309-318.

Provan, F., Jensen, L., Uleberg, K., Larssen, E., Rajalahti, T., Mullins, J. & Obach, A. (2013). Proteomic analysis of epidermal mucus from sea lice–infected Atlantic salmon, *Salmo salar* L., *Journal of Fish Diseases*, vol. 36, no. 3, pp. 311-321.

Rach, J.J., Howe, G.E. & Schreier, T.M. (1997). Safety of formalin treatments on warm-and cool water fish eggs, *Aquaculture*, vol. 149, no. 3, pp. 183-191.

Radonic, A., Thulke, S., Bae, H.G., Muller, M.A., Siegert, W. & Nitsche, A. (2005). Reference gene selection for quantitative real-time PCR analysis in virus infected cells: SARS corona virus, Yellow fever virus, Human Herpesvirus-6, Camelpox virus and Cytomegalovirus infections, *Virology journal*, vol. 2, pp. 7.

Rae, G.H. (2002). Sea louse control in Scotland, past and present, *Pest Management Science*, vol. 58, no. 6, pp. 515-520.

Rajan, B., Fernandes, J.M., Caipang, C., Kiron, V., Rombout, J.H. & Brinchmann, M.F. (2011). Proteome reference map of the skin mucus of Atlantic cod (*Gadus morhua*) revealing immune competent molecules, *Fish & Shellfish Immunology*, vol. 31, no. 2, pp. 224-231.

Rakers, S., Niklasson, L., Steinhagen, D., Kruse, C., Schauber, J., Sundell, K. & Paus, R. (2013). Antimicrobial peptides (AMPs) from fish epidermis: perspectives for investigative dermatology, *Journal of Investigative Dermatology*, vol. 133, no. 5, pp. 1140-1149.

Ramsey, M.H., Geelhoed, B., Wood, R. & Damant, A.P. (2011). Improved evaluation of measurement uncertainty from sampling by inclusion of between-sampler bias using sampling proficiency testing, *Analyst*, vol. 136, no. 7, pp. 1313-1321.

Randelli, E., Buonocore, F., & Scapigliati, G. (2008). Cell markers and determinants in fish immunology. *Fish & Shellfish Immunology* 25 (326-340).

Rebl, A., Korytár, T., Köbis, J.M., Verleih, M., Krasnov, A., Jaros, J., Kühn, C., Köllner, B. & Goldammer, T. (2014). Transcriptome profiling reveals insight into distinct immune responses to *Aeromonas salmonicida* in gill of two Rainbow Trout Strains, *Marine Biotechnology*, vol. 16, no. 3, pp. 333-348.

Reid, I.M. (1980). Morphometric methods in veterinary pathology: a review, *Veterinary Pathology*, vol. 17, no. 5, pp. 522-543.

Reite, O.B. & Evensen, Ø. (2006). Inflammatory cells of teleostean fish: a review focusing on mast cells/eosinophilic granule cells and rodlet cells. Fish & Shellfish Immunology, vol. 20, no. 2, pp. 192-208.

Reynolds, W., McCauley, R., Casterlin, M. & Crawshaw, L. (1976). Body temperatures of behaviorally thermoregulating largemouth blackbass (*Micropterus salmoides*), *Comparative Biochemistry and Physiology Part A: Physiology*, vol. 54, no. 4, pp. 461-463.

Rijkers, G.T., Frederix-Wolters, E.M. & van Muiswinkel, W.B. (1980). The immune system of cyprinid fish. Kinetics and temperature dependence of antibody-producing cells in carp (*Cyprinus carpio*), *Immunology*, vol. 41, no. 1, pp. 91-97.

Robbins, S., Cotran, R. (1979). *Pathologic basis of disease*. 2nd ed., *Philadelphia, PA*: Saunders, pp. 402-1404.

Roberts, S.D. & Powell, M.D. (2003). Comparative ionic flux and gill mucous cell histochemistry: effects of salinity and disease status in Atlantic salmon (*Salmo salar* L.), *Comparative Biochemistry and Physiology Part A: Molecular & Integrative Physiology,* vol. 134, no. 3, pp. 525-537.

Roberts, R.J., & Rodger, H.D., (2012). The pathophysiology and systematic pathology of teleosts. In: R.J. Roberts, eds. *Fish Pathology*, 4th Edition, Blackwell Publishing Ltd, pp. 62-143.

Roberts, R., (2012), Fish Pathology, 4th Edition, Blackwell Publishing Ltd, pp. 62-143.

Rodgers, C.J. (1990). Immersion vaccination for control of fish Furunculosis. *Diseases of Aquatic Organisms*. vol 8, pp. 69–72.

Rodger, H. & McArdle, J. (1996). An outbreak of amoebic gill disease in Ireland, *Veterinary Record,* vol. 139, pp. 348-348.

Rodger, H. (2007). Gill disorders: an emerging problem for farmed Atlantic salmon (*Salmo salar*) in the marine environment, *Fish Veterinary Journal,* vol. 9, pp. 38-48.

Rodger, H.D. (2010). *Fish Disease Manual*. Vet-Aqua International, Oranmore, Co. Galway, Ireland, Grant-Aid Agreement No. PBA/AF/08/003.

Rodger, H.D., Murphy, K., Mitchell, S.O. & Henry, L. (2011). Gill disease in marine farmed Atlantic salmon at four farms in Ireland, *The Veterinary Record,* vol. 168, no. 25, pp. 668.

Rojo, M.G., Garcia, G.B., Mateos, C.P., Garcia, J.G. & Vicente, M.C. (2006). Critical comparison of 31 commercially available digital slide systems in pathology. *International Journal of Surgical Pathology*. vol. 14, no. 4, pp. 285-305.

Rombough, P. & Garside, E. (1977). Hypoxial death inferred from thermally induced injuries at upper lethal temperatures, in the banded killifish, *Fundulus diaphanus* (LeSueur), *Canadian Journal of Zoology,* vol. 55, no. 10, pp. 1705-1719.

Rombout, J.W., Blok, L.J., Lamers, C.H. & Egberts, E. (1986). Immunization of carp (*Cyprinus carpio*) with a *Vibrio anguillarum* bacterin: indications for a common mucosal immune system, *Developmental & Comparative Immunology,* vol. 10, no. 3, pp. 341-351.

Rombout, J., Bot, H. & Taverne-Thiele, J. (1989). Immunological importance of the second gut segment of carp., *Journal of Fish Biology,* vol. 35, no. 2, pp. 167-178.

Rombout, J.H., Taverne-Thiele, A.J. & Villena, M.I. (1993). The gut-associated lymphoid tissue (GALT) of carp (*Cyprinus carpio* L.): An immunocytochemical analysis, *Developmental & Comparative Immunology,* vol. 17, no. 1, pp. 55-66.

Rombout, J.H., Abelli, L., Picchietti, S., Scapigliati, G. & Kiron, V. (2011). Teleost intestinal immunology, *Fish & Shellfish Immunology,* vol. 31, no. 5, pp. 616-626.

Rombout, J.H., Van der Tuin, S., Yang, G., Schopman, N., Mroczek, A., Hermsen, T. & Taverne-Thiele, J. (2008). Expression of the polymeric Immunoglobulin Receptor (pIgR) in mucosal tissues of common carp (*Cyprinus carpio* L.), *Fish & Shellfish Immunology,* vol. 24, no. 5, pp. 620-628.

Rombout, J.H., Yang, G. & Kiron, V. (2014). Adaptive immune responses at mucosal surfaces of teleost fish, *Fish & Shellfish Immunology,* vol. 40, no. 2, pp. 634-643.

Romstad, A.B., Reitan, L.J., Midtlyng, P., Gravningen, K. & Evensen, Ø. (2013). Antibody responses correlate with antigen dose and *in vivo* protection for oil-adjuvanted, experimental furunculosis (*Aeromonas salmonicida* subsp. *salmonicida*) vaccines in Atlantic salmon (*Salmo salar* L.) and can be used for batch potency testing of vaccines, *Vaccine,* vol. 31, no. 5, pp. 791-796.

Roque, A., Yildiz, H.Y., Carazo, I. & Duncan, N. (2010). Physiological stress responses of sea bass (*Dicentrarchus labrax*) to hydrogen peroxide (H_2O_2) exposure, *Aquaculture,* vol. 304, no. 1, pp. 104-107.

Roy, P., Witten, P., Hall, B. & Lall, S. (2002). Effects of dietary phosphorus on bone growth and mineralisation of vertebrae in haddock (*Melanogrammus aeglefinus* L.), *Fish Physiology and Biochemistry,* vol. 27, no. 1-2, pp. 35-48.

Ruane, N., Rodger, H., Mitchell, S., Doyle, T., Baxter, E. & Fringuelli, E. (2013). *GILPAT: An Investigation into Gill Pathologies in Marine Reared Finfish,* Marine Institute, Rinville, Oranmore, Co. Galway.

Ruangsri, J., Fernandes, J.M., Brinchmann, M. & Kiron, V. (2010). Antimicrobial activity in the tissues of Atlantic cod (*Gadus morhua* L.), *Fish & Shellfish Immunology,* vol. 28, no. 5, pp. 879-886.

Russell Hayman, J., Bly, J.E., Paul Levine, R. & Lobb, C.J. (1992). Complement deficiencies in channel catfish (*Ictalurus punctatus*) associated with temperature and seasonal mortality, *Fish & Shellfish Immunology,* vol. 2, no. 3, pp. 183-192.

Saha, N.R., Suetake, H. & Suzuki, Y. (2005). Analysis and characterization of the expression of the secretory and membrane forms of IgM heavy chains in the puffer fish, *Takifugu rubripes*, *Molecular Immunology,* vol. 42, no. 1, pp. 113-124.

Salinas, I., Zhang, Y. & Sunyer, J.O. (2011). Mucosal immunoglobulins and B cells of teleost fish, *Developmental & Comparative Immunology,* vol. 35, no. 12, pp. 1346-1365.

Sandritter W. (1976). Color atlas and textbook of tissue md cellular pathology. *Year Book Medical Publishers*, Chicago,

Santos, M.A. & Pacheco, M. (1996). *Anguilla anguilla* L. Stress biomarkers recovery in clean water and secondary-treated pulp mill effluent, *Ecotoxicology and environmental safety,* vol. 35, no. 1, pp. 96-100.

Scapigliati, G., Buonocore, F., Randelli, E., Casani, D., Meloni, S., Zarletti, G., Tiberi, M., Pietretti, D., Boschi, I. & Manchado, M. (2010). Cellular and molecular immune responses of the sea bass (*Dicentrarchus labrax*) experimentally infected with betanodavirus, *Fish & Shellfish Immunology,* vol. 28, no. 2, pp. 303-311.

Schmid, O.J., and Mann, H. (1961). Action of a detergent (dodecylbenzene sulphormate) on the gills of the trout. Nature (Ld.) 192: 675.

Schmittgen, T.D. & Livak, K.J. (2008). Analyzing real-time PCR data by the comparative Ct method, *Nature Protocols,* vol. 3, no. 6, pp. 1101-1108.

Scott, A.L., Rogers, W. & Klesius, P.H. (1985). Chemiluminescence by peripheral blood phagocytes from channel catfish: function of opsonin in and temperature, *Developmental & Comparative Immunology,* vol. 9, no. 2, pp. 241-250.

Sealey, W., Craig, S. & Gatlin, D.M. (2001). Dietary cholesterol and lecithin have limited effects on growth and body composition of hybrid striped bass (*Morone chrysops, M. saxatilis*), *Aquaculture Nutrition,* vol. 7, no. 1, pp. 25-31.

Secombes, C. (1996). The nonspecific immune system: cellular defenses, In: *The Fish Immune System*: *Organism, Pathogen, and Environment*, edi. Iwama G., Nakanishi T., pp. 63-103,

Secombes, C. & Fletcher, T. (1992). The role of phagocytes in the protective mechanisms of fish. *Annual Review of Fish Diseases*, vol. 2, pp. 53-71.

Segers, J., Temmink, J., Van den Berg, J. & Wegman, R. (1984). Morphological changes in the gill of carp (*Cyprinus carpio* L.) exposed to acutely toxic concentrations of methyl bromide, *Water Research,* vol. 18, no. 11, pp. 1437-1441.

Segner, H., Sundh, H., Buchmann, K., Douxfils, J., Sundell, K.S., Mathieu, C., Ruane, N., Jutfelt, F., Toften, H. & Vaughan, L. (2012). Health of farmed fish: its relation to fish welfare and its utility as welfare indicator, *Fish Physiology and Biochemistry,* vol. 38, no. 1, pp. 85-105.

Sepúlveda, M.S., Gallagher, E.P., Wieser, C.M. & Gross, T.S. (2004). Reproductive and biochemical biomarkers in largemouth bass sampled downstream of a pulp and paper mill in Florida, *Ecotoxicology and Environmental Safety,* vol. 57, no. 3, pp. 431-440.

Sfacteria, A., Brines, M. & Blank, U. (2014). The mast cell plays a central role in the immune system of teleost fish, *Molecular immunology,* Vol 63, no 1, pp 3-8.

Sharon, N. & Lis, H. (1989). Lectins as cell recognition molecules, *Science (New York, N.Y.),* vol. 246, no. 4927, pp. 227-234.

Shephard, K.L. (1994). Functions for fish mucus, *Reviews in Fish Biology and Fisheries,* vol. 4, no. 4, pp. 401-429.

Shinn, A., Gibson, D. & Sommerville, C. (2001). Morphometric discrimination of *Gyrodactylus salaris* Malmberg (Monogenea) from species of *Gyrodactylus* parasitising British salmonids using novel parameters, *Journal of Fish Diseases,* vol. 24, no. 2, pp. 83-97.

Shoemaker, C.A., Klesius, P.H. & Evans, J.J. (2001). Prevalence of *Streptococcus iniae* in tilapia, hybrid striped bass, and channel catfish on commercial fish farms in the United States, *American Journal of Veterinary Research,* vol. 62, no. 2, pp. 174-177.

Skidmore, J. & Tovell, P. (1972). Toxic effects of zinc sulphate on the gills of rainbow trout, *Water Research,* vol. 6, no. 3, pp. 217-IN4.

Solem, S.T. & Stenvik, J. (2006). Antibody repertoire development in teleosts—a review with emphasis on salmonids and *Gadus morhua* L, *Developmental & Comparative Immunology,* vol. 30, no. 1, pp. 57-76.

Sollid, J., De Angelis, P., Gundersen, K. & Nilsson, G.E. (2003). Hypoxia induces adaptive and reversible gross morphological changes in crucian carp gills, *The Journal of Experimental Biology,* vol. 206, no. 20, pp. 3667-3673.

Sollid, J., Weber, R.E. & Nilsson, G.E. (2005). Temperature alters the respiratory surface area of crucian carp *Carassius carassius* and goldfish *Carassius auratus*, *The Journal of Experimental Biology,* vol. 208, no. 6, pp. 1109-1116.

Sommerset, I., Skern, R., Biering, E., Bleie, H., Fiksdal, I.U., Grove, S. & Nerland, A.H. (2005). Protection against Atlantic halibut nodavirus in turbot is induced by recombinant capsid protein vaccination but not following DNA vaccination, *Fish & Shellfish Immunology,* vol. 18, no. 1, pp. 13-29.

Speare, D.J. & Ferguson, H. (1989). Fixation artifacts in rainbow trout (*Salmo gairdneri*) gills: a morphometric evaluation, *Canadian Journal of Fisheries and Aquatic Sciences,* vol. 46, no. 5, pp. 780-785.

Speare, D.J., Carvajal, V. & Horney, B.S. (1999). Growth suppression and branchitis in trout exposed to hydrogen peroxide, *Journal of Comparative Pathology,* vol. 120, no. 4, pp. 391-402.

Star, B. & Jentoft, S. (2012). Why does the immune system of Atlantic cod lack MHC II?, *Bioessays,* vol. 34, no. 8, pp. 648-651.

Steinum, T., Kvellestad, A., Colquhoun, D.J., Heum, M., Mohammad, S., Grontvedt, R.N. & Falk, K. (2010). Microbial and pathological findings in farmed Atlantic salmon *Salmo salar* with proliferative gill inflammation, *Diseases of Aquatic Organisms,* vol. 91, no. 3, pp. 201-211.

Stenvik, J., Schrøder, M., Olsen, K., Zapata, A. & Jørgensen, T.Ø. (2001). Expression of immunoglobulin heavy chain transcripts (VH-families, IgM, and IgD) in head kidney and spleen of the Atlantic cod (*Gadus morhua* L.), *Developmental & Comparative Immunology,* vol. 25, no. 4, pp. 291-302.

Stenvik, J. & Jørgensen, T.Ø. (2000). Immunoglobulin D (IgD) of Atlantic cod has a unique structure, *Immunogenetics,* vol. 51, no. 6, pp. 452-461.

Stien, L.H., Kiessling, A. & Manne, F. (2007). Rapid estimation of fat content in salmon fillets by colour image analysis, *Journal of Food Composition and Analysis,* vol. 20, no. 2, pp. 73-79.

Sundh, H., Kvamme, B.O., Fridell, F., Olsen, R.E., Ellis, T., Taranger, G.L. & Sundell, K. (2010). Intestinal barrier function of Atlantic salmon (*Salmo salar* L.) post smolts is reduced by common sea cage environments and suggested as a possible physiological welfare indicator, *BMC Physiology,* vol. 10, pp. 22-6793-10-22.

Sunyer, O., Zhang, Y., Li, J., Parra, D. & LaPatra, S.E. (2009). Is IgT the evolutionary equivalent of IgA? Insights into its structure and function, *Journal of Immunology,* vol. 182, pp. 81-21.

Sunyer, J.O. (2012). Evolutionary and functional relationships of B cells from fish and mammals: insights into their novel roles in phagocytosis and presentation of particulate antigen, *Infectious Disorders Drug Targets,* vol. 12, no. 3, pp. 200-212.

Sunyer, J.O. (2013). Fishing for mammalian paradigms in the teleost immune system, *Nature Immunology*, vol. 14, no. 4, pp. 320-326.

Szalai, A.J., Bly, J. & Clem, L. (1994). Changes in serum concentrations of channel catfish (*Ictalurus punctatus* Rafinesque) phosphorylcholine-reactive protein (PRP) in response to inflammatory agents, low temperature-shock and infection by the fungus *Saprolegnia* sp., *Fish & Shellfish Immunology*, vol. 4, no. 5, pp. 323-336.

Tadiso, T.M., Krasnov, A., Skugor, S., Afanasyev, S., Hordvik, I. & Nilsen, F. (2011a). Gene expression analyses of immune responses in Atlantic salmon during early stages of infection by salmon louse (*Lepeophtheirus salmonis*) revealed bi-phasic responses coinciding with the copepod-chalimus transition, *BMC Genomics*, vol. 12, pp. 141-2164-12-141.

Tadiso, T.M., Lie, K.K. & Hordvik, I. (2011b). Molecular cloning of IgT from Atlantic salmon, and analysis of the relative expression of τ, μ and δ in different tissues, *Veterinary Immunology and Immunopathology*, vol. 139, no. 1, pp. 17-26.

Tadiso, T.M. (2012). Molecular characterisation of key components of the mucosal immune system in Atlantic salmon (*Salmo salar* L) and transcriptome analysis of responses against the salmon louse (*Lepeophtheirus salmonis*). PhD Thesis, University of Bergen.

Tafalla, C., Bøgwald, J. & Dalmo, R.A. (2013). Adjuvants and immunostimulants in fish vaccines: current knowledge and future perspectives, *Fish & Shellfish Immunology*, vol. 35, no. 6, pp. 1740-1750.

Tatner, M.F. & Findlay, C. (1991). Lymphocyte migration and localisation patterns in rainbow trout *Oncorhynchus mykiss*, studied using the tracer sample method, *Fish & Shellfish Immunology*, vol. 1, no. 2, pp. 107-117.

Temmink, J., Bouwmeister, P., De Jong, P. & Van Den Berg, J. 1983, An ultrastructural study of chromate-induced hyperplasia in the gill of rainbow trout (*Salmo gairdneri*), *Aquatic toxicology*, vol. 4, no. 2, pp. 165-179.

Thomassen, J. M. (1993). Hydrogen peroxide as a delousing agent for Atlantic salmon. In: Pathogens of wild and farmed fish, Boxhall, G. A. & Defaye, D., Ellis Horwood, Chichester: 290-295.

Tian, J., Sun, B., Luo, Y., Zhang, Y. & Nie, P. (2009). Distribution of IgM, IgD and IgZ in mandarin fish, *Siniperca chuatsi* lymphoid tissues and their transcriptional changes after *Flavobacterium columnare* stimulation, *Aquaculture*, vol. 288, no. 1, pp. 14-21.

Toranzo, A.E., Magariños, B. & Romalde, J.L. (2005). A review of the main bacterial fish diseases in mariculture systems, *Aquaculture*, vol. 246, no. 1, pp. 37-61.

Tort, L., Puigcerver, M., Crespo, S. & Padros, F. (2002). Cortisol and haematological response in sea bream and trout subjected to the anaesthetics clove oil and 2-phenoxyethanol, *Aquaculture Research*, vol. 33, no. 11, pp. 907-910.

Tort, L., Balasch, J. & Mackenzie, S. (2003). Fish immune system. A crossroads between innate and adaptive responses, *Inmunología*, vol. 22, no. 3, pp. 277-286.

Tort, L. (2011). Stress and immune modulation in fish, *Developmental & Comparative Immunology*, vol. 35, no. 12, pp. 1366-1375.

Treasurer, J., Wadsworth, S. & Grant, A. (2000)., Resistance of sea lice, *Lepeophtheirus salmonis* (Krøyer), to hydrogen peroxide on farmed Atlantic salmon, *Salmo salar* L., *Aquaculture Research*, vol. 31, no. 11, pp. 855-860.

Valdenegro-Vega, V.A., Crosbie, P., Bridle, A., Leef, M., Wilson, R. & Nowak, B.F. (2014). Differentially expressed proteins in gill and skin mucus of Atlantic salmon (*Salmo salar*) affected by amoebic gill disease, *Fish & Shellfish Immunology*, vol. 40, no. 1, pp. 69-77.

Vallejo, A.N., Miller, N.W. & William Clem, L. (1992). Antigen processing and presentation in teleost immune responses, *Annual Review of Fish Diseases*, vol. 2, pp. 73-89.

Van Valin, C.C., Andrews, A.K. & Eller, L.L. (1968)., Some effects of mirex on two warm-water fishes, *Transactions of the American Fisheries Society*, vol. 97, no. 2, pp. 185-196.

Vanden Bergh, P. & Frey, J. (2013). *Aeromonas salmonicida* subsp. *salmonicida* in the light of its type-three secretion system, *Microbial biotechnology.* Vol. 7(5), 381–400.

Vandesompele, J., De Preter, K., Pattyn, F., Poppe, B., Van Roy, N., De Paepe, A. & Speleman, F. (2002). Accurate normalization of real-time quantitative RT-PCR data by geometric averaging of multiple internal control genes, *Genome Biology,* vol. 3, no. 7, pp.

Verdugo, P. (1990). Goblet cells secretion and mucogenesis, *Annual Review of Physiology,* vol. 52, no. 1, pp. 157-176.

Verlhac, V., Sage, M. & Deschaux, P. (1990). Cytotoxicity of carp (*Cyprinus carpio*) leucocytes induced against TNP-modified autologous spleen cells and influence of acclimatization temperature, *Developmental & Comparative Immunology,* vol. 14, no. 4, pp. 475-480.

Villarroel, F., Bastías, A., Casado, A., Amthauer, R. & Concha, M.I. (2007). Apolipoprotein AI, an antimicrobial protein in *Oncorhynchus mykiss*: Evaluation of its expression in primary defence barriers and plasma levels in sick and healthy fish, *Fish & Shellfish Immunology,* vol. 23, no. 1, pp. 197-209.

Vivas, J., Riaño, J., Carracedo, B., Razquin, B.E., López-Fierro, P., Naharro, G. & Villena, A.J. (2004). The auxotrophic aroA mutant of *Aeromonas hydrophila* as a live attenuated vaccine against *A. salmonicida* infections in rainbow trout (*Oncorhynchus mykiss*), *Fish & Shellfish Immunology,* vol. 16, no. 2, pp. 193-206.

Vogel, C. & Marcotte, E.M. (2012). Insights into the regulation of protein abundance from proteomic and transcriptomic analyses, *Nature Reviews Genetics,* vol. 13, no. 4, pp. 227-232.

Waagbø, R. (2006). Feeding and disease resistance in fish, *Biology of growing animals,* vol. 4, pp. 387-415.

Walters, G. & Plumb, J. (1980). Environmental stress and bacterial infection in channel catfish, *Ictalurus punctatus* Rafinesque, *Journal of Fish Biology,* vol. 17, no. 2, pp. 177-185.

Weiss, E. & Avtalion, R.R. (1977). Regulatory effect of temperature and antigen upon immunity in ectothermic vertebrates. II. Primary enhancement of anti-hapten antibody response at high and low temperatures, *Developmental & Comparative Immunology,* vol. 1, no. 2, pp. 93-103.

Wetzel, A.W., Gilbertson, J., Zheng, L., Gilespie, J., Swalwell, J., Yagi, Y., Kim, S., Emmert-Buck, M. & Becich, M.J. (2000). Three-dimensional reconstruction for genomic analysis of prostate cancer, *28th AIPR Workshop: 3D Visualization for Data Exploration and Decision Making,* International Society for Optics and Photonics

Whittington, I., Shinn, A., Bron, J. & Deveney, M. (2011). Innovative solutions for aquaculture: assessment of in situ monitoring techniques and life history parameters for monogenean skin and gill parasites, Aquaculture Research Reports, *Fisheries Research and Development Corporation. The University of Adelaide*., Australia.

Whyte, S.K. (2007). The innate immune response of finfish–a review of current knowledge, *Fish & Shellfish Immunology,* vol. 23, no. 6, pp. 1127-1151.

Wilbur, D.C., Madi, K., Colvin, R.B., Duncan, L.M., Faquin, W.C., Ferry, J.A., Frosch, M.P., Houser, S.L., Kradin, R.L. & Lauwers, G.Y. (2009). Whole-slide imaging digital pathology as a platform for teleconsultation: a pilot study using paired subspecialist correlations, *Archives of Pathology & Laboratory Medicine,* vol. 133, no. 12, pp. 1949-1953.

Wolf, J.C., Baumgartner, W.A., Blazer, V.S., Camus, A.C., Engelhardt, J.A., Fournie, J.W., Frasca, S.,Jr, Groman, D.B., Kent, M.L., Khoo, L.H., Law, J.M., Lombardini, E.D., Ruehl-Fehlert, C., Segner, H.E., Smith, S.A., Spitsbergen, J.M., Weber, K. & Wolfe, M.J. (2014). Nonlesions, misdiagnoses, missed diagnoses, and other interpretive challenges in fish histopathology studies: A Guide for Investigators, Authors, Reviewers, and Readers, *Toxicologic pathology.* Published online 11 August 2014, DOI: 10.1177/0192623314540229 .

Wolke, R.E., Murchelano, R.A., Dickstein, C.D. & George, C.J. (1985) Preliminary evaluation of the use of macrophage aggregates (MA) as fish health monitors, *Bulletin of environmental contamination and toxicology,* vol. 35, no. 1, pp. 222-227.

Wood, C.M. & Randall, D. (1973), The influence of swimming activity on water balance in the rainbow trout (*Salmo gairdneri*), *Journal of Comparative Physiology A: Neuroethology, Sensory, Neural, and Behavioral Physiology,* vol. 82, no. 3, pp. 257-276.

Workenhe, S.T., Wadowska, D.W., Wright, G.M., Kibenge, M.J. & Kibenge, F.S. (2007). Demonstration of infectious salmon anaemia virus (ISAV) endocytosis in erythrocytes of Atlantic salmon, *Virology journal*, vol. 4, pp. 13.

Wynne, J.W., O'Sullivan, M.G., Cook, M.T., Stone, G., Nowak, B.F., Lovell, D.R. & Elliott, N.G. (2008). Transcriptome analyses of amoebic gill disease-affected Atlantic salmon (*Salmo salar*) tissues reveal localized host gene suppression, *Marine Biotechnology*, vol. 10, no. 4, pp. 388-403.

Xu, Z., Parra, D., Gomez, D., Salinas, I., Zhang, Y.A., von Gersdorff Jorgensen, L., Heinecke, R.D., Buchmann, K., LaPatra, S. & Sunyer, J.O. (2013). Teleost skin, an ancient mucosal surface that elicits gut-like immune responses, *Proceedings of the National Academy of Sciences of the United States of America*, vol. 110, no. 32, pp. 13097-13102.

Yano, T., H. Ando and M. Nakao (1984). Optimum conditions for the assay of hemolytic complement titer of carp and seasonal variation of the titers. J. Faculty of . Agriculture., Kyushu University. Vol. 29, pp. 91-101.

Yoshimizu, M. and H. Kasai (2007). Prevention and control of fish viral disease. JVPA Digest, 27, 1–16

Young, N., Crosbie, P., Adams, M., Nowak, B. & Morrison, R. (2007). *Neoparamoeba perurans* n. sp., an agent of amoebic gill disease of Atlantic salmon (*Salmo salar*), *International Journal for Parasitology*, vol. 37, no. 13, pp. 1469-1481

Zapata, A., Torroba, M., Sacedon, R., Varas, A. & Vicente, A. (1996). Structure of the lymphoid organs of elasmobranchs, *Journal of Experimental Zoology*, vol. 275, no. 2-3, pp. 125-143.

Zelikoff, J.T. (1998). Biomarkers of immunotoxicity in fish and other non-mammalian sentinel species: predictive value for mammals? *Toxicology*, vol. 129, no. 1, pp. 63-71.

Zhang, Y., Salinas, I., Li, J., Parra, D., Bjork, S., Xu, Z., LaPatra, S.E., Bartholomew, J. & Sunyer, J.O. (2010). IgT, a primitive immunoglobulin class specialized in mucosal immunity, *Nature immunology*, vol. 11, no. 9, pp. 827-835.

Zhang, Y., Salinas, I. & Sunyer, O. J., (2011). Recent findings on the structure and function of teleost IgT, *Fish & Shellfish Immunology*, vol. 31, no. 5, pp. 627-634.

Zhao, X., Findlay, R.C. & Dickerson, H.W. (2008). Cutaneous antibody-secreting cells and B cells in a teleost fish, *Developmental & Comparative Immunology*, vol. 32, no. 5, pp. 500-508.

Zou, J., Carrington, A., Collet, B., Dijkstra, J.M., Yoshiura, Y., Bols, N. & Secombes, C. (2005). Identification and bioactivities of IFN-gamma in rainbow trout *Oncorhynchus mykiss*: the first Th1-type cytokine characterized functionally in fish, *Journal of immunology*, vol. 175, no. 4, pp. 2484-2494.

Zuchelkowski, E.M., Pinkstaff, C.A. & Hinton, D.E. (1985) Mucosubstance histochemistry in control and acid-stressed epidermis of brown bullhead catfish, *Ictalurus nebulosus* (LeSueur), *The Anatomical Record*, vol. 212, no. 4, pp. 327-335.

Zwollo, P., Haines, A., Rosato, P. & Gumulak-Smith, J. (2008). Molecular and cellular analysis of B-cell populations in the rainbow trout using Pax5 and immunoglobulin markers, *Developmental & Comparative Immunology*, vol. 32, no. 12, pp. 1482-1496.

APPENDIX I

General Buffers

Phosphate buffered saline, pH 7.4 (PBS)

NaH_2PO_4 (VWR)	0.438g
Na_2HPO_4 (VWR)	1.28g
Sodium chloride	4.385g

Dissolve in 400ml distilled water, pH to 7.4 make up to 500ml and autoclave.

Tris buffered saline (TBS), pH 7.6

Trisma base	1.21g
Sodium chloride	14.62g

Dissolve in 400ml distilled water, pH to 7.2-7.6 and make up to 500ml.

Stains

Mayer's Haematoxylin

Haematoxylin		2g
Sodium iodate		0.4g
Potassium alum	100g	
Citric acid		2g
Chloral hydrate	100g	
Distilled water		2L

Allow haematoxylin, potassium alum and sodium iodate to dissolve in distilled water overnight. Add chloral hydrate and citric acid and boil for 5 min.

Eosin

1% Eosin		40ml
Putt's Eosin		80ml
Eosin yellowish	20g	

Pre-dissolve in 600ml distilled water and then make up to 2L.

Putt's Eosin

Eosin yellowish	4g	
Potassium dichromate		2g
Saturated aqueous picric acid		40ml
Absolute alcohol		40ml
Distilled water		320ml

Dissolve eosin and potassium dichromate in the ethanol, add the water and then the picric acid.

Scott's tap water substitute

Sodium bicarbonate	3.5g
Magnesium sulphate	20g
Tap water	1L

Dissolve by heating if necessary and add a few thymol crystals to preserve.

Molecular Biology

TAE buffer (x50)

Tris base	242g
Glacial acetic acid	57.1 ml
$Na_2EDTA.H_2O$	81.61 g

Adjust the final volume to 1000 ml and pH 8.5

Agarose gel

Agarose	1g
TAE	100ml

Dissolve in the microwave. Add 50 µl ethidium bromide (1 mg/l) when the gel temperature < 60°C.

APPENDIX II

Table 1 Samples and measurement parameters for conducted feed trial

	Type of sample	Measurements or parameter
1.	Total weight and fork length	Specific growth rate, K factor (condition factor)
2.	Liver weight (6 fish per tank per diet)	Hepatosomatic index (ratio of live weight to body weight) (HIS)
3.	Blood samples (6 fish per tank per diet)	Blood smears for leukocyte identification, Haematocrit Haemoglobin Total protein and Albumen Diluted blood for RBC and WBC count Plasma collection for later lysozyme assay
4.	Head kidney samples (6 fish per tank per diet)	Isolation of macrophages for phagocytosis and respiratory burst assay
5.	Gut tissues (6 fish per tank per diet)	Sections for H&E stains, AB-PAS staining, immunohistochemistry and mucus fixation for later SEM and TEM processing
6.	Gill samples (3 fish per tank per diet)	Sections for H&E stains, AB-PAS staining, immunohistochemistry and mucus fixation for later SEM and TEM processing

Table 2 Step by step user guide operations for gill image analysis (GIA)

Table 2. User guide operations for gill image analysis (GIA)
1. Load the image
2. Load the calibration
3. Enter sample details *e.g*. histology sample identity
4. Carry out back ground correction if necessary
5. Rotate the image to give dorsal ventral orientation to secondary lamellae
6. Capture predefine cropped of image (2250X1200 pixels)
7. Draw bounding box to capture 5 dorsal and 5 ventral lamellae passing through primary filament
8. Using intensity thresholding the segment tissue from back ground using threshold sliders. Output binary image.
9. Draw interactively to separate fused or touching secondary lamellae
10. Marked end point of captured tissue to be used in calculating perimeter length of secondary lamellae
11. Interactively mark lowest point of inter lamellae space (ILS) at dorsal and ventral surface of primary lamellae
12. In ILS interactively mark basement membrane to define epithelium of primary lamellae
13. Mark CVS / cartilage for segmentation
14. Measure depth of primary tissue filament at extremities of captured tissue
15. Use colour thresholding to segment mucous cells (HLS colour model) using recursive addition of blue pixels
16. Draw a line along individual secondary lamellae to measure length
17. Draw a line to delineate the dorsal and ventral boundaries of interlamellar spaces
18. Selecting interlamellar space and exclude artefacts if necessary
19. Select segmented total gill tissue
20. Draw a line interactively separate secondary gill lamellae at their bases
21. Use intensity thresholding to segment vacuoles in epithelial tissue / secondary lamellae
22. Check selection of mucous cells on primary lamellae and deselect accidental inclusions
23. Check selection of mucous cells on secondary lamellae and deselect accidental inclusions
24. Select secondary lamellae for measurement
25. Check capture of CVS / cartilage
26. Check capture of vacuole in secondary lamellae
27. Check capture of vacuole in primary lamellae
28. Check capture of primary lamellae epithelium
29. Audible notification of program completion.

Table 3 summary of different raw materials in formulated diets and their proximate analysis. (Skretting ARC, Norway)

Dietary formulation			
	Diet A (control)	Diet B (high soya)	Diet C (functional ingredients)
Raw Material	%	%	%
Fish meal (Scandinavian)	25.00	25.00	25.00
Soya Bean Meal (unrefined)	0.00	25.00	0.00
Soya concentrate (refined)	20.00	0.00	20.00
Wheat	18.73	9.88	18.33
Wheatgluten	13.72	15.81	13.72
Astaxanthin 10%	0.05	0.05	0.05
Fishoil South-American	20.85	22.91	20.85
Natumix (plant extracts/organic acid)	0.00	0.00	YES
Macrogard GLUCAN	0.00	0.00	YES
Nucelotides	0.00	0.00	YES
Proximate analysis			
Nutrient	Analysis	Analysis	Analysis
Dry matter	92.5	92.8	92.5
Moisture	7.5	7.2	7.5
Protein	42.0	42.1	42.0
Fat	26.0	27.7	26.0

Table 4 Hypothetical correlation of morphometric parameters with conventional histopathological descriptions published in the literature

Parameter/morphometric variable	**Related histopathological lesions**	**Hypothetical relationship**
Secondary lamellae area (SLA)	Epithelial hyperplasia and hypertrophy, fusion of secondary lamellae, clubbing of secondary lamellae	Positively correlated
Total gill area (TGA)	Epithelial hyperplasia and hypertrophy,	Positively correlated
Secondary lamellar perimeter length (SFPL)	Shortening of filament Epithelial hyperplasia and hypertrophy	Negatively correlated Positively correlated
Median secondary lamellar length (MedianSLL)	Shortening of filament Lengthening of filament	Negatively correlated Positively correlated
Primary lamellae epithelial area (PLEA)	Epithelial hyperplasia and hypertrophy	Positively correlated
TMCA / SLA	Mucous cell hypertrophy	Positively correlated
TMCN/(SLA+PLEA)	Mucous cell hyperplasia	Positively correlated

Table 5 Results of immune gene analysis from experiment 1. Data was analysed using GLM univariate analysis. Normalised gene expression was calibrated against A10 (control diet at control temperature)

	IgM			IgT			mIgM			mIgT			pIgR		
Dietary groups	**Mean**	**Std Error**	**p value**	**Mean**	**Std Error**	**p value**	**Mean**	**Std Error**	**p value**	**Mean**	**Std Error**	**p value**	**Mean**	**Std Error**	**p value**
A4	1.1833	±0.22688	0.997	0.8171	±0.19902	0.958	1.059	±0.29535	1.000	0.6808	±0.17628	0.971	1.0618	±0.12439	1.000
B4	1.0935	±0.23738	1.000	0.6963	±0.12228	0.747	1.1245	±0.28265	1.000	0.6565	±0.09386	0.948	0.7583	±0.15824	0.862
A10 (control group)	1.0311	±0.12112	1.000	1.0088	±0.05717	1.000	1.017	±0.08836	1.000	1.2605	±0.38226	1.000	1.0102	±0.06400	1.000
B10	1.2561	±0.27240	0.980	1.2674	±0.12386	0.865	1.2675	±0.27251	0.992	1.8001	±0.58051	1.000	1.0324	±0.13526	1.000
A16	1.2761	±0.16958	0.971	1.5251	±0.18171	0.244	1.4415	±0.37119	0.923	0.7373	±0.10043	0.982	0.8637	±0.12094	0.990
B16	1.5745	±0.28290	0.540	2.1053	±0.2261	0.001*	1.8502	±0.43149	0.418	2.0817	±1.31992	1.000	1.0083	±0.31148	1.000